Beyond the typical fluctuations : a journey to the large deviations in the Kardar-Parisi-Zhang growth model

Alexandre Krajenbrink

PSL
UNIVERSITÉ PARIS

THÈSE DE DOCTORAT
DE L'UNIVERSITÉ PSL

Préparée à l'École Normale Supérieure

Beyond the typical fluctuations: a journey to the large deviations in the Kardar-Parisi-Zhang growth model

Soutenue par
Alexandre Krajenbrink
Le 20 juin 2019

École doctorale n°564
Physique en Île-de-France

Spécialité
Physique Théorique

Composition du jury :

Bernard DERRIDA Collège de France	*Président*
Paul BOURGADE Courant Institute, New York University	*Rapporteur*
Malte HENKEL Université de Lorraine Nancy	*Rapporteur*
Sandrine PÉCHÉ Université Paris Diderot	*Examinatrice*
Grégory SCHEHR Université Paris-Sud	*Examinateur*
Herbert SPOHN Technische Universität München	*Examinateur*
Pierre LE DOUSSAL École Normale Supérieure	*Directeur de thèse*

ENS | PSL

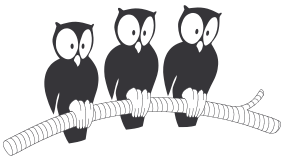

Contents

Remerciements

Je tiens à exprimer dans les quelques lignes qui suivent mes plus profonds remerciements et ma plus sincère gratitude et affection à ma famille, mes amis, mes mentors et mes collaborateurs sans qui je ne serais pas en train de conclure ces trois dernières années par cette présente thèse.

Il serait inconcevable pour moi de commencer ces remerciements autrement que par mes parents. C'est grâce à eux que j'ai été éveillé aux sciences et que je me suis dirigé vers des études scientifiques: cette thèse en est l'aboutissement. Merci pour tout.

Je garde une place toute particulière dans ces remerciements pour Marie-Anne Pavée-Callu qui supporte au quotidien mes élucubrations de physicien théoricien. Sa présence et sa complicité sont plus qu'importantes pour moi et je tenais à lui témoigner ma reconnaissance à travers ces quelques mots.

Des remerciements de thèse ne seraient rien sans l'éloge de mon directeur de thèse Pierre Le Doussal. Pierre est quelqu'un avec qui j'ai réellement appris la physique, que ce soit la physique statistique, la physique mathématique, la physique des équations (!), la physique des appendices de papiers scientifiques (!!), la physique des matrices aléatoires, la physique des polymères, la physique des fermions ou bien encore la physique de l'équation KPZ. Il a été (et est encore au moment précis de l'écriture de ce manuscrit) un directeur de thèse extrêment bienveillant et généreux. Généreux en temps, généreux scientifiquement, généreux humainement et généreux en voyages: ce qui m'a conduit à voyager presque six mois de ma thèse à l'étranger vers des destinations aussi exotiques que Santa Barbara en Californie.

Comme la thèse ne s'arrête pas au quotidien à l'École Normale, il m'incombe de remercier mes amis dont l'amitié et le soutien permanent m'ont été plus que vitaux durant ma thèse. Tout particulièrement et de manière plus personnelle, je tiens à exprimer ma gratitude à Jonathan Lacotte pour son amitié sans faille et pour nos longues discussions diurnes et souvent nocturnes sur notre recherche respective et son impact ; à Hedi Hadiji, Maxime Louis, Pierre-Luc Vautrey, Léo Miolane et Clément Le Priol avec qui j'ai partagé de nombreuses séances d'escalade et énigmes mathématiques ; à Tristan Gautié, Clément Roussel et José Moran, mes successeurs à l'École Normale, avec qui j'ai partagé nombre d'élèves en cours particuliers ; à Maxence Ernoult avec qui j'ai partagé nombre d'aventures à Cambridge (UK) et Cambridge (USA) ; à Elyar Abiar, mon ami co-fondateur de Pandoteχ ; à Gary Bécigneul avec qui j'ai pu discuter de matrices aléatoires au sommet du Stromboli en Sicile ; à Victor Godet, sûrement un de mes plus proches amis de Ginette, avec qui j'espère pouvoir continuer à partager ma passion pour la physique, et finalement à mon ami de plus longue date Guillaume Lucas-Rabner pour sa présence constante à mes côtés.

Je ne pourrais également oublier de mentionner mes co-thésards du (feu) Laboratoire de Physique Théorique: Tony Jin, De-liang Zhong, Ioannis Lavdas, Zhihao Duan et Dongsheng Ge. Nous sommes tous rentrés au LPT en même temps et avons eu la joie de partager ensemble nos premières publications, nos recherches respectives de postdocs et les péripéties des uns et

des autres en conférences à l'autre bout du monde. Je suis réellement heureux de les avoir rencontrés, et encore plus d'avoir eu le plaisir de collaborer avec De-liang et Tony sur des sujets aussi passionants que le calcul de diagrammes *fishnet* ou l'étude des chaînes de spins stochastiques en espérant tout bas voir apparaître des statistiques KPZ.

J'ai également eu la chance de vivre l'aventure de Physique pour Tous avec Tony Jin, Louis Garrigue et Mathias Casiulis durant ces trois années de thèse. J'ai pris plaisir à leur côté à enseigner la physique à un public de littéraires, de philosophes, de géographes et d'économistes et je tenais à le souligner une dernière fois ici.

Je n'oublierai pas tous les échanges que j'ai eus avec Satya Majumdar, Grégory Schehr, Alberto Rosso et Guillaume Barraquand qui m'ont prodigué de nombreux conseils durant ma thèse. J'ai réellement apprécié leur bienveillance, leur proximité, leur curiosité scientifique et j'ai énormément appris à leurs côtés.

Au delà de mon travail direct avec mon directeur de thèse, Pierre Le Doussal, j'ai pu collaborer avec un certain nombre de physiciens et de mathématiciens au côté desquels j'ai énormément appris: Ivan Corwin, Sylvain Prolhac, Promit Ghosal, Bertrand Lacroix-A-Chez-Toine pour ne citer que mes co-auteurs. Je tiens une nouvelle fois à les remercier et j'espère avoir la chance de pouvoir continuer à chercher *et* trouver avec eux dans le futur.

J'ai eu durant ma thèse une double casquette où j'étais également chercheur au sein de Cambridge Quantum Computing. J'ai pu me pencher avec mes collaborateurs et amis Alexander Cowtan, Silas Dilkes, Ross Duncan, Will Simmons et Seyon Sivarajah sur des problèmes de routage de qubits dans des ordinateurs quantiques. J'espère avoir la chance de poursuivre mon travail avec eux dans cette période excitante de prémice de l'informatique quantique!

Je tiens à remercier Paul Bourgade et Malte Henkel pour avoir gentiment accepté d'être les rapporteurs de ma thèse. Un grand merci également à Bernard Derrida, Sandriné Péché, Grégory Schehr et Herbert Spohn pour avoir accepté de faire partie de mon jury de soutenance ainsi qu'à Jean-Philippe Bouchaud et Camille Aron qui ont été respectivement mon parrain et mon tuteur de thèse.

Je remercie chaleureusement Nikos Zygouras, Neil O'Connell, Sylvain Prolhac, Alexander Hartmann, Grégory Schehr, Yan Fyodorov et Malte Henkel pour m'avoir invité au sein de leur laboratoires afin d'exposer ma recherche ou de collaborer avec eux.

Je souhaite également remercier Eugénie Pezé-Heidsieck qui a joué une part importante dans le choix de ma thèse et qui m'a accompagné durant son début.

Je remercie le LPTENS ainsi que ses deux directeurs Costas Bachas et Denis Bernard pour m'avoir acceuilli en thèse ainsi qu'Adel Bilal pour son soutien. Ma thèse n'aurait pas pu se dérouler comme elle l'a été sans l'aide de Viviane Sébille, Sandrine Patacchini, Ouissem Trabelsi, Laura Baron-Ledez, Jean-François Allemand et l'ensemble du personnel administratif de l'École Normale: je leur suis très reconnaissant. Un très grand merci également à Jean Souphanplixa qui a été d'une aide plus que précieuse durant ma scolarité et mon apprentissage de la physique.

Je terminerai ces remerciements avec une pensée spéciale pour mes enseignants en classes préparatoires à Ginette, tout particulièrement Michel Volcker, Hugues Mesnil et Thibaud Naulet, et mes professeurs à l'École polytechnique, qui m'ont tous, tour à tour, donné goût pour les sciences.

Introduction, goal and outline

> "*I would rather have questions that can't be answered than answers that can't be questioned.*"
>
> — Richard Feynman

This Thesis will be devoted to the celebrated Kardar-Parisi-Zhang (KPZ) equation, the corner stone of continuous stochastic non-linear growth models. The goal of this Thesis is two-fold. Firstly, it aims to review the state of the art and provide a detailed picture of the search of exact solutions to the KPZ equation, of their properties in terms of large deviations and also of their applications to random matrix theory or stochastic calculus. Secondly, is it intended to formulate a number of open questions connecting the Kardar-Parisi-Zhang with integrability theory, random matrix theory and Coulomb gas theory.

This Thesis is divided in three distinct parts:

Part I will be devoted to a general introduction to the physics of the Kardar-Parisi-Zhang equation and its exact solutions at all times, shedding some light on the reason why this equation is considered nowadays as a landmark to study systems driven out-of-equilibrium. In addition, Part I will include a presentation of some elements of Random Matrix Theory and of Large Deviation Theory required to understand the recent developments surrounding this equation. Finally, Part I will also bring to light intriguing connections of the solutions of the KPZ equation to other problems arising in probability theory.

Part II will focus on the short-time properties of the solutions to the KPZ equation from the point of view of Large Deviation Theory. Two frameworks will be introduced to that aim: *(i)* the Weak Noise Theory, interpreted as a perturbation theory on the magnitude of the noise of the KPZ equation and *(ii)* a general methodology developed in this Thesis, the cumulant method based on the recently established Fredholm representation of some solutions to the KPZ equation. In addition, the predictions for the short-time KPZ solutions will be confronted to remarkable high-precision numerical simulations of discrete directed polymers obtained by Markov-chain Monte Carlo methods combined with the idea of importance sampling.

Part III will focus on the late-time properties of the solutions to the KPZ equation again from the point of view of Large Deviation Theory. Quite remarkably, the question of determining the large fluctuations of the KPZ solutions at large time will unveil a more general problem which is the study of truncated linear statistics at the edge of Gaussian random matrices. Four original methods, historically dedicated to the large-time large deviations of the KPZ solutions and a priori unrelated, will be presented and unified within Part III. These methods originate from different backgrounds involving a generalized Painlevé II equation, the Stochastic Airy Operator, the theory of Coulomb gases and an extended cumulant expansion for determinantal point processes.

We will present in this Thesis a number of original results obtained during the three years of its completion. These results will be equally distributed in the three parts composing this Thesis and can be summarized as follows.

In Part I, we will introduce a new solution to the Kardar-Parisi-Zhang equation valid at all times in a half-space for the so-called droplet initial condition in presence of a wall at the origin characterized by a coefficient $A \geqslant -\frac{1}{2}$ and for the Brownian initial condition with a positive drift equal to $A + \frac{1}{2}$ in presence of a hard-wall at the origin. We will additionally present a new application of the exact KPZ solutions to the study of a Brownian functional, called the pairwise coincidence time, in various geometries (Brownian motions, Brownian bridges...). Finally, on a more technical note, we will provide a new Lemma to manipulate a certain class of Fredholm Pfaffians including matrix-valued kernels and to transform them into Fredholm determinants with scalar-valued kernels.

In Part II, we will construct a new method, the cumulant method, to establish at short time a Large Deviation Principle for the solutions of the KPZ equation. The assumption required for the use of this method will be the availability of a representation of the KPZ solution in terms of Fredholm determinant, which was recently found for various initial conditions. This method will appear as an analog to the Szegö theorem for Toeplitz determinants. From an exhaustive study of the short-time properties of the KPZ solutions obtained for many initial conditions, we will hint to some form of universality in the distribution of the large fluctuations at short time. Finally, on a more numerical note, we will validate the conclusions of the cumulant method by comparing the probability distribution of the large fluctuations down to values as small as 10^{-500}.

In Part III, we will develop a new systematic expansion of the Fredholm determinant related to the solution of the Kardar-Parisi-Zhang equation for the droplet initial condition. The aim of this expansion is to *(i)* uncover the presence of a Gaussian Free Field in the atypical fluctuations of the KPZ solution at short time and *(ii)* bring corrections at arbitrary order in time in a form similar to a Szegö theorem to study the intermediate-time regime. This systematic expansion will allow to shift smoothly from the short-time regime to the large-time regime in order to establish a Large Deviation Principle at late time for the solutions of the KPZ equation as well as for the linear statistics problem. This expansion will in addition be a central pillar for our resolution of the problem of truncated linear statistics at the edge of Gaussian random matrices and for the discovery of a new family of phase transitions exhibiting a continuous order larger or equal to three. To finish on a more practical note, we applied our results on the truncated linear statistics to investigate non-intersecting Brownian interfaces subject to a needle-like potential that could potentially be realized with the help of the tip of a Scanning Tunneling Microscope.

Let us conclude this outline and this list of results by saying that we hope this Thesis will properly portray the recent progress on the Kardar-Parisi-Zhang equation and will as well serve as a basis for a review on the associated literature.

Publications related to this Thesis

[1] A. Hartmann, A. Krajenbrink, P. Le Doussal, *Probing the large deviations of the Kardar-Parisi-Zhang equation with an importance sampling of directed polymers in random media.* arXiv:1909.03841, (2019).

[2] A. Krajenbrink, P. Le Doussal, *Replica Bethe Ansatz solution to the Kardar-Parisi-Zhang equation on the half-line.* arXiv:1905.05718, (2019).

[3] A. Krajenbrink, B. Lacroix-A-Chez-Toine, P. Le Doussal, *Distribution of Brownian coincidences.* J Stat Phys (2019) 177: 119, (2019).

[4] A. Krajenbrink, P. Le Doussal, *Linear statistics and pushed Coulomb gas at the edge of the β-random matrices: four paths to large deviations.* Europhysics Letters **125** 20009. Supplementary materials available at arXiv:1811.00509, (2018).

[5] A. Krajenbrink, P. Le Doussal, S. Prolhac, *Systematic time expansion for the Kardar-Parisi-Zhang equation, linear statistics of the GUE at the edge and trapped fermions.* Nuclear Physics B, **936** 239–305, (2018).

[6] A. Krajenbrink, P. Le. Doussal, *Large fluctuations of the KPZ equation in a half-space.* SciPost Phys. **5**, 032, (2018).

[7] I. Corwin, P. Ghosal, A Krajenbrink, P. Le Doussal, L-C Tsai, *Coulomb-Gas Electrostatics Controls Large Fluctuations of the Kardar-Parisi-Zhang Equation* Phys. Rev. Lett. **121**, 060201, (2018).

[8] A. Krajenbrink, P. Le Doussal, *Simple derivation of the $(-\lambda H)^{5/2}$ large deviation tail for the 1D KPZ equation*, J. Stat. Mech. 063210, (2018).

[9] A. Krajenbrink, P. Le Doussal, *Exact short-time height distribution in the one-dimensional Kardar-Parisi-Zhang equation with Brownian initial condition*, Phys. Rev. E **96**, 020102, (2017).

Index of notations and abbreviations

$\mathbb{R}_+$	Positive numbers: $[0, +\infty[$
$\mathbb{E}$	Expectation with respect to a random variable
$\overline{\cdots}$	Average over disorder
$\Theta(x)$	Heaviside Theta function
$\Gamma(x)$	Gamma function
$W(x)$	Lambert W function
$\mathrm{Ai}(x)$	Airy function
$\mathrm{Li}_s(x)$	Polylogarithm of order s
$\zeta(x)$	Riemann zeta function
$\mathrm{Erf}(x)$	Error function: $\mathrm{Erf}(x) = \frac{2}{\sqrt{\pi}} \int_0^z \mathrm{d}t\, e^{-t^2}$
$\mathrm{Erfc}(x)$	Complementary error function: $\mathrm{Erfc}(x) = 1 - \mathrm{Erf}(x)$
$(x)_+$	$\max(0, x)$
$⨍$	Cauchy principal value
Det	Determinant
Pf	Pfaffian

BB	Brownian Bridge
BM	Brownian Motion
DP	Directed Polymer
EW	Edwards-Wilkinson
GβE	Gaussian Beta Ensemble of Random Matrix Theory
GOE	Gaussian Orthogonal Ensemble
GUE	Gaussian Unitary Ensemble
GSE	Gaussian Symplectic Ensemble
JPDF	Joint Probability Distribution Function
KPZ	Kardar-Parisi-Zhang
MGF	Moment Generating Function
PDF	Probability Distribution Function
RBA	Replica Bethe Ansatz
RMT	Random Matrix Theory
SAO	Stochastic Airy Operator
SHE	Stochastic Heat Equation
TW	Tracy-Widom
WKB	Wentzel-Kramers-Brilloin
WNT	Weak Noise Theory

Part I

Introduction to the Kardar-Parisi-Zhang equation and elements of Random Matrix Theory

Abstract

In the first part of this Thesis, we will introduce the Kardar-Parisi-Zhang equation and explain why it is considered nowadays as a landmark to study systems driven out of equilibrium. In addition, we will present some elements of Random Matrix Theory and Large Deviation Theory required to fully understand the narrative behind the recent mathematical developments surrounding this equation such as its exact solutions and its intriguing connections with models of polymers and Brownian functionals. The pinnacle of this first part will be the presentation of a new solution to the Kardar-Parisi-Zhang on the half-line for the droplet initial condition in the presence of a wall at the origin.

Chapter 1

The Kardar-Parisi-Zhang equation

1.1 Birth of the model

Classifying physics in terms of critical phenomena is one of the great ambition of statistical physics [10]. The concept of universality classes embodies this idea as many unrelated systems such as liquid-vapor systems, magnets and binary liquid mixtures share the same critical behavior. One of the first theoretical manifestation of this notion arose from the work of Onsager on the two-dimensional Ising model [11] which predicted the existence of critical behavior far from the prediction of mean field theory. Later on, the concept of universality emerged again from the work of Wilson on the renormalization group [12], providing a practical way to classify critical phenomena. Nonetheless, most historical developments did concern systems at thermal equilibrium.

There has been a recent shift in statistical physics from systems at equilibrium towards systems out-of-equilibrium. The field of active matter, which consists in studying active agents consuming and spending energy to move such as flocks of birds [13], is one of the many concrete examples showing recent interest in such problems. In the context of out-of-equilibrium physics, a class of models called the Kardar-Parisi-Zhang (KPZ) universality class [14] is proposed as a potential candidate to represent a large class of models out-of-equilibrium. The KPZ universality class consists of a family of models representing the stochastic growth of interfaces. It is nowadays related to countless physical phenomena exhibiting non-equilibrium fluctuations such as directed polymers, stirred fluids and stochastic particle transport [15–20]. Quite intriguingly, this universality class in 1+1 dimensions was also connected these past years to integrable systems, both classical and quantum and to random matrix theory. The discovery of these connections triggered intense investigation of the properties of the models in this class on both theoretical and experimental sides.

The physics of stochastic interface growth has a rich history and an even richer scope of applications. It emerges for instance in the physics of molecular deposition or film growth [21] essential in the industry of semi-conductors, in the physics of slow combustion [22] or cell replication where one can be interested in the front evolution of cancer cell colonies [23] and also in the physics of population dynamics where one can be interested in the border delimiting two populations [24] or two phases having different stability as in the famous liquid crystal growth experiment of Takeuchi and Sano [25–31]. For all these phenomena, it has been observed and suggested that the interface fluctuations become larger and larger as time increases. This phenomenon, called the kinetic roughening [15], was largely observed in multiple situations and appears to be a universal feature of any surface growing with stochastic local interactions.

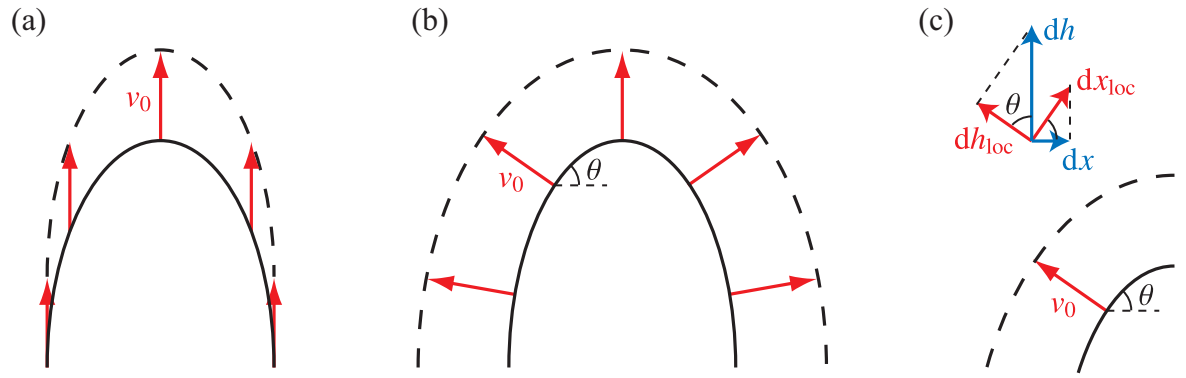

Figure 1.1: Interface growing according to the Edwards-Wilkinson equation, the noise is neglected for graphical purpose. **Left** (a) anisotropic growth along one direction. **Center** (b) isotropic growth along the local normal direction. **Right** (c) geometrical construction of local coordinates. Figure borrowed from Ref. [20] which was inspired from Ref. [15]

To investigate whether a common physics is hidden in all these systems, one should search for some universal feature. Similarly to systems at equilibrium, a feature of interest is scale invariance. For an interface parametrized by a function $h(x,t)$, a scale invariance implies that the statistical properties of the fluctuations $\delta h(x,t) = h(x,t) - \mathbb{E}[h(x,t)]$ are kept invariant under the transformation

$$x \to bx, \quad t \to b^z t, \quad \delta h \to b^\alpha \delta h, \tag{1.1.1}$$

The physics of these growing interfaces and of the kinetic roughening will therefore be described by the set of exponents $\{\alpha, z\}$.

Having in mind the idea of universality and of critical exponents, the natural exercise is to construct phenomenologically an equation driving a growing interface subject to external noise due for instance to heterogeneities. In this Thesis we will be interested in surfaces growing in one direction in space and one direction in time, thus we will build an equation in 1+1 dimensions. Under the usual symmetries: space-time translation, space inversion, rotation and height translation, the simplest diffusion equation in this setting is the heat equation with an additive white noise:

$$\partial_t h(x,t) = v_0 + \nu\, \partial_x^2 h(x,t) + \sqrt{D}\, \xi(x,t)\ . \tag{1.1.2}$$

This equation is the celebrated Edwards-Wilkinson equation [32]. This equation allows interfaces to grow as one can translate the height field by a linear drift term $h \to h + v_0 t$ to obtain a diffusion equation in the presence of a white noise. Here $\nu > 0$ denotes the strength of the diffusive relaxation which smoothens irregularities and $\xi(x,t)$ is a centered Gaussian white noise with $\mathbb{E}\left[\xi(x,t)\xi(x',t')\right] = \delta(x-x')\delta(t-t')$. This equation is also symmetric under height inversion $h \to -h$ which is unrealistic for many physical problems. Imposing an invariance of the Edwards-Wilkinson equation with respect to the rescaling (1.1.1) yields in $1+1$ dimensions the following values for the critical exponents

$$\alpha = \frac{1}{2}, \qquad z = 2. \tag{1.1.3}$$

These exponents are the landmark of the Edwards-Wilkinson universality class [32]. Moreover, it is possible to solve the Edwards-Wilkinson equation in Fourier space and show that the resulting height $h(x,t)$ has Gaussian fluctuations.

From microscopic considerations, the Edwards-Wilkinson equation assumes that the interface growth occurs solely along one direction, hence anisotropically, as we depict in Fig. 1.1 (a) which we borrowed from Ref. [20]. Physically we expect growth processes to be isotropic and the growth

direction to be along the local normal of the interface, therefore the Edwards-Wilkinson cannot describe globally the growth but rather locally in system of coordinates $(x_{\rm loc}, h_{\rm loc})$ defined by the local tangent and normal of the interface as seen in Fig. 1.1 (b)-(c). The transformation of local coordinates to global coordinates is obtained by considering the local slope of the interface $\tan\theta = |\partial_x h|$ as in Fig. 1.1 (b)-(c), then

$$\mathrm{d}h = \frac{\mathrm{d}h_{\rm loc}}{\cos\theta}, \qquad \mathrm{d}x = \mathrm{d}x_{\rm loc}\cos\theta\ . \tag{1.1.4}$$

Now, taking the Edwards-Wilkinson equation with the local variables $(x_{\rm loc}, h_{\rm loc})$ and inserting the global coordinates (x, h) leads at the lowest-order in $|\partial_x h|$ to the celebrated Kardar-Parisi-Zhang (KPZ) equation [14–19, 33].

$$\partial_t h(x,t) = \nu\,\partial_x^2 h(x,t) + \frac{\lambda_0}{2}\left(\partial_x h(x,t)\right)^2 + \sqrt{D}\,\xi(x,t)\ . \tag{1.1.5}$$

The reason to introduce a coefficient λ_0 in front of the non-linearity is because we only considered non-linearity arising from slope effects whereas in practical situations it can come from the interactions between different particles or other physics phenomena. In the rest of this Thesis, we shall consider the KPZ equation starting from a given initial condition $h(x, t = 0)$ and we shall use units of space, time and heights such that $\lambda_0 = D = 2$ and $\nu = 1$.

Remark 1.1.1. *This is equivalent to use everywhere the following units of space, time and heights*

$$x^* = \frac{2^3\nu^3}{D\lambda_0^2}, \quad t^* = \frac{2^6\nu^5}{D^2\lambda_0^4}, \quad h^* = \frac{2\nu}{\lambda_0}\ . \tag{1.1.6}$$

The addition of the non-linearity in the KPZ equation breaks the invariance under height inversion $h \to -h$, which is physically more acceptable for a growth process. In $1+1$ dimensions (one in space and one in time), the stationary distribution of the KPZ equation is known (and can be obtained from the related Fokker-Planck equation) as

$$P(\{h(x)\}) \sim \exp\left(-\frac{1}{2}\int_{\mathbb{R}} \mathrm{d}x (\partial_x h)^2\right) \tag{1.1.7}$$

This represents an interface with Brownian longitudinal fluctuations. In addition, the renormalization group and symmetry invariance arguments allow to obtain critical exponents [14, 33, 34] different from the ones of the Edwards-Wilkinson equation as

$$\alpha = \frac{1}{2}, \qquad z = \frac{3}{2}. \tag{1.1.8}$$

These exponents are the landmark of another universality class: the Kardar-Parisi-Zhang universality class [14, 35, 36]. They have also been probed experimentally and we refer the reader to Ref. [37] for a discussion on this matter. Let us for the moment provide some more background on this universality class before coming back to the KPZ equation.

1.2 Some elements around the KPZ universality class

The Kardar-Parisi-Zhang universality class in 1+1 dimensions includes a host of models [18, 38]: discrete versions of stochastic interface growth such as the polynuclear growth (PNG) model [39, 40], exclusion processes such as the totally asymmetric simple exclusion process (TASEP), the asymmetric simple exclusion process (ASEP) [41], the q-TASEP and other variants [42–45], discrete or semi-discrete [46–54] models of directed polymers, random walks in time dependent random media [55, 56], dimer models, random tilings, random permutations [57]. It also includes

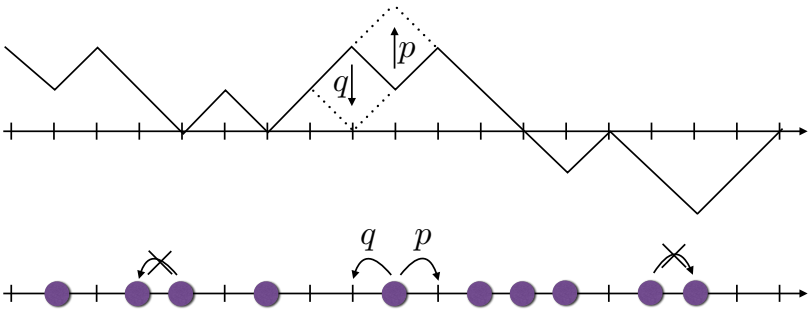

Figure 1.2: Pictorial representation of the mapping between the ASEP and an interface growth problem. Taken from Ref. [64]

the study of some correlation function in quantum condensates [58, 59]. A common aspect of all the models inside the KPZ class is that in the large-time limit the KPZ height field (which can be defined for all members of the class) fluctuates on the scale $t^{1/3}$ with t the time since the beginning of the growth. This universality extends beyond the scaling in time: the one point distribution of the height, when appropriately scaled, converges to a few number of universal distributions, most of them appear in random matrix theory, for instance the Tracy-Widom distributions for the largest eigenvalue of large Gaussian random matrices [60, 61]. We will extensively discuss this point in the rest of this Thesis. The distribution characterizing the fluctuations of the height at large times depends on some broad features of the initial condition [35, 62]. There has been recent progress in physics and mathematics in the study of the KPZ universality class, thanks to the discovery of exact solutions and the development of powerful methods to address stochastic integrability [63].

For completeness, let us describe in more details one of the models aforementioned: the ASEP. This is one of the models in non-equilibrium statistical physics that plays a central role in the exact studies of the KPZ equation. It is defined on a lattice with time $t > 0$ and coordinate $x \in \mathbb{Z}$ where each site it either occupied or empty. The particles on the lattice can hop to a neighboring site stochastically and independently, to the right at rate p and to the left at rate $q < p$, unless the new site is already occupied: this characterizes the exclusion. It turns out that the ASEP can be mapped to a model of interface growth, the so-called single-step model, by replacing the occupied and empty sites with downward and upward increments (see Fig. 1.2). Therefore the height increase $h(x,t) - h(x,0)$ is given by the total number of particles that went through the position x to the right during a time t. The work of Tracy-Widom in Ref. [44] on the ASEP was important to determine exact solutions to the Kardar-Parisi-Zhang equation 1+1 dimensions. The reason for that is that the KPZ equation is known to be linked to a certain asymmetric limit of ASEP, see Ref. [65]. Indeed, setting the hopping rates of ASEP as $p - q = \mathcal{O}(\sqrt{\epsilon})$ with $\epsilon \ll 1$, it was shown that $\sqrt{\epsilon} h(\lfloor x/\epsilon \rfloor, t/\epsilon^2)$ in the limit $\epsilon \to 0$ satisfies the KPZ equation. More generally it is conjectured that the KPZ equation itself is the universal scaling limit of weakly asymmetric growth models in $1+1$ dimensions, this is illustrated by the notion of weak asymmetry universality [36].

To conclude this Section, let us understand the following fundamental property of the KPZ equation which states that its dynamics describes the trajectory in the space of models from the Edwards-Wilkinson fixed point to the Kardar-Parisi-Zhang fixed point. To understand this, we come back to the dimensional analysis for the KPZ equation, if $h(x,t)$ solves the KPZ equation then the rescaled field

$$\tilde{h}(\tilde{x}, \tilde{t}) := b^{-\alpha} h(x = b\tilde{x}, t = b^z \tilde{t}) \tag{1.2.1}$$

solves the rescaled equation (dropping the tildes)

$$\partial_t h(x,t) = b^{z-2}\partial_x^2 h(x,t) + b^{\alpha+z-2}(\partial_x h(x,t))^2 + b^{(z-2\alpha-1)/2}\sqrt{2}\xi(x,t). \tag{1.2.2}$$

By comparing the diffusion and the non-linearity terms for small and large b, since the exponents z and α are positive, it is clear that the non-linearity is irrelevant at short time while the diffusion part of the equation is irrelevant at large time. From the point of view of renormalization group, these two terms dictate the value of the critical exponents $\{\alpha, z\}$, hence the relative relevance of the two terms at short and large times indicates that the dynamics of the KPZ equation describes the flow from the Edwards-Wilkinson fixed point (irrelevance of the non-linearity) [32] towards the Kardar-Parisi-Zhang fixed point (irrelevance of the diffusion) [35].

1.3 Some mappings of the KPZ equation

Let us now come back to the KPZ equation (1.1.5) and discuss some of its properties. It enjoys a special Galilean invariance called the statistical tilt symmetry. For a given realization of the white noise $\xi(x,t)$, if $h(x,t)$ is a solution of the KPZ equation, then

$$h_v(x,t) = h(x-vt,t) - vx + \frac{1}{2}v^2 t, \tag{1.3.1}$$

is a solution of the KPZ equation in the noise $\xi_v(x,t) = \xi(x-vt,t)$. What is more, the quantity $u(x,t) = \partial_x h(x,t)$ solves the equation

$$\partial_t u(x,t) = \partial_x^2 u(x,t) + 2u(x,t)\partial_x u(x,t) + \sqrt{2}\partial_x \xi(x,t). \tag{1.3.2}$$

This is the Burgers's equation for a randomly forced fluid, much studied in the literature in the context of turbulence: $u(x,t)$ is interpreted as the velocity field of a one-dimensional fluid, see Ref. [66]. In this framework the Galilean symmetry reads $u_v(x,t) = u(x-vt,t) - v$.

The most important mapping of the KPZ equation is not on Burger's equation but rather to another stochastic process driven by the so-called Stochastic Heat Equation (SHE) which we now present. The Cole-Hopf mapping of the Kardar-Parisi-Zhang equation consists in defining the following change of variable

$$Z(x,t) = \exp(h(x,t)) \tag{1.3.3}$$

so that $Z(x,t)$ which we will call the partition sum verifies in the Ito prescription the celebrated Stochastic Heat Equation[1]:

$$\partial_t Z(x,t) = \partial_x^2 Z(x,t) + \sqrt{2\bar{c}}\,\xi(x,t)Z(x,t)\ . \tag{1.3.4}$$

There has been an important amount of work undertaken to properly define mathematically the KPZ equation which lead to the development of the theory of rough paths and regularity structures [17].

Remark 1.3.1. *The SHE can either be considered on the full-line, i.e. $x \in \mathbb{R}$ or on the half-line $x \in \mathbb{R}_+$, in which case one generally imposes at all times a Robin boundary condition at the origin $\partial_x Z(x,t)\,|_{x=0} = AZ(0,t)$. In terms of the KPZ equation, this corresponds to fixing the slope of the height at the origin, i.e. $\partial_x h(x,t)\,|_{x=0} = A$.*

[1] Note that we have inserted an extra factor $\bar{c}$ in the partition function for later purpose which amounts to choose a system of units such that $D = 2\bar{c}$. At the very end of the calculation, we will set $\bar{c}$ back to unity.

As a first comment on this equation, let us observe that we have traded the KPZ equation which is non-linear with an additive noise with the SHE which is linear but has a multiplicative noise viewed as a source term. Secondly, from the point of view of stochastic differential equations, let us note that the Cole-Hopf mapping is non-trivial as its validity depends on whether the solution to the SHE remains positive at all times. Fortunately, the partition sum is almost surely strictly positive at all times as proved by Mueller in Ref. [67]. See also Refs. [68, 69] for more recent developments.

One of the most remarkable properties of the SHE is that its solution, the partition sum, can be seen as the partition function of a directed polymer in a random medium. Indeed, consider an elastic polymer of length t and fixed endpoints x_0 and y, in a random potential $\xi(x,t)$ which partition function is given by

$$\mathcal{Z}(y,x_0,t) = \int_{x(0)=x_0}^{x(t)=y} \mathcal{D}x(\tau) e^{-\int_0^t \left[\frac{\dot{x}(\tau)^2}{4} + \sqrt{2c}\,\xi(x(\tau),\tau)\right] \mathrm{d}\tau}. \tag{1.3.5}$$

By the standard Feynman-Kăc path integral argument, $Z(x,t) = \mathcal{Z}(y,x_0,t)$ solves the SHE under the initial condition $Z(x,0) = \delta(x-x_0)$. Furthermore, the first endpoint of the polymer x_0 can be chosen to have a distribution over the real line with a probability density $Z(x,0) = e^{h(x,0)}$ in which case the full solution to the SHE with initial condition $Z(x,0)$ reads

$$Z(x,t) = \int_{\mathbb{R}} \mathrm{d}x_0 Z(x_0,0)\mathcal{Z}(y,x_0,t). \tag{1.3.6}$$

Historically, since the KPZ equation is non-linear, it has been extremely hard to extract quantitative information from it. There has been controversy on the solvability of the equation to the point where Barabàsi and Stanley stated at the beginning of the Chapter 6 of Ref. [70] that *"the KPZ equation cannot be solved in closed form due to its nonlinear character"*. As we shall see in the rest of this Thesis, this statement is nevertheless wrong.

Indeed, recently exact solutions have also been obtained for the KPZ equation at all times for various initial conditions [2, 71–80]: this was achieved by various routes. First by studying scaling limits of solvable discrete models [18, 43, 80], which allowed for rigorous treatments. The second on which we will elaborate longer, pioneered by Kardar [81], is non-rigorous, but leads to a more direct solution: it starts from the directed polymer formulation, uses the so-called replica method together with a mapping to the attractive delta-Bose gas, or Lieb-Liniger model, which is then studied using the Bethe ansatz, nowadays denoted the replica Bethe ansatz (RBA) method. More recently, Borodin and Corwin introduced the Macdonald process to account for the integrable structure of many discrete and continuous models [42, 82]. They also developed the study of stochastic vertex models.

1.4 The Replica Bethe Ansatz

Let us describe in more details the approach initiated by Kardar. From the Cole-Hopf mapping, we now know that the solution of the KPZ equation can be mapped to the SHE which is linear, hence easier to manipulate. The quantities of interest for us in the SHE will be the moments of the solution $Z(x,t)$. As the SHE has been obtained under the Ito prescription the first moment of the solution, i.e. the expected value $\mathbb{E}_{\mathrm{KPZ}}[Z(x,t)]$, verifies the standard heat equation. Regarding the higher moments, we will firstly define the N-point correlation function at equal time of the solution to the SHE

$$\Psi(x_1,\ldots,x_N,t) = \mathbb{E}_{\mathrm{KPZ}}\left[Z(x_1,t)\ldots Z(x_N,t)\right]. \tag{1.4.1}$$

Since we study N copies of the solution to the SHE, we call this object the replica. Since the correlator of the noise is $\mathbb{E}\left[\xi(x,t)\xi(x',t')\right] = \delta(x-x')\delta(t-t')$, standard Ito manipulations show that the replica verifies a Schrödinger equation which is the celebrated delta Bose gas, or Lieb-Liniger model [83]

$$\partial_t \Psi(x_1,\dots,x_N,t) = -\hat{\mathcal{H}}_N \Psi(x_1,\dots,x_N,t), \tag{1.4.2}$$

where the Lieb-Liniger Hamiltonian is given as

$$\hat{\mathcal{H}}_N = -\sum_{j=1}^{N} \frac{\partial^2}{\partial x_j^2} - 2\bar{c} \sum_{1\leqslant i<j\leqslant N} \delta(x_i - x_j). \tag{1.4.3}$$

The definition of the replica is fully symmetric by the exchange of positions $\{x_i \leftrightarrow x_j\}$, or equivalently by exchange of the copies of the SHE solution, therefore the quantum mechanical problem will describe bosons with contact interactions. For $\bar{c} < 0$ the model is a repulsive one while for $\bar{c} > 0$ it is attractive which corresponds to the physics of the Kardar-Parisi-Zhang equation. The precise boundary conditions are such that

1. if the model is considered on a full-line, we shall impose a periodic boundary condition at $x = 0$ and $x = L$ and the real line will be considered by the limit $L \to +\infty$.

2. if the model is considered on a half-line, the variables $\{x_j\}$ will take value on $[0, L]$ and the wavefunctions Ψ will verify a Robin boundary condition at the origin

$$\forall t > 0, \forall i \in [1,N], \qquad \partial_{x_i} \Psi(x_1,\dots,x_N,t)_{x_i=0} = A\Psi(x_1,\dots,x_N,t)_{x_i=0} \tag{1.4.4}$$

   Another boundary condition should be imposed at $x = L$ to define the problem properly. In practice, as we will be interested in the limit $L \to +\infty$ this boundary can be chosen arbitrarily and we will decide to choose a hard-wall, i.e. $A = +\infty$ at $x = L$.

The Lieb-Liniger is integrable on the full-line and its energy spectrum and eigenfunctions were obtained long ago using the Bethe ansatz [83] which is a generalization of single particle plane waves to N particles. It is an interesting model for quantum gases which has received a revived interest from experimental realizations in dilute cold atomic gases [84]. Its properties have been studied in non-equilibrium and equilibrium both theoretically and experimentally, and are quite different in the attractive case $\bar{c} > 0$ and the repulsive case $\bar{c} < 0$.

In the repulsive case, a proper fixed-density thermodynamic limit exists, and the bosons form a one-dimensional super-fluid with quasi long-range order, a sea with particle-hole excitations, and collective modes [83] well described at low energy by the bosonisation (i.e. Luttinger liquid) theory [85]. In the attractive case, relevant to analyze the Kardar-Parisi-Zhang, the ground state is a bound state of all the N bosons, and the excitations are obtained by splitting it into a collection of quasi-independent, smaller bound states, which behave almost as free particles, called string states [86]. The dynamical correlations have been studied in [87, 88]. It is an interesting strongly correlated model [89] with nontrivial bound states, also observed in experiments [90, 91]. Recently its non-equilibrium properties have received a large attention, in particular after a quantum quench [92–94].

Quite interestingly for the KPZ equation, the delta Bose gas is integrable both on the full-line and on the half-line. In the latter case, we refer the readers to the following references [95–97] (see also section 5.1 of [98]) for the Dirichlet boundary condition (i.e. $A = +\infty$) and for arbitrary A, we refer to the following extensive list of references [79, 98–103].

Having in mind the properties of the Lieb-Liniger model, one can formally express the solution to delta Bose gas as

$$\mathbb{E}_{\mathrm{KPZ}}\left[Z(x_1,t)\dots Z(x_N,t)\right] = \langle x_1\dots x_N|e^{-t\hat{\mathcal{H}}_N}|\Psi(t=0)\rangle. \tag{1.4.5}$$

The initial state for the Lieb-Liniger model is denoted

$$\mathbb{E}_{\mathrm{KPZ}}\left[Z(x_1,t=0)\dots Z(x_N,t=0)\right] = \langle x_1\dots x_N|\Psi(t=0)\rangle. \tag{1.4.6}$$

As this initial state corresponds to the initial condition of the SHE, we must take the initial state $|\Psi(t=0)\rangle$ as

$$\langle x_1\dots x_N|\Psi(t=0)\rangle = \Phi_0(x_1,\dots,x_N) := \prod_{j=1}^{N} Z(z_j,0) \tag{1.4.7}$$

Let us note nonetheless that this is valid solely for deterministic initial conditions and we will present later on in this Thesis an extension to random initial conditions for the KPZ equation.

To obtain the N-th moment of the solution to the SHE $Z(x,t)$, one can now take the position of all N-replica to coincide to some value x and use the spectral decomposition of the evolution operator $e^{-t\hat{\mathcal{H}}_N}$ in terms of the eigenstates of the Lieb-Liniger Hamiltonian $\hat{\mathcal{H}}_N$ as

$$\mathbb{E}_{\mathrm{KPZ}}\left[Z(x,t)^N\right] = \sum_{\mu} \Psi_\mu(x,\dots,x)\langle\Psi_\mu|\Phi_0\rangle \frac{1}{||\mu||^2} e^{-tE_\mu} \tag{1.4.8}$$

Here the un-normalized eigenfunctions of $\hat{\mathcal{H}}_n$ are denoted Ψ_μ (of norm denoted $||\mu||$) with eigenenergies E_μ. Since only symmetric eigenstates contribute (as the initial and final states are fully symmetric in the x_i), the $\sum_\mu$ denotes a sum over all bosonic eigenstates of the Lieb-Liniger model, and $\langle\Psi_\mu|\Phi_0\rangle$ denotes the overlap, i.e. the Hermitian scalar product of the initial state with the eigenstate Ψ_μ. Assuming that the moments $\mathbb{E}_{\mathrm{KPZ}}\left[Z(x,t)^N\right]$ have been calculated for all integer N, the final step of the RBA method consists in the summation of these moments to obtain the generating function of the solution to the SHE, of equivalently the generating function of the exponential of the KPZ height

$$g(\varsigma) = \mathbb{E}_{\mathrm{KPZ}}\left[\exp(-\varsigma e^{h(x,t)})\right] = \mathbb{E}_{\mathrm{KPZ}}\left[\exp(-\varsigma Z(x,t))\right] = 1 + \sum_{N=1}^{\infty} \frac{(-\varsigma)^N}{N!}\mathbb{E}_{\mathrm{KPZ}}\left[Z(t)^N\right] . \tag{1.4.9}$$

Remark 1.4.1. *The RBA was said earlier to be non-rigorous. One of the reasons is that the formal series (1.4.9) does not converge in general, but there exist tricks such as the Mellin-Barnes summation formula, Lemma 3.5.3, allowing to give a meaning to the series.*

In practice, an important question is to determine the probability distribution function (PDF) for the height at one point, $h(0,t)$, given an initial condition $h(x,t=0)$. Remarkably, for all initial conditions that were solved, the generating function (1.4.9) can always be expressed in terms of algebraic objects called Fredholm determinants and Fredholm Pfaffians which are common objects in Random Matrix Theory [104,105] representing expectation values over determinantal and Pfaffian point processes. From these, it was shown that in the large-time limit the shifted height $H(t) = h(0,t) + \frac{t}{12}$ has fluctuations of magnitude $t^{1/3}$ as predicted from the KPZ universality class and they are described by the celebrated Tracy-Widom distributions [60,61], i.e. the distributions of the largest eigenvalues of standard Gaussian random matrix ensembles [104, 105]. Quite surprisingly, some of these Fredholm determinants are also related to the physics of trapped fermions at finite temperature in quantum mechanics [106] where the temperature T of the fermions is related to the time t of the KPZ dynamics as $T \propto t^{-1/3}$.

1.5 The full-space problem

For the rest of this Chapter, let us introduce and discuss some initial conditions of the Kardar-Parisi-Zhang equation. In this Section we shall focus on the full-space problem and after that we shall turn to the half-space one. One of the most general initial condition studied so far for the Kardar-Parisi-Zhang equation in full-space is the following:

$$h(x,t=0) = \begin{cases} w_L x + \sigma_L B_L(-x) & x \leqslant 0, \\ -w_R x + \sigma_R B_R(x) & x \geqslant 0. \end{cases} \tag{1.5.1}$$

where B_L and B_R are independent one-sided unit Brownian motions with $B_L(0) = B_R(0) = 0$. The two point correlators are given by $\mathbb{E}\left[B_R(x)B_R(x')\right] = \min(x,x')$. The parameters w_L and w_R measure the slope of the initial profile on each side of zero and the parameters σ_L and σ_R describe the variance of the randomness on each side of zero. At the time of completion of this manuscript, all solvable cases of the Kardar-Parisi-Zhang equation in full-space can be considered by choosing the parameters σ_L and σ_R in $\{0,1\}^2$. Indeed, the list of solvable cases are the following:

1. The wedge initial condition where we choose $\sigma_R = \sigma_L = 0$. In this case, *(i)* $w_L = w_R = \omega \to \infty$ describes the droplet initial condition, *(ii)* $w_L = \infty$, $w_R = 0$ (resp. $w_R = \infty$ and $w_L = 0$), describes the half-flat initial condition and *(iii)* $w_L = w_R = 0$ describes the flat initial condition. Taking $w_L = w_R = \omega$ enables to study a cross-over between the flat and droplet initial condition.

2. The Brownian initial condition where we choose $\sigma_L = \sigma_R = 1$. In this case, $w_L = w_R = 0$ describes the stationary initial condition. Taking $w_L = w_R = w$ enables to study a cross-over between the stationary and droplet initial condition.

3. The Flat-Brownian initial condition where we choose $\sigma_L = 0$. Taking $w_L \to \infty$ describes the half-Brownian and taking $w_R \to \infty$ describes the half-flat. Note that by symmetry we can study a symmetric situation with $L \leftrightarrow R$.

As indicated during the introduction to the Replica Bethe Ansatz method, the generating function of the solution to the KPZ equation can be expressed in terms of Fredholm determinants which provide a direct connection between random matrix ensembles and the KPZ equation. Anticipating the rest of this Thesis, the droplet initial condition is related to the Tracy-Widom distribution for the Gaussian Unitary Ensemble (GUE), the flat initial condition to the Tracy-Widom distribution for the Gaussian Orthogonal Ensemble (GOE) and the stationary initial condition to the so-called Baik Rains distribution.

The full-space problem with droplet initial condition was originally the first one to be solved exactly. Although the KPZ equation appeared in 1986, its first solution appeared in 2010 highlighting its complexity and the effort engaged both in the physics and mathematics community. In addition, recent impressive experiments on liquid crystals from Takeuchi and Sano have been able to validate the large-time random matrix statistics of the KPZ height fluctuation [25–30].

1.6 The half-space problem

Although most of these results have been obtained on the full space, it is interesting for applications to study also half-space models, e.g. defined only on the half line $x \in \mathbb{R}_+$. Recently indeed experiments were able to access the half-space geometries [31]. Moreover there are strong theoretical motivations since integrability properties are sometimes preserved by going to the half-space, with the proper boundary conditions. Progress started with discrete models, notably

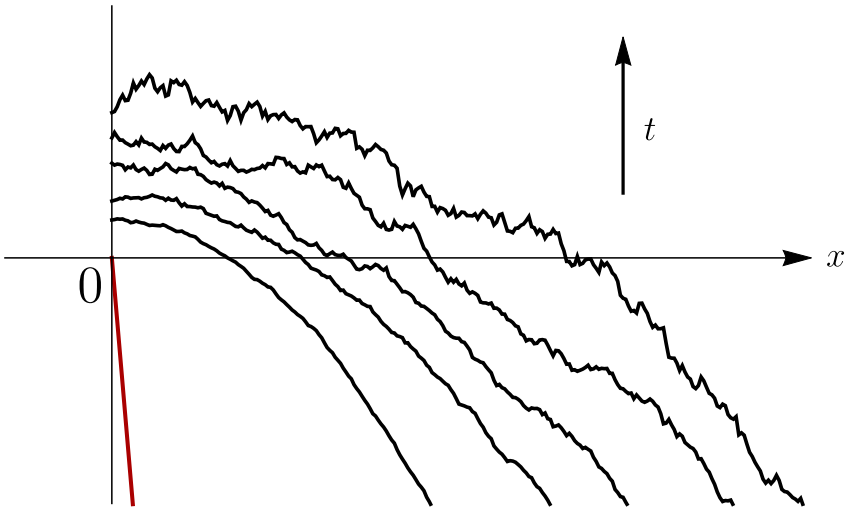

Figure 1.3: Representation of the time evolution of the KPZ height $h(x,t)$ (black lines) at different times from the droplet initial condition (red line) and with a wall at the origin. We here consider the fluctuations of the height $h(x,t)$ next to the wall. Courtesy of J. De Nardis in Ref. [112].

in mathematics. Indeed, the half-space problem has been addressed for some models in the KPZ universality class. In a pioneering paper, Baik and Rains [107] studied the longest increasing sub-sequences (LIS) of *symmetrized* random permutations which maps to a discrete zero temperature model of a directed polymer in a half-space, with a tunable parameter α which makes the boundary more attractive as α increases. They found, in the limit of large polymer length t, a transition when α reaches the critical value $\alpha_c = 1$. For $\alpha < \alpha_c$ the PDF of the fluctuations of the directed polymer energy is given by the Tracy-Widom distribution for the Gaussian Symplectic Ensemble (GSE) of random matrices [61] on the characteristic KPZ scale $t^{1/3}$. For $\alpha > \alpha_c$ the PDF is Gaussian on the scale $t^{1/2}$, as the directed polymer paths are bound to the diagonal line. At the critical point, $\alpha = \alpha_c$ the PDF is given by the GOE Tracy-Widom distribution on the $t^{1/3}$ scale. A similar transition was found for the height distribution in the discrete PNG growth model on a half-line, with a source at the origin, as the nucleation rate at the origin is increased above a threshold [108]. Finally, some results were also obtained for the TASEP in a half-space [45] and for the (finite temperature) log-gamma DP with symmetric weights [109, 110] and in half-quadrant geometries [111].

For the coming presentation of the KPZ equation on a half-line, we will borrow some elements from Ref. [112]. The KPZ equation (1.1.5) on the half-line considers the space variable $x \in \mathbb{R}^+$ along with a Neumann boundary condition (b.c.)

$$\forall t > 0, \quad \partial_x h(x,t) \,|_{x=0} = A \quad \Leftrightarrow \quad (\partial_x - A) Z(x,t) \,|_{x=0} = 0. \tag{1.6.1}$$

A is a real parameter which describes the interaction with the boundary (a wall at $x = 0$). The wall is repulsive for $A > 0$ and attractive for $A < 0$, in addition the case $A = +\infty$ imposes $Z(x = 0, t) = 0$, i.e. an infinitely repulsive or absorbing wall. On the contrary, $A = 0$ is seen as a reflecting wall. For the half-space problem, we need in addition to regularize the initial condition when it is not properly defined at $x = 0$, as it is the case for a hard-wall with boundary coefficient $A = +\infty$. In this case, the droplet initial condition for instance reads

$$h(x, t = 0) = -\frac{|x - \kappa|}{\eta} - \log \eta \quad , \quad \eta \to 0^+ \quad \Leftrightarrow \quad Z(x, t = 0) = \delta(x - \kappa) \, . \tag{1.6.2}$$

Historically the height at the origin $H(t)$ was studied. For finite A it reads $H(t) = h(\kappa = 0, t) + \frac{t}{12}$ and for $A = +\infty$ it reads $H(t) = h(\kappa, t) - \log \kappa + \frac{t}{12}$ with $\kappa \to 0^+$ since a regularization is needed.

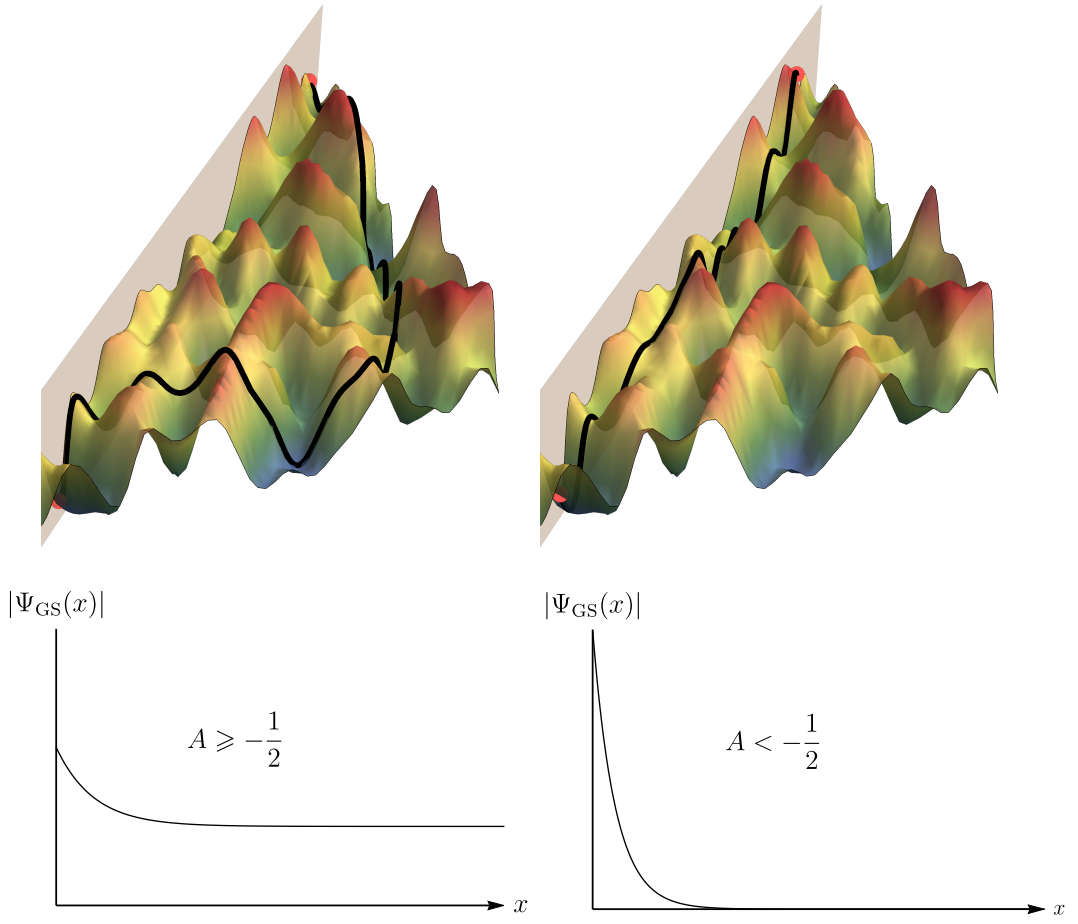

Figure 1.4: Top. The directed polymer in random environment with a wall on the left and fixed endpoints along the wall. The attraction to the wall is parametrized by the parameter A. At $A = -1/2$ there is a phase transition, for $A < -1/2$ the polymer spends most of the next to the wall, while at $A \geqslant -1/2$ the polymer is unpinned. Depending on the value of A, the statistics of the fluctuations of the corresponding free energy, equivalent to the KPZ height, changes from Gaussian ($A < -1/2$), to GOE Tracy-Widom ($A = -1/2$) and GSE Tracy-Widom ($A > -1/2$). **Bottom**. The same transition is observed for the ground state eigenstate of the attractive Lieb-Liniger model for bosons on the half-line (the wall is at the left of the origin). The wave function changes from being delocalized ($A \geqslant -1/2$) to being localized at the boundary ($A < -1/2$) where all particles are bounded to the wall. Courtesy of J. De Nardis in Ref. [112].

The time evolution of the KPZ height from the droplet initial condition in a half-space then resembles Fig. 1.3.

The half-space problem was considered by Kardar in Ref. [113] in the equivalent representation in terms of a directed polymer in a half space bounded by a wall. A binding transition to the wall, that was termed *depinning by quenched randomness*, was predicted for $A = -1/2$ from heuristic considerations on the ground state of the delta Bose gas in the presence of a wall. The phase transition, which we represent in Fig. 1.4, separates a phase where the directed polymer is bound to the wall for $A < -\frac{1}{2}$ to an unbound phase for $A \geqslant -\frac{1}{2}$, as the attraction to the wall is decreased. Numerical studies also addressed the half-line problem: the convergence to the GSE was explored [31] in a half-space geometry aiming to open the way for an experimental confirmation. In addition, connections to conductance fluctuations in Anderson localization were explored [114].

More recently, exact solutions to the KPZ equation were obtained for three specific values of A, i.e. $A = +\infty, 0, -1/2$ [71, 79, 80] for the droplet initial condition. In all three cases the

solution can be expressed in terms of a Fredholm Pfaffian [6, 71, 79, 80]. For $A = +\infty$, the infinitely repulsive wall, it was found [71] that the PDF of the scaled height, $H(t)/t^{1/3}$, converges at large t to the GSE Tracy-Widom distribution [61, 104, 105]. For $A = 0$, it was also found that the large-time limit of the PDF corresponds to the GSE Tracy-Widom distribution [79]. Both cases used the mapping to the delta Bose gas, with use of respectively the RBA for $A = +\infty$ and nested contour integral representations of the moments for $A = 0$. The critical case $A = -\frac{1}{2}$ was solved instead using a continuum limit from the ASEP model with an open boundary [80, 115]. It was found that at large time the PDF converges to the GOE Tracy-Widom distribution which thus describes the large-time behavior at the transition.

It is natural to conjecture that the transition for the KPZ equation at $A = -1/2$ is in the same universality class, in the large-time limit, as the one discovered by Baik and Rains in [107] and that this universality is common to the full KPZ universality class, see Ref. [115]. Baik and Rains performed a detailed analysis on a scale $\alpha - 1 = wt^{-1/3}$ around the transition. They found that the PDF depends continously on w and interpolates between the GSE/GOE/Gaussian distributions as w is increased. This transition PDF was obtained as a solution of Painlevé type system of equations. Further results were obtained recently using Pfaffian-Schur processes, for variants of TASEP models and last passage percolation in a half-quadrant [116, 117]. Not only the one-point, but also the multi-point height distributions were studied and for arbitrary positions with respect to the wall. A Fredholm Pfaffian was obtained with an explicit expression around the GSE/GOE/Gaussian transition, hence we may conjecture that it is compatible with the Painlevé system of [107].

1.7 Cross-over between fixed points of the KPZ equation

So far we have explored the Kardar-Parisi-Zhang universality class but it is in fact possible to go beyond and to define subclasses of universality in terms of initial or boundary conditions. As a concrete example, let us recall that for the KPZ equation in a half-space, we discussed the fact that the Robin boundary condition A controls the statistics of the fluctuations of the one-point KPZ height at large time. Therefore, varying this parameter allows to realize a cross-over between different large-time distributions, also seen as basin of attraction of the dynamics.

More generally, for the family of initial conditions previously introduced, it is possible to define by dimensional analysis other cross-over, or relevant, parameters [2, 6, 118, 119]. Indeed, the slope of the wedge initial condition or the drift of the Brownian initial condition play a cross-over role both at short time and at large time in terms of the distribution of the solution to the KPZ equation. We represent in Table 1.1 the relevant parameters at short time and at large time found in the literature describing various cross-overs and indicate explicitly the related interpolation at large time. The cross-overs are realized when the relevant parameter is increased from 0 to $+\infty$.

This Table has to be understood in the following way:

- At short time, all boundary conditions with finite A will behave as the reflecting wall $A = 0$. All initial conditions with finite w or ω will behave as the stationary initial condition $w = 0$ or the flat initial condition $\omega = 0$. The singular cases will be the hard-wall $A = +\infty$ and the droplet initial condition $w = \tilde{w} = +\infty$.

- At late time, all boundary conditions with $A > -1/2$ will behave as the hard-wall $A = +\infty$. All initial conditions with finite w or ω will behave as the droplet initial condition. The

singular cases will be the critical wall $A = -1/2$, the stationary initial condition $w = 0$ and the flat initial condition $\omega = 0$.

Crossover parameter	Short time	Large time	large-time crossover
Robin boundary condition in half-space with droplet initial condition			
A	$\tilde{A} = A\sqrt{t}$	$\bar{A} = (A + \frac{1}{2})t^{1/3}$	GOE $\leftrightarrow$ GSE
Brownian initial condition with variance 1 and drift			
w	$\tilde{w} = w\sqrt{t}$	$\bar{w} = wt^{1/3}$	GUE $\leftrightarrow$ Baik Rains
Wedge initial condition with slope			
ω	$\tilde{\omega} = \omega\sqrt{t}$	$\bar{\omega} = \omega t^{1/3}$	GUE $\leftrightarrow$ GOE

Table 1.1: Table of parameters in the KPZ equation controlling a cross-over between Random Matrix Ensembles. All relevant parameters are supposed to be positive and the cross-over occurs between the value at 0 and at $+\infty$.

This leads us to define new fixed points in terms of initial conditions:

- For the full-space problem, the fixed points for both short and large times are the droplet giving the GUE TW at late time, the stationary giving the Baik Rains distribution at late time and the flat initial condition giving the GOE TW at late time.
- For the half-space problem, the short-time fixed points are the reflecting wall ($A = 0$) and the hard-wall ($A = +\infty$). At large time, they are the critical wall ($A = -1/2$) giving the GOE Tracy-Widom distribution and the hard-wall ($A = +\infty$) giving the GSE Tracy-Widom distribution.

These cross-overs have been studied at the origin $x = 0$, it would be interesting to obtain a complete phase diagrams of the various cross-overs taking into account the position of the KPZ height. Physically, if we probe the KPZ height far from the origin in a half-space, we expect that the boundary condition at the origin to become more and more irrelevant, hence there can additionally exist cross-overs between full-space and half-space distributions.

Chapter 2

Elements of Random Matrix Theory

Random Matrix Theory [104, 105, 120, 121] was first introduced by Eugene Wigner in the context of nuclear physics. He proposed to model the statistical properties of the spectrum (eigenvalues) of the nuclei Hamiltonian by a random matrix, hence considering the nuclei as a black box whose constituting elements interact randomly. Since Wigner, this theory has been proven fruitful in many contexts: statistics and finance [122], disordered systems, non-intersecting random walks [123], trapped fermions [106, 124–130], lattice quantum chromodynamics (QCD), string theory [131, 132], number theory, Anderson localization [133], quantum chaos, transport and entanglement [134–138] and much more.

From the point of view of Number Theory, the Riemann zeta function and its generalizations the L-functions are intimately related both to the distribution of prime numbers and to Random Matrix Theory [139–143]. The celebrated Riemann hypothesis states that all non-trivial zeros of zeta lie on a critical axis of real part equal to one-half. Many theorems and conjecture nowadays state or imply that the unfolded zeros of zeta have the same statistical properties as the eigenvalues of a random matrix of large size.

In physics, one of the applications of random matrices lies in the field of disordered systems (for instance spin glasses) where a defect or an impurity is modeled by a random potential [144–149]. For this class of model, this naturally leads to the notion of random energy landscape in which the stability of stationary points is described by the Hessian of the random potential which is a random matrix by essence.

Quite surprisingly, Random Matrix Theory has also found applications in the context of non-intersecting random walks, see Ref. [150] for an extensive review on this topic. These connections are in some sense an implication of the seminal work of Karlin and McGregor [151]. It has been showed that in this model, the joint distribution of the position of the random walkers is exactly the distribution of the eigenvalues of a random matrix [152].

More recently, random matrices have appeared in the context of the Kardar-Parisi-Zhang equation and its universality class in a quite profound way. The investigation of this connection is a major part of this Thesis. To that aim, we shall now introduce the Gaussian ensemble of random matrices which we will extensively use throughout this Thesis.

2.1 Gaussian β matrices

In this Thesis, we will focus solely on the Gaussian β ensemble (GβE) of random matrices [104]. To this aim, we consider a matrix of size $N \times N$ such that its eigenvalues are real and labeled $\{\lambda_i\}$, and such that their joint probability distribution function (JPDF) has the form

$$P[\{\lambda_i\}] \propto \exp\left(\beta \sum_{1 \leqslant i < j \leqslant N} \log|\lambda_i - \lambda_j| - \frac{\beta N}{4} \sum_{i=1}^{N} \lambda_i^2\right). \tag{2.1.1}$$

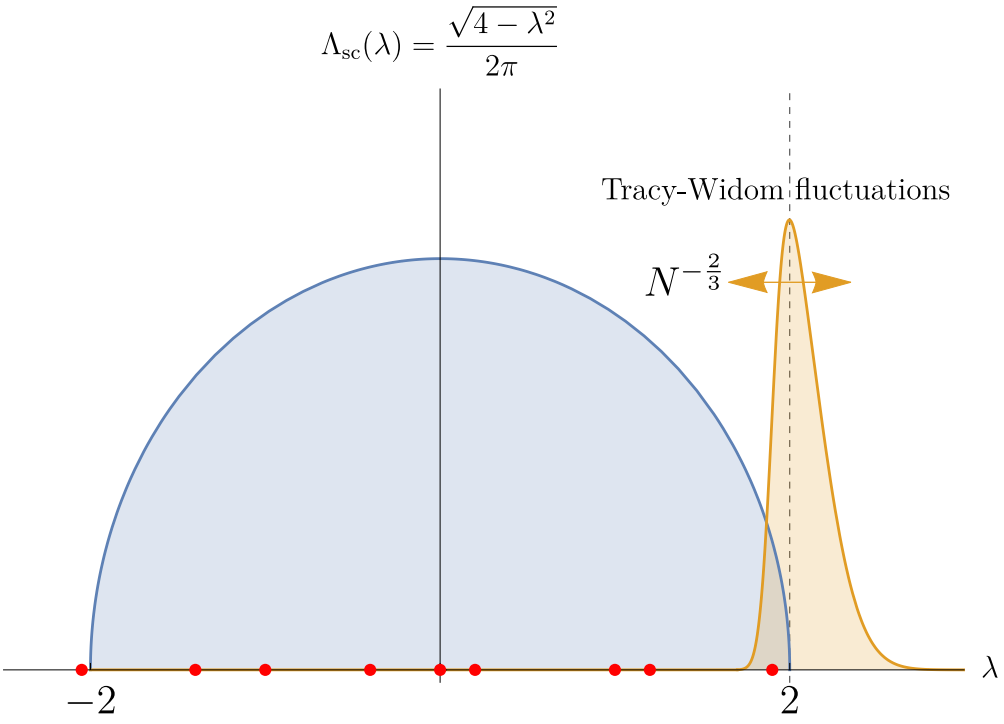

Figure 2.1: Representation of Wigner semi-circle distribution (blue line) with support $[-2, 2]$ for a random matrix of size $N \times N$ in the limit of large N and the Tracy-Widom distributions arising at the edge on a scale $N^{-2/3}$.

Let us first comment on the fact that the Gaussian weight in Eq. (2.1.1) is the reason for the name of the ensemble. The logarithmic contribution of the JPDF also takes the form of a Vandermonde factor $\prod_{i<j}|\lambda_i - \lambda_j|^\beta$, inducing a strong correlation between the eigenvalues. Under our conventions, in the large N limit the empirical measure $\Lambda_N(\lambda) := N^{-1}\sum_{i=1}^N \delta_{\lambda_i}(\lambda)$ converges to the celebrated Wigner semi-circle distribution [104] with density $\Lambda_{\rm sc}(\lambda) = \frac{1}{2\pi}\sqrt{4-\lambda^2}\mathbb{1}_{\{|\lambda|<2\}}$ which we represent in Fig. 2.1.

Historically, matrix representations for the GβE were obtained solely for $\beta = 1, 2, 4$ and are referred to as the orthogonal (GOE), unitary (GUE) and symplectic (GSE) ensembles (due to a conjugacy symmetry of the matrix leaving the spectrum invariant) [104]. For completeness of this introduction, let us describe the construction of a GOE matrix. Denote M the $N \times N$ real symmetric matrix whose entries above the diagonal are independent random Gaussian variables with mean zero and variance

$$\mathbb{E}\left[M_{ij}^2\right] = \frac{1+\delta_{ij}}{N}. \tag{2.1.2}$$

Then the probability measure of M is given, up to normalization, by

$$P(M) \propto \exp(-\frac{N}{4}\mathrm{Tr}M^2) \tag{2.1.3}$$

and the JPDF of its eigenvalues is given up to normalization by Eq. (2.1.1). Since the pioneer work of Dumitriu and Edelman around 2002 [153], matrix representations of the Gaussian ensemble were obtained for any β in a tridiagonal form. Indeed, let H_β be the following tridiagonal matrix of size $N \times N$,

$$H_\beta = \frac{1}{\sqrt{N\beta}} \begin{pmatrix} \mathcal{N}(0,2) & \chi_{(N-1)\beta} & & & & & \mathbf{0} \\ \chi_{(N-1)\beta} & \mathcal{N}(0,2) & \chi_{(N-2)\beta} & & & & \\ & \ddots & \ddots & \ddots & & & \\ & & \ddots & \ddots & \ddots & & \\ & & & \chi_{2\beta} & \mathcal{N}(0,2) & \chi_\beta & \\ \mathbf{0} & & & & \chi_\beta & \mathcal{N}(0,2) & \end{pmatrix} \tag{2.1.4}$$

where the diagonal terms are Gaussian random variables and the off-diagonal elements are χ-distributed with parameters $k\beta$ for $k \in [1, N-1]$ so that their PDF reads

$$P(\chi) = \frac{2^{1-a/2}}{\Gamma(a/2)} \chi^{a-1} e^{-\chi^2/2} \Theta(\chi) \tag{2.1.5}$$

where a is the parameter of the random variable χ_a. The eigenvalues $\{\lambda_i\}$ of H_β then admit Eq. (2.1.1) as their joint probability distribution. This matrix can also be understood from the point of view of a discrete hopping model on a one-dimensional lattice. The problem is not translation-invariant as the hopping rates $\chi_{(N-k)\beta}$ depend on the position on the lattice.

Due to the presence of the β factor, the JPDF (2.1.1) can be seen as the Gibbs measure of a Coulomb gas (CG) with logarithmic repulsion between the eigenvalues, which, at large N, are described by a continuous density. In addition, this JPDF is the stationary measure of the β Dyson Brownian motion [154] which represents particles $\{\lambda_i\}$ driven by a Brownian motion and interacting with a logarithmic potential $\log|\lambda_i - \lambda_j|$. In addition, in the case of $\beta = 2$, if we see the eigenvalues $\{\lambda_i\}$ as the positions of identical non-interacting fermionic particles as in Ref. [106, 129], then the JPDF can be represented as the square modulus of the related N-body fermionic wave function, i.e. the quantum probability.

The particular feature of the random eigenvalues of H_β which will be of interest in this Thesis concerns their behavior around the edge of the spectrum located at $\lambda = 2$ for large N. Near the edge, the fluctuations of the eigenvalues are stronger than in the bulk of the spectrum and a non-trivial behavior is found in a window of width $\sim N^{-2/3}$ around the edge. In that window for large N, the scaled eigenvalues $a_i \equiv N^{2/3}(\lambda_i - 2)$ define the Airy$_\beta$ point process (APP) which thus describes the few largest eigenvalues of a large GβE matrix.

In the case of $\beta = 2$, the Airy$_2$ point process has the special structure of a determinantal point process, see Section 2.2 below for more details. It is an infinite random point configuration $\mathbf{a} = (a_1 > a_2 > \cdots)$ on $\mathbb{R}$. Its mean density $\rho(a)$ (seen as the average of the empirical density of a) is equal to

$$\rho(a) = K_{\mathrm{Ai}}(a, a) \tag{2.1.6}$$

with the standard Airy kernel K_{Ai}, see Appendix A.3. For large negative argument the mean density should match the Wigner semi-circle density of the bulk $\rho(a) \simeq_{a\to-\infty} \frac{1}{\pi}\sqrt{|a|}$. More generally, the k-th correlation function $\rho_k(x_1, \ldots, x_k)$ for all $k \geqslant 1$ takes a determinantal form

$$\rho_k(x_1, \ldots, x_k) = \det[K_{\mathrm{Ai}}(x_i, x_k)]_{i,j=1}^k. \tag{2.1.7}$$

The connection between the tridiagonal matrix and the Airy$_\beta$ point process is made in the large

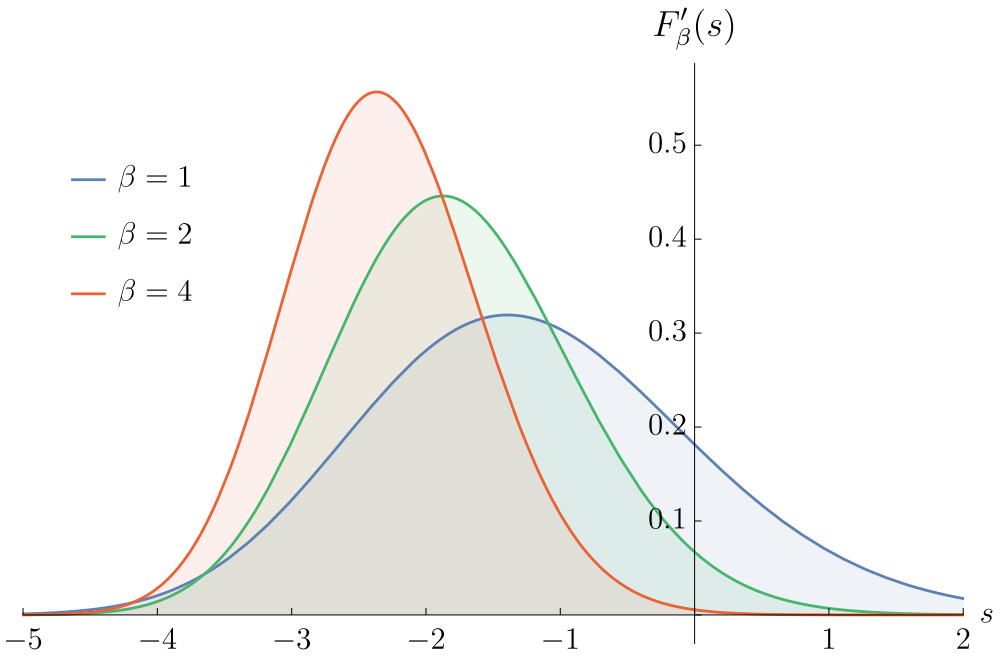

Figure 2.2: Tracy-Widom distributions for the GOE, $\beta = 1$ (blue line), the GUE, $\beta = 2$ (green line) and the GSE, $\beta = 4$ (red line). The plots were performed on Mathematica with the dedicated Tracy-Widom distribution function.

N limit by the convergence of H_β to an operator called the Stochastic Airy Operator (SAO) [155].

$$N^{2/3}(2I - H_\beta) \underset{N\to+\infty}{\to} \mathcal{H}_{\mathrm{SAO}} = -\frac{\mathrm{d}^2}{\mathrm{d}y^2} + y + \frac{2}{\sqrt{\beta}}V(y) \tag{2.1.8}$$

where $V(y)$ is a standard white noise. The operator $\mathcal{H}_{\mathrm{SAO}}$ acts on $\mathbb{L}^2([0,+\infty[)$ with Dirichlet boundary conditions at the origin and its eigenvalues are the opposite of the Airy points, i.e. $\varepsilon_i = -a_i$ by construction. From a quantum mechanical point of view, this Hamiltonian describes a quantum particle in a linear potential with an additional random potential.

Remark 2.1.1. *To understand this convergence, note that the only space-dependent quantities in H_β are the off-diagonal elements and that for fixed k and in the limit $N \to \infty$,*

$$\frac{1}{\sqrt{N\beta}}\chi_{(N-k)\beta} \simeq_{N\gg 1} 1 - \frac{k}{2N} + \mathfrak{g} \tag{2.1.9}$$

where $\mathfrak{g}$ is a Gaussian random variable. From the asymptotics of the χ random variable at large N, the discrete hopping model can be understood with a linear field, corresponding to the factor k/N in the asymptotics.

For $\beta = 1, 2, 4$, the cumulative distribution of the largest Airy point a_1 is the celebrated Tracy-Widom (TW) distribution [60, 61, 156, 157]. Equivalently, denoting $\lambda_{\max}$ the largest eigenvalue of H_β, we have

$$\lim_{N\to+\infty} \mathbb{P}\left(\frac{\lambda_{\max} - 2}{N^{-2/3}} \leqslant s\right) = \mathbb{P}(a_1 \leqslant s) := F_\beta(s) \tag{2.1.10}$$

In addition, we present in Fig. 2.2 the plot of the Tracy-Widom PDF F'_β for $\beta = 1, 2, 4$. For arbitrary $\beta > 0$, the CDF $F_\beta(s)$ or equivalently the PDF $F'_\beta(s)$ has asymmetric tails [158],

$$F'_\beta(s) \simeq \begin{cases} \exp\left(-\frac{\beta}{24}|s|^3\right), & s \to -\infty \\ \exp\left(-\frac{2\beta}{3}s^{3/2}\right), & s \to +\infty \end{cases} \tag{2.1.11}$$

Before we turn to some properties determinantal point processes and their extension to Pfaffian point processes, let us discuss in some details the Tracy-Widom distributions in terms of their determinantal and Painlevé representations.

2.1.1 Tracy-Widom β in terms of Fredholm determinants

We shall now present multiple properties of the Tracy-Widom distributions in terms of Fredholm determinants anticipating the Section 2.2 for the precise definitions of these objects. For $s \in \mathbb{R}$, let P_s be the projector onto $[s, +\infty[$ represented by the kernel $P_s(x,y) = \Theta(x-s)\delta(x-y)$ and let B_{Ai} be the integral operator constructed from the kernel

$$\mathsf{B}_{\mathrm{Ai}}(x,y) = \mathrm{Ai}(x+y) \tag{2.1.12}$$

where Ai is the standard Airy function, see Appendix A.2. Note that the Airy integral operator represented by the Airy kernel can be rewritten in terms of B_{Ai} as $K_{\mathrm{Ai}} = \mathsf{B}_{\mathrm{Ai}} P_0 \mathsf{B}_{\mathrm{Ai}}$. The Tracy-Widom distributions for $\beta = 2, 1, 4$ admit determinantal representations as

- $F_2(s) = \mathrm{Det}[I - P_s K_{\mathrm{Ai}}]$
- $F_1(s) = \sqrt{\mathrm{Det}(I - P_s K_{\mathrm{Forr}})} = \mathrm{Det}[I - P_s \mathsf{B}_{\mathrm{Ai}}]$
- $F_4(s) = \sqrt{\mathrm{Det}(I - P_s K^{\mathrm{GLD}})} = \frac{1}{2}\left(\mathrm{Det}[I - P_s \mathsf{B}_{\mathrm{Ai}}] + \mathrm{Det}[I + P_s \mathsf{B}_{\mathrm{Ai}}]\right)$

All operators are considered on $\mathbb{L}^2(\mathbb{R})$ and the intermediate kernels K_{Forr} and K_{GLD} are given by

$$\begin{aligned} K_{\mathrm{Forr}}(x,y) &= K_{\mathrm{Ai}}(x,y) - \mathrm{Ai}(x)\left(1 - \int_0^{+\infty} \mathrm{d}\lambda \mathrm{Ai}(y+\lambda)\right), \\ K^{\mathrm{GLD}}(x,y) &= K_{\mathrm{Ai}}(x,y) - \frac{1}{2}\mathrm{Ai}(x)\int_0^{+\infty} \mathrm{d}\lambda \mathrm{Ai}(y+\lambda). \end{aligned} \tag{2.1.13}$$

The kernel K_{Forr} was shown by Forrester in Ref. [159] to be related to the GOE Tracy-Widom distribution function $F_1(s)$, the kernel B_{Ai} was proved to be related to $F_1(s)$ by Ferrari and Spohn in Ref. [160] and the kernel K^{GLD} was shown by Gueudré and Le Doussal in Ref. [71] to be related to the GSE Tracy-Widom distribution function $F_4(s)$.

Remark 2.1.2. *Here $F_4(s)$ is the cumulative distribution function of the GSE-TW distribution, as defined in [161]. Another convention, which we denote $\tilde{F}_4$ with $F_4(s) = \tilde{F}_4(\frac{s}{\sqrt{2}})$, is given in [61, 160].*

2.1.2 Tracy-Widom β in terms of solutions to a Painlevé equation

Define q to be the solution of the Painlevé II equation for $r \in \mathbb{R}$,

$$q'' = rq + 2q^3 \tag{2.1.14}$$

which satisfies the asymptotic condition $q(r) \sim_{r\to+\infty} \mathrm{Ai}(r)$. Let $U(s) = \frac{1}{2}\int_s^{+\infty} \mathrm{d}r q(r)$, then the Tracy-Widom distributions for $\beta = 2, 1, 4$ are given by [60, 61]

- $F_2(s) = \exp\left(-\int_s^{+\infty} \mathrm{d}r (r-s) q^2(r)\right)$
- $F_1(s) = \exp\left(-U(s)\right) F_2(s)^{1/2}$
- $F_4(s) = \cosh\left(U(s)\right) F_2(s)^{1/2}$

It allows to obtain the following relation between the three distributions:

$$F_4(s) = \frac{1}{2}(F_1(s) + \frac{F_2(s)}{F_1(s)}) \tag{2.1.15}$$

The Painlevé II equation is part of a family of nonlinear ordinary differential equations that generalize the classical theory of linear differential equations in the complex plane. Indeed, the Painlevé II equation may be viewed as a nonlinear generalization of the Airy differential equation. In the context of the Korteweg-de Vries equation, Hastings and McLeod [162] established the existence of a solution to the Painlevé II equation satisfying the Airy asymptotic condition.

2.2 Determinantal and Pfaffian point processes

In this Section, we shall review the very basic properties of Determinantal and Pfaffian point processes required to understand the recent developments on the exact solutions to the Kardar-Parisi-Zhang equation. In pedestrian words, a determinantal point process [163] is a set of random points on the real line $\{x_i\}$ such that every correlation function of these points is the determinant of a kernel K called the correlation kernel

$$\forall k \geqslant 1, \qquad \rho_k(x_1, \dots, x_k) = \det\left[K(x_i, x_j)\right]_{i,j=1}^{k} \tag{2.2.1}$$

Remark 2.2.1. *In this Thesis, we shall consider integral linear operators acting on the Lebesgue space $\mathbb{L}^2(\Omega)$ with Ω a subspace of $\mathbb{R}$ represented by a kernel $K : (x, y) \mapsto K(x, y)$. In addition, let us mention that the correlation kernel is not unique. If K is a correlation kernel, then the conjugation of K with any positive weight ω provides an equivalent correlation kernel*

$$\mathsf{K}(x, y) = \omega(x)K(x, y)\omega(y)^{-1} \tag{2.2.2}$$

describing the process.

Determinantal processes are the landmark of exclusion models as the determinantal representation forbids two points to be equal. They are sometimes referred in the physics literature as Fermionic processes due to the Pauli exclusion principle and the Wick's theorem in quantum mechanics inducing determinantal structures in various correlation functions.

An important property of determinantal point processes is that any linear statistics of the points can be expressed as a Fredholm determinant. Indeed, for any function f and any determinantal point process $\{a_i\}$ with correlation kernel K acting on $\mathbb{L}^2(\Omega)$ we have

$$\mathbb{E}\left[\prod_{i=1}^{\infty}(1 - f(a_i))\right] := \mathrm{Det}\left[I - fK\right]_{\mathbb{L}^2(\Omega)} \tag{2.2.3}$$

where I is the identity kernel.

Remark 2.2.2. *Averages such as the one in the left hand side of Eq. (2.2.3) often appear in the context of linear statistics. Quite generally, linear statistics problems consist in calculating the probability distribution of sums of the type $\mathcal{L} = \sum_i \phi(a_i)$. Averaging over the exponential of such sums lead to averaging over products such as the one in the left hand side of Eq. (2.2.3).*

The right hand side of Eq. (2.2.3) is called a Fredholm determinant and it can be represented by the following series

$$\mathrm{Det}\left[I - fK\right]_{\mathbb{L}^2(\Omega)} = 1 + \sum_{n=1}^{\infty}\frac{(-1)^n}{n!}\prod_{i=1}^{n}\int_{\Omega}\mathrm{d}x_i f(x_i)\det\left[K(x_i, x_j)\right]_{i,j=1}^{n} \tag{2.2.4}$$

A rigorous construction of Fredholm determinants can be found in [105, 164].

Remark 2.2.3. *By default, all integrations are considered with the uniform Lebesgue measure on the space Ω, it is also possible and equivalent to consider the function f as a part of the integration measure.*

A generalization of determinantal point processes are Pfaffian point processes whose correlation functions are expressed in terms of a Pfaffian of a correlation kernel K.

$$\forall k \geqslant 1, \qquad \rho_k(x_1, \dots, x_k) = \mathrm{Pf}\left[K(x_i, x_j)\right]_{i,j=1}^{k} \tag{2.2.5}$$

We recall that the Pfaffian of an anti-symmetric matrix A of size $2N \times 2N$ is defined by

$$\mathrm{Pf}(A) = \sqrt{\mathrm{Det}(A)} = \sum_{\substack{\sigma \in S_{2N} \\ \sigma(2p-1) < \sigma(2p)}} \mathrm{sign}(\sigma) \prod_{p=1}^{N} A_{\sigma(2p-1),\sigma(2p)} \tag{2.2.6}$$

In this Thesis, our interest will focus on Pfaffian point processes where the kernel K is not scalar valued but rather 2×2 matrix valued. We represent such a kernel K as

$$K(x,y) = \begin{pmatrix} K_{11}(x,y) & K_{12}(x,y) \\ K_{21}(x,y) & K_{22}(x,y) \end{pmatrix}. \tag{2.2.7}$$

For such a kernel to be anti-symmetric, we shall also require $K_{21}(x,y) = -K_{12}(y,x)$.

Remark 2.2.4. *If we take the diagonal elements of K to be zero, i.e. $K_{11} = K_{22} = 0$, then*

$$\mathrm{Pf}[K(x_i, x_j)]_{i,j=1}^{k} = \det[K_{12}(x_i, x_j)]_{i,j=1}^{k} \tag{2.2.8}$$

In this case the Pfaffian point process reduces to a determinantal point process with kernel K_{12}. Therefore in a certain sense, Pfaffian point processes are more general than determinantal point processes.

The direct generalization of the Fredholm determinant is the Fredholm Pfaffian, i.e. for any function f and any Pfaffian point process $\{a_i\}$ with kernel K acting on $\mathbb{L}^2(\Omega)$ we have

$$\mathbb{E}\left[\prod_{i=1}^{\infty}(1 - f(a_i))\right] := \mathrm{Pf}\left[J - fK\right]_{\mathbb{L}^2(\Omega)} \tag{2.2.9}$$

where the matrix kernel J is defined by $J(r,r') = \begin{pmatrix} 0 & 1 \\ -1 & 0 \end{pmatrix} \mathbb{1}_{r=r'}$ and the right hand side, called a Fredholm Pfaffian, stands for the following series

$$\mathrm{Pf}\left[J - K\right]_{\mathbb{L}^2(\Omega)} = 1 + \sum_{n_s=1}^{\infty} \frac{(-1)^{n_s}}{n_s!} \prod_{p=1}^{n_s} \int_{\Omega} \mathrm{d}r_p \; f(r_p) \mathrm{Pf}[K(r_i, r_j)]_{i,j=1}^{n_s} \tag{2.2.10}$$

The relation between a Pfaffian and a Determinant extends to their Fredholm counterpart as

$$\mathrm{Pf}[J - K]^2 = \mathrm{Det}[I + JK] \tag{2.2.11}$$

For the precise definition and properties of Fredholm Pfaffians see Section 8 in [165], as well as e.g. Section 2.2. in [116], Appendix B in [41] and Appendix G in [76].

In this Thesis, we will need two special determinant and Pfaffian: the Cauchy determinant and the Schur Pfaffian expressed as

$$\det\left[\frac{1}{x_i + y_j}\right]_{i,j=1}^{k} = \frac{\prod_{1 \leqslant i < j \leqslant k}(x_j - x_i)\prod_{1 \leqslant i < j \leqslant k}(y_j - y_i)}{\prod_{i,j}(x_i + y_j)}, \quad \mathrm{Pf}\left[\frac{x_i - x_j}{x_i + x_j}\right]_{i,j=1}^{k} = \prod_{1 \leqslant i < j \leqslant k} \frac{x_i - x_j}{x_i + x_j}. \tag{2.2.12}$$

In the rest of this Chapter, we will present several manipulations on Fredholm determinants and Pfaffians which will play a capital role in the study of the exact solutions to the Kardar-Parisi-Zhang equation later on in this Thesis.

2.2.1 Trace expansion of a Fredholm Pfaffian

Let us recall here the first terms in the series expansion of a Fredholm Pfaffian (2.2.9) in powers of its kernel. Here K denotes a generic 2×2 matrix valued kernel, hence this expansion is also valid for a Fredholm Determinant by taking the diagonal elements of the kernel to be zero.

$$\mathrm{Pf}(J-K)_{\mathbb{L}^2([s,+\infty[)} = 1 + \sum_{n_s=1}^{\infty} \frac{(-1)^{n_s}}{n_s!} \prod_{p=1}^{n_s} \int_s^{+\infty} \mathrm{d}r_p \, \mathrm{Pf}[K(r_i,r_j)]_{i,j=1}^{n_s} \tag{2.2.13}$$

More explicitly we write (with the convention that $K_{21}(r,r') = -K_{12}(r',r)$)

$$\begin{aligned}
&\mathrm{Pf}[J-K]_{\mathbb{L}^2([s,+\infty[)} = 1 - \int_s^{+\infty} \mathrm{d}r \mathrm{Pf} \begin{pmatrix} 0 & K_{12}(r,r) \\ -K_{12}(r,r) & 0 \end{pmatrix} \\
&+ \frac{1}{2!} \iint_s^{+\infty} \mathrm{d}r_1 \mathrm{d}r_2 \mathrm{Pf} \begin{pmatrix} 0 & K_{12}(r_1,r_1) & K_{11}(r_1,r_2) & K_{12}(r_1,r_2) \\ K_{21}(r_1,r_1) & 0 & K_{21}(r_1,r_2) & K_{22}(r_1,r_2) \\ K_{11}(r_2,r_1) & K_{12}(r_2,r_1) & 0 & K_{12}(r_2,r_2) \\ K_{21}(r_2,r_1) & K_{22}(r_2,r_1) & K_{21}(r_2,r_2) & 0 \end{pmatrix} \\
&- \frac{1}{3!} \iiint_s^{+\infty} \mathrm{d}r_1 \mathrm{d}r_2 \mathrm{d}r_3 \\
&\mathrm{Pf} \begin{pmatrix} 0 & K_{12}(r_1,r_1) & K_{11}(r_1,r_2) & K_{12}(r_1,r_2) & K_{11}(r_1,r_3) & K_{12}(r_1,r_3) \\ K_{21}(r_1,r_1) & 0 & K_{21}(r_1,r_2) & K_{22}(r_1,r_2) & K_{21}(r_1,r_3) & K_{22}(r_1,r_3) \\ K_{11}(r_2,r_1) & K_{12}(r_2,r_1) & 0 & K_{12}(r_2,r_2) & K_{11}(r_2,r_3) & K_{12}(r_2,r_3) \\ K_{21}(r_2,r_1) & K_{22}(r_2,r_1) & K_{21}(r_2,r_2) & 0 & K_{21}(r_2,r_3) & K_{22}(r_2,r_3) \\ K_{11}(r_3,r_1) & K_{12}(r_3,r_1) & K_{11}(r_3,r_2) & K_{12}(r_3,r_2) & 0 & K_{12}(r_3,r_3) \\ K_{21}(r_3,r_1) & K_{22}(r_3,r_1) & K_{21}(r_3,r_2) & K_{22}(r_3,r_2) & K_{21}(r_3,r_3) & 0 \end{pmatrix} + \mathcal{O}(K^4) \\
&= 1 - \mathrm{Tr}K_{12} + \frac{1}{2}\left[(\mathrm{Tr}K_{12})^2 - \mathrm{Tr}K_{12}^2 + \mathrm{Tr}K_{11}K_{22}\right] \\
&- \frac{1}{6}\left[(\mathrm{Tr}K_{12})^3 + 2\mathrm{Tr}K_{12}^3 - 3\mathrm{Tr}K_{12}\mathrm{Tr}K_{12}^2 + 3\mathrm{Tr}K_{12}\mathrm{Tr}K_{11}K_{22} - 6\mathrm{Tr}K_{12}K_{11}K_{22}\right] + \mathcal{O}(K^4),
\end{aligned} \tag{2.2.14}$$

where all integrations in the traces run onto $[s,+\infty[$. The fourth order of the expansion can be found in Appendix G of Ref. [76]. This expansion is called the trace expansion of a Fredholm Pfaffian.

Remark 2.2.5. *In the case where K_{12} is rank 1 operator, we have for all integer n, $\mathrm{Tr}(K_{12}^n) = (\mathrm{Tr}K_{12})^n$, simplifying the expansion dramatically. In that case it becomes [76]*

$$\mathrm{Pf}[J-K]_{\mathbb{L}^2([s,+\infty[)} = 1 - \mathrm{Tr}K_{12} + \frac{1}{2}\mathrm{Tr}K_{11}K_{22} + \frac{1}{2}(2\mathrm{Tr}K_{12}K_{11}K_{22} - \mathrm{Tr}K_{12}\mathrm{Tr}K_{11}K_{22}) + \mathcal{O}(K^4) \tag{2.2.15}$$

2.2.2 Cumulant expansion of a Fredholm determinant

In this Section, we will define the so-called cumulant expansion of a Determinantal point process. This type of expansion first originated from the evaluation of the general quantity

$$\mathbb{E}_K \left[\exp\left(-\sum_{i=1}^{+\infty} \varphi(a_i) \right) \right] \tag{2.2.16}$$

where $\{a_i\}_{i\in\mathbb{N}}$ forms a determinantal point process with kernel K and φ is an arbitrary function. This expansion will later be extremely useful to investigate the exact short and large times

behaviors of the solution to the Kardar-Parisi-Zhang equation and thus we introduce it with great care. As we study a Determinantal point process, the linear statistics of Eq. (2.2.16) can be cast onto a Fredholm determinant.

$$\mathbb{E}_K\left[\exp\left(-\sum_{i=1}^{+\infty}\varphi(a_i)\right)\right] = \mathrm{Det}[I-(1-e^{-\varphi})K] \tag{2.2.17}$$

Taking the logarithm of both sides of this equality, using the property $\log\mathrm{Det} = \mathrm{Tr}\log$ and Taylor expanding the logarithm leads to the following expansion in $e^{-\varphi}$ (see also Ref. [121])

$$\log\mathbb{E}_K\left[\exp\left(-\sum_{i=1}^{+\infty}\varphi(a_i)\right)\right] = \log\mathrm{Det}[I-(1-e^{-\varphi})K] = -\sum_{p=1}^{+\infty}\frac{1}{p}\mathrm{Tr}[\Big((1-e^{-\varphi})K\Big)^p] \tag{2.2.18}$$

The expansion of all factors $1-e^{-\varphi}$ allows us to the definition of the cumulant expansion.

Definition 2.2.6 (*Cumulant expansion of a determinantal process*)

The n-th cumulant $\kappa_n(\varphi)$ of the linear statistics problem defined in (2.2.16) is $n!$ times the term of order φ^n in the following series

$$\log\mathbb{E}_K\left[\exp\left(-\sum_{i=1}^{\infty}\varphi(a_i)\right)\right] = \sum_{n=1}^{\infty}\frac{\kappa_n(\varphi)}{n!} \tag{2.2.19}$$

As an example, the expansion to the third-order of $1-e^{-\varphi}$ allows us to obtain the first three cumulants.

1. *p=1*
$$-\mathrm{Tr}[(1-e^{-\varphi})K] = -\mathrm{Tr}(\varphi K)+\frac{1}{2}\mathrm{Tr}(\varphi^2K)-\frac{1}{6}\mathrm{Tr}(\varphi^3K) \tag{2.2.20}$$
2. *p=2*
$$-\frac{1}{2}\mathrm{Tr}[\Big((1-e^{-\varphi})K\Big)^2] = -\frac{1}{2}\mathrm{Tr}(\varphi K\varphi K)+\frac{1}{2}\mathrm{Tr}(\varphi K\varphi^2K) \tag{2.2.21}$$
3. *p=3*
$$-\frac{1}{3}\mathrm{Tr}[\Big((1-e^{-\varphi})K\Big)^3] = -\frac{1}{3}\mathrm{Tr}(\varphi K\varphi K\varphi K) \tag{2.2.22}$$

Grouping the various terms, we end up having

$$\begin{aligned}\kappa_1(\varphi) &= -\mathrm{Tr}(\varphi K), \qquad \kappa_2(\varphi) = \mathrm{Tr}(\varphi^2K)-\mathrm{Tr}(\varphi K\varphi K),\\ \kappa_3(\varphi) &= -\mathrm{Tr}(\varphi^3K)+3\mathrm{Tr}(\varphi K\varphi^2K)-2\mathrm{Tr}(\varphi K\varphi K\varphi K).\end{aligned} \tag{2.2.23}$$

The formula for the general cumulant can be found in Ref. [166] where similar problems of linear statistics have been studied

$$\kappa_n(\varphi) = \sum_{\ell=1}^{n}\frac{(-1)^{n+\ell+1}}{\ell}\sum_{\substack{m_1,\dots,m_\ell\geqslant 1\\ m_1+\cdots+m_\ell=n}}\frac{n!}{m_1!\cdots m_\ell!}\mathrm{Tr}(\varphi^{m_1}K\varphi^{m_2}K\dots\varphi^{m_\ell}K). \tag{2.2.24}$$

2.2.3 Extension of the cumulant expansion to Fredholm Pfaffians

Although initially introduced for Determinantal point processes, we shall extend the use of cumulant expansions to Fredholm Pfaffians. The reason for this is the intrinsic relation between the solutions to the Kardar-Parisi-Zhang equation and algebraic processes which scope is not only limited to Determinantal processes but also to Pfaffian processes. When the set $\{a_i\}$ forms a Pfaffian point process, the linear statistics admits a Fredholm Pfaffian representation

$$\mathbb{E}_K\left[\exp\left(-\sum_{i=1}^{+\infty}\varphi(a_i)\right)\right] = \mathrm{Pf}[J-(1-e^{-\varphi})K] \tag{2.2.25}$$

We will subsequently assume that the kernel K is matrix valued and is represented by a 2×2 matrix $K = \begin{pmatrix} K_{11} & K_{12} \\ K_{21} & K_{22} \end{pmatrix}$. The key property to obtain the cumulant expansion for Pfaffian processes is the following

$$\mathrm{Pf}\left[J-(1-e^{-\varphi})K\right]^2 = \mathrm{Det}\left[1+(1-e^{-\varphi})JK\right] \tag{2.2.26}$$

Upon the use of the same procedure as in the Determinantal case, the linear statistics for Pfaffian processes reads

$$\log\mathbb{E}_K\left[\exp\left(-\sum_{i=1}^{\infty}\varphi(a_i)\right)\right] = -\frac{1}{2}\sum_{p=1}^{\infty}\frac{1}{p}\mathrm{Tr}\left[(e^{-\varphi}-1)JK\right]^p \tag{2.2.27}$$

As before, the expansion in powers of φ provides the cumulant expansion. For the rest of this Thesis, we will only require the expression of the first cumulant which reads

$$\kappa_1 = \frac{1}{2}\mathrm{Tr}(\varphi JK) = -\mathrm{Tr}(\varphi K_{12}) \tag{2.2.28}$$

2.3 From two to one-dimensional kernels

Later in this Thesis, when encountering exact solutions to the Kardar-Parisi-Zhang equation we will need to juggle between matrix-valued kernels and scalar value kernels. For this purpose, we present in this Section an equivalent representation of a class of Fredholm Pfaffians with 2×2 block kernels in terms of a Fredholm determinant with a scalar valued kernel. Consider a measure $\mathrm{d}\mu$ on a contour $C\in\mathbb{C}$ and another measure $\mathrm{d}\nu_z$ on the real line $\mathbb{R}$, depending on a real parameter z. Consider the quantities $Q(z)$ defined by

$$Q(z) = 1+\sum_{n_s=1}^{\infty}\frac{(-1)^{n_s}}{n_s!}Z(n_s,z) \tag{2.3.1}$$

and

$$\begin{aligned} Z(n_s,z) = \prod_{p=1}^{n_s}\int_{\mathbb{R}}\mathrm{d}\nu_z(r_p)\iint_{C^2}\mathrm{d}\mu(X_{2p-1})\mathrm{d}\mu(X_{2p}) \\ \phi_{\mathrm{odd}}(X_{2p-1})\phi_{\mathrm{even}}(X_{2p})e^{-r_p[X_{2p-1}+X_{2p}]}\,\mathrm{Pf}\left[\frac{X_i-X_j}{X_i+X_j}\right]_{i,j=1}^{2n_s} \end{aligned} \tag{2.3.2}$$

Then, we have the following equivalent representations for $Q(z)$.

Lemma 2.3.1 (*Fredholm Schur Pfaffian*)

$Q(z)$ is equal to a Fredholm Pfaffian with a 2×2 matrix valued skew-symmetric kernel

$$Q(z) = \mathrm{Pf}\left[J - K\right]_{\mathbb{L}^2(\mathbb{R},\nu_z)} \tag{2.3.3}$$

For $(r,r')\in\mathbb{R}^2$ the matrix kernel K is given by

$$\begin{aligned}
K_{11}(r,r') &= \iint_{C^2} \mathrm{d}\mu(v)\mathrm{d}\mu(w)\frac{v-w}{v+w}\phi_{\mathrm{odd}}(v)\phi_{\mathrm{odd}}(w)e^{-rv-r'w}\\
K_{22}(r,r') &= \iint_{C^2} \mathrm{d}\mu(v)\mathrm{d}\mu(w)\frac{v-w}{v+w}\phi_{\mathrm{even}}(v)\phi_{\mathrm{even}}(w)e^{-rv-r'w}\\
K_{12}(r,r') &= \iint_{C^2} \mathrm{d}\mu(v)\mathrm{d}\mu(w)\frac{v-w}{v+w}\phi_{\mathrm{odd}}(v)\phi_{\mathrm{even}}(w)e^{-rv-r'w}\\
K_{21}(r,r') &= \iint_{C^2} \mathrm{d}\mu(v)\mathrm{d}\mu(w)\frac{v-w}{v+w}\phi_{\mathrm{even}}(v)\phi_{\mathrm{odd}}(w)e^{-rv-r'w}
\end{aligned} \tag{2.3.4}$$

and the matrix kernel J is defined by $J(r,r') = \begin{pmatrix} 0 & 1\\ -1 & 0\end{pmatrix}\mathbb{1}_{r=r'}$.

Proof. This Lemma is a direct consequence of Bruijn's theorem, see Ref. [167]. □

Note that $K_{21}(r,r') = -K_{12}(r',r)$ so the kernel is skew-symmetric. The type of kernel presented in this Lemma appear in the context of Pfaffian Schur processes. Quite remarkably, we have shown in [6] that the associated Fredholm Pfaffian can be cast in a Fredholm determinant with a scalar kernel.

Proposition 2.3.2 (*Krajenbrink & Le Doussal, Proposition B.2 of Ref. [6]*)

$Q(z)$ is equal to the square root of a Fredholm determinant with scalar valued kernel

$$Q(z) = \sqrt{\mathrm{Det}\left[I - \bar{K}\right]_{\mathbb{L}^2(\mathbb{R}_+)}} \tag{2.3.5}$$

where $\mathbb{L}^2(\mathbb{R}_+)$ is considered with the uniform measure. Introducing the functions

$$f_{\mathrm{odd}}(r) = \int_C \mathrm{d}\mu(v)\,\phi_{\mathrm{odd}}(v)e^{-rv}, \quad f_{\mathrm{even}}(r) = \int_C \mathrm{d}\mu(v)\,\phi_{\mathrm{even}}(v)e^{-rv} \tag{2.3.6}$$

which are assumed to be in $\mathbb{L}^2(\mathbb{R})$, the scalar kernel $\bar{K}$ is given, for $(x,y)\in\mathbb{R}_+^2$, by

$$\bar{K}(x,y) = 2\partial_x \int_{\mathbb{R}} \mathrm{d}\nu_z(r)\,\left[\mathrm{f}_{\mathrm{even}}(x+r)\mathrm{f}_{\mathrm{odd}}(r+y) - \mathrm{f}_{\mathrm{odd}}(x+r)\mathrm{f}_{\mathrm{even}}(r+y)\right] \tag{2.3.7}$$

and the scalar kernel I is the identity kernel $I(x,y) = \mathbb{1}_{x=y}$.

The form (2.3.7) is quite reminiscent of a Christoffel-Darboux representation of kernels. This might also indicate another integral rewriting of the bracket involving odd and even functions. It is also useful to note the effect of similarity transformations on the kernel obtained. Rescaling the variables by a factor a, i.e. $(x,y)\to(ax,ay)$, leads to the kernel $\tilde{K}$ with $\tilde{K}(x,y) = a\bar{K}(ax,ay)$.

Proof. We start back from the definition of the matrix valued kernel K in Eq. (2.3.4) and use the following identity $\frac{v-w}{v+w} = \frac{w}{w} - \frac{2w}{v+w}$ along with the identities valid for $\Re(w) > 0$ and $\Re(v+w) > 0$

$$\frac{1}{w} = \int_0^{+\infty} \mathrm{d}x e^{-xw}, \quad \frac{1}{v+w} = \int_0^{+\infty} \mathrm{d}x e^{-x(v+w)}, \quad we^{-r'w} = -\partial_{r'} e^{-r'w} \tag{2.3.8}$$

These identities are used to separate the integrals w.r.t the variables v and w. One can now introduce the odd and even functions, $f_{\mathrm{odd}}(r) = \int_C \mu(\mathrm{d}v)\, \phi_{\mathrm{odd}}(v) e^{-rv}$ and $f_{\mathrm{even}}(r) = \int_C \mu(\mathrm{d}v)\, \phi_{\mathrm{even}}(v) e^{-rv}$, to write the elements of the kernel K as

$$\begin{aligned}
K_{11}(r,r') &= \int_0^{+\infty} \mathrm{d}x \ \left[2\mathrm{f}_{\mathrm{odd}}(r+x)\mathrm{f}'_{\mathrm{odd}}(r'+x) - \mathrm{f}_{\mathrm{odd}}(r)\mathrm{f}'_{\mathrm{odd}}(r'+x)\right] \\
K_{22}(r,r') &= \int_0^{+\infty} \mathrm{d}x \ \left[2\mathrm{f}_{\mathrm{even}}(r+x)\mathrm{f}'_{\mathrm{even}}(r'+x) - \mathrm{f}_{\mathrm{even}}(r)\mathrm{f}'{}_{\mathrm{even}}(r'+x)\right] \\
K_{12}(r,r') &= \int_0^{+\infty} \mathrm{d}x \ \left[2\mathrm{f}_{\mathrm{odd}}(r+x)\mathrm{f}'_{\mathrm{even}}(r'+x) - \mathrm{f}_{\mathrm{odd}}(r)\mathrm{f}'{}_{\mathrm{even}}(r'+x)\right] \\
K_{21}(r,r') &= \int_0^{+\infty} \mathrm{d}x \ \left[2\mathrm{f}_{\mathrm{even}}(r+x)\mathrm{f}'_{\mathrm{odd}}(r'+x) - \mathrm{f}_{\mathrm{even}}(r)\mathrm{f}'_{\mathrm{odd}}(r'+x)\right]
\end{aligned} \tag{2.3.9}$$

Consider the notation for the matrix valued kernel

$$K(r,r') = \begin{pmatrix} K_{11}(r,r') & K_{12}(r,r') \\ K_{21}(r,r') & K_{22}(r,r') \end{pmatrix} \tag{2.3.10}$$

One of the two main steps of the proof is to notice that the kernel K can be factorized as a product of a matrix that depends only on r and another matrix that depends only on r'.

$$K(r,r') = \int_0^{+\infty} \mathrm{d}x \begin{pmatrix} 2\mathrm{f}_{\mathrm{odd}}(r+x) - \mathrm{f}_{\mathrm{odd}}(r) \\ 2\mathrm{f}_{\mathrm{even}}(r+x) - \mathrm{f}_{\mathrm{even}}(r) \end{pmatrix} \begin{pmatrix} \mathrm{f}'_{\mathrm{odd}}(r'+x) \\ \mathrm{f}'_{\mathrm{even}}(r'+x) \end{pmatrix}^T \tag{2.3.11}$$

We now write this matrix product as an operator product, $K(r,r') = \int_0^{+\infty} \mathrm{d}x\, A^{(1)}(r,x) A^{(2)}(x,r')$, where the operator $A^{(1)} : \mathbb{L}^2(\mathbb{R}, \nu_z) \to \mathbb{L}^2(\mathbb{R}_+)$ is defined by

$$A^{(1)}(r,x) = \begin{pmatrix} 2\mathrm{f}_{\mathrm{odd}}(r+x) - \mathrm{f}_{\mathrm{odd}}(r) \\ 2\mathrm{f}_{\mathrm{even}}(r+x) - \mathrm{f}_{\mathrm{even}}(r) \end{pmatrix} \tag{2.3.12}$$

and $A^{(2)} : \mathbb{L}^2(\mathbb{R}_+) \to \mathbb{L}^2(\mathbb{R}, \nu_z)$ is defined by

$$A^{(2)}(x,r') = \begin{pmatrix} \mathrm{f}'_{\mathrm{odd}}(r'+x) \\ \mathrm{f}'_{\mathrm{even}}(r'+x) \end{pmatrix}^T \tag{2.3.13}$$

We further suppose that both operators are Hilbert-Schmidt. Let us summarize this factorization by the following notation $\mathrm{Pf}\,[J-K]_{\mathbb{L}^2(\mathbb{R},\nu_z)} = \mathrm{Pf}\left[J - A^{(1)}A^{(2)}\right]_{\mathbb{L}^2(\mathbb{R},\nu_z)}$. Using that for a skew-symmetric kernel K, $\mathrm{Pf}[J-K]^2 = \mathrm{Det}[I+JK]$, (see [165], Lemma 8.1), where the scalar kernel I is the identity kernel $I(x,y) = \mathbb{1}_{x=y}$, this gives

$$\mathrm{Pf}\,[J-K]^2_{\mathbb{L}^2(\mathbb{R},\nu_z)} = \mathrm{Det}\left[I + JA^{(1)}A^{(2)}\right]_{\mathbb{L}^2(\mathbb{R},\nu_z)} \tag{2.3.14}$$

Following [156, 168], one uses the "needlessly fancy" general relation $\det(I+AB) = \det(I+BA)$ for arbitrary Hilbert-Schmidt operators A and B. They may act between different spaces as long as the products make sense. In the present context $\det(I+AB)$ is the Fredholm determinant of a matrix valued kernel whilst $\det(I+BA)$ is a Fredholm determinant of scalar valued kernel.

$$\mathrm{Pf}\,[J-K]^2_{\mathbb{L}^2(\mathbb{R},\nu_z)} = \mathrm{Det}\left[I + A^{(2)}JA^{(1)}\right]_{\mathbb{L}^2(\mathbb{R}_+)} \tag{2.3.15}$$

Let us compute the scalar valued kernel of the operator $A^{(2)}JA^{(1)} : \mathbb{L}^2(\mathbb{R}_+) \to \mathbb{L}^2(\mathbb{R}_+)$.

$$\begin{aligned}
A^{(2)}JA^{(1)}(x,y) &= \int_{\mathbb{R}} \mathrm{d}\nu_z(r)\, A^{(2)}(x,r) JA^{(1)}(r,y) \\
&= \mathcal{K}(x,y) - \frac{1}{2}\mathcal{K}(x,0)
\end{aligned} \tag{2.3.16}$$

where $\mathcal{K} : \mathbb{L}^2(\mathbb{R}_+) \to \mathbb{L}^2(\mathbb{R}_+)$ is defined by

$$\mathcal{K}(x,y) = 2\int_{\mathbb{R}} \mathrm{d}\nu_z(r)\ \left[\mathrm{f}'_{\mathrm{odd}}(r+x)\mathrm{f}_{\mathrm{even}}(r+y) - \mathrm{f}'_{\mathrm{even}}(r+x)\mathrm{f}_{\mathrm{odd}}(r+y)\right] \tag{2.3.17}$$

We observe that $\mathcal{K}$ can be written as a partial derivative w.r.t its first variable $\mathcal{K}(x,y) = \partial_x k(x,y)$ where k is a skew-symmetric scalar kernel given by

$$k(x,y) = 2\int_{\mathbb{R}} \mathrm{d}\nu_z(r)\ \left[\mathrm{f}_{\mathrm{odd}}(r+x)\mathrm{f}_{\mathrm{even}}(r+y) - \mathrm{f}_{\mathrm{even}}(r+x)\mathrm{f}_{\mathrm{odd}}(r+y)\right] \tag{2.3.18}$$

The operator $(x,y) \mapsto \mathcal{K}(x,0)$ is of rank 1 and can be written as $\mathcal{K}\left|\delta\right\rangle\left\langle 1\right|$ where all products have to be taken in the sense of Hilbert-Schmidt integral operator products. Here δ is the δ-function at $x = 0$ and 1 denotes the function $1(x) = 1$ for all $x \geqslant 0$. This leads to the equality

$$\mathrm{Pf}\left[J-K\right]^2_{\mathbb{L}^2(\mathbb{R},\nu_z)} = \mathrm{Det}\left[I + \mathcal{K}\left(I - \frac{1}{2}\left|\delta\right\rangle\left\langle 1\right|\right)\right]_{\mathbb{L}^2(\mathbb{R}_+)} \tag{2.3.19}$$

As $\left|\delta\right\rangle\left\langle 1\right|$ is of rank 1, by the matrix determinant lemma, we have

$$\mathrm{Pf}\left[J-K\right]^2_{\mathbb{L}^2(\mathbb{R},\nu_z)} = \mathrm{Det}\left[I+\mathcal{K}\right]_{\mathbb{L}^2(\mathbb{R}_+)}\left(1 - \frac{1}{2}\left\langle 1\right|\mathcal{K}(I+\mathcal{K})^{-1}\left|\delta\right\rangle\right) \tag{2.3.20}$$

We now want to prove the following identity to be able to conclude

$$\left\langle 1\right|\mathcal{K}(I+\mathcal{K})^{-1}\left|\delta\right\rangle = 0 \tag{2.3.21}$$

The main ingredient to prove this is the remarkable fact that $\mathcal{K}$ is expressed as a product $\mathcal{K} = Dk$, where $D = \partial_x$ and k is a skew-symmetric kernel as introduced in (2.3.18). Hence, we rewrite the identity (2.3.21) as $Q = \left\langle 1\right|\mathcal{K}(I+\mathcal{K})^{-1}\left|\delta\right\rangle = -\left\langle\delta\right|k(I+Dk)^{-1}\left|\delta\right\rangle$ where we used for any function f that $\left\langle 1\right|Df = -\left\langle\delta\right|f$. Note also the commutation relation $k(I+Dk)^{-1} = (I+kD)^{-1}k$. We recall that D is the derivative operator defined by its matrix element $\left\langle f\right|D\left|g\right\rangle = \int_{\mathbb{R}_+}\mathrm{d}x\, f(x)g'(x)$. By integration by part, the adjoint of D is $D^T = -D - \left|\delta\right\rangle\left\langle\delta\right|$. Taking the adjoint of the operator $k(I+Dk)^{-1}$, we have

$$Q = -\left\langle\delta\right|(I+k^TD^T)^{-1}k^T\left|\delta\right\rangle = \left\langle\delta\right|\left(I+kD+k\left|\delta\right\rangle\left\langle\delta\right|\right)^{-1}k\left|\delta\right\rangle \tag{2.3.22}$$

We can use the Sherman-Morrison identity since the last term in the inverse is a rank 1 operator.

$$\begin{aligned} Q &= \left\langle\delta\right|(I+kD)^{-1}k\left|\delta\right\rangle - \frac{\left\langle\delta\right|(I+kD)^{-1}k\left|\delta\right\rangle\left\langle\delta\right|(I+kD)^{-1}k\left|\delta\right\rangle}{1+\left\langle\delta\right|(I+kD)^{-1}k\left|\delta\right\rangle} \\ &= -Q - \frac{Q^2}{1-Q} \end{aligned} \tag{2.3.23}$$

which implies $Q = 0$ or $Q = 2$. Since the amplitude of k can be increased continuously from 0 to any value, by continuity, the solution is $Q = 0$. Defining $\bar{K} = -\mathcal{K}$ and taking the square root on both sides of Eq. (2.3.20) ends the proof. □

2.3.1 Equivalence of different matrix kernels at the level of Fredholm Pfaffians

To conclude this Section of the transformation of matrix valued kernels to scalar kernels, let us mention for completeness a useful proposition which states the equivalence at the level of Fredholm Pfaffians of different kernels. The reason why we mention this result is that some kernels appearing in the literature are not directly suited to the Proposition 2.3.2 but are equivalent to kernels verifying its hypothesis by the use of the following Proposition 2.3.3.

Proposition 2.3.3 (*Matrix kernel equivalence, Proposition 5.2 of Ref. [116]*)

Let $\mathbf{A} : \mathbb{R}^2 \to \mathrm{Skew}_2(\mathbb{R})$ *be a kernel of the form*

$$\mathbf{A}(x,y) = \begin{pmatrix} A(x,y) & -\partial_y A(x,y) \\ -\partial_x A(x,y) & \partial_x \partial_y A(x,y) \end{pmatrix},$$

where A *is smooth, antisymmetric, and* $\mathbf{A}$ *satisfies the following decay hypotheses: there exist constants* $C > 0$ *and* $a > b \geqslant 0$ *such that*

$$|A(x,y)| < Ce^{-ax-ay}, \quad |\partial_y A(x,y)| < Ce^{-ax+by}, \quad |\partial_x \partial_y A(x,y)| < Ce^{bx+by}.$$

Let $\mathbf{B}$ *be the kernel*

$$\mathbf{B}(x,y) = \begin{pmatrix} A(x,y) & -2\partial_y A(x,y) \\ -2\partial_x A(x,y) & 4\partial_x \partial_y A(x,y) + \delta'(x,y) \end{pmatrix}.$$

where δ' *is a distribution on* $\mathbb{R}^2$ *such that*

$$\iint f(x,y)\delta'(x,y)\mathrm{d}x\mathrm{d}y = \int \Big(\partial_y f(x,y) - \partial_x f(x,y)\Big)\Big|_{y=x} \mathrm{d}x, \tag{2.3.24}$$

for smooth and compactly supported test functions f*. Then for any* $s \in \mathbb{R}$*,*

$$\mathrm{Pf}[J - \mathbf{A}]_{\mathbb{L}^2([s,+\infty[)} = \mathrm{Pf}[J - \mathbf{B}]_{\mathbb{L}^2([s,+\infty[)}. \tag{2.3.25}$$

Remark 2.3.4. *Our work on the half-space Kardar-Parisi-Zhang solution in Ref. [2] strongly suggests that this proposition is a particular case of a more general identity. Indeed, this Proposition was introduced in Ref. [116] to study different kernels leading to the same GSE Fredholm Pfaffian. In Ref. [2], we hint that a same phenomenon should occur for the GOE Fredholm Pfaffian.*

Chapter 3

Exact solutions to the Kardar-Parisi-Zhang equation

In this Chapter, we will browse the recent achievements regarding the exact solutions to the Kardar-Parisi-Zhang equation, from its first solution which arose in 2010 from multiple research teams at the same time to the last solution obtained by us in [2].

3.1 A brief historical note

Since 2010, there has been a revival in both physics and mathematics communities in the search of exact solutions to the Kardar-Parisi-Zhang equation. So far, without taking into account this Thesis, in full-space three initial conditions have been solved and in half-space the droplet initial condition has been solved for three specific boundary conditions. We present in the Table 3.1 the chronology of the discovery of these exact solutions.

Initial condition	Authors	Year	Ref.
Full space			
Droplet	Sasamoto, Spohn	2010	[72]
	Calabrese, Le Doussal, Rosso		[73]
	Dotsenko		[74]
	Amir, Corwin, Quastel ($\star$)		[75]
Flat	Calabrese, Le Doussal	2011	[76]
Brownian	Imamura, Sasamoto	2012	[77]
	Borodin, Corwin, Ferrari, Veto ($\star$)	2014	[78]
Half space			
Droplet with hard wall	Gueudré, Le Doussal	2012	[71]
Droplet with reflecting wall	Borodin, Bufetov, Corwin	2015	[79]
Droplet with critical wall	Barraquand, Borodin, Corwin, Wheeler ($\star$)	2017	[80]
Droplet with general $A \geqslant -\frac{1}{2}$	Krajenbrink, Le Doussal	2019	[2]
Brownian with hard wall	Krajenbrink, Le Doussal		[2]

Table 3.1: Chronology of the discovery of exact solutions to the KPZ equation. In half-space, we use the shorthand notatons: Reflective wall for $A = 0$, hardwall for $A = \infty$ and critical wall for $A = -\frac{1}{2}$. The solutions displayed with a ($\star$) were obtained rigorously.

At the end of this Chapter, we will present two new solutions to the Kardar-Parisi-Zhang equation in half-space: the Brownian with a hard-wall and the droplet with arbitrary boundary coefficient larger than $-1/2$.

3.2 Solutions at all times in full-space

For the completeness of the presentation, we shall recall here the exact expressions for the solutions to the KPZ equation at all times. We will focus on the droplet and Brownian initial conditions in full and half-space and we will not discuss the solution to the flat initial condition, expressed in Ref. [76], as we will not use its exact expression in this Thesis. In particular, we will be interested in the generating function of the exponential of the KPZ height which exhibits a Fredholm representation for all aforementioned initial conditions .

3.2.1 Droplet initial condition

The moment generating function of the exponential shifted height $H(t) = h(0,t) + \frac{t}{12}$ is given in terms of a Fredholm determinant with the Airy kernel and the so-called Fermi factor measure. The solution was found originally by several research groups and was presented in Refs. [72–75].

$$\mathbb{E}_{\mathrm{KPZ}}\left[\exp\left(-ze^{H(t)}\right)\right] = \mathrm{Det}[I - \sigma_{z,t}K_{\mathrm{Ai}}]_{\mathbb{L}^2(\mathbb{R})}\,. \tag{3.2.1}$$

where K_{Ai} is the Airy kernel, $K_{\mathrm{Ai}}(u,u') = \int_0^\infty \mathrm{d}r\ \mathrm{Ai}(r+u)\mathrm{Ai}(r+u')$, and the weight of the Airy kernel $\sigma_{z,t}$ is the Fermi factor expressed as

$$\sigma_{z,t}(u) = \frac{z}{z + e^{-t^{1/3}u}} \tag{3.2.2}$$

Remark 3.2.1. *The only time-dependence of the Fredholm determinant lies in the Fermi factor.*

To further study properties of the Fredholm determinant and the droplet solution in this Thesis, we additionally need the following facts:

- To investigate the short-time behavior of the droplet solution, we will need the behavior of the diagonal element of the kernel K_{Ai} for large argument. Up to exponentially small corrections, it is given by [169]

$$K_{\mathrm{Ai}}(vt^{-1/3}, vt^{-1/3}) \simeq_{t\ll 1} \frac{\sqrt{|v|}}{\pi} t^{-1/6}\Theta(-v). \tag{3.2.3}$$

- To investigate the late-time behavior of the droplet solution, it is useful to change variable and define $z = e^{-st^{1/3}}$. From the work of Amir, Corwin and Quastel [75], it has been proved that the Fredholm determinant (3.2.1) also has a representation in terms of a solution of a generalized Painlevé II equation[2]. Indeed,

$$\mathrm{Det}[I - \sigma_{z,t}K_{\mathrm{Ai}}]_{\mathbb{L}^2(\mathbb{R})} = \exp\left(-\int_s^{+\infty} \mathrm{d}r(r-s)\Psi_t(r)\right) \tag{3.2.4}$$

  where Ψ_t and q_t verify the following differential equations

$$\begin{aligned} \Psi_t(r) &= \int_{\mathbb{R}} \mathrm{d}v[q_t(r,v)]^2\sigma'_{1,t}(v), \\ \partial_r^2 q_t(r,v) &= [v + r + 2\Psi_t(r)]q_t(r,v). \end{aligned} \tag{3.2.5}$$

  with asymptotic behavior $q_t(r,v) \simeq_{r\to+\infty} \mathrm{Ai}(r+v)$.

[2] This is interpreted as a finite-time version of the Painlevé property of the Tracy-Widom distribution for $\beta = 2$.

At late time, the Fermi factor becomes a projector: $\sigma_{z,t}(u) \to_{t\to+\infty} \Theta(u-s)$, the double exponential becomes an indicator function $e^{-e^{\lambda(\cdot)}} \to_{\lambda\to+\infty} \mathbb{1}(\cdot \leqslant 0)$ and hence we find that the cumulative distribution of the shifted height $H(t) = h(0,t) + \frac{t}{12}$ converges to the Tracy-Widom distribution for $\beta = 2$.

$$\lim_{t\to+\infty} \mathbb{P}(\frac{H(t)}{t^{1/3}} \leqslant s) = \mathrm{Det}[I - K_{\mathrm{Ai}}]_{\mathbb{L}^2([s,+\infty[)} := F_2(s) \tag{3.2.6}$$

The Tracy-Widom fluctuations at large time are a landmark of the Kardar-Parisi-Zhang universality class.

3.2.2 Brownian initial condition

Another initial condition that has been solved is the Brownian one, sometimes also called the stationary interface in the case of zero drift. Mathematically, it is described by a two-sided Brownian interface pinned at $x = 0$ and in addition to averaging over realizations of the dynamic stochastic process, one has to average over all possible initial pinned Brownian interfaces with diffusivity ν. Imamura and Sasamoto [77, 170] and Borodin, Corwin, Ferrari, Veto [78] derived exact explicit representations for the generating function of the exponential KPZ height in terms of a Fredholm determinant. They also showed that, in the long-time limit and for typical fluctuations, the cumulative distribution of the KPZ height converges to the so-called Baik-Rains distribution which is also encountered in the studies of the stationary TASEP, polynuclear growth and last passage percolation.

For the Brownian initial condition $h(x,0) = B(x) - w|x|$, the exact solution is written in terms of an additional random variable χ independent of $h(x,t)$, with probability density $p(\chi)\mathrm{d}\chi = e^{-2w\chi - e^{-\chi}}/\Gamma(2w)\mathrm{d}\chi$. As announced the generating function of $e^{H(t)+\chi}$, where $H(t)$ is the shifted height $H(t) = h(0,t) + \frac{t}{12}$, exhibits a Fredholm determinant representation [77, 78, 170] given by

$$\mathbb{E}_{\mathrm{KPZ},B}\left[\exp\left(-ze^{H(t)}\right)\right] = \mathrm{Det}[I - \sigma_{z,t}K_{\mathrm{Ai},\Gamma}]_{\mathbb{L}^2(\mathbb{R})}\ . \tag{3.2.7}$$

where $\sigma_{z,t}$ is the Fermi factor previously introduced in Eq. (3.2.2) and $K_{\mathrm{Ai},\Gamma}$ is the deformed Airy kernel which expression is

$$K_{\mathrm{Ai},\Gamma}(u,u') = \int_0^{+\infty} \mathrm{d}r\, \mathrm{Ai}_\Gamma^\Gamma(r+u, t^{-\frac{1}{3}}, w, w)\mathrm{Ai}_\Gamma^\Gamma(r+u', t^{-\frac{1}{3}}, w, w)\ , \tag{3.2.8}$$

where the deformed Airy function is equal to

$$\mathrm{Ai}_\Gamma^\Gamma(a,b,c,d) := \int_{\mathbb{R}+i\epsilon} \frac{\mathrm{d}\eta}{2\pi} \exp\left(i\frac{\eta^3}{3} + ia\eta\right) \frac{\Gamma(ib\eta + d)}{\Gamma(-ib\eta + c)}\ . \tag{3.2.9}$$

where Γ is the Gamma function and $\epsilon \in [0, \Re(d/b)[$ due to the pole of the Γ function.

Remark 3.2.2. *Contrary to the droplet initial condition, the time-dependence lies both in the Fermi factor and in the kernel itself. Note also that the generating function over the KPZ height comprises an average over the initial Brownian condition.*

To further study properties of the Fredholm determinant and the Brownian solution in this Thesis, we additionally need the following facts:

- At short time, the relevant physical parameter is $\tilde{w} = wt^{1/2}$ and whereas at large time it is $\bar{w} = wt^{1/3}$.

- To investigate the short-time behavior of the Brownian solution, we shall need the behavior of the diagonal element of the kernel $K_{\mathrm{Ai},\Gamma}$ for large argument. Up to exponentially small corrections, it is given by [9]

$$K_{\mathrm{Ai},\Gamma}(vt^{-1/3}, vt^{-1/3}) \simeq_{t\ll 1} \frac{\sqrt{W_0(\tilde{w}^2 e^{-\hat{v}+\tilde{w}^2}) - \tilde{w}^2}}{\pi} t^{-1/6}\Theta(-\hat{v}). \tag{3.2.10}$$

  where $\hat{v} = v + \log \tilde{w}^2 - \log t$ and W_0 is the first real branch of the Lambert function.

3.3 Solutions at all times in half-space

We now turn to the solutions of the Kardar-Parisi-Zhang on the half-line. A common feature of all known solutions is that the generating function of the exponential KPZ height is expressed as a Fredholm Pfaffian rather than a Fredholm determinant. Here we shall solely focus on the droplet initial condition, which is the only initial condition studied until this Thesis. We recall on the half-line of the presence of a wall with parameter A. We shall present the three known solutions for $A = -1/2, 0, +\infty$.

3.3.1 Critical case $A = -\frac{1}{2}$

Defining the shifted height $H(t) = h(0,t) + \frac{t}{12}$, Barraquand, Borodin, Corwin and Wheeler obtained in Ref. [80] the following Pfaffian representation of the generating function of the exponential height for $A = -\frac{1}{2}$

$$\mathbb{E}_{\mathrm{KPZ}}\left[\exp(-\frac{z}{4}e^{H(t)})\right] = \mathbb{E}_{\mathrm{GOE}}\left[\prod_{i=1}^{\infty}\frac{1}{\sqrt{1+ze^{t^{1/3}a_i}}}\right]_{\mathbb{L}^2(\mathbb{R})} \tag{3.3.1}$$

where the set $\{a_i\}$ forms a Pfaffian GOE point process.

Remark 3.3.1. *The only time-dependence of the Fredholm Pfaffian lies in the measure which is here the square root of the Fermi factor.*

At large time, the cumulative distribution of the shifted height will converge to the Tracy-Widom distribution for $\beta = 1$.

$$\lim_{t\to+\infty} \mathbb{P}(\frac{H(t)}{t^{1/3}} \leqslant s) = F_1(s) \tag{3.3.2}$$

3.3.2 Reflective (symmetric) wall $A = 0$

A solution to the case $A = 0$ was obtained in [79] by Borodin, Bufetov and Corwin. The generating function of the exponential shifted height $H(t) = h(0,t) + \frac{t}{12}$ shows the following Pfaffian representation for $z \geqslant 0$.

$$\mathbb{E}_{\mathrm{KPZ}}\left[\exp\left(-\frac{z}{4}e^{H(t)}\right)\right] = 1 + \sum_{n_s=1}^{\infty}\frac{(-1)^{n_s}}{n_s!}\prod_{p=1}^{n_s}\int_{\mathbb{R}}\mathrm{d}r_p \frac{z}{z+e^{-t^{1/3}r_p}}\mathrm{Pf}\left[K(r_i,r_j)\right]_{n_s\times n_s} \tag{3.3.3}$$

where K is a 2×2 block matrix with the following elements

$$\begin{aligned}
K_{11}(r,r') &= \frac{1}{4t^{1/3}}\int_{C_v}\int_{C_w}\frac{\mathrm{d}v\mathrm{d}w}{4\pi^2}\frac{v-w}{v+w}\frac{\Gamma(\frac{1}{2}-vt^{-\frac{1}{3}})}{\Gamma(1-vt^{-\frac{1}{3}})}\frac{\Gamma(\frac{1}{2}-wt^{-\frac{1}{3}})}{\Gamma(1-wt^{-\frac{1}{3}})}e^{-rv-r'w+\frac{v^3+w^3}{3}}\\
K_{22}(r,r') &= \frac{1}{4t^{1/3}}\int_{C_v}\int_{C_w}\frac{\mathrm{d}v\mathrm{d}w}{4\pi^2}\frac{v-w}{v+w}\frac{\Gamma(vt^{-\frac{1}{3}})}{\Gamma(\frac{1}{2}+vt^{-\frac{1}{3}})}\frac{\Gamma(wt^{-\frac{1}{3}})}{\Gamma(\frac{1}{2}+wt^{-\frac{1}{3}})}e^{-rv-r'w+\frac{v^3+w^3}{3}}\\
K_{12}(r,r') &= \frac{1}{4t^{1/3}}\int_{C_v}\int_{C_w}\frac{\mathrm{d}v\mathrm{d}w}{4\pi^2}\frac{v-w}{v+w}\frac{\Gamma(\frac{1}{2}-vt^{-\frac{1}{3}})}{\Gamma(1-vt^{-\frac{1}{3}})}\frac{\Gamma(wt^{-\frac{1}{3}})}{\Gamma(\frac{1}{2}+wt^{-\frac{1}{3}})}e^{-rv-r'w+\frac{v^3+w^3}{3}}\\
K_{21}(r,r') &= -K_{12}(r',r)
\end{aligned} \tag{3.3.4}$$

The contours C_v and C_w are such that $C_{v,w}=\frac{1}{2}a_{v,w}+i\mathbb{R}$ for $a_{v,w}\in]0,1[$.

Remark 3.3.2. *Contrary to the critical case, the time-dependence lies both in the Fermi factor and in the kernel itself, similarly to the Brownian initial condition in full-space.*

This representation can be cast in a Fredholm Pfaffian form

$$\mathbb{E}_{\mathrm{KPZ}}\left[\exp\left(-\frac{z}{4}e^{H(t)}\right)\right]=\mathrm{Pf}[J-\sigma_{t,z}K]_{\mathbb{L}^2(\mathbb{R})}\,. \tag{3.3.5}$$

To further study properties of the Fredholm Pfaffian in this Thesis, we additionally need the following facts:

- To investigate the short-time behavior of the solution with parameter $A=0$, we shall need the behavior of the off-diagonal element of the kernel K_{12} for large argument. Up to exponentially small corrections, it is given by [6]

$$K_{12}(vt^{-1/3},vt^{-1/3})\simeq_{t\ll 1}\frac{\sqrt{|v|}}{2\pi}t^{-1/6}\Theta(-v) \tag{3.3.6}$$

- The large-time limit of the K was obtained in Ref. [79] as the GSE kernel so that the cumulative distribution of the shifted height converges to the Tracy-Widom distribution for $\beta=4$.

$$\lim_{t\to+\infty}\mathbb{P}(\frac{H(t)}{t^{1/3}}\leqslant s)=F_4(s) \tag{3.3.7}$$

3.3.3 Hard wall $A=+\infty$

The droplet initial condition with a hard-wall was originally studied in [71] and we revisited it in Ref. [6] to provide a new identity for the generating function of the exponential KPZ height. The generating function of the exponential shifted height $H(t)=h(\varepsilon,t)+\frac{t}{12}-2\log\varepsilon$ for $\varepsilon\ll 1$ is given for $z\geqslant 0$ as a Fredholm Pfaffian

$$\mathbb{E}_{\mathrm{KPZ}}\left[\exp\left(-ze^{H(t)}\right)\right]=1+\sum_{n_s=1}^{\infty}\frac{(-1)^{n_s}}{n_s!}\prod_{p=1}^{n_s}\int_{\mathbb{R}}\mathrm{d}r_p\frac{z}{z+e^{-t^{1/3}r_p}}\mathrm{Pf}\left[K(r_i,r_j)\right]_{n_s\times n_s} \tag{3.3.8}$$

The expected value of the l.h.s of (3.3.8) is taken over the realization of the KPZ white noise, and K is a 2×2 block matrix with elements

$$\begin{aligned}
K_{11}(r,r') &= \frac{1}{\pi t^{1/3}}\int_{C_v}\int_{C_w}\frac{\mathrm{d}v\mathrm{d}w}{(2i\pi)^2}\frac{v-w}{v+w}\Gamma(2vt^{-\frac{1}{3}})\Gamma(2wt^{-\frac{1}{3}})\cos(\pi vt^{-\frac{1}{3}})\cos(\pi wt^{-\frac{1}{3}})e^{-rv-r'w+\frac{v^3+w^3}{3}}\\
K_{22}(r,r') &= \frac{1}{\pi t^{1/3}}\int_{C_v}\int_{C_w}\frac{\mathrm{d}v\mathrm{d}w}{(2i\pi)^2}\frac{v-w}{v+w}\Gamma(2vt^{-\frac{1}{3}})\Gamma(2wt^{-\frac{1}{3}})\sin(\pi vt^{-\frac{1}{3}})\sin(\pi wt^{-\frac{1}{3}})e^{-rv-r'w+\frac{v^3+w^3}{3}}\\
K_{12}(r,r') &= \frac{1}{\pi t^{1/3}}\int_{C_v}\int_{C_w}\frac{\mathrm{d}v\mathrm{d}w}{(2i\pi)^2}\frac{v-w}{v+w}\Gamma(2vt^{-\frac{1}{3}})\Gamma(2wt^{-\frac{1}{3}})\cos(\pi vt^{-\frac{1}{3}})\sin(\pi wt^{-\frac{1}{3}})e^{-rv-r'w+\frac{v^3+w^3}{3}}\\
K_{21}(r,r') &= -K_{12}(r',r)
\end{aligned} \tag{3.3.9}$$

The contours C_v and C_w pass at the right of 0 as $C_{v,w} = \frac{1}{2}a_{v,w} + i\mathbb{R}$ for $a_{v,w} \in]0,1[$.

Remark 3.3.3. *As in the case of the reflecting wall, the time-dependence lies both in the Fermi factor and in the kernel itself.*

This representation can be cast in a Fredholm Pfaffian form

$$\mathbb{E}_{\mathrm{KPZ}}\left[\exp\left(-ze^{H(t)}\right)\right] = \mathrm{Pf}[J - \sigma_{t,z}K]_{\mathbb{L}^2(\mathbb{R})}\,. \tag{3.3.10}$$

To further study properties of the Fredholm Pfaffian in this Thesis, we additionally need the following facts:

- To investigate the short-time behavior of the solution with parameter $A = +\infty$, we shall need the behavior of the off-diagonal element of the kernel K_{12} for large argument. Up to exponentially small corrections, it is given by [6]

$$K_{12}(vt^{-1/3}, vt^{-1/3}) \simeq_{t\ll 1} \frac{1}{2\pi}\left(\sqrt{-W_{-1}(-\frac{t}{4}e^r)} - \sqrt{-W_0(-\frac{t}{4}e^r)}\right) t^{-1/6}\Theta\left(-1-r-\log(\frac{t}{4})\right) \tag{3.3.11}$$

  where W_0 and W_{-1} are the two real branches of the Lambert function, see [171] and the Appendix A.1. The extremal value $r + \log(\frac{t}{4}) = -1$ corresponds to evaluating the Lambert functions $W(z)$ at $z = -e^{-1}$ which is the lower edge of the domain of definition of $W(z)$ to remain real valued. From the definition of the Fermi factor, one can substitute $r + \log(\frac{t}{4}) \to r$ up to the replacement $z \to \frac{t}{4}z$ as seen from the definition of $\sigma_{t,z}$ in (3.2.2).

- The large-time limit of the K was obtained in Ref. [79] as the GSE kernel so that the cumulative distribution of the shifted height converges to the Tracy-Widom distribution for $\beta = 4$.

$$\lim_{t\to+\infty} \mathbb{P}(\frac{H(t)}{t^{1/3}} \leqslant s) = F_4(s) \tag{3.3.12}$$

3.4 A new duality in half-space and general solution to the droplet initial condition

Until this Thesis, the KPZ equation in half-space for general boundary condition A has resisted the analysis. There have been attempts to extend the Replica Bethe Ansatz approach for the hard-wall configuration [71] to general A [79, 112, 172] using the fact that the associated Bose gas is integrable. The structure for generic A is nevertheless much more complicated as multi-particle states bound to the wall arises in the spectrum of the associated delta Bose gas [112, 172]. This problem did not impact the study in [71] since for $A = +\infty$ there are no boundary bound states. Here we will provide the solution to half-space puzzle for an extended range of $A > -1/2$ which is obtained through a recent breakthrough in the mathematics community. Another approach was followed recently: the full structure of the states bound to the wall was obtained [112, 172] leading to improved formulae for the moments on the partition sum a priori valid for all A.

3.4.1 The game changer for the half-space problem

Quite recently in the mathematics community, a game changer theorem has been presented in Ref. [173] relating the problem of the half-space KPZ equation with droplet initial condition in the presence of a wall of parameter A and the Brownian initial condition in the presence of a hard-wall but with a drift equal to $A + \frac{1}{2}$. We now present this Theorem and explain how we can manipulate it solve the half-space KPZ problem [2].

Theorem 3.4.1 (*Parekh. Theorem 1.1 of Ref. [173]*)

For $A \in \mathbb{R}$, let $Z(x,t)$ denote the solution of the SHE on the half-line with Robin-boundary parameter A and droplet initial condition $Z(x,0) = \delta(x)$. Let $Z_{\mathrm{Br}}(x,t)$ be the solution to the SHE with Brownian initial condition with drift $A + \frac{1}{2}$, i.e. $Z_{\mathrm{Br}}(x,0) = e^{B(x)-(A+\frac{1}{2})x}$, where B is a (zero drift) Brownian motion with Dirichlet boundary condition on the half-line $Z_{\mathrm{Br}}(0,t) = 0$. Then one has the following equality in distributions

$$Z(0,t) = \lim_{\kappa \to 0} \frac{Z_{\mathrm{Br}}(\kappa, t)}{\kappa} \tag{3.4.1}$$

Remark 3.4.2. *This theorem comes as a limit of an identity proved in Ref. [110], Proposition 8.1, on half-space Macdonald processes.*

Let us quote the author of Ref. [173] which summarizes well the strategy we implemented in Ref. [2] to obtain a new solution to the KPZ equation in half-space.

> " Mathematically, we believe that [Theorem 3.4.1] is interesting because it hints at an intriguing *duality* between the initial data of a solution to the half-space SHE and the boundary conditions one imposes on it. This duality can in turn be exploited in order to obtain useful results on quantities of interest. " (Taken from Ref. [173])

We thus choose to study, rather than our original problem with parameter A, the KPZ problem on the half-line with Dirichlet boundary conditions, but with Brownian initial conditions. To be able to apply the theorem we choose the drift of the Brownian to be $A + \frac{1}{2}$. Since the boundary conditions are Dirichlet (i.e. $A = +\infty$) we can apply the same Replica Bethe Ansatz (RBA) method as in [71]. The only technical difficulty is the calculation of the "overlap" of the Brownian initial condition with the eigenstates of the delta Bose gas, which we are able to perform. We then obtain a formula for the n-th integer moment of $Z_{\mathrm{Br}}(x,0)$, which then leads us to a formula for the moments of the droplet initial condition for generic A using the theorem. Mathematically, defining the limit $\hat{Z}_{\mathrm{Br}}(t) = \lim_{\kappa \to 0^+} Z_{\mathrm{Br}}(\kappa, t)/\kappa$, we shall use the following consequence of Theorem 3.4.1.

$$\mathbb{E}_{\mathrm{KPZ,B}}\left[\hat{Z}_{\mathrm{Br}}(t)^n\right] = \mathbb{E}_{\mathrm{KPZ}}\left[Z(t)^n\right] \tag{3.4.2}$$

To relate to the Kardar-Parisi-Zhang problem in half-space, we shall study in a single unified calculation the statistics of

1. $Z(t) = e^{h(t)}$ and $H(t) = h(0,t) + \frac{t}{12}$ where $h(t)$ is the KPZ height at $x = 0$ with droplet initial condition in the presence of a wall of parameter A;
2. $\hat{Z}_{\mathrm{Br}}(t) = e^{h_{\mathrm{Br}}(t)} = \lim_{\kappa \to 0^+} e^{h_{\mathrm{Br}}(\kappa,t) - \log \kappa}$ and $H_{\mathrm{Br}}(t) = h_{\mathrm{Br}}(t) + \frac{t}{12}$ where $h_{\mathrm{Br}}(\kappa, t)$ is the KPZ height at $x = \kappa$ with Brownian initial condition with a drift $A + \frac{1}{2}$ in the presence of a hard-wall.

The ultimate goal of this Section will be the calculation of the generating function of the exponential KPZ heights which, from the Theorem 3.4.1 of Parekh in [173], are related for any $\varsigma > 0$ as

$$\mathbb{E}_{\mathrm{KPZ,Brownian}}\left[\exp(-\varsigma e^{H_{\mathrm{Br}}(t)})\right] = \mathbb{E}_{\mathrm{KPZ}}\left[\exp(-\varsigma e^{H(t)})\right] \tag{3.4.3}$$

The expected value of the left hand side is taken over the white noise of the KPZ equation and the Brownian initial condition while the expected value of the right hand side is taken over the white noise of the KPZ equation. Note that although the Theorem is valid for any $A \in \mathbb{R}$, we will only make use of it for $A > -1/2$.

3.4.2 The Replica Bethe Ansatz solution for the half-space problem

Before entering the details of the calculation of the RBA for the Brownian initial condition, we shall state our main result, obtained in Ref. [2], valid for all times $t \geqslant 0$ and all parameter $A > -\frac{1}{2}$ for the generating function for $\varsigma > 0$ of the exponential KPZ height in terms of its representation as a Fredholm Pfaffian.

Result 3.4.3 (*Finite-time Fredholm Pfaffian solution to the half-space KPZ problem*)

The generating function of the exponential KPZ height at $x = 0$ for the droplet initial condition in half-space in the presence of a wall of parameter $A > -1/2$ is given at all times by the following Fredholm Pfaffian.

$$\mathbb{E}_{\mathrm{KPZ}}\left[\exp(-\varsigma e^{H(t)})\right] = 1 + \sum_{n_s=1}^{+\infty} \frac{(-1)^{n_s}}{n_s!} \prod_{p=1}^{n_s} \int_{\mathbb{R}} \mathrm{d}r_p \frac{\varsigma}{\varsigma + e^{-r_p}} \mathrm{Pf}\left[K(r_i, r_j)\right]_{n_s \times n_s} \tag{3.4.4}$$

where kernel K is matrix valued and represented by a 2×2 block matrix with elements

$$\begin{aligned}
K_{11}(r,r') &= \iint_{C^2} \frac{\mathrm{d}w}{2i\pi} \frac{\mathrm{d}z}{2i\pi} \frac{w-z}{w+z} \frac{\Gamma(A+\frac{1}{2}-w)}{\Gamma(A+\frac{1}{2}+w)} \frac{\Gamma(A+\frac{1}{2}-z)}{\Gamma(A+\frac{1}{2}+z)} \\
&\qquad \times \Gamma(2w)\Gamma(2z)\cos(\pi w)\cos(\pi z) e^{-rw-r'z+t\frac{w^3+z^3}{3}}, \\
K_{22}(r,r') &= \iint_{C^2} \frac{\mathrm{d}w}{2i\pi} \frac{\mathrm{d}z}{2i\pi} \frac{w-z}{w+z} \frac{\Gamma(A+\frac{1}{2}-w)}{\Gamma(A+\frac{1}{2}+w)} \frac{\Gamma(A+\frac{1}{2}-z)}{\Gamma(A+\frac{1}{2}+z)} \\
&\qquad \times \Gamma(2w)\Gamma(2z)\frac{\sin(\pi w)}{\pi}\frac{\sin(\pi z)}{\pi} e^{-rw-r'z+t\frac{w^3+z^3}{3}}, \\
K_{12}(r,r') &= \iint_{C^2} \frac{\mathrm{d}w}{2i\pi} \frac{\mathrm{d}z}{2i\pi} \frac{w-z}{w+z} \frac{\Gamma(A+\frac{1}{2}-w)}{\Gamma(A+\frac{1}{2}+w)} \frac{\Gamma(A+\frac{1}{2}-z)}{\Gamma(A+\frac{1}{2}+z)} \\
&\qquad \times \Gamma(2w)\Gamma(2z)\cos(\pi w)\frac{\sin(\pi z)}{\pi} e^{-rw-r'z+t\frac{w^3+z^3}{3}}, \\
K_{21}(r,r') &= -K_{12}(r',r).
\end{aligned} \tag{3.4.5}$$

In this formula the contours C are parallel to the imaginary axis and cross the real axis between 0 and $A + \frac{1}{2}$.

Remark 3.4.4. *For a visual illustration of the block structure in the Pfaffians of matrix valued kernel, appearing in Eq. (3.4.4), see e.g. Eq. (2.2.14).*

The series in Eq. (3.4.4) can also be interpreted as a Fredholm Pfaffian, see Eq. (3.4.34), implying a duality between the generating function of the exponential KPZ height and an average of a "Fermi factor" over a Pfaffian point process

$$\mathbb{E}_{\mathrm{KPZ}}\left[\exp(-\varsigma e^{H(t)})\right] = \mathbb{E}_K\left[\prod_{i=1}^{+\infty} \frac{1}{1+\varsigma e^{a_i}}\right] \tag{3.4.6}$$

where the set $\{a_i\}$ forms a Pfaffian point process with kernel K. At large time, we have additionally obtained in Ref. [2] the following limit behavior of the solution of the Kardar-Parisi-Zhang equation.

Result 3.4.5 (*Late-time cumulative distribution of the KPZ solution*)

The late-time KPZ height has Tracy-Widom type fluctuations for any $A \geqslant -1/2$, i.e.

- *For any $A > -\frac{1}{2}$, the one-point KPZ height fluctuations follow the Tracy-Widom GSE distribution*

$$\lim_{t\to\infty} \mathbb{P}\left(\frac{h(0,t)+\frac{t}{12}}{t^{1/3}} \leqslant s\right) = F_4(s) \tag{3.4.7}$$

- *For $A = -\frac{1}{2}$, the one-point KPZ height fluctuations follow the Tracy-Widom GOE distribution.*

$$\lim_{t\to\infty} \mathbb{P}\left(\frac{h(0,t)+\frac{t}{12}}{t^{1/3}} \leqslant s\right) = F_1(s) \tag{3.4.8}$$

What is more, near the transition point $A = -1/2$, there is a critical regime for $A + \frac{1}{2} \to 0$ and $t \to +\infty$ simultaneously, with the crossover parameter $\epsilon = (A + \frac{1}{2})t^{1/3}$ being kept fixed and of order 1. Under a proper rescaling of the kernel (3.4.5) we obtain a large-time limit of the matrix kernel which depends continuously on ϵ and name it the transition kernel. Its expression, K^{ϵ}, is given in two equivalent forms in Eqs. (3.4.41) and in Eqs. (3.4.48) for $\epsilon > 0$. In the limit $\epsilon \to +\infty$ this transition kernel becomes equal to the standard kernel of the GSE. The transition around $A = -1/2$ for the KPZ equation is believed to be in the same universality class than the one for last passage percolation in a half-quadrant. For the latter an explicit Fredholm Pfaffian was obtained in Ref. [116, 117] and we provide a conjecture on the equivalence between our Fredholm Pfaffian of Ref. [2] and theirs. Finally, although we do not address the case $A < -1/2$ or $\epsilon < 0$ we conjectured in Ref. [2] from the equivalence of our cross-over kernel with the kernel of Ref. [116, 117] that for any $A < -\frac{1}{2}$, the one-point KPZ height has Gaussian fluctuations.

Conjecture 3.4.6 (*Late-time cumulative distribution for $A < -1/2$*)

The late-time KPZ height grows with a velocity equal to $(A + \frac{1}{2})^2 - \frac{1}{12}$ and has Gaussian fluctuations for $A < -1/2$

$$\lim_{t\to\infty} \mathbb{P}\left(\frac{h(0,t)+t(\frac{1}{12}-(A+\frac{1}{2})^2)}{t^{1/2}\sqrt{2A+1}} \leqslant s\right) = \frac{1}{\sqrt{2\pi}}\int_{-\infty}^{s} \mathrm{d}y e^{-\frac{y^2}{2}} \tag{3.4.9}$$

3.4.3 Bethe ansatz formula for the moments of the partition sum

Let us recall that the partition sum $Z_{\mathrm{Br}}(x,t)$ verifies the Stochastic Heat Equation on the half-line $x \geqslant 0$ and that the general equal time moments of the solution of the SHE, $Z_{\mathrm{Br}}(x,t)$, over the KPZ noise can be expressed [81] as quantum mechanical expectation values of the evolution operator in imaginary time of the Lieb Liniger model [83].

$$\mathbb{E}_{\mathrm{KPZ,B}}\left[Z_{\mathrm{Br}}(x_1,t)\dots Z_{\mathrm{Br}}(x_n,t)\right] = \langle x_1\dots x_n|e^{-t\hat{\mathcal{H}}_n}|\Psi(t=0)\rangle \tag{3.4.10}$$

where $\hat{\mathcal{H}}_n$ is the Hamiltonian of the Lieb-Liniger model [83] for n quantum particles with attractive delta function interactions of strength $c = -\bar{c} < 0$. The initial state for the Lieb-Lininer model is denoted

$$\mathbb{E}_{\mathrm{KPZ,B}}\left[Z_{\mathrm{Br}}(x_1,t=0)\dots Z_{\mathrm{Br}}(x_n,t=0)\right] = \langle x_1\dots x_n|\Psi(t=0)\rangle \tag{3.4.11}$$

and since we are considering the Brownian initial condition and we are interested in averages both over the Brownian and the KPZ noise we must take the initial state $|\Psi(t=0)\rangle$ as

$$\langle x_1\dots x_n|\Psi(t=0)\rangle = \Phi_0(x_1,\dots,x_n) := \mathbb{E}_B\left[\prod_{j=1}^{n} e^{B(x_j)-(A+\frac{1}{2})x_j}\right]. \tag{3.4.12}$$

A simple calculation shows that $\Phi_0(x_1,\dots,x_n)$ is the fully symmetric function which in the sector $0\leqslant x_1\leqslant\cdots\leqslant x_n$ takes the form

$$\Phi_0(x_1,\dots,x_n)=\prod_{j=1}^{n}e^{\frac{1}{2}(2n-2j+1)x_j-(A+\frac{1}{2})x_j}\ . \tag{3.4.13}$$

We can now rewrite the quantum mechanical problem (3.4.10) at coinciding points using the spectral decomposition of the evolution operator $e^{-t\hat{\mathcal{H}}_n}$ in terms of the eigenstates of the Lieb-Liniger Hamiltonian $\hat{\mathcal{H}}_n$ as

$$\mathbb{E}_{\mathrm{KPZ,B}}\left[Z_{\mathrm{Br}}(x,t)^n\right]=\sum_{\mu}\Psi_\mu(x,\dots,x)\langle\Psi_\mu|\Phi_0\rangle\frac{1}{||\mu||^2}e^{-tE_\mu}\ . \tag{3.4.14}$$

Here the un-normalized eigenfunctions of $\hat{\mathcal{H}}_n$ are denoted Ψ_μ (of norm denoted $||\mu||$) with eigenenergies E_μ. Here we used the fact that only symmetric (i.e. bosonic) eigenstates contribute since the initial and final states are fully symmetric in the x_i. Hence the $\sum_\mu$ denotes a sum over all bosonic eigenstates of the Lieb-Liniger model, also called delta Bose gas, and $\langle\Psi_\mu|\Phi_0\rangle$ denotes the overlap, i.e. the Hermitian scalar product of the initial state (3.4.13) with the eigenstate Ψ_μ.

From the Bethe ansatz the eigenstates Ψ_μ are thus Bethe states, i.e. superpositions of plane waves over all permutations P of the n rapidities λ_j for $j\in[1,n]$ with an additional summation over opposite pairs $\pm\lambda_j$ due to the infinite hard wall. The bosonic (fully symmetric) eigenstates can be obtained everywhere from their expression in the sector $x_1<\cdots<x_n$, which reads

$$\begin{aligned}\Psi_\mu(x_1,\dots,x_n)&=\frac{1}{(2i)^n}\sum_{P\in S_n}\prod_{p=1}^{n}\left(\sum_{\varepsilon_p=\pm1}\varepsilon_p e^{i\varepsilon_p x_p\lambda_{P(p)}}\right)A[\varepsilon_1\lambda_{P(1)},\varepsilon_2\lambda_{P(2)},\dots,\varepsilon_n\lambda_{P(n)}]\\ A[\lambda_1,\dots,\lambda_n]&=\prod_{n\geqslant\ell>k\geqslant1}(1+\frac{i\bar{c}}{\lambda_\ell-\lambda_k})(1+\frac{i\bar{c}}{\lambda_\ell+\lambda_k})\end{aligned} \tag{3.4.15}$$

This wavefunction automatically satisfies both

1. The matching condition arising from the $\delta(x_i-x_j)$ interaction

$$\left(\partial_{x_{i+1}}-\partial_{x_i}+\bar{c}\right)\Psi_\mu(x_1,\dots,x_n)\mid_{x_{i+1}=x_i}=0 \tag{3.4.16}$$

2. The hardwall boundary condition $\Psi_\mu(x_1,\dots,x_n)=0$ if some $x_i=0$.

The allowed values for the rapidities λ_i, which parametrize the true physical eigenstates are determined by the Bethe equations arising from the boundary conditions at $x=L$. One will find that the normalized eigenstates $\psi_\mu=\Psi_\mu/||\mu||$ vanish as $(\lambda_i-\lambda_j)$ or $(\lambda_i+\lambda_j)$ when two rapidities become equal or opposite: hence the rapidities obey an exclusion principle.

The detailed Bethe equations, which determine the allowed values for the set of rapidities $\{\lambda_j\}$, depend on the choice of boundary condition at $x=L$. However, in the $L\to+\infty$ limit, these details do not matter. For simplicity we choose another hardwall at $x=L$. The Bethe equations then read

$$e^{2i\lambda_j L}=\prod_{\ell\neq j}\frac{\lambda_j-\lambda_\ell-i\bar{c}}{\lambda_j-\lambda_\ell+i\bar{c}}\frac{\lambda_j+\lambda_\ell-i\bar{c}}{\lambda_j+\lambda_\ell+i\bar{c}} \tag{3.4.17}$$

In the case of the infinite hardwall, these equations are also given in Ref. [97] and their solutions in the large L limit were studied in Ref. [174]. The structure of the general states for

infinite L are built by partitioning the n particles into a set of n_s bound-states formed by $m_j \geqslant 1$ particles with $n = \sum_{j=1}^{n_s} m_j$. Each bound state is a *perfect string* [86] , i.e. a set of rapidities

$$\lambda^{j,a} = k_j + \frac{i\bar{c}}{2}(m_j + 1 - 2a) \tag{3.4.18}$$

where $a \in [1, m_j]$ labels the rapidities within the string. Such eigenstates have momentum and energy

$$K_\mu = \sum_{j=1}^{n_s} m_j k_j, \qquad E_\mu = \sum_{j=1}^{n_s} m_j k_j^2 - \frac{\bar{c}^2}{12} m_j (m_j^2 - 1). \tag{3.4.19}$$

The difference with the standard case is that the states are now invariant by a sign change of any of the momenta $\lambda_j \to -\lambda_j$, i.e. $k_j \to -k_j$. From now on, we shall denote the wavefunctions of the string states as $\Psi_{\{k_\ell, m_\ell\}}$. The inverse of the squared norm of an arbitrary string state was obtained in Ref. [71] as

$$\begin{aligned}
\frac{1}{||\mu||^2} &= \frac{1}{n!}\bar{c}^{n-n_s} 2^{n_s} \prod_{i=1}^{n_s} S_{k_i,m_i} \prod_{1 \leqslant i < j \leqslant n_s} D_{k_i,m_i,k_j,m_j} L^{-n_s} \\
D_{k_1,m_1,k_2,m_2} &= \frac{4(k_1-k_2)^2 + (m_1-m_2)^2 c^2}{4(k_1-k_2)^2 + (m_1+m_2)^2 c^2} \frac{4(k_1+k_2)^2 + (m_1-m_2)^2 c^2}{4(k_1+k_2)^2 + (m_1+m_2)^2 c^2} \\
S_{k,m} &= \frac{2^{2m-2}}{m^2} \prod_{p=1}^{[m/2]} \frac{4k^2 + c^2(m-2p)^2}{4k^2 + c^2(m+1-2p)^2}
\end{aligned} \tag{3.4.20}$$

Note that we have only kept the leading term in L as $L \to +\infty$. Inserting the norm formula Eq. (3.4.20) into the spectral decomposition of the n-th moment of Z_{Br}, we obtain the starting formula for the integer moments of the partition sum with Brownian weight on the endpoint in the limit $L \to +\infty$

$$\begin{aligned}
\mathbb{E}_{\mathrm{KPZ,B}}\left[Z_{\mathrm{Br}}(x,t)^n\right] = \sum_{n_s=1}^{n} \frac{2^{n_s}\bar{c}^n}{n_s! \bar{c}^{n_s} n!} \prod_{p=1}^{n_s} \sum_{m_p \geqslant 1} \int_{\mathbb{R}} \frac{\mathrm{d}k_p}{2\pi} m_p S_{k_p,m_p} e^{(m_p^3 - m_j)\frac{\bar{c}^2 t}{12} - m_p k_p^2 t} \\
\times \delta_{n, \sum_{j=1}^{n_s} m_j} \prod_{i<j}^{n_s} D_{k_i,m_i,k_j,m_j} \Psi_{\{k_\ell,m_\ell\}}(x,\ldots,x) \langle \Psi_{\{k_\ell,m_\ell\}} | \Phi_0 \rangle
\end{aligned} \tag{3.4.21}$$

Remark 3.4.7. *Here the Kronecker delta enforces the constraint $\sum_{j=1}^{n_s} m_j = n$ with $m_j \geqslant 1$ and in the summation over states we used $\sum_{k_j} \to m_j L \int_{\mathbb{R}} \frac{\mathrm{d}k}{2\pi}$ which holds also here in the large L limit.*

An important identity, which makes the problem solvable, is that the inverse norms of the states can be expressed as a Schur Pfaffian. Introducing the reduced variables $X_{2p-1} = m_p + 2ik_p$ and $X_{2p} = m_p - 2ik_p$ for $p \in [1, n_s]$, the factor D reads

$$\prod_{1 \leqslant i < j \leqslant n_s} D_{k_i,m_i,k_j,m_j} = \prod_{j=1}^{n_s} \frac{m_j}{2ik_j} \underset{2n_s \times 2n_s}{\mathrm{Pf}} \left[\frac{X_i - X_j}{X_i + X_j}\right] \tag{3.4.22}$$

Since we are interested in the wave-function near the wall, i.e. $\hat{Z}_{\mathrm{Br}}(t) = \lim_{x \to 0^+} \frac{Z_{\mathrm{Br}}(x,t)}{x}$, we can simplify the factor $\Psi_{\{k_\ell,m_\ell\}}(x,\cdots,x)$ in (3.4.21) by taking its small x limit,

$$\Psi_\mu(x,\ldots,x) = n! x^n \prod_{j=1}^{n} \lambda_j + \mathcal{O}(x^{n+1}) \tag{3.4.23}$$

To obtain the n-th moment of $\hat{Z}_{\mathrm{Br}}(t)$ from (3.4.21) we need to calculate the overlap $\langle \Psi_\mu | \Phi_0 \rangle$ where Φ_0 is given in (3.4.13). In general it involves sums over permutations and leads to complicated

expressions but in this case, we have found in Ref. [2] that the overlap in the half-space for Brownian initial conditions is quite simple

$$\langle \Psi_\mu | \Phi_0 \rangle = n! \prod_{j=1}^{n} \frac{\lambda_j}{A^2 + \lambda_j^2}. \tag{3.4.24}$$

Remark 3.4.8. *It is important to note that the formula (3.4.24) for the overlap of the string states with the Brownian initial condition is valid only when the integrals are convergent. This requires the condition $n/2 < A + \frac{1}{2}$ and hence the above formula for the integer moments $\mathbb{E}_{\mathrm{KPZ,B}}\left[\hat{Z}_{\mathrm{Br}}(t)^n\right]$ is valid only when the drift is large enough, for each value of n. This requirement is identical to the one obtained in the full space, for the Brownian initial condition in [77, 170]. There, it was shown how to use these restricted moment formula to construct the full solution for the generating function of the moments at finite time. In Ref. [2] we have followed the same path.*

Inserting the rapidities λ_j of the string state and taking $\bar{c} = 1$, one gathers the contribution from the S term, from the overlap of the Bethe wave functions with the Brownian initial condition and from the value of the Bethe wave at small x in the following quantity factor

$$B_{k,m} = \frac{2k}{\pi} \sinh(2\pi k) \Gamma(2ik + m) \Gamma(-2ik + m) \frac{\Gamma(\frac{1-m}{2} + A + ik)}{\Gamma(\frac{1+m}{2} + A + ik)} \frac{\Gamma(\frac{1-m}{2} + A - ik)}{\Gamma(\frac{1+m}{2} + A - ik)} \tag{3.4.25}$$

After some simple manipulations on various Γ functions on the initial formula for the moments $\mathbb{E}_{\mathrm{KPZ,B}}\left[\hat{Z}_{\mathrm{Br}}(t)^n\right]$ in Eq. (3.4.21), we obtained in Ref. [2] an intermediate representation for the moments of our two equivalent problems (droplet initial conditions with any A, and Brownian initial condition with drift $A + 1/2$ and Dirichlet).

Result 3.4.9 (*Moments of the partition function in a Pfaffian representation*)

The moments of the partition sums for the droplet and Brownian initial conditions have the following Pfaffian representation.

$$\begin{aligned} &\mathbb{E}_{\mathrm{KPZ}}\left[Z(t)^n\right] = \mathbb{E}_{\mathrm{KPZ,B}}\left[\hat{Z}_{\mathrm{Br}}(t)^n\right] \\ &= \sum_{n_s=1}^{n} \frac{n!}{n_s!} \prod_{p=1}^{n_s} \sum_{m_p \geqslant 1} \int_{\mathbb{R}} \frac{\mathrm{d}k_p}{2\pi} \frac{B_{k_p,m_p}}{4ik_p} e^{(m_p^3 - m_p)\frac{t}{12} - m_p k_p^2 t} \delta_{n, \sum_{j=1}^{n_s} m_j} \underset{2n_s \times 2n_s}{\mathrm{Pf}} \left[\frac{X_i - X_j}{X_i + X_j}\right] \end{aligned} \tag{3.4.26}$$

where the factor B_{k_p,m_p} was introduced in Eq. (3.4.25).

We shall now write the generating function for the moments of $Z(t)$, i.e. focusing on the droplet initial condition with generic $A > -1/2$ and with some efforts, we will be able to extend it to $A = -1/2$ the critical case. Since the problems of the droplet and Brownian initial conditions are in correspondence due to the theorem of Parekh in [173], the solution for the droplet initial condition and wall parameter A will have the same range of validity as for the Brownian initial condition.

3.4.4 Generating function in terms of a Fredholm Pfaffian

The generating function is defined, for $\varsigma > 0$, as

$$g(\varsigma) = \mathbb{E}_{\mathrm{KPZ}}\left[\exp(-\varsigma e^{H(t)})\right] = \mathbb{E}_{\mathrm{KPZ}}\left[\exp(-\varsigma e^{\frac{t}{12}} Z(t))\right] = 1 + \sum_{n=1}^{\infty} \frac{(-\varsigma e^{\frac{t}{12}})^n}{n!} \mathbb{E}_{\mathrm{KPZ}}\left[Z(t)^n\right] \tag{3.4.27}$$

The constraint $\sum_{i=1}^{n_s} m_i = n$ in Eq. (3.4.26) can then be relaxed by reorganizing the series according to the number of strings:

$$g(\varsigma) = 1 + \sum_{n_s=1}^{\infty} \frac{1}{n_s!} Z(n_s, \varsigma) \tag{3.4.28}$$

where $Z(n_s, \varsigma)$ is the partition sum at fixed number of strings. As we shall see, the generating function exhibits the remarkable structure of a Fredholm Pfaffian arising thanks to the Schur Pfaffian nature of the inverse norm of the Bethe wave functions in half-space.

Let us first manipulate the partition sum at fixed number of strings expressed in terms of the reduced variables $X_{2p-1} = m_p + 2ik_p$ and $X_{2p} = m_p - 2ik_p$ for $p \in [1, n_s]$.

$$Z(n_s, \varsigma) = \prod_{p=1}^{n_s} \sum_{m_p \geqslant 1} \int_{\mathbb{R}} \frac{\mathrm{d}k_p}{2\pi} (-\varsigma)^{m_p} \frac{B_{k_p, m_p}}{4ik_p} e^{-t m_p k_p^2 + \frac{t}{12} m_p^3} \underset{2n_s \times 2n_s}{\mathrm{Pf}} \left[\frac{X_i - X_j}{X_i + X_j} \right] \tag{3.4.29}$$

where $B_{k,m}$ was given in (3.4.25). The summation over the variables m_p can be done using the usual Mellin-Barnes summation trick, see Lemma 3.5.3. To this aim, let us define a contour $C_0 = a + i\mathbb{R}$ with $a \in]0, \min(2A+1, 1)[$, then denoting f the function gathering all the integer terms in (3.4.29), we have

$$\sum_{m_p \geqslant 1} (-\varsigma)^{m_p} f(m_p) = -\int_{\mathbb{R}} \mathrm{d}r_p \frac{\varsigma}{\varsigma + e^{-r_p}} \int_{C_0} \frac{\mathrm{d}w_p}{2i\pi} f(w_p) e^{-w_p r_p}. \tag{3.4.30}$$

For each m_p we therefore introduce two variables r_p and w_p and we redefine the reduced variables X_{2p} and X_{2p-1} under the minimal replacement $m_p \to w_p$ imposed by the Mellin-Barnes formula.

We will require one last trick of calculation to present our final expression for the partition sum at fixed number of strings. By anti-symmetrization, we separate the following term of $B_{k,m}$ in X_{2p} and X_{2p-1} as

$$\sinh(2\pi k) = \sin(\frac{\pi}{2}(X_{2p} - X_{2p-1})) \to 2\sin(\frac{\pi}{2} X_{2p}) \cos(\frac{\pi}{2} X_{2p-1}). \tag{3.4.31}$$

Finally, rescaling all variables X by a factor 2, we obtain our final expression for $Z(n_s, \varsigma)$.

Result 3.4.10 (*Partition sum at fixed number of strings*)

Let C be a contour of the form $C = \frac{a}{2} + i\mathbb{R}$ where $a \in]0, A + \frac{1}{2}[$. The partition sum at fixed number of strings then reads

$$\begin{aligned} Z(n_s, \varsigma) =& (-1)^{n_s} \prod_{p=1}^{n_s} \int_{\mathbb{R}} \mathrm{d}r_p \frac{\varsigma}{\varsigma + e^{-r_p}} \iint_{C^2} \frac{\mathrm{d}X_{2p-1}}{2i\pi} \frac{\mathrm{d}X_{2p}}{2i\pi} \frac{\sin(\pi X_{2p}) \cos(\pi X_{2p-1})}{\pi} \\ & \times \Gamma(2X_{2p-1}) \Gamma(2X_{2p}) \frac{\Gamma(A + \frac{1}{2} - X_{2p})}{\Gamma(A + \frac{1}{2} + X_{2p})} \frac{\Gamma(A + \frac{1}{2} - X_{2p-1})}{\Gamma(A + \frac{1}{2} + X_{2p-1})} \\ & \times e^{-(X_{2p-1} + X_{2p}) r_p + t(\frac{X_{2p-1}^3}{3} + \frac{X_{2p}^3}{3})} \underset{2n_s \times 2n_s}{\mathrm{Pf}} \left[\frac{X_i - X_j}{X_i + X_j} \right] \end{aligned} \tag{3.4.32}$$

This partition sum and the generating function (3.4.28) are now perfectly suited for the application of our Lemma 2.3.1 leading to the introduction of a Fredholm Pfaffian representation for $g(\varsigma)$.

Let us define the functions

$$\begin{aligned}\phi_{2p}(X) &= \frac{\sin(\pi X)}{\pi}\Gamma(2X)\frac{\Gamma(A+\frac{1}{2}-X)}{\Gamma(A+\frac{1}{2}+X)}e^{-r_pX+t\frac{X^3}{3}}\\ \phi_{2p-1}(X) &= \cos(\pi X)\Gamma(2X)\frac{\Gamma(A+\frac{1}{2}-X)}{\Gamma(A+\frac{1}{2}+X)}e^{-r_pX+t\frac{X^3}{3}}\end{aligned} \tag{3.4.33}$$

Lemma 2.3.1 precisely states that the generating function $g(\varsigma)$ admits a closed form in terms of a Fredholm Pfaffian, which is our main result for the generating function at finite time together with the explicit expression of the kernel given in Eqs. (3.4.5) in the Result 3.4.3.

$$g(\varsigma) = 1 + \sum_{n_s=1}^{\infty}\frac{(-1)^{n_s}}{n_s!}\prod_{p=1}^{n_s}\int_{\mathbb{R}}\mathrm{d}r_p\frac{\varsigma}{\varsigma+e^{-r_p}}\underset{n_s\times n_s}{\mathrm{Pf}}\left[K(r_k,r_\ell)\right] = \mathrm{Pf}(J-\sigma_\varsigma K)_{\mathbb{L}^2(\mathbb{R})} \tag{3.4.34}$$

The function σ_ς is given by $\sigma_\varsigma(r) = \frac{\varsigma}{\varsigma+e^{-r}}$. Finally, recalling that the generating function $g(\varsigma)$ is precisely the generating function of the exponential height, i.e. $g(\varsigma) = \mathbb{E}_{\mathrm{KPZ}}\left[\exp(-\varsigma e^{H(t)})\right]$, we finished the derivation of our main result 3.4.3 for the KPZ solution at all times.

3.4.5 An equivalent kernel

To study the cumulative distribution of the KPZ solution at large time, we shall need to introduce a new kernel, equivalent to the one presented in Eqs. (3.4.5). We recall that for the antisymmetrization procedure, we used the trigonometric decomposition

$$\sin(\pi(X_{2p}-X_{2p-1})) = \sin(\pi X_{2p})\cos(\pi X_{2p-1}) - \cos(\pi X_{2p})\sin(\pi X_{2p-1}) \tag{3.4.35}$$

which lead to the replacement showed in Eq. (3.4.31). It turns out that this decomposition can be made more general. For any real α, we decompose the sine function as

$$\sin(\pi(X_{2p}-X_{2p-1})) = \sin(\pi(X_{2p}-\alpha))\cos(\pi(X_{2p-1}-\alpha)) - \cos(\pi(X_{2p}-\alpha))\sin(\pi(X_{2p-1}-\alpha)) \tag{3.4.36}$$

and we call this the α-*decomposition*. To study the limit $A\to+\infty$, we use $\alpha=0$ and for the limit $A\to-\frac{1}{2}$, we use $\alpha = A+\frac{1}{2}$. Following the same derivation for the Fredholm Pfaffian, the α-decomposition leads to an α-extension of our functions ϕ (Eq. (3.4.33)).

$$\begin{aligned}\phi_{2p}(X) &= \frac{\sin(\pi(X-\alpha))}{\pi}\Gamma(2X)\frac{\Gamma(A+\frac{1}{2}-X)}{\Gamma(A+\frac{1}{2}+X)}e^{-r_pX+t\frac{X^3}{3}}\\ \phi_{2p-1}(X) &= \cos(\pi(X-\alpha))\Gamma(2X)\frac{\Gamma(A+\frac{1}{2}-X)}{\Gamma(A+\frac{1}{2}+X)}e^{-r_pX+t\frac{X^3}{3}}\end{aligned} \tag{3.4.37}$$

We see that this choice $\alpha = A+\frac{1}{2}$ can be interesting since it suppresses the pole at $X = A+\frac{1}{2}$ in the function ϕ_{2p}. At the end we obtain a similar Fredholm Pfaffian expression for the generating function, with the minimal replacement in the kernel (3.4.5)

$$\sin(\pi X)\to\sin(\pi(X-\alpha)), \qquad \cos(\pi X)\to\cos(\pi(X-\alpha)) \tag{3.4.38}$$

Remark 3.4.11. *We emphasize that all the kernels parametrized by α yield the same Fredholm Pfaffian by construction.*

3.4.6 Large-time limit of the Fredholm Pfaffian and the distribution of the KPZ height

We will now study the large-time limit of our kernel and of the KPZ height. At the moment, the time factor is only present in the cubic exponential in Eqs. (3.4.5) and we precisely want to eliminate the time factor in the exponential. This implies that we have to perform the following change of variable in the kernel.

$$(w,z) = t^{-1/3}(\tilde{w},\tilde{z}), \qquad r = t^{1/3}\tilde{r}, \qquad A + \frac{1}{2} = \epsilon t^{-1/3}. \tag{3.4.39}$$

Furthermore, in the large-time limit, the Gamma, cosine and sine functions simplify using that for small positive argument

$$\Gamma(x) \simeq \frac{1}{x}, \qquad \cos(x) \simeq 1, \qquad \sin(x) \simeq x. \tag{3.4.40}$$

This rescaling introduces a new kernel K^ϵ the large-time kernel which is obtained equivalently from the kernel (3.4.5) as $K_{11}(t^{1/3}\tilde{r}, t^{1/3}\tilde{r}') = K^\epsilon_{11}(\tilde{r},\tilde{r}')$, $K_{22}(t^{1/3}\tilde{r}, t^{1/3}\tilde{r}') = t^{-2/3}K^\epsilon_{22}(\tilde{r},\tilde{r}')$, $K_{12}(t^{1/3}\tilde{r}, t^{1/3}\tilde{r}') = t^{-1/3}K^\epsilon_{12}(\tilde{r},\tilde{r}')$. This produces a factor $t^{-n_s/3}$ from the Pfaffian (Eq. (3.4.4), compensating for the change of measure $\prod_p \mathrm{d}r_p = t^{n_s/3}\prod_p \mathrm{d}\tilde{r}_p$.

Result 3.4.12 (*Large-time kernel for the half-space KPZ problem*)

The large-time kernel K^ϵ of the Fredholm Pfaffian of the solution to the Kardar-Parisi-Zhang equation in half-space with droplet initial condition in the presence of a wall with parameter A (such that $\epsilon = (A+\frac{1}{2})t^{1/3}) > 0$ is

$$\begin{aligned}
K^\epsilon_{11}(r,r') &= \frac{1}{4}\iint_{C^2}\frac{\mathrm{d}w}{2i\pi}\frac{\mathrm{d}z}{2i\pi}\frac{w-z}{w+z}\frac{1}{wz}\frac{\epsilon+w}{\epsilon-w}\frac{\epsilon+z}{\epsilon-z}e^{-rw-r'z+\frac{w^3+z^3}{3}}\\
K^\epsilon_{22}(r,r') &= \frac{1}{4}\iint_{C^2}\frac{\mathrm{d}w}{2i\pi}\frac{\mathrm{d}z}{2i\pi}\frac{w-z}{w+z}\frac{\epsilon+w}{\epsilon-w}\frac{\epsilon+z}{\epsilon-z}e^{-rw-r'z+\frac{w^3+z^3}{3}}\\
K^\epsilon_{12}(r,r') &= \frac{1}{4}\iint_{C^2}\frac{\mathrm{d}w}{2i\pi}\frac{\mathrm{d}z}{2i\pi}\frac{w-z}{w+z}\frac{1}{w}\frac{\epsilon+w}{\epsilon-w}\frac{\epsilon+z}{\epsilon-z}e^{-rw-r'z+\frac{w^3+z^3}{3}}
\end{aligned} \tag{3.4.41}$$

The contours C have now to be understood as $C = \tilde{a} + i\mathbb{R}$, where $\tilde{a} \in]0,\epsilon[$. We emphasize that the contours all lie at the left of the poles at $X = \epsilon$.

Besides, as usual for the study of the late-time KPZ dynamics, let us choose the variable ς as $\varsigma = e^{-st^{1/3}}$ so that at large time, the "Fermi factor" becomes an indicator function

$$\lim_{t\to+\infty}\sigma_\varsigma(rt^{1/3}) = \Theta(r-s) \tag{3.4.42}$$

where Θ is the Theta Heaviside function. The Fredholm Pfaffian formula for the generating function then becomes in the limit

$$\lim_{t\to+\infty} g(\varsigma = e^{-st^{1/3}}) = \mathrm{Pf}(J - K^\epsilon)_{\mathbb{L}^2([s,+\infty[)}. \tag{3.4.43}$$

On the other hand, at large time, the Laplace transform of the distribution of the exponential of the KPZ height converges towards the cumulative probability of the height, i.e.

$$\begin{aligned}
g(\varsigma = e^{-st^{1/3}}) = \mathbb{E}_{\mathrm{KPZ}}\left[\exp(-e^{H(t)-st^{1/3}})\right] &\simeq_{t\to+\infty} \mathbb{E}_{\mathrm{KPZ}}\left[\Theta(st^{1/3}-H(t))\right]\\
&\simeq_{t\to+\infty} \mathbb{P}(\frac{H(t)}{t^{1/3}} \leqslant s)
\end{aligned} \tag{3.4.44}$$

where Θ is the Theta Heaviside function. From this, we obtain the CDF of the height distribution in the large-time limit as a Fredholm Pfaffian

$$\lim_{t\to+\infty} \mathbb{P}(\frac{H(t)}{t^{1/3}} \leqslant s) = \mathrm{Pf}(J - K^\epsilon)_{\mathbb{L}^2([s,+\infty[)} \tag{3.4.45}$$

in terms of the matrix kernel given in (3.4.41), also called the transition kernel, as it describes the critical region around the transition. As shown in Ref. [2], it describes the crossover from GSE/GOE/Gaussian expected from universality arguments. Our formula for the kernel is limited at this stage to $\epsilon > 0$.

3.4.7 General ϵ behavior of the matrix valued kernel at large time

Performing the large-time limit at any fixed $A > -1/2$ corresponds to the previous calculation with $\epsilon = +\infty$. As the contours of kernel K^ϵ are parallel to the imaginary axis and cross the real axis between 0 and ϵ, we can push the limit $\epsilon \to \infty$ without any ambiguity and the kernel in this limit K^∞ reads

$$\begin{aligned}
K^\infty_{11}(r,r') &= \frac{1}{4}\iint_{C^2} \frac{\mathrm{d}w}{2i\pi}\frac{\mathrm{d}z}{2i\pi}\frac{w-z}{w+z}\frac{1}{wz} e^{-rw-r'z+\frac{w^3+z^3}{3}} \\
K^\infty_{22}(r,r') &= \frac{1}{4}\iint_{C^2} \frac{\mathrm{d}w}{2i\pi}\frac{\mathrm{d}z}{2i\pi}\frac{w-z}{w+z} e^{-rw-r'z+\frac{w^3+z^3}{3}} \\
K^\infty_{12}(r,r') &= \frac{1}{4}\iint_{C^2} \frac{\mathrm{d}w}{2i\pi}\frac{\mathrm{d}z}{2i\pi}\frac{w-z}{w+z}\frac{1}{w} e^{-rw-r'z+\frac{w^3+z^3}{3}}
\end{aligned} \tag{3.4.46}$$

This is the kernel associated to the GSE random matrices as given in Lemma 2.7. of Ref. [116]. Hence the distribution of the KPZ height at $x = 0$ converges at large time for boundary conditions such that $\epsilon \to \infty$ (e.g. for any fixed $A > -1/2$) to the GSE Tracy-Widom distribution.

$$\lim_{t\to\infty} \mathbb{P}(\frac{h(0,t) + \frac{t}{12}}{t^{1/3}} \leqslant s) = F_4(s) \tag{3.4.47}$$

To study the general ϵ behavior of our kernel, we shall compare it with the transition kernel obtained in in Ref. [116] from the solution of discrete models, i.e. last passage percolation and facilitated TASEP.

To this aim, it is useful to return to the α-decomposition and choose $\alpha = A + \frac{1}{2}$. Inserting the replacement (3.4.38) into the finite-time kernel (3.4.5) and repeating the same steps one obtains a large-time kernel equivalent to (3.4.41) (which, for simplicity, we shall also denote by K^ϵ).

$$\begin{aligned}
K^\epsilon_{11}(r,r') &= \frac{1}{4}\iint_{C^2} \frac{\mathrm{d}w}{2i\pi}\frac{\mathrm{d}z}{2i\pi}\frac{w-z}{w+z}\frac{1}{wz}\frac{\epsilon+w}{w-\epsilon}\frac{\epsilon+z}{z-\epsilon} e^{-rw-r'z+\frac{w^3+z^3}{3}} \\
K^\epsilon_{22}(r,r') &= \frac{1}{4}\iint_{C^2} \frac{\mathrm{d}w}{2i\pi}\frac{\mathrm{d}z}{2i\pi}\frac{w-z}{w+z}\frac{(z+\epsilon)(w+\epsilon)}{wz} e^{-rw-r'z+\frac{w^3+z^3}{3}} \\
K^\epsilon_{12}(r,r') &= \frac{1}{4}\iint_{C^2} \frac{\mathrm{d}w}{2i\pi}\frac{\mathrm{d}z}{2i\pi}\frac{w-z}{w+z}\frac{z+\epsilon}{wz}\frac{\epsilon+w}{w-\epsilon} e^{-rw-r'z+\frac{w^3+z^3}{3}}
\end{aligned} \tag{3.4.48}$$

Remark 3.4.13. *As advertized above, this choice of $\alpha = A + \frac{1}{2}$ has decreased the number of poles for w or z equal to ϵ, which will be useful below.*

An important conjecture of our work in Ref. [2] is that our transition kernel K^ϵ in Eq. (3.4.48) is equivalent to the cross-over kernel[3] K_{cross} in Ref. [116] Definition 2.9.

[3] This kernel appeared previously in Refs. [175, 176].

Conjecture 3.4.14 (*Fredholm Pfaffian equivalence*)

The transition kernel found for the solution to the KPZ equation in half-space with crossover parameter $\epsilon > 0$ is equivalent to the one found at the transition for the last passage percolation and facilitated TASEP models in a half-space.

$$\mathrm{Pf}(J - K^{\epsilon})_{\mathbb{L}^2([s,+\infty[)} = \mathrm{Pf}(J - K_{\mathrm{cross}})_{\mathbb{L}^2([s,+\infty[)} \tag{3.4.49}$$

We recall from Ref. [116] Definition 2.9 that the cross-over kernel K_{cross} is the sum of two kernels I and R, the latter having a single non-zero component R_{22}. In our notations and contour conventions, these kernels read for $\epsilon > 0$

$$\begin{aligned}
I_{11}(r,r') &= \iint_{C^2} \frac{\mathrm{d}z}{2i\pi}\frac{\mathrm{d}w}{2i\pi}\frac{w-z}{w+z}\frac{w+\epsilon}{w}\frac{z+\epsilon}{z}e^{-r'z-rw+\frac{w^3+z^3}{3}},\\
I_{12}(r,r') &= \frac{1}{2}\iint_{C^2} \frac{\mathrm{d}z}{2i\pi}\frac{\mathrm{d}w}{2i\pi}\frac{w-z}{w+z}\frac{w+\epsilon}{w}\frac{1}{\epsilon-z}e^{-r'z-rw+\frac{w^3+z^3}{3}},\\
I_{22}(r,r') &= \frac{1}{4}\iint_{C^2} \frac{\mathrm{d}z}{2i\pi}\frac{\mathrm{d}w}{2i\pi}\frac{w-z}{w+z}\frac{1}{\epsilon-z}\frac{1}{\epsilon-w}e^{-r'z-rw+\frac{w^3+z^3}{3}},\\
I_{21}(r,r') &= -I_{12}(r',r),\\
R_{22}(r,r') &= \frac{1}{4}\mathrm{sgn}(r'-r)e^{-|r-r'|\epsilon}.
\end{aligned} \tag{3.4.50}$$

where we recall that the contour C is parallel to the imaginary axis and crosses the real axis between 0 and ϵ.

Remark 3.4.15. *With these definitions the above formula holds for $\epsilon > 0$. The kernel of Ref. [116] is also valid for $\epsilon < 0$, with various changes on the contours.*

Since it is already proved in Ref. [116] that in the large positive $\epsilon \to +\infty$ limit, the kernel K_{cross} is the GSE kernel, we see that in this limit it is equivalent to ours. For general $\epsilon > 0$ we have expanded in Ref. [2] the Fredholm Pfaffians on both sides of Eq. (3.4.49) in series of their traces up to the third-order in Airy function with perfect matching. Thus we have a strong case for the conjecture of the full equivalence of the Fredholm Pfaffians.

3.4.8 Solution for the KPZ generating function at all times for generic A in terms of a scalar kernel

The general kernel we have obtained in Eq. (3.4.5) has a particular structure in the form of a Schur Pfaffian. With this structure, the kernel verifies the hypothesis of Proposition 2.3.2 which we have proved in Ref. [6]. This proposition states that we can transform the Fredholm Pfaffian of Eq. (3.4.34) which involves a matrix valued kernel, into a Fredholm determinant of a scalar kernel. To proceed, let us first define the functions

$$\begin{aligned}
f_{\mathrm{odd}}(r) &= \int_C \frac{\mathrm{d}w}{2i\pi}\frac{\Gamma(A+\frac{1}{2}-w)}{\Gamma(A+\frac{1}{2}+w)}\Gamma(2w)\cos(\pi w)e^{-rw+t\frac{w^3}{3}}\\
f_{\mathrm{even}}(r) &= \int_C \frac{\mathrm{d}z}{2i\pi}\frac{\Gamma(A+\frac{1}{2}-z)}{\Gamma(A+\frac{1}{2}+z)}\Gamma(2z)\frac{\sin(\pi z)}{\pi}e^{-rz+t\frac{z^3}{3}}
\end{aligned} \tag{3.4.51}$$

and the kernel $\bar{K}_{t,\varsigma}$ such that for all $(x,y) \in \mathbb{R}_+^2$

$$\begin{aligned}
\bar{K}_{t,\varsigma}(x,y) &= 2\partial_x \int_{\mathbb{R}} \mathrm{d}r \frac{\varsigma}{\varsigma+e^{-r}}[f_{\mathrm{even}}(r+x)f_{\mathrm{odd}}(r+y) - f_{\mathrm{odd}}(r+x)f_{\mathrm{even}}(r+y)]\\
&= 2\partial_x \int_{\mathbb{R}} \mathrm{d}r \frac{\varsigma}{\varsigma+e^{-r}} \iint_{C^2} \frac{\mathrm{d}w\mathrm{d}z}{(2i\pi)^2}\frac{\Gamma(A+\frac{1}{2}-w)}{\Gamma(A+\frac{1}{2}+w)}\frac{\Gamma(A+\frac{1}{2}-z)}{\Gamma(A+\frac{1}{2}+z)}\\
&\qquad \times \Gamma(2w)\Gamma(2z)\frac{\sin(\pi(z-w))}{\pi}e^{-xz-yw-rw-rz+t\frac{w^3+z^3}{3}}
\end{aligned} \tag{3.4.52}$$

Then, the generating function of the exponential of the KPZ height admits the Fredholm determinant representation with a scalar valued kernel.

Result 3.4.16 (*Scalar kernel Fredholm determinant for the KPZ generating function*)

The generating function of the exponential KPZ height enjoys a Fredholm determinant representation with a scalar kernel.

$$g(\varsigma) = \mathbb{E}_{\mathrm{KPZ}}\left[\exp(-\varsigma e^{H(t)})\right] = \mathrm{Pf}(J - \sigma_\varsigma K)_{\mathbb{L}^2(\mathbb{R})} = \sqrt{\mathrm{Det}(I - \bar{K}_{t,\varsigma})_{\mathbb{L}^2(\mathbb{R}_+)}} \tag{3.4.53}$$

To obtain the large-time limit of (3.4.53) one performs the same rescaling as in Sec. 3.4.6, namely one chooses $\varsigma = e^{-t^{1/3}s}$ and one rescales $(w, z) \to t^{-1/3}(w, z)$, $r \to t^{1/3}r$. The Fermi factor σ_ς produces a Heaviside function $\Theta(r-s)$ and then (3.4.53) allows us to obtain a transition kernel for $\epsilon > 0$ as

$$\bar{K}(x, y) = \frac{1}{2}\iint_{C^2} \frac{\mathrm{d}w\mathrm{d}z}{(2i\pi)^2} \frac{\epsilon + w}{\epsilon - w}\frac{\epsilon + z}{\epsilon - z}\frac{w - z}{w + z}\frac{1}{w} e^{-xz-yw+\frac{w^3+z^3}{3}} \tag{3.4.54}$$

The contours C are parallel to the imaginary axis and cross the real axis between 0 and ϵ. This additionally allows us to obtain the cumulative distribution of the one-point KPZ height in terms of a Fredholm determinant as

$$\lim_{t\to\infty} \mathbb{P}\left(\frac{H(t)}{t^{1/3}} \leqslant s\right) = \sqrt{\mathrm{Det}(I - \bar{K})_{\mathbb{L}^2([s,+\infty[)}} \tag{3.4.55}$$

We will now be interested in the $\epsilon \to 0^+$ limit which is extremely delicate to handle, but via a careful analysis we will show that it converges towards the scalar kernel of the GOE-TW distribution.

3.4.9 Small ϵ limit of the scalar kernel and convergence to the GOE

To investigate the small ϵ behavior of the scalar kernel, one proceeds by moving the contours C of the scalar kernel of Eq. (3.4.54) to the right of ϵ (and we denote $\hat{C}$ the corresponding contour), and collecting all residues along the way. Doing so, we rewrite the scalar kernel as

$$\begin{aligned}\bar{K}(x, y) = \frac{1}{2}\iint_{\hat{C}^2} \frac{\mathrm{d}w\mathrm{d}z}{(2i\pi)^2} \frac{\epsilon + w}{\epsilon - w}\frac{\epsilon + z}{\epsilon - z}\frac{w - z}{w + z}\frac{1}{w} e^{-xz-yw+\frac{w^3+z^3}{3}} \\ - \epsilon e^{-\epsilon x+\frac{\epsilon^3}{3}} \int_0^{+\infty} \mathrm{d}\lambda \mathrm{Ai}(y + \lambda) + \mathrm{Ai}(x) e^{-\epsilon y+\frac{\epsilon^3}{3}}\end{aligned} \tag{3.4.56}$$

It would be tempting at this stage to set $\epsilon = 0$ in the last two terms, but this is wrong and that is the whole subtlety. Indeed the operator product of the third term with the second one leads to a non trivial contribution for small but finite ϵ. We now study the $\epsilon \to 0^+$ delicate limit in details. We first conjugates the kernel on the left by the multiplication of $e^{-\epsilon x}$ and on the right by the multiplication of $e^{\epsilon y}$ which leaves the associated Fredholm determinant unchanged. The new kernel obtained by this manipulation is the following

$$\begin{aligned}\mathsf{K}(x, y) = \frac{1}{2}\iint_{\hat{C}^2} \frac{\mathrm{d}w\mathrm{d}z}{(2i\pi)^2} \frac{\epsilon + w}{\epsilon - w}\frac{\epsilon + z}{\epsilon - z}\frac{w - z}{w + z}\frac{1}{w} e^{-xz-yw+\epsilon y-\epsilon x+\frac{w^3+z^3}{3}} \\ - \epsilon e^{-2\epsilon x+\epsilon y+\frac{\epsilon^3}{3}} \int_0^{+\infty} \mathrm{d}\lambda \mathrm{Ai}(y + \lambda) + \mathrm{Ai}(x) e^{-\epsilon x+\frac{\epsilon^3}{3}}\end{aligned} \tag{3.4.57}$$

As the devil hides in the details, the $\epsilon \to 0$ limit of this kernel is not trivial and we have shown in Ref. [2] that is it equal to

$$\lim_{\epsilon\to 0} \mathsf{K}(x, y) = K^{\mathrm{GLD}}(x, y) - \frac{1}{2}\delta_\infty(x) \int_0^{+\infty} \mathrm{d}\lambda \mathrm{Ai}(y + \lambda) + \mathrm{Ai}(x) \tag{3.4.58}$$

where δ_∞ is a distribution on $\mathbb{R}$ such that $\int_{\mathbb{R}} \mathrm{d}x f(x)\delta_\infty(x) = \lim_{X\to+\infty} f(X)$.

Remark 3.4.17. *As generic kernels decay fast enough at infinity, one would think that the δ_∞ contribution should not play any role. That is indeed wrong as the third term in Eq. (3.4.58) does not show decay in its second variable.*

Our last effort in Ref. [2] was to prove that the Fredholm determinant of K for $\epsilon = 0$ was identical to the one of the GOE-TW distribution. We achieved this by manipulating the Fredholm determinant of K with the Sherman-Morrison formula and with the matrix determinant lemma. We were able to show that our Fredholm determinant is equal to the one of Forrester in Ref. [159] which directly relates to the GOE Tracy-Widom cumulative distribution F_1.

$$\mathrm{Det}\,(I-\mathsf{K})_{\mathbb{L}^2([s,+\infty[)} = \mathrm{Det}\,\left(I - K_{\mathrm{Ai}} - |\mathrm{Ai}\rangle\,\langle 1|\,(1-\mathrm{Ai})\right)_{\mathbb{L}^2([s,+\infty[)} = F_1(s)^2 \tag{3.4.59}$$

Hence, we concluded in Ref. [2] that for $\epsilon \to 0^+$, the cumulative probability of the one-point KPZ height field is given by the GOE TW distribution.

$$\lim_{t\to\infty} \mathbb{P}\left(\frac{H(t)}{t^{1/3}} \leqslant s\right) = F_1(s) \tag{3.4.60}$$

Conclusion and summary

In this Chapter we have extended the replica Bethe ansatz solution to the KPZ equation in a half-space for droplet initial condition near the wall to generic value of $A > -1/2$. Despite much progress in the topic of exact solutions for the KPZ equation, this has remained a challenge for several years. A recent theorem which maps this problem to the case of a hardwall with a Brownian initial condition was the key tool to find this solution.

It allows to demonstrate the convergence to the GSE Tracy-Widom distribution at large time in this phase and to the GOE Tracy-Widom distribution for $A = -\frac{1}{2}$. We have also obtained the crossover or transition kernel valid in the critical region $A + \frac{1}{2} = \epsilon t^{-1/3}$. Additionally, let us note that the phase diagram we have presented for the solution to the KPZ equation echoes the one obtained in Ref. [110] Section 8 for the log-gamma polymer. Let us close by mentioning that the physics content of the mapping between the Brownian initial condition and the droplet initial condition with different interactions with the wall remains to be understood deeper.

Before investigating several applications and connections of the solutions to the KPZ equation to other mathematical oddities, let us formulate various open questions regarding the exact solutions to the KPZ equation.

3.5 Open questions regarding the exact solutions to the KPZ equation

The open directions we would like to introduce point towards the relation of the solutions to the Kardar-Parisi-Zhang equation and the family of Painlevé equations and towards the nature of the kernels involved in the Fredholm determinant and Pfaffian representation of the generating function of the exponential KPZ heights.

3.5.1 Relation between KPZ solutions and Painlevé equations

So far, a proper relation has been established between a finite-time generalization of the Painlevé II equation and the solution to the KPZ equation for droplet initial condition. This relation was established in [75] by algebraic manipulations on the Fredholm determinant involving the Airy

kernel and the Fermi factor.

We may wonder whether there exists a way to obtain this correspondence directly from the Replica Bethe Ansatz. If so it would be of great importance to obtain such a correspondence with Painlevé equations for all solved initial conditions of the Kardar-Parisi-Zhang equation.

Finally, if some sort of connection between the solved initial conditions and Painlevé equations was established, it would also be paramount to determine whether the general solution to the KPZ equation can be expressed in the Painlevé language. The reason for such a question is that it is not known at the moment whether the general solution to the KPZ equation has a determinantal or Pfaffian representation or if it is the luxury of a few initial conditions.

3.5.2 Time-dependence of the kernels

At the moment, all known solutions to the Kardar-Parisi-Zhang equation exhibit a determinantal or Pfaffian representation for their generating function. These Pfaffians or determinants always exhibit a weight interpreted as a Fermi factor or as the square root of a Fermi factor. Nonetheless, the associated kernels look generally quite complicated and involve various Gamma functions incorporating a non-trivial time-dependence, allowing a Random Matrix interpretation only at infinite time. The only counter-examples to this observation are the droplet initial condition in full-space and in half-space for the critical parameter $A = -1/2$ where respectively the GUE and GOE kernels appear at all times.

From our work in Ref. [2] on the half-space KPZ problem with droplet initial condition in the presence of a wall of parameter $A \geqslant -1/2$, we have seen that at all times the kernel (3.4.5) involves a Fermi factor and multiple Gamma functions. For the case $A = -1/2$, this seems a priori in contradiction with the work of [80] where the GOE kernel appears at all times: the resulting kernel does not present any time-dependence. The natural question to ask ourselves is how we can reconcile both results.

It would be extremely interesting to sort this question out. At the moment, the Gamma functions simplify only at large time onto rational fractions leading to the late-time transition kernel. Although we have no technical claim of the following, we would like to formulate a conjecture on this matter for the half-space KPZ problem.

Conjecture 3.5.1 (*Fredholm representation at all times with the cross-over kernel*)

> *The generating function of the exponential of the KPZ height with droplet initial condition in the presence of a wall with parameter A can be expressed at all times as a Fredholm Pfaffian with the infinite time transition kernel and a weight generalizing the Fermi factor carrying a non-trivial time-dependence.*

Remark 3.5.2. *If this conjecture were true, it would provide an additional formulation of the solution to the Brownian initial condition in full-space.*

Although we have at the moment no calculation to corroborate this conjecture, we have identified a possible mechanism to tackle this problem which we named the extended Mellin-Barnes summation.

The Mellin Barnes summation trick and its generalization

Most derivations of the solutions at all times to the Kardar-Parisi-Zhang equation require at some point the use of the Mellin-Barnes summation trick which allows to transform a series into an

integral in the complex plane. We first present the usual Mellin-Barnes summation and briefly discuss it before introducing its extended version. We suppose here and below that all interchange of integrals and series are benign.

Lemma 3.5.3 (*Mellin-Barnes summation trick*)

Let $\Gamma = a + i\mathbb{R}$ for some $a \in]0,1[$ be a contour in the complex plane, parallel to the imaginary axis and $z \in \mathbb{C}$ such that $\Re(z) > 0$. The Mellin-Barnes summation formula allows to substitute a summation over integers to an integral over Γ.

$$\sum_{m \geqslant 1} (-z)^m f(m) = -\int_{\mathbb{R}} \mathrm{d}r \, \frac{z}{z + e^{-r}} \int_{\Gamma} \frac{\mathrm{d}w}{2i\pi} e^{-wr} f(w) \tag{3.5.1}$$

For completeness, we provide a short non-rigorous proof of the classical Mellin-Barnes summation formula, see Ref. [42] Lemma 3.2.13 for some more convergence details.

Proof. By a residue calculus (and ignoring any convergence issue), we note the identity

$$\sum_{m \geqslant 1} (-z)^m f(m) = -\int_{\Gamma} \frac{\mathrm{d}w}{2i\pi} \frac{\pi}{\sin(\pi w)} z^w f(w) \tag{3.5.2}$$

using that $\mathrm{Res}_{w=m}[\pi/\sin(\pi w)] = (-1)^m$. Furthermore, we note the second identity for $\Re(z) > 0$

$$\frac{\pi}{\sin(\pi w)} z^w = \int_{\mathbb{R}} \mathrm{d}r \frac{z}{z + e^{-r}} e^{-wr} \tag{3.5.3}$$

where the r.h.s can be viewed as a Mellin transform of a Fermi factor. □

The issue with the classical Mellin-Barnes trick is that there is no way to obtain another function than a Fermi factor[4] $(z, r) \mapsto \frac{z}{z+e^{-r}}$. There is nonetheless a certain freedom in the Mellin-Barnes formula that has not been exploited yet in the literature. When introducing the function $w \mapsto \pi/\sin(\pi w)$, we corrected for the residue by proceeding to the change $(-z)^m \to z^w$. One could introduce more general functions that would still have some poles at the positive integers and correct the corresponding residue in the integral. We claim to extend the classical Mellin-Barnes formula by the following assertion.

Claim 3.5.4 (*Extended Mellin-Barnes summation*)

For any function g such that all summations and interchanges of integrals are benign, we have the identity

$$\sum_{m \geqslant 1} (-z)^m f(m) = \int_{\mathbb{R}} \mathrm{d}r \int_{\Gamma} \frac{\mathrm{d}w}{2i\pi} \, e^{-wr} \frac{f(w)}{g(w)} \sum_{m \geqslant 1} e^{rm} g(m) (-z)^m \tag{3.5.4}$$

Although we expect a rigorous proof to emerge from complex analysis, in the same spirit as the regular Mellin-Barnes trick, we provide here another way to introduce this extended trick, which is closer to some calculation of Sasamoto and Imamura in Ref. [77, 170] in the case of the stationary initial condition for the KPZ equation in full-space.

[4] Note that we can interpret this function as a Fermi factor where $\log z$ plays the role of a chemical potential and r of an energy.

Physicist's heuristics. We introduce an auxiliary function g such that for all m

$$(-z)^m f(m) = \int_{\mathbb{R}} \mathrm{d}y\, \delta(y)(-z)^m \frac{f(m+iy)}{g(m+iy)} g(m) \tag{3.5.5}$$

We express the δ-function in Fourier space and proceed to the change of variable $w = m + iy$

$$(-z)^m f(m) = \int_{m+i\mathbb{R}} \mathrm{d}w \int_{\mathbb{R}} \frac{\mathrm{d}r}{2i\pi}\, e^{r(m-w)}(-z)^m \frac{f(w)}{g(w)} g(m) \tag{3.5.6}$$

Suppose that we can shift the contour of integration of w such that there is no m dependency anymore. Let's call Γ this new contour. We then have

$$(-z)^m f(m) = \int_{\Gamma} \frac{\mathrm{d}w}{2i\pi} \int_{\mathbb{R}} \mathrm{d}r\, e^{r(m-w)}(-z)^m \frac{f(w)}{g(w)} g(m) \tag{3.5.7}$$

Let us now proceed to the m summation

$$\sum_{m\geqslant 1} (-z)^m f(m) = \int_{\Gamma} \frac{\mathrm{d}w}{2i\pi} \int_{\mathbb{R}} \mathrm{d}r\, e^{-wr} \frac{f(w)}{g(w)} \sum_{m\geqslant 1} e^{rm} g(m)(-z)^m \tag{3.5.8}$$

□

We hope that this extended summation will be able to solve some of our open question and to motivate its use, we now exhibit some particular cases of this formula.

Example 3.5.5 (The binomial case $g(m) = \frac{\Gamma(\beta+m)}{\Gamma(\beta)\Gamma(m+1)}$)**.**
In this case $\sum_{m\geqslant 1} e^{rm} g(m)(-z)^m = \frac{1}{(1+ze^r)^\beta} - 1$ *and hence*

$$\sum_{m\geqslant 1} (-z)^m f(m) = \int_{\Gamma} \frac{\mathrm{d}w}{2i\pi} \int_{\mathbb{R}} \mathrm{d}r\, e^{-rw} \frac{\Gamma(w+1)\Gamma(\beta)}{\Gamma(w+\beta)} f(w) \left[\frac{1}{(1+ze^r)^\beta} - 1 \right] \tag{3.5.9}$$

In particular,

- $\beta = 1$ *recovers the usual Fermi factor,*
- $\beta = \frac{1}{2}$ *introduces the square root of the Fermi factor,*

$$\sum_{m\geqslant 1} (-z)^m f(m) = \int_{\Gamma} \frac{\mathrm{d}w}{2i\pi} \int_{\mathbb{R}} \mathrm{d}r\, e^{-rw} \sqrt{\pi} \frac{\Gamma(w+1)}{\Gamma(w+\frac{1}{2})} f(w) \left[\frac{1}{\sqrt{1+ze^r}} - 1 \right] \tag{3.5.10}$$

Remark 3.5.6 (Other applications of the extended Mellin-Barnes trick)**.** *We expect that this new summation identity readily applies to other problems such as the Riemann ζ function. Indeed, the integral representation of ζ*

$$\zeta(s) = \frac{1}{\Gamma(s)} \int_0^{+\infty} \mathrm{d}x \frac{x^{s-1}}{e^x - 1} \tag{3.5.11}$$

can be obtained within a line of calculation with the standard Mellin-Barnes trick and the term $1/(e^x - 1)$ is seen as a Bose factor. It would be interesting to obtain more general integral representations of the ζ function.

Chapter 4

Connections and applications of the Kardar-Parisi-Zhang equation

In this Chapter, we shall introduce and discuss some unexpected connections and applications of the Kardar-Parisi-Zhang equation with Random Matrix Theory and Brownian functionals. As we shall see, these connections open more questions than they actually answer, which makes the discussion even more interesting leading to new research directions.

4.1 Hidden connections between RMT and KPZ: the Gorin-Sodin Mapping

As a first connection, we discuss here a mapping that was unveiled by Gorin and Sodin in Ref. [177] between the partition function of walker on a random complete graph in the thermodynamic limit and the solution of the Stochastic Heat Equation for two particular initial conditions.

For the next Theorem to come, we shall suppose that the GOE and GUE ensembles of size $N \times N$ are defined with the convention that the edge of their spectrum is located at $2\sqrt{N}$ rather than 2 as presented before. The result of Gorin and Sodin is the following.

Theorem 4.1.1 (*Gorin & Sodin, Corollary 1.5 of Ref. [177]*)

Let M_N be a $N \times N$ Hermitian (resp. symmetric) matrix with independent (up to symmetry) complex (resp. real) elements, so that the moments of the matrix elements $\mathbb{E}[M_N]_{i,j}^k \overline{[M_N]_{i,j}^\ell}$ with $k + l \leqslant 4$ match those of GUE (resp. GOE) - in this case, we write the matrix $M_N^{(\beta)}$ with $\beta = 1$ for the GOE matching (resp. $\beta = 2$ for the GUE matching) - and suppose that $\sup_N \max_{1 \leqslant i,j \leqslant N} \mathbb{E}\big|[M_N]_{i,j}\big|^{C_0} < \infty$ where C_0 is the absolute constant from Ref. [178]. Then for all $t > 0$, one has the equality in law

$$\lim_{N \to +\infty} \frac{N}{\beta} \left[\left(\frac{M_N^{(\beta)}}{2\sqrt{N}} \right)^{2\lfloor t^{1/3} N^{2/3} \rfloor} + \left(\frac{M_N^{(\beta)}}{2\sqrt{N}} \right)^{2\lfloor t^{1/3} N^{2/3} \rfloor + 1} \right]_{1,1} = Z^{(\beta)}(0,t) \exp\left(\frac{t}{12}\right) \tag{4.1.1}$$

where $Z^{(\beta=1)}$ is the solution of the Stochastic Heat Equation in half-space for droplet initial condition and the critical Robin boundary condition $A = -1/2$ and where $Z^{(\beta=2)}$ is the solution in full-space for droplet initial condition. The factor t is then the true time of the Kardar-Parisi-Zhang dynamics.

There is a striking heuristic interpretation of the theorem of Gorin and Sodin. On the right hand side of Eq. (4.1.1), the solution to the Stochastic Heat Equation represents the partition function of a continuum directed polymer in a space-time random medium. For the case of the point to point polymer (or point to line), the partition function sums all paths from the initial point to the final points, each path being weighted by the successive random weights of the bonds encountered by the polymer. On the other hand, a random matrix can be seen as an adjacency matrix of a complete random graph. Taking a matrix M to some power k and evaluating its element $(1,1)$ amounts to calculate the total weight of the bonds encountered by a directed polymer on this graph, proceeding to a loop from the node labeled by 1 back to the same node in k discrete steps. Hence taking an adjacency matrix to some power (left hand side of Eq. (4.1.1)) has also the interpretation of a partition function although of a different problem. In this problem, the disorder is time independent. This makes the connection between the two problems highly non trivial.

Besides, from the theory of tridiagonal random matrix ensembles, we know that a GOE or GUE matrix can also be constructed in a tridiagonal fashion, it is shown in Ref. [177] Proposition 1.7 that Eq. (4.1.1) also applies to tridiagonal matrices given in Eq. (2.1.4). Keeping in mind the adjacency matrix interpretation stated above, we can now represent the directed polymer not on a complete graph, but rather on one dimensional lattice closed at its ends with symmetric transition probability $\chi_{\beta i}$ between sites $(i \leftrightarrow i+1)$ and a probability $\mathcal{N}(0, \frac{2}{\beta})$ to remain at the same site. Such lattice and hopping rate are represented in Fig. 4.1. Another consequence of the result of Gorin and Sodin is that the partition function of the directed polymer on this one-dimensional lattice is equal in law to the partition function of a polymer in a space-time random environment which partition sum is the solution to the SHE (right hand side of Eq. (4.1.1)). We would like to highlight that this graph theoretical interpretation is highly non trivial and this could serve conversely as a cornerstone to map one-dimensional random hopping models to directed polymers on complete graphs with possible applications to stochastic spin chains.

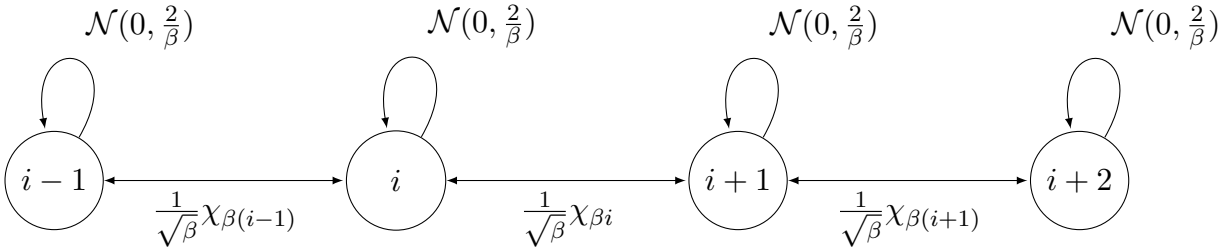

Figure 4.1: Representation of a random walk on a one dimensional lattice with symmetric transition probability χ distributed with parameters βi between sites $(i \leftrightarrow i+1)$ and a probability $\mathcal{N}(0, 2/\beta)$ to remain at the same site. We recall that the density of a χ variable with parameter $a > 0$ is $P(\chi) = \Theta(\chi) 2^{1-a/2}/\Gamma(a/2)\chi^{a-1}e^{-\chi^2/2}$ where Θ is the Theta Heaviside function.

To understand how this result arises, let us recall the two identities regarding the generating function of the solutions to the Stochastic Heat Equation $Z^{(\beta)}(0,t)$. For all $t > 0$ and $z \geqslant 0$,

- For $\beta = 2$,

$$\mathbb{E}_{\mathrm{KPZ}}\left[\exp(-zZ^{(\beta=2)}(0,t)e^{\frac{t}{12}})\right] = \mathbb{E}_{\mathrm{Ai},\beta=2}\left[\prod_{k=1}^{+\infty}\frac{1}{1+ze^{t^{1/3}a_k}}\right] \tag{4.1.2}$$

- For $\beta = 1$,

$$\mathbb{E}_{\mathrm{KPZ}}\left[\exp(-zZ^{(\beta=1)}(0,t)e^{\frac{t}{12}})\right] = \mathbb{E}_{\mathrm{Ai},\beta=1}\left[\prod_{k=1}^{+\infty}\frac{1}{\sqrt{1+4ze^{t^{1/3}a_k}}}\right] \tag{4.1.3}$$

The Theorem of Gorin and Sodin was proved showing an equality between the Laplace transform of both random variables of appearing in Eq. (4.1.1). From the point of view of random matrices, the important observation is that for GOE/GUE ensembles, the eigenvectors are independent from the spectrum. Besides, they are uniformly distributed on the unit sphere (of $\mathbb{R}^N$ for $\beta = 1$ and of $\mathbb{C}^N$ for $\beta = 2$) and as $N \to \infty$ their components become independent Gaussians, hence the squared norm of each component becomes χ^2 distributed with parameter β. Now, the key point to make Fermi factors appear is the following lemma:

Lemma 4.1.2 (*Laplace transform of χ^2 variables*)

Let $z \geqslant 0$ and χ_β be a random variable χ-distributed with parameter β. For the case of integer β, a χ^2_β variable corresponds to the sum of β squared standard Gaussians. Then we have the following Laplace transform:

$$\mathbb{E}[e^{-z\chi^2_\beta}] = \frac{1}{(1+2z)^{\frac{\beta}{2}}} \tag{4.1.4}$$

Remark 4.1.3. *If we read the fine lines of the paper of Gorin and Sodin, the "Fermi factor" is interpreted as the Laplace transform of the distribution of eigenvectors of the related random matrix. Hence, if one finds a solution to the Kardar-Parisi-Zhang equation that takes the form of a Fredholm determinant with the kernel of a usual matrix ensemble but with a different measure than the Fermi factor, then this solution will be related to a random matrix that can be constructed entirely based on the knowledge of the distribution of the eigenvectors (determined from the measure of the Fredholm determinant replacing the "Fermi factor") and the related spectrum (which correlation function is determined from the kernel of the Fredholm determinant).*

For completeness, we discuss the choice of scaling in the theorem of Gorin and Sodin. Using a spectral decomposition of the matrix M_N and denoting Ψ^j_a the a-th coordinate of the eigenvectors associated to the eigenvalue λ_a of M_N for $a \in [1, N]$, we have

$$\frac{N}{\beta}\left[\left(\frac{M_N^{(\beta)}}{2\sqrt{N}}\right)^{2\lfloor t^{1/3}N^{2/3}\rfloor}\right]_{1,1} = \frac{N}{\beta}\sum_{j=1}^{N}\left|\Psi^j_1\right|^2\left(\frac{\lambda_j}{2\sqrt{N}}\right)^{2\lfloor t^{1/3}N^{2/3}\rfloor} \tag{4.1.5}$$

As we have the convergence for large N of the eigenvalues to the Airy-β process $\lambda_j \simeq 2\sqrt{N} + a_j N^{-1/6}$, the eigenvalue factor converges towards $\left(\frac{\lambda_j}{2\sqrt{N}}\right)^{2\lfloor t^{1/3}N^{2/3}\rfloor} \simeq \exp(t^{1/3}a_j)$. The Laplace transform of the l.h.s of Eq. (4.1.5) is now easy to evaluate using the independence of $\left|\Psi^j\right|^2$ and a_j and the fact that $N|\Psi|^2$ is χ distributed with parameter β. We refer to Refs. [179, 180] for further details. Finally, the reason why the Theorem of Gorin and Sodin contains two terms shifted by a power one is to break the symmetry of the left and right edges of the spectrum to keep only the right one.

We would like to end the discussion on this surprising connexion between RMT and the KPZ equation with several open questions:

- The Theorem of Gorin and Sodin relates the element $(1, 1)$ of a GOE/GUE type matrix to the solution of the KPZ equation at position $x = 0$. Can this discussion be pursued further to obtain a position $x \neq 0$ of the KPZ solution and if yes, would this be translated in other elements of the matrix (such as (i, j)) ?

- Is there a possible interpretation of the multi-time joint distribution of $[M_N^{\lfloor 2t_1^{1/3}N^{2/3}\rfloor}]_{11}$ and $[M_N^{\lfloor 2t_2^{1/3}N^{2/3}\rfloor}]_{11}$? Similarly, is there an interpretation for the multi-space joint distribution of $[M_N^{\lfloor 2t^{1/3}N^{2/3}\rfloor}]_{ii}$ and $[M_N^{\lfloor 2t^{1/3}N^{2/3}\rfloor}]_{jj}$?
- Is there a similar interpretation or theorem using perturbed matrices such as the one of Baik, Ben Arous and Péché ? If yes, a possible candidate on the Kardar-Parisi-Zhang side would be the solution for the stationary initial condition.

4.2 Coincidence of Brownians walkers and exponential moments of KPZ

In this Section, we introduce another intriguing application of the exact solution to the Stochastic Heat Equation to some Brownian functional which we call the *coincidence time* of independent Brownian walkers. We refer to Ref. [3] for the further details on the calculations and some extensions and discussions not presented here.

To this aim, we consider a model of Brownian walkers identified to a Langevin evolution of particles of positions $x_i(\tau)$ on the time interval $\tau \in [0,t]$ such that

$$\dot{x}_i(\tau) = \eta_i(\tau) \;\text{ with }\; \langle \eta_i(\tau)\rangle = 0 \;\; \langle \eta_i(\tau)\eta_j(\tau')\rangle = 2D\delta_{i,j}\delta(\tau-\tau') \; . \tag{4.2.1}$$

and consider the case where the walkers start at $t=0$ from a single source $x_i(0)=x_0$ for $i \in [1,N]$. The time spent by the walkers in at a distance at most ℓ to each other is

$$T_N(\ell,t) = \sum_{i\neq j}^{N} \int_0^t \mathrm{d}\tau \; \Theta\left[\frac{\ell}{2} - |x_i(\tau)-x_j(\tau)|\right], \tag{4.2.2}$$

We are particularly interested in the limit where the length ℓ is small compared to all the other scales of the problem and therefore define in the limit $\ell \to 0$,

$$\mathcal{T}_N(t) = \lim_{\ell\to 0} \frac{1}{\ell} T_N(\ell,t) = \sum_{i\neq j}^{N} \int_0^t \delta[x_i(\tau)-x_j(\tau)]\mathrm{d}\tau \; . \tag{4.2.3}$$

We refer to this observable as the *coincidence time* of N random walkers, *i.e.* the amount of time that these independent particles spend crossing each other. Note however that $\mathcal{T}_N(t)$ does not have the dimension of a time, which is a usual property of the local time of a stochastic process [181–183]. Using the Brownian scaling, the process has a simple rescaling to the time interval $\tau \in [0,1]$, and we obtain the equality $\mathcal{T}_N(t=1) = \mathcal{T}_N = \frac{\mathcal{T}_N(t)}{\sqrt{t}}$. The N-dependence is what makes the problem highly non-trivial. Indeed, the case $N=2$ is solved easily by considering the process $z(\tau) = \frac{1}{\sqrt{2}}(x_1(\tau)-x_2(\tau))$ which is also a diffusion process of same diffusion coefficient D (which we take to be $D=1$),

$$\dot{z}(\tau) = \xi(\tau) \; , \;\; \text{with} \;\; \langle \xi(\tau)\rangle = 0 \;\; \langle \xi(\tau)\xi(\tau')\rangle = 2D\delta(\tau-\tau') \; . \tag{4.2.4}$$

The coincidence time $\mathcal{T}_2$ of the two Brownian particles can be expressed in terms of the local time $L_t(x)$ of the process $z(\tau)$ defined as $L_t(x) = \int_0^t \mathrm{d}\tau \delta(z(\tau)-x)$. Setting $x=0$, we obtain

$$L_t(0) = \int_0^t \mathrm{d}\tau \delta(z(\tau)) = \int_0^t \mathrm{d}\tau \delta\left(\frac{1}{\sqrt{2}}(x_1(\tau)-x_2(\tau))\right) = \frac{\mathcal{T}_2(t)}{\sqrt{2}} \; . \tag{4.2.5}$$

The joint Probability Distribution Function (PDF) of the local time $L_t(0) = L$ and the final position $z(t) = x_f$ was obtained by Borodin [182] and further exploited by Pitman [183]. However, as soon as $N = 3$, one cannot define independent processes for which our coincidence time is a simple observable. The goal of the remaining of this Section is to study the coincidence time for an arbitrary number N of walkers.

In particular, we study the PDF of $\mathcal{T}_N$ for two cases, Brownian motions and Brownian bridges. In the first case (Brownian motion) one defines the Moment Generating Function (MGF) $\langle e^{-c\mathcal{T}_N(t)}\rangle_{\mathbf{x}_0}$, where $\langle \dots \rangle_{\mathbf{x}_0}$ denotes the expectation value with respect to the PDF of $\mathcal{T}_N(t)$ for given initial conditions $\mathbf{x}(\tau = 0) = \mathbf{x}_0 = (x_0, \dots, x_0)$. This MGF can be expressed in the Feynman-Kač framework as an N-dimensional path integral

$$\langle e^{-c\mathcal{T}_N(t)}\rangle_{\mathbf{x}_0} = \int_{\mathbb{R}^N} \mathrm{d}\mathbf{y} Z_N(\mathbf{y}, t|\mathbf{x}_0; c) \ , \quad \text{with} \ , \tag{4.2.6}$$

$$Z_N(\mathbf{y}, t|\mathbf{x}_0; c) = \int_{\mathbf{x}(0)=\mathbf{x}_0}^{\mathbf{x}(t)=\mathbf{y}} \mathcal{D}\mathbf{x}(\tau)\ e^{-\int_0^t \left[\sum_{i=1}^N \frac{\dot{x}_i(\tau)^2}{4} + 2c\sum_{i<j}^N \delta[x_i(\tau) - x_j(\tau)]\right] \mathrm{d}\tau} \ , \tag{4.2.7}$$

where $\mathbf{x}(\tau) = (x_1(\tau), x_2(\tau), \cdots, x_N(\tau))$. As the final point $\mathbf{y}$ is arbitrary, we integrated here over all the possible realisations. In the second case (Brownian bridges) we define the MGF as the following expectation value with fixed initial and final positions

$$\langle e^{-c\mathcal{T}_N(t)}\rangle_{\mathbf{x}_0,\mathbf{y}} = \frac{Z_N(\mathbf{y}, t|\mathbf{x}_0; c)}{Z_N(\mathbf{y}, t|\mathbf{x}_0; c = 0)} \tag{4.2.8}$$

where $Z_N(\mathbf{y}, t|\mathbf{x}_0; c = 0) = (4\pi t)^{-N/2} e^{-(\mathbf{y}-\mathbf{x}_0)^2/(4t)}$ is the free propagator. This situation is depicted in Fig. 4.2. The function $Z_N(\mathbf{y}, t|\mathbf{x}_0; c)$ can be interpreted as the imaginary time N-body propagator of the bosonic Lieb-Liniger Hamiltonian [83]

$$-\partial_t Z_N = \hat{\mathcal{H}}_N(c) Z_N \ \text{ with } \ \hat{\mathcal{H}}_N(c) = \sum_{i=1}^N \hat{p}_i^2 + 2c\sum_{i<j}^N \delta(\hat{x}_i - \hat{x}_j) \ . \tag{4.2.9}$$

We therefore see that this MGF, eq. (4.2.8), for non-interacting diffusing classical particles is mapped onto the propagator of a quantum problem of identical bosons with a contact interaction and hence this problem is also related to the directed polymer in a random potential through the Stochastic Heat Equation and equivalently to the Kardar-Parisi-Zhang equation.

The MGF of our diffusion problem, or N independent Brownian bridges, and negative value of the parameter $c = -\bar{c}$ is thus related to the moments of the solution of the SHE as follows

$$\langle e^{\bar{c}\mathcal{T}_N(t)}\rangle_{\mathbf{0},\mathbf{0}} = \frac{\overline{\mathcal{Z}(0,0,t)^N}}{\mathcal{Z}_0(0,0,t)^N} \tag{4.2.10}$$

where $\mathcal{Z}_0(x, 0, t) = \frac{1}{\sqrt{4\pi t}} e^{-x^2/(4t)}$ is the free Brownian propagator (for $c = 0$). Note that all initial and final points here are set to 0. The moments of the solution of the SHE being the exponential moments of the solution of the KPZ equation, the connexion is now unveiled.

In the following, we will present exact formulae for the Laplace transform of the coincidence time $\langle e^{-c\mathcal{T}_N(t)}\rangle$ and we will denote the case of N independent Brownian bridges $\langle e^{-c\mathcal{T}_N(t)}\rangle_{\mathrm{BB}} \equiv \langle e^{-c\mathcal{T}_N(t)}\rangle_{\mathbf{0},\mathbf{0}}$, and the case of N Brownian motions all starting from, $x_0 = 0$, with free final points, $\langle e^{-c\mathcal{T}_N(t)}\rangle_{\mathrm{BM}} \equiv \langle e^{-c\mathcal{T}_N(t)}\rangle_{\mathbf{0}}$. We will be able to invert the Laplace transform in the two cases and to obtain the small and large T asymptotics of the PDF of $\mathcal{T}_N(t)$.

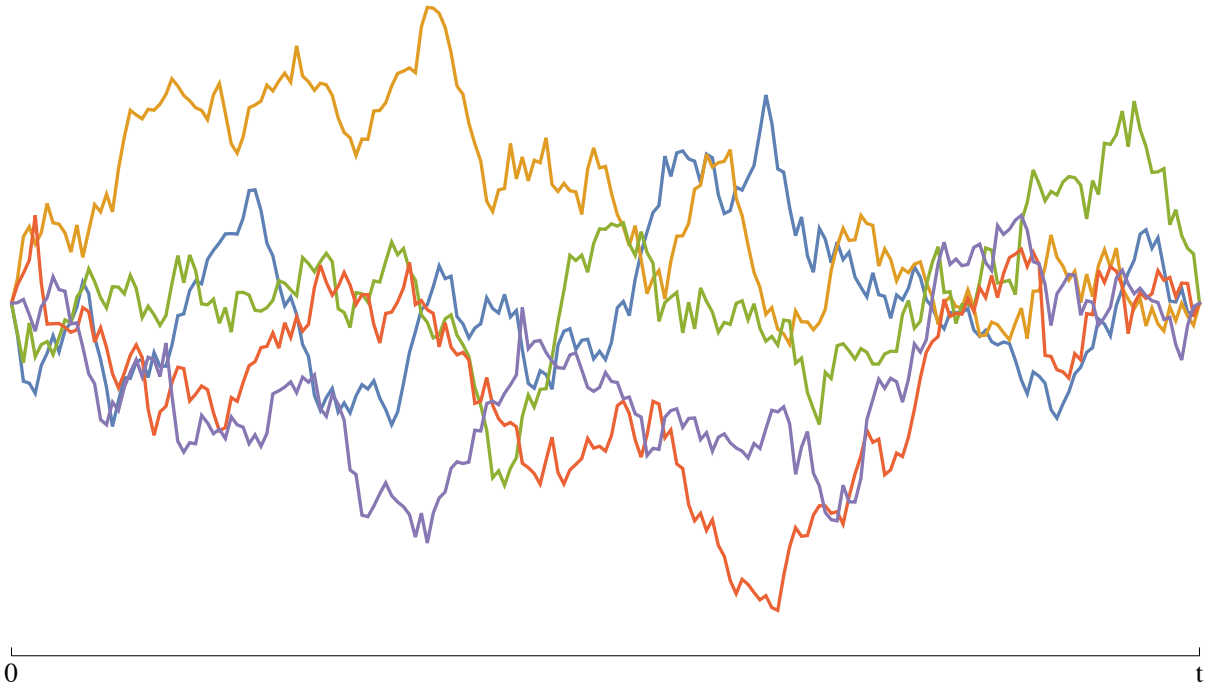

Figure 4.2: Plot of a simulation of $N = 5$ Brownian bridges for a diffusion coefficient $D = 1$ starting from $x_0 = (0; 0; 0)$ and endpoints in $y = (0; 0; 0)$.

4.2.1 Coincidence time for Brownian bridges and the KPZ equation with droplet initial conditions

The Lieb-Liniger Hamiltonian in Eq. (4.2.9) is exactly solvable using the Bethe ansatz. Here we need only the symmetric eigenstates of $\hat{\mathcal{H}}_N(c)$, which in the repulsive case $c > 0$, are single particle states. We recall here that the eigen-energies $E_{\mathbf{k}}$ of this system form a continuum indexed by N real momenta $\{k_i\}$'s such that

$$\hat{\mathcal{H}}_N(c)|\Psi^c_{\mathbf{k}}\rangle = E_{\mathbf{k}}|\Psi^c_{\mathbf{k}}\rangle\ , \quad \text{with} \quad E_{\mathbf{k}} = \mathbf{k}^2 = \sum_{i=1}^{N} k_i^2\ , \tag{4.2.11}$$

$$\langle \mathbf{x}|\Psi^c_{\mathbf{k}}\rangle = \frac{C^c_{\mathbf{k}}}{N!}\sum_{\sigma\in S_N}\prod_{i<j}\left(1 - \frac{ic\,\mathrm{sign}(x_j - x_i)}{k_{\sigma(j)} - k_{\sigma(i)}}\right) e^{i\sum_{j=1}^{N} x_j k_{\sigma(j)}}\ , \tag{4.2.12}$$

$$C^c_{\mathbf{k}} = \left(\prod_{i<j}\frac{(k_i - k_j)^2}{(k_i - k_j)^2 + c^2}\right)^{1/2}\ . \tag{4.2.13}$$

where the $|\Psi^c_{\mathbf{k}}\rangle$ denote the eigenstates of $\hat{\mathcal{H}}_N(c)$. The calculation is similar to the one in Refs. [73, 74] except that we retain here for $c > 0$ only the particle states, meaning that the momenta $\{k_i\}$ are real and do not carry a complex component. Consider the imaginary time propagator at coinciding endpoints

$$Z_N(\mathbf{0}, t|\mathbf{0}; c) = \langle \mathbf{0}|e^{-\hat{\mathcal{H}}_N(c)t}|\mathbf{0}\rangle = \int_{\mathbb{R}^N}\frac{\mathrm{d}\mathbf{k}}{(2\pi)^N}\langle \mathbf{0}|\Psi^c_{\mathbf{k}}\rangle\langle\Psi^c_{\mathbf{k}}|\mathbf{0}\rangle e^{-E_{\mathbf{k}}t}\ . \tag{4.2.14}$$

Using that $\langle \mathbf{0}|\Psi_{\mathbf{k}}^{c}\rangle = C_{\mathbf{k}}^{c}$, we arrive at the following Laplace transform for the PDF of the coincidence time for N Brownian bridges

$$\langle e^{-c\mathcal{T}_N(t)}\rangle_{\mathrm{BB}} = (4\pi t)^{\frac{N}{2}} \int_{\mathbb{R}^N} \frac{\mathrm{d}\mathbf{k}}{(2\pi)^N} e^{-\mathbf{k}^2 t} \prod_{i<j} \frac{(k_i-k_j)^2}{(k_i-k_j)^2+c^2} \,. \tag{4.2.15}$$

where we have divided by the result at $c=0$ which coincides with the free propagator $Z_N(\mathbf{0},t|\mathbf{0};0) = (4\pi t)^{-\frac{N}{2}}$ to ensure that the l.h.s is equal to unity when c is zero.

Remark 4.2.1. *There is an alternative formula for the moments of the directed polymer problem, which was derived using Macdonald processes, see Refs. [42, 184].*

Having determined the Laplace transform of the coincidence time of the N Brownian bridges, we now pursue and obtain from Eq. (4.2.15) an expression for the PDF of their coincidence time. To this aim, we first first recall the Cauchy identity

$$\prod_{i<j} \frac{(k_i-k_j)^2}{(k_i-k_j)^2+c^2} = \det_{1\leqslant \ell,m\leqslant N} \left(\frac{c}{c+i(k_\ell-k_m)} \right) \tag{4.2.16}$$

Expanding the determinant as a sum over permutations and exponentiating each denominator by introducing auxiliary variables $\mathbf{r} = (r_1,\cdots,r_N)$ yields

$$\prod_{i<j} \frac{(k_i-k_j)^2}{(k_i-k_j)^2+c^2} = c^N \sum_{\sigma\in S_N} \mathrm{sign}(\sigma) \int_{\mathbb{R}_+^N} \mathrm{d}\mathbf{r}\; e^{-c\sum_\ell r_\ell} \prod_{\ell=1}^{N} e^{-ik_\ell(r_\ell - r_{\sigma(\ell)})} \,. \tag{4.2.17}$$

Proceeding to the replacement of the integrand of Eq. (4.2.15), we are able to compute the integrals over the momenta $\mathbf{k}$ and sum back over all permutations, yielding

$$\langle e^{-c\mathcal{T}_N(t)}\rangle_{\mathrm{BB}} = c^N \int_{\mathbb{R}_+^N} \mathrm{d}\mathbf{r}\; e^{-c\sum_\ell r_\ell} \det_{1\leqslant i,j\leqslant N} \left(e^{-\frac{(r_i-r_j)^2}{4t}} \right) \tag{4.2.18}$$

The inversion of the Laplace transform is now straightforward, and we conclude this calculation by giving the PDF $P_{N,\mathrm{BB}}(T)$ of the rescaled coincidence time $\mathcal{T}_N = \mathcal{T}_N(t=1)$.

Result 4.2.2 (*PDF of the coincidence time for N Brownian bridges*)

The probability distribution function of the coincidence time of N independent Brownian bridges is given by

$$P_{N,\mathrm{BB}}(T) = \partial_T^{N+1} \int_{\mathbb{R}_+^N} \mathrm{d}\mathbf{r}\; \Theta\left(T - \sum_{\ell=1}^{N} r_\ell \right) \det_{1\leqslant i,j\leqslant N} \left(e^{-\frac{(r_i-r_j)^2}{4}} \right) \tag{4.2.19}$$

Having the full distribution $P_{N,\mathrm{BB}}(T)$ of the rescaled coincidence time $\mathcal{T}_N = \mathcal{T}_N(t)/\sqrt{t}$, we now investigate for arbitrary N its tails respectively for small $T\to 0$ and large $T\to\infty$.

To obtain the small T limit of $P_{N,\mathrm{BB}}(T)$, it is convenient to consider the $c\to+\infty$ limit of the Laplace transform $\langle e^{-c\mathcal{T}_N}\rangle_{\mathrm{BB}}$, which is given in Eq. (4.2.15). The interpretation of such consideration is that the trajectories of Brownian bridges which contribute to a small coincidence time are repelled from each others. In the Lieb-Liniger picture, this is consistent with the repulsive case where the states are described as single particle states rather than bound state, meaning that each particle has own momentum that does not carry a complex part. Taking the large $c\to+\infty$ limit of Eq. (4.2.15), we obtain

$$\langle e^{-c\mathcal{T}_N}\rangle_{\mathrm{BB}} \approx \pi^{-\frac{N}{2}} c^{-N(N-1)} \int_{\mathbb{R}^N} \mathrm{d}\mathbf{k} e^{-\mathbf{k}^2} \prod_{i<j} (k_i-k_j)^2 = 2^{-\frac{N(N-1)}{2}} \frac{G(N+2)}{c^{N(N-1)}} \,, \tag{4.2.20}$$

where $G(n) = \prod_{k=1}^{n-2} k!$ is the Barnes G function and where have used the Mehta integral formula e.g. (1.5)-(1.6) in [185]. Inverting this approximate Laplace transform, we obtain the small T behavior of the PDF of $P_{N,\mathrm{BB}}(T)$ as

Result 4.2.3 (*Small T limit of the PDF of the coincidence time of Brownian bridges*)

The small T limit of the PDF $P_{N,\mathrm{BB}}(T)$ is given by

$$P_{N,\mathrm{BB}}(T) \underset{T\to 0}{=} 2^{-\frac{N(N-1)}{2}} \frac{G(N+2)}{\Gamma(N(N-1))} T^{N(N-1)-1} + \mathcal{O}(T^{N(N-1)+1}). \tag{4.2.21}$$

We now turn to the large T limit of $P_{N,\mathrm{BB}}(T)$ and in this case, we need to investigate the $c \to -\infty$ limit of the expectation $\langle e^{-c\mathcal{T}_N}\rangle_{\mathrm{BB}}$ which is dominated by large values of $\mathcal{T}_N$. The trajectories which contribute to a large coincidence time are attracted to each others. In the Lieb-Liniger picture, this corresponds to the attractive case, where particles form bound states called strings, in which the momenta of the particles share the same real part but also have a quantized imaginary part. Upon increasing $\bar{c} = -c$, the potential becomes more and more attractive and the trajectories become dominated by the configuration where all particles are bounded into a single string.

Mathematically, for $c = -\bar{c} < 0$ the expression of the moments of the directed polymer partition function is more involved as it involves a sum over string states, see the extensive list of publications [42, 73, 74, 186] on this topic for further details. Nonetheless, in the limit $\bar{c} \to +\infty$, the energy spectrum of the Lieb-Liniger model is dominated by its ground state which is a single string containing all particles with energy $E_0(N) = -\bar{c}^2 \frac{N(N^2-1)}{12}$. It follows from the contribution of the ground state to the moment (see for instance Eqs. (65-66) in the Supp. Mat. of Ref. [187] replacing t by $\bar{c}^2 t$ and multiplying by c^N) that

$$\langle e^{-c\mathcal{T}_N}\rangle_{\mathrm{BB}} = \frac{N!(4\pi)^{\frac{N-1}{2}}}{N^{3/2}} \bar{c}^{N-1} e^{\bar{c}^2 \frac{N(N^2-1)}{12}} \left[1 + \mathcal{O}(e^{-\frac{1}{4}N(N-1)\bar{c}^2})\right] \tag{4.2.22}$$

This behavior is consistent with the following $T \to \infty$ asymptotics:

Result 4.2.4 (*Large T limit of the PDF of the coincidence time of Brownian bridges*)

The large T asymptotics of the PDF $P_{N,\mathrm{BB}}(T)$ is given by

$$P_{N,\mathrm{BB}}(T) \underset{T\to\infty}{=} \frac{N!2^{N-1}\pi^{\frac{N}{2}-1}}{N^{3/2}} \sqrt{\alpha_N} (-\partial_T)^{N-1} e^{-\alpha_N T^2} + \mathcal{O}(e^{-\beta_N T^2}) \tag{4.2.23}$$

$$= \frac{N!2^{N-1}\pi^{\frac{N}{2}-1}}{N^{3/2}} \alpha_N^{\frac{N}{2}} H_{N-1}\left(\sqrt{\alpha_N} T\right) e^{-\alpha_N T^2} + \mathcal{O}(e^{-\beta_N T^2}) \,, \tag{4.2.24}$$

where $H_p(x) = e^{x^2}(-\partial_x)^p e^{-x^2}$ is the Hermite polynomial of degree p. The exponential factors are equal to

$$\alpha_N = \frac{3}{N(N^2-1)}, \qquad \beta_N = \frac{3}{N^3 - 3N^2 + 2N} \tag{4.2.25}$$

This is in particular verified by calculating the Laplace transform of the aproximate PDF of Eq. (4.2.23) using a saddle point approximation. The saddle point $T^* = \bar{c}(2\alpha_N)^{-1} > 0$ is therefore on the contour of integration for $\bar{c} = -c > 0$ making our approximations valid.

In addition to the asymptotics, we calculated in Ref. [3] the mean and variance of the coincidence time for N Brownian bridges, the result is the following:

Result 4.2.5 (*Mean value and variance of $\mathcal{T}_{N,\mathrm{BB}}$*)

The mean value of coincidence time for Brownian bridges with diffusion coefficient $D = 1$ is

$$\langle \mathcal{T}_N \rangle_{\mathrm{BB}} = \frac{N(N-1)}{2}\sqrt{\frac{\pi}{2}}. \tag{4.2.26}$$

The variance of the coincidence time for Brownian bridges with diffusion coefficient $D = 1$ is

$$\mathrm{Var}\left(\mathcal{T}_N\right)_{\mathrm{BB}} = N(N-1)(N-2)\left[\frac{8\pi}{9\sqrt{3}} - \frac{\pi}{2}\right] + N(N-1)\left[1 - \frac{\pi}{4}\right]. \tag{4.2.27}$$

4.2.2 Coincidence time for Brownian motions and the KPZ equation with flat initial condition

We now turn to the case of the Brownian motion, where the final points are not fixed (i.e. they are integrated upon). This is connected to the directed polymer problem with one free endpoint and equivalently to the Kardar-Parisi-Zhang equation with a flat initial condition. A solution for the latter was given in Refs. [76]. As in the case of the Brownian bridges, we shall use the solution to the KPZ equation both for $c > 0$ and $c < 0$. Since the calculation of the moments of solution to the SHE for flat initial is quite intricate and involves first the half-flat initial condition, we start by recalling some results on the half-flat solution first. The half-flat initial condition corresponds for our problem to N Brownians all starting at 0 and ending on a given half line.

Let us discuss the Bethe ansatz solution of the Lieb-Liniger model for half-flat initial condition. To this aim, consider the partition sum of the directed polymer with half-flat initial condition

$$\mathcal{Z}_w(x,t) = \int_{-\infty}^{0} \mathrm{d}y e^{wy} \mathcal{Z}(x,y,t) \tag{4.2.28}$$

From Eq (52) in [119], or Eq. (88) in [76], we have the following: restoring the factors of $\bar{c}$ (by a change of units), with $c = -\bar{c}$, restricting to $c \geqslant 0$ and retaining only the single particle states (as they are the only states of the repulsive Lieb-Liniger model, this is the same argument as for the Brownian bridges), we obtain

$$\overline{\mathcal{Z}_w(x,t)^N} = \prod_{j=1}^{N} \int_{\mathbb{R}} \frac{\mathrm{d}k_j}{2\pi} \frac{e^{-k_j^2 t - i x k_j}}{i k_j + w} \prod_{1 \leqslant i < j \leqslant N} \frac{(k_i - k_j)^2}{(k_i - k_j)^2 + c^2} \frac{i k_i + i k_j + 2w + c}{i k_i + i k_j + 2w} \tag{4.2.29}$$

From this we obtain the Laplace transform of the coincidence time of N Brownian walkers which start at a position x and reach the negative half line $]-\infty, 0]$, as

$$\langle e^{-c\mathcal{T}_N} \rangle_{\mathrm{half-BM}} = \frac{\overline{\mathcal{Z}_w(x,t)^N}}{\mathcal{Z}_w^0(x,t)^N} \quad , \quad \mathcal{Z}_w^0(x,t) = \int_{\mathbb{R}} \frac{\mathrm{d}k}{2\pi} \frac{e^{-k^2 t - i x k}}{i k + w} \tag{4.2.30}$$

Remark 4.2.6. *The extra weight e^{wx} is a regularization prescription and it will be considered in the limit $w = 0^+$.*

The knowledge of the half-flat initial condition is actually enough to get information for the flat case: indeed, as was shown in Refs. [76] the flat initial conditions can be viewed as a certain limit of the half-flat. More particularly, the moments of the partition function of the directed

polymer with one free endpoint i.e. $\mathcal{Z}_{\text{flat}}(t) = \int_{\mathbb{R}} \mathrm{d}y \mathcal{Z}(x,y,t)$, associated to the Kardar-Parisi-Zhang equation with flat initial condition, can be obtained from the ones for the half-flat initial condition in the double limit $x \to -\infty$ and $w \to 0^+$. We refer the readers to Ref. [76] for the fine details on this double limit. Taking the language of the Bethe ansatz, in this double limit only paired strings and strings with zero momenta remain: this then provides the Laplace transform of the coincidence time of unconstrained Brownians walkers all starting at 0.

After having taken the double limit and using the formulae for the moments of Refs. [76], we determine that the Laplace transform of the coincidence time of N Brownian motions depends on the parity of N as:

For N even

$$\langle e^{-c\mathcal{T}_N}\rangle_{\text{BM}} = \frac{(2c)^{\frac{N}{2}}N!}{(\frac{N}{2})!}\prod_{p=1}^{\frac{N}{2}}\int_{\mathbb{R}}\frac{\mathrm{d}k_p}{2\pi}\frac{e^{-2k_p^2}}{4k_p^2+c^2}\prod_{1\leqslant p<q\leqslant\frac{N}{2}}\frac{(k_p-k_q)^2}{(k_p-k_q)^2+c^2}\frac{(k_p+k_q)^2}{(k_p+k_q)^2+c^2} \tag{4.2.31}$$

For N odd

$$\langle e^{-c\mathcal{T}_N}\rangle_{\text{BM}} = \frac{(2c)^{\frac{N-1}{2}}N!}{(\frac{N-1}{2})!}\prod_{p=1}^{\frac{N-1}{2}}\int_{\mathbb{R}}\frac{\mathrm{d}k_p}{2\pi}\frac{k_p^2e^{-2k_p^2}}{(k_p^2+c^2)(4k_p^2+c^2)}\prod_{1\leqslant p<q\leqslant\frac{N-1}{2}}\frac{(k_p-k_q)^2}{(k_p-k_q)^2+c^2}\frac{(k_p+k_q)^2}{(k_p+k_q)^2+c^2} \tag{4.2.32}$$

These results are obtained from Eq. (108) in [76] by noting that for $c > 0$ and N even only particle states (meaning each particle carries its own real momentum) with paired momenta $(k_1, -k_1, \ldots, k_{N/2}, -k_{-N/2})$ contribute, while for N odd there are $N-1$ paired momenta and one zero momentum. This is the reason why the parity of N plays a role.

As in the case of Brownian bridges, we manipulate the Laplace transform to be able to invert it. In the following, we will indeed obtain from Eqs. (4.2.31) and (4.2.32) an expression for the PDF of the coincidence time for N Brownian motions. Nonetheless, the calculation is more intricate than for the Brownian bridges as it will involve Pfaffians rather than determinants. We first carry the calculation for N even and then we will pursue with the odd case.

For N even For $p \in [1, N/2]$, we define the conjugate variables

$$X_{2p} = c - 2ik_p, \quad X_{2p-1} = c + 2ik_p \tag{4.2.33}$$

and rewrite the factor coupling different momenta in terms of these variables,

$$\frac{(k_p-k_q)^2}{(k_p-k_q)^2+c^2}\frac{(k_p+k_q)^2}{(k_p+k_q)^2+c^2} = \frac{(X_{2q}-X_{2p})(X_{2q-1}-X_{2p-1})(X_{2q-1}-X_{2p})(X_{2q}-X_{2p-1})}{(X_{2p}+X_{2q})(X_{2p-1}+X_{2q-1})(X_{2p-1}+X_{2q})(X_{2p}+X_{2q-1})}. \tag{4.2.34}$$

Then using the explicit values of X_{2p} and X_{2p-1}, one rewrites Eq. (4.2.31) as

$$\langle e^{-c\mathcal{T}_N}\rangle_{\text{BM}} = \frac{c^N N!}{(\frac{N}{2})!}\prod_{p=1}^{\frac{N}{2}}\int_{\mathbb{R}}\frac{\mathrm{d}k_p}{2\pi}\frac{ie^{-2k_p^2}}{k_p}\prod_{p=1}^{N}\frac{1}{X_p}\prod_{1\leqslant p<q\leqslant N}\frac{X_q-X_p}{X_q+X_p} \tag{4.2.35}$$

Using formulae (9.1) and (9.4) from Bruijn, see Ref. [167], we write the last part of (4.2.35) as a form that is amenable to a Laplace inversion

$$\prod_{p=1}^{N}\frac{1}{X_p}\prod_{1\leqslant p<q\leqslant N}\frac{X_q-X_p}{X_q+X_p} = \int_{\mathbb{R}_+^N}\mathrm{d}\mathbf{r}\, e^{-c\sum_\ell r_\ell}\prod_{1\leqslant k<\ell\leqslant N}\text{sign}(r_k-r_\ell)\prod_{p=1}^{\frac{N}{2}}e^{-2ik_p(r_{2p-1}-r_{2p})} \tag{4.2.36}$$

From this identity, after anti-symmetrizing the last exponential with respect to r_{2p} and r_{2p-1} we obtain for the Laplace transform of the coincidence time the following expression

$$\begin{aligned}
&\langle e^{-c\mathcal{T}_N}\rangle_{\mathrm{BM}} \\
&= \frac{c^N N!}{(\frac{N}{2})!}\int_{\mathbb{R}_+^N} \mathrm{d}\mathbf{r}\; e^{-c\sum_\ell r_\ell} \prod_{1\leqslant k<\ell\leqslant N} \mathrm{sign}(r_k - r_\ell) \prod_{p=1}^{\frac{N}{2}} \int_{\mathbb{R}} \frac{\mathrm{d}k_p}{2\pi} e^{-2k_p^2} \frac{\sin(2k_p(r_{2p-1}-r_{2p}))}{k_p} \\
&= \frac{c^N N!}{2^{\frac{N}{2}}(\frac{N}{2})!}\int_{\mathbb{R}_+^N} \mathrm{d}\mathbf{r}\; e^{-c\sum_\ell r_\ell} \prod_{1\leqslant k<\ell\leqslant N} \mathrm{sign}(r_k - r_\ell) \prod_{p=1}^{\frac{N}{2}} \mathrm{erf}\left(\frac{r_{2p-1}-r_{2p}}{\sqrt{2}}\right)
\end{aligned} \tag{4.2.37}$$

where we computed the integral w.r.t $\{k_p\}$'s. The final trick consists in *(i)* changing the labels in the r variables in the error function from r_{2p} to $r_{\sigma(2p)}$ where σ belongs to the symmetric group S_N, *(ii)* using the fact that there are $N!/(2^{N/2}(N/2)!)$ ways of pairing N objects (N is even) and *(iii)* using the definition of the Pfaffian of an anti-symmetric matrix $\mathrm{Pf}(A) = \sum_{\sigma\in S_N, \sigma(2p-1)<\sigma(2p)} \mathrm{sign}(\sigma) \prod_{p=1}^{N/2} A_{\sigma(2p-1),\sigma(2p)}$ to finally obtain

$$\langle e^{-c\mathcal{T}_N}\rangle_{\mathrm{BM}} = c^N \int_{\mathbb{R}_+^N} \mathrm{d}\mathbf{r}\; e^{-c\sum_\ell r_\ell} \prod_{1\leqslant k<\ell\leqslant N} \mathrm{sign}(r_k - r_\ell) \underset{1\leqslant k,\ell\leqslant N}{\mathrm{Pf}} \left[\mathrm{erf}\left(\frac{r_k - r_\ell}{\sqrt{2}}\right)\right] \tag{4.2.38}$$

The Laplace inversion is now as straightforward as in the Brownian case and we obtain the PDF $P_{N,\mathrm{BM}}(T)$ of the rescaled coincidence time $\mathcal{T}_N = \mathcal{T}_N(t=1)$ as:

Result 4.2.7 (*PDF of the coinidence time for N even Brownian motions*)

The probability distribution function of the coincidence time of N (even) independent Brownian motions is given by

$$P_{N,\mathrm{BM}}(T) = \partial_T^{N+1} \int_{\mathbb{R}_+^N} \mathrm{d}\mathbf{r}\; \Theta\left(T - \sum_{\ell=1}^N r_\ell\right) \prod_{1\leqslant k<\ell\leqslant N} \mathrm{sign}(r_k - r_\ell) \underset{1\leqslant k,\ell\leqslant N}{\mathrm{Pf}} \left[\mathrm{erf}\left(\frac{r_k - r_\ell}{\sqrt{2}}\right)\right] \tag{4.2.39}$$

Remark 4.2.8. *Even though the product of sign functions can itself be written as a Pfaffian, we have not tried to simplify further Eq.* (4.2.39).

We now pursue with the odd case.

For N odd For $p \in [1, (N-1)/2]$, define the conjugate variables

$$X_{2p} = c - 2ik_p, \quad X_{2p-1} = c + 2ik_p, \quad X_N = c \tag{4.2.40}$$

Then, in a similar fashion as the even N case, one rewrites the Laplace transform for the odd N case Eq. (4.2.32) as

$$\langle e^{-c\mathcal{T}_N}\rangle_{\mathrm{BM}} = \frac{c^N N!}{(\frac{N-1}{2})!} \prod_{p=1}^{\frac{N-1}{2}} \int_{\mathbb{R}} \frac{\mathrm{d}k_p}{2\pi} \frac{i e^{-2k_p^2}}{k_p} \prod_{p=1}^{N} \frac{1}{X_p} \prod_{1\leqslant p<q\leqslant N} \frac{X_q - X_p}{X_q + X_p} \tag{4.2.41}$$

By the same argument as in the even N case, using Bruijn's results of Ref. [167], the Laplace transform of the coincidence time is written in a form amenable to inversion as

$$\langle e^{-c\mathcal{T}_N}\rangle_{\mathrm{BM}} = \frac{c^N N!}{2^{\frac{N-1}{2}}(\frac{N-1}{2})!} \int_{\mathbb{R}_+^N} \mathrm{d}\mathbf{r}\; e^{-c\sum_\ell r_\ell} \prod_{1\leqslant k<\ell\leqslant N} \mathrm{sign}(r_k - r_\ell) \prod_{p=1}^{\frac{N-1}{2}} \mathrm{erf}\left(\frac{r_{2p-1}-r_{2p}}{\sqrt{2}}\right) \tag{4.2.42}$$

We have to be careful in the odd case as there are N variables r but only $N-1$ of them are involved in the error functions whereas all N variables are involved in the product of sign functions. We now wish to employ the same Pfaffian trick as the even N case and hence have to consider all $(N-1)!/(2^{\frac{N-1}{2}}(\frac{N-1}{2})!)$ ways of pairings $N-1$ objects. Hence, we obtain our final expression for the Laplace transform in the odd N case

$$\langle e^{-c\mathcal{T}_N}\rangle_{\rm BM} = Nc^N \int_{\mathbb{R}_+^N} {\rm d}\mathbf{r}\; e^{-c\sum_\ell r_\ell} \prod_{1\leqslant k<\ell\leqslant N} {\rm sign}(r_k-r_\ell) \underset{1\leqslant k,\ell\leqslant N-1}{\rm Pf}\left[{\rm erf}\left(\frac{r_k-r_\ell}{\sqrt{2}}\right)\right] \tag{4.2.43}$$

Once again, the inversion is straightforward and we obtain the PDF $P_{N,\rm BM}(T)$ of the rescaled coincidence time $\mathcal{T}_N = \mathcal{T}_N(t=1)$ as

Result 4.2.9 (*PDF of the coinidence time for N odd Brownian motions*)

The probability distribution function of the coincidence time of N (odd) independent Brownian motions is given by

$$P_{N,\rm BM}(T) = N\partial_T^{N+1}\int_{\mathbb{R}_+^N} {\rm d}\mathbf{r}\;\Theta\left(T-\sum_{\ell=1}^N r_\ell\right)\prod_{1\leqslant k<\ell\leqslant N}{\rm sign}(r_k-r_\ell)\underset{1\leqslant k,\ell\leqslant N-1}{\rm Pf}\left[{\rm erf}\left(\frac{r_k-r_\ell}{\sqrt{2}}\right)\right] \tag{4.2.44}$$

As for the Brownian bridges, having the full distribution $P_{N,\rm BM}(T)$ of the rescaled coincidence time $\mathcal{T}_N = \mathcal{T}_N(t)/\sqrt{t}$ for Brownian motions, we now investigate for arbitrary N its tails respectively for small $T\to 0$ and large $T\to\infty$.

We first discuss the small T behavior of the PDF $P_{N,\rm BM}(T)$ of $\mathcal{T}_N = \mathcal{T}_N(t)/\sqrt{t}$. It can be extracted from the $c\to+\infty$ limit of $\langle e^{-c\mathcal{T}_N}\rangle_{\rm BM}$ as for the Brownian bridges. When c is increased, the interaction in the Lieb-Liniger model becomes more repulsive and the corresponding Brownian trajectories with small coincidence time are those where none of the Brownian are bounded together. Taking the large $c\to+\infty$ limit of Eqs. (4.2.31) and (4.2.32) we see that the leading term is in all cases $c^{-N(N-1)/2}$. Inverting the effective Laplace transform, we obtain the small T behavior of $P_{N,\rm BM}(T)$ as

Result 4.2.10 (*Small T limit of the PDF of the coincidence time of Brownian motions*)

The small T limit of the PDF $P_{N,\rm BM}(T)$ is given by

$$P_{N,\rm BM}(T) \underset{T\to 0}{=} I_N T^{\frac{N(N-1)}{2}-1} + \mathcal{O}(T^{\frac{N(N-1)}{2}+1}), \tag{4.2.45}$$

where I_N is determined as

$$I_N = \frac{1}{2^{\frac{N(N-1)}{4}}\Gamma(\frac{N(N-1)}{2})}(\frac{2}{\sqrt{\pi}})^N\prod_{j=1}^N\Gamma(1+\frac{j}{2}) \tag{4.2.46}$$

It is quite surprising that the small T limit does not depend on the parity of N bearing in mind that all other formulae do. From the $c\to+\infty$ limit, the factors I_N do appear differently for N even and odd but at the end of the calculation they coincide to a formula that do not depend on the parity of N. Indeed, we see that

For N even

$$I_N = \frac{2^{\frac{N}{2}} N!}{(\frac{N}{2})!\Gamma\left(\frac{N(N-1)}{2}\right)} \prod_{p=1}^{\frac{N}{2}} \int_{\mathbb{R}} \frac{\mathrm{d}k_p}{2\pi} e^{-2k_p^2} \prod_{1\leqslant p<q\leqslant \frac{N}{2}} (k_p^2 - k_q^2)^2 \tag{4.2.47}$$

For N odd

$$I_N = \frac{2^{\frac{N-1}{2}} N!}{(\frac{N-1}{2})!\Gamma\left(\frac{N(N-1)}{2}\right)} \prod_{p=1}^{\frac{N-1}{2}} \int_{\mathbb{R}} \frac{\mathrm{d}k_p}{2\pi} k_p^2 e^{-2k_p^2} \prod_{1\leqslant p<q\leqslant \frac{N-1}{2}} (k_p^2 - k_q^2)^2. \tag{4.2.48}$$

The k integrals are typical examples of Selberg-Mehta integrals, and further details can be found in Ref. [185] in Section 1.4 or Formulae (1.5)-(1.6). In both cases, the calculation yields the result of Eq. (4.2.46).

Similarly to the Brownian bridges, we determine the large T tail of the PDF $P_{N,\mathrm{BB}}(T)$ of $\mathcal{T}_N = \mathcal{T}_N(t)/\sqrt{t}$ by investigating the $c \to -\infty$ limit of the Lieb-Liniger model. It again determined by the same ground state as for the Brownian bridges. From Eqs. (65-66) of Ref. [187], it follows that the Laplace transform in the $c \to -\infty$ limit reads

$$\langle e^{-c\mathcal{T}_N} \rangle_{\mathrm{BM}} = 2^{N-1} e^{\tilde{c}^2 \frac{N(N^2-1)}{12}} \left[1 + \mathcal{O}(e^{-\frac{1}{4}N(N-1)\tilde{c}^2})\right] \tag{4.2.49}$$

This behavior is consistent with the following $T \to \infty$ asymptotics:

Result 4.2.11 (*Large T limit of the PDF of the coincidence time of Brownian motions*)

The large T asymptotics of the PDF $P_{N,\mathrm{BM}}(T)$ is given by

$$P_{N,\mathrm{BM}}(T) \underset{T\to\infty}{=} 2^N \sqrt{\frac{\alpha_N}{4\pi}} e^{-\alpha_N T^2} + \mathcal{O}(e^{-\beta_N T^2}) \tag{4.2.50}$$

with the exponential factors again given by eqs. (4.2.25), i.e. $\alpha_N = \frac{3}{N(N^2-1)}$ and $\beta_N = \frac{3}{N^3-3N^2+2N}$.

Finally, in addition to the asymptotics, we calculated in Ref. [3] the mean and variance of the coincidence time for N Brownian motions, the result is the following:

Result 4.2.12 (*Mean value and variance of $\mathcal{T}_{N,\mathrm{BM}}$*)

The mean value of coincidence time of N independent Brownian motions with diffusion coefficient $D = 1$ is

$$\langle \mathcal{T}_N \rangle_{\mathrm{BM}} = \frac{N(N-1)}{2}\sqrt{\frac{2}{\pi}}. \tag{4.2.51}$$

The variance of the coincidence time for Brownian motions with diffusion coefficient $D = 1$ is

$$\mathrm{Var}\left(\mathcal{T}_N\right)_{\mathrm{BM}} = N(N-1)(N-2)\left[\frac{2}{3} - \frac{2}{\pi}\right] + N(N-1)\left[\frac{1}{2} - \frac{1}{\pi}\right]. \tag{4.2.52}$$

In conclusion, we have investigated the probability distribution function $P_N(T)$ of the total pairwise coincidence time $\mathcal{T}_N = T$ of N independent Brownian walkers in one dimension. Our main results have been obtained for two special geometries: *(i)* Brownian motions (BM) starting from the same point 0 and *(ii)* Brownian bridges (BB). We have obtained explicit expressions for the moment generating function (MGF), i.e. the expectation of $e^{-c\mathcal{T}_N}$. We have mapped, through

a Feynman-Kač path integral representation, the determination of the MGF to the calculation of a Green function in the Lieb-Liniger model of quantum particles interacting with a pairwise delta interaction. Restricting to Brownians all starting all at 0 allows to consider only bosonic states, i.e. the delta Bose gas. For $c > 0$ the MGF is the standard Laplace transform of $P_N(T)$, for which we obtained a formula for any N using the eigenstate (spectral) decomposition of the repulsive Bose gas. A Laplace inversion then led us to a compact formula for $P_N(T)$ for each geometry, one involving a determinant (for the BB) and the other one a Pfaffian (for the BM). We have shown that for $c < 0$ the MGF is related to the exponential moments of the one dimensional Kardar-Parisi-Zhang (KPZ) equation, equivalently to the moments of the directed polymer in a random potential. These moments are calculated using a summation over the eigenstates of the attractive Lieb-Liniger model. These include bound states called strings. Here we obtained the large T asymptotics of $P_N(T)$ from the contribution of the ground state of the Lieb-Liniger model, for the BB and the BM. Our main result is that the PDF of the coincidence time has a universal decay at large T, of the form $P_N(T) \sim \exp(-3T^2/(N^3 - N))$, and only the pre-exponential factor depends on the geometry. For the BB we used the connection to the droplet solution of the KPZ equation, and for the BM to the flat initial condition. It is possible to extend some of the above considerations to other geometries, for instance Brownian motions starting at different points, or to relate the problem to other initial conditions of the Kardar-Parisi-Zhang equation, and we refer the readers to Ref. [3] for further details and discussion. We hope this work will motivate further studies of the coincidence properties of multiple diffusion processes.

4.2.3 Open questions

Apart from being a technical exercise, the study of the coincidence time PDF raises one important question. The Lieb-Liniger model for $c > 0$ only comprises particle states and there is no string structure at that level: this is why it was easy to evaluate the moment generating function $\langle e^{-c\mathcal{T}_N} \rangle_{\rm BB}$. A question is whether one could do things conversely and start from the knowledge of the PDF $P_{N,\rm BB}(T)$ to study the physics of the Kardar-Parisi-Zhang equation. This is stunning as obtaining its solutions requires solving the Lieb-Liniger model for a coupling constant $c < 0$. In this regime, the so-called attractive regime, additional states appear in the Lieb-Liniger model: these are the string states representing particles bounded together.

To obtain the moments of the directed polymer for a coefficient $c < 0$, one can equivalently evaluate this generating function

$$\langle e^{c\mathcal{T}_N} \rangle_{\rm BB} = \int_0^\infty {\rm d}T \, e^{cT} P_{N,\rm BB}(T). \tag{4.2.53}$$

As the PDF $P_{N,\rm BB}(T)$ has the particular structure,

$$P_{N,\rm BB}(T) = \partial_T^{N+1} \int_{\mathbb{R}_+^N} {\rm d}\mathbf{r} \; \Theta\left(T - \sum_{\ell=1}^N r_\ell\right) \det_{1 \leqslant i,j \leqslant N} \left(e^{-\frac{(r_i - r_j)^2}{4}} \right), \tag{4.2.54}$$

the new generating function can be calculated by simple integrations by part and it is well-defined thanks to the fact that the distribution of the coincidence time has a Gaussian tail.

The open questions are: *(i)* how one could extract the string structure out of this generating function and *(ii)* what the algebraic structure in this approach between the cases $c > 0$ and $c < 0$ is. In particular we have to manipulate $N+1$ integrations by part, each of them induces a bracket that can be controlled by the small and large T asymptotics of the PDF $P_{N,\rm BB}(T)$ given in the Results. (4.2.3) and (4.2.4), providing an interpretation of the brackets could be interesting by itself.

Chapter 5

Introduction to the large deviations of the KPZ equation

To investigate the distribution of the Kardar-Parisi-Zhang height field in certain regimes of time, namely at short time and at large time, we shall require the use of Large Deviation Principles. The theory of Large Deviations [188, 189] can be understood through the point of view of Extreme Value Statistics. Extreme Value Statistics describes the fluctuations of a random variable far away from its typical value. It models the probability that rare and extreme events occur, which is of paramount importance in many domains, e.g. statistics of records, genetic mutations or risk analysis on financial markets.

Extreme Value Statistics has been also studied in the context of Random Matrix Theory [158, 164] where a lot of effort has been engaged to obtain the large deviations of the distribution of the largest eigenvalue a random matrix. It is known since the work of Tracy and Widom that the fluctuations of the largest eigenvalue of a random matrix converges to the so-called Tracy-Widom distribution [60]. Since the eigenvalues of a random matrix are strongly correlated, the largest eigenvalue can be seen as the maximum of correlated random variables which is an order of magnitude harder to study than non-correlated random variables for which the maximum is described by either the Gumbel, Fréchet or Weibull distributions [190, 191]. Nonetheless, the Tracy-Widom distribution describes only the typical fluctuations of the largest eigenvalue around its average. The determination of *large fluctuations* requires different methods. In the context of Random Matrix Theory, a fruitful method to investigate the Large Deviations is the Coulomb gas method [120, 192]. As we shall see in this Thesis, Coulomb gas methods can also be adapted to investigate the Large Deviations of the solution to the Kardar-Parisi-Zhang equation at large time.

More generally, large deviation theory play an important role in the study of non-equilibrium systems [193–201] and the central object is the Large Deviation rate function which controls the atypical fluctuations: this function can be viewed as an non-equilibrium analog of the free energy for a system at equilibrium. In the context of the KPZ equation in this Thesis, we will be interested in large deviations in two situations: at short time and at large time.

At large time in 1+1 dimensions, the KPZ equation belongs to the Kardar-Parisi-Zhang universality class. The feature of interest for us is that this class is characterized by various growth models and experimental systems which share asymptotically the same scaling behavior of the typical fluctuations of the associated height δh at a position x

$$\delta h \sim t^{1/3} \sim x^{1/2} \tag{5.0.1}$$

It is besides understood that these typical fluctuations are the universal Tracy-Widom distributions. The question of the large deviations within the KPZ universality class remains has not

been explored in details before. In the Section 5.2, we will put in place some elements to understand how to build a large deviation theory for the KPZ equation. Although the large deviations functions related to the KPZ equation are not expected to be universal within the KPZ class, our hope is to present some mechanisms which will turn to be useful to understand the problem in the whole class.

At short time, the motivation to study large deviations is completely different. Since, the dynamics of the KPZ equation describes the flow from the Edwards-Wilkinson fixed point to the Kardar-Parisi-Zhang fixed point, it is important to know how the fluctuations of the solutions to the KPZ equation depart from their initial Gaussian distribution. As we have seen in the first Chapter, in the short-time regime by contrast with the scaling of the KPZ class; the scaling of the typical height fluctuations is Gaussian and verifies the Edwards-Wilkinson exponents [32],

$$\delta h \sim t^{1/4} \sim x^{1/2} \tag{5.0.2}$$

As we will see in the rest of this Thesis, the large deviations at short time will allow us to understand how the solution to the KPZ equation becomes non-Gaussian.

Before introducing some particular ideas relevant to the short and large times regimes, let us conclude by mentioning that unlike diffusive interacting particle systems for which powerful methods [199,201] were developed to quantify large deviations, the Kardar-Parisi-Zhang equation requires new theoretical efforts. One of the objective of this Thesis was to understand the physical mechanisms behind these large deviations.

5.1 Large deviations at short time

By a dimensional analysis of the Kardar-Parisi-Zhang equation, the natural time scale of the dynamics is

$$t_0 = \frac{2^6 \nu^5}{D^2 \lambda_0^4} \tag{5.1.1}$$

The dynamics occurring at times t very small compared to t_0 will be considered as the short-time dynamics. By a naive perturbation theory in the time t, the KPZ equation boils down at the leading order to the Edwards-Wilkinson equation, easily solvable in Fourier space since it is linear. In the Edwards-Wilkinson world, the typical fluctuations of the centered height $H(t)$ at one space point are Gaussian and their distribution takes the form

$$P(H,t) \asymp \exp(-c_0 \frac{H^2}{\sqrt{t}}) \tag{5.1.2}$$

Nevertheless, away from the typical fluctuations where the centered height is of order $\mathcal{O}(1)$, the presence of the KPZ non-linearity plays a increasingly important role, even at very small times. Anticipating from the second part of this Thesis, the large deviations of the KPZ height are far from the Gaussian realm and their distribution takes the following form

$$P(H,t) \asymp \exp(-\frac{\Phi(H)}{\sqrt{t}}) \tag{5.1.3}$$

where the Large Deviation function Φ is highly asymmetric with the following asymptotic

$$\Phi(H) = \begin{cases} c_{-\infty}|H|^{5/2}, & H \to -\infty \\ c_{+\infty} H^{3/2}, & H \to +\infty \end{cases} \tag{5.1.4}$$

Remark 5.1.1. *The matching of the typical Edwards-Wilkinson fluctuations imposes that at small argument, the function Φ is quadratic. Besides, the coefficients $c_0, c_\infty, c_{+\infty}$ will highly depend on the initial condition.*

Quite amazingly, as we will see in the rest of this Thesis, the exponents 5/2 and 3/2 will be conserved by the dynamics of the Kardar-Parisi-Zhang equation. What is more, the exponent 3/2 is a landmark of the fluctuations of models lying in the KPZ universality class and is also the exponent of the right tail of the Tracy-Widom fluctuations.

The daunting work regarding the short-time large deviations of the solutions to the KPZ equation is the exact evaluation of the function Φ. In particular, it is of utter importance to determine whether which information in Φ depends on the initial condition and which is universal. In addition, as the large deviation function is the analog of the free energy for systems at equilibrium, the search for non-analyticities in Φ will amount to investigate the existence of dynamical phase transitions for the solutions of the Kardar-Parisi-Zhang equation.

Before turning to the large deviations at late time for the KPZ equation, let us emphasize that the rate of the deviations $1/\sqrt{t}$ was obtained thanks to the results on the Edwards-Wilkinson fixed point. At late time, an additional difficulty comes from the fact that we also have to determine the corresponding rate.

5.2 Large deviations at large time

To introduce the large deviations at late time for the KPZ equation, we shall heavily borrow the elegant arguments and presentation of Refs. [158, 187]. We have already seen in the introduction to the exact solutions to the KPZ equation that at large time, the typical fluctuations of the height are of magnitude $t^{1/3}$ and are given by the celebrated Tracy-Widom distributions. It was recently emphasized [158] that in several systems having Tracy-Widom fluctuations there is a hidden third-order phase transition between a strong and a weak coupling phase. Tracy-Widom distributions appear in these systems as a finite-size cross-over function connecting the free energies of the two phases across the critical point. In the strong coupling phase, the degrees of freedom of the system act collectively while in the weak coupling phase, there is a single dominant degree of freedom. The appearance of the Tracy-Widom distributions in the growth models in the KPZ universality class therefore raises the natural question: is there a third-order phase transition ? If yes, what is the interpretation of the two related phases ?

As in the short time case, we shall first recall some properties about the typical fluctuations before investigating the large deviations. From our introduction to the solutions of the KPZ equation, we know that at large time, the PDF $P(H,t)$ of the shifted scaled height $H(t) \propto h(0,t) + \frac{t}{12}$ rescaled by $t^{1/3}$ is equal to the PDF of a Tracy-Widom β random variable F'_β, for some β depending on the precise initial or boundary condition.

$$P(H,t) = \frac{1}{t^{1/3}} F'_\beta\left(\frac{H}{t^{1/3}}\right) \tag{5.2.1}$$

The Tracy-Widom β PDF admits the following asymptotics (dismissing any prefactor) [158]

$$F'_\beta(s) = \begin{cases} \exp\left(-\frac{\beta}{24}|s|^3\right), & s \to -\infty \\ \exp\left(-\frac{2\beta}{3}s^{3/2}\right), & s \to +\infty \end{cases} \tag{5.2.2}$$

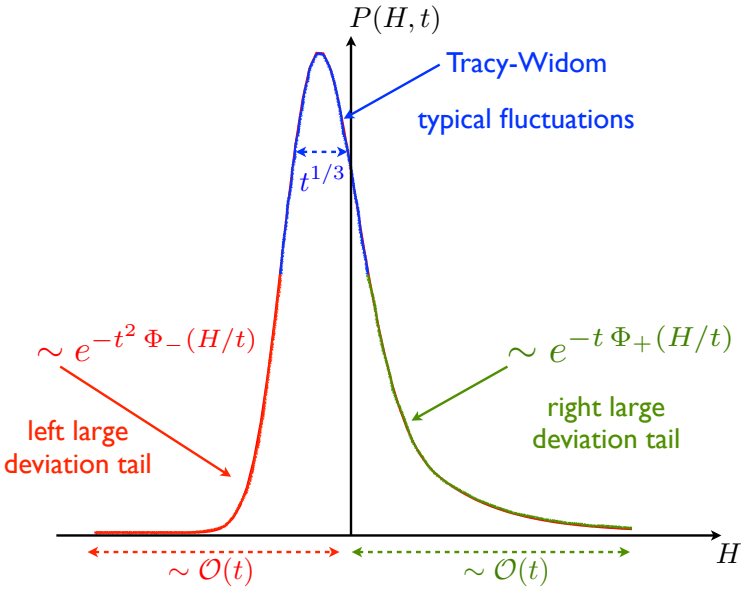

Figure 5.1: A schematic picture of the height distribution at the origin at large time. The typical fluctuations $H \sim \mathcal{O}(t^{1/3})$ around the mean are distributed according to a Tracy-Widom β law (blue line). The atypical large fluctuations to the left (red line) and to the right (green line) are described respectively by the left and right large deviation functions in Eq (5.2.4). Figure courtesy of P. Le Doussal, S. N. Majumdar and G. Schehr [187].

which translates for $P(H,t)$ into

$$P(H,t) = \begin{cases} \exp\left(-\frac{\beta}{24}\frac{|H|^3}{t}\right), & H \to -\infty \\ \exp\left(-\frac{2\beta}{3}\frac{H^{3/2}}{\sqrt{t}}\right), & H \to +\infty \end{cases} \tag{5.2.3}$$

Having the information about the typical fluctuation regime, we now want to turn to the large deviation one, bearing in mind that we will have to match for small arguments the Tracy-Widom asymptotics of Eq. (5.2.3).

Remark 5.2.1. *It is quite remarkable to observe that the exponents of the right tail of the typical regime at large time presented in* (5.2.3) *match perfectly the asymptotic of the right large deviations of the height at short time as displayed in Eq.* (5.1.4)

Anticipating the rest of this Section, the solutions to the KPZ equation admit at large time a Large Deviation principle when the centered height is of order $\mathcal{O}(t)$. Such fluctuations are of the order of magnitude of the velocity of the interface, which means that these large deviations will be interpreted as the interface having an anomalous velocity or growth rate: physically this corresponds to having an excess growth or a mass die-out. Nevertheless, contrary to the short-time regime, the rate of the large deviations will be asymmetric: the rate will be t^2 for the left large deviations and t for the right large deviations. The goal of the rest of this Section will be to explain heuristically why. We summarize in Fig. 5.1 our discussion on the typical and atypical fluctuation regimes and present the large deviations result for $P(H,t)$ in Eq. (5.2.4).

$$P(H,t) \sim \begin{cases} \exp\left(-t^2\Phi_-(\frac{H}{t})\right), & H \sim \mathcal{O}(t) < 0 \\ \exp\left(-t\Phi_+(\frac{H}{t})\right), & H \sim \mathcal{O}(t) > 0 \end{cases} \tag{5.2.4}$$

For the large deviations to match the typical ones, we additionally require

$$\begin{aligned} \Phi_-(z) &\sim_{z\to 0^-} |z|^3 \\ \Phi_+(z) &\sim_{z\to 0^+} z^{3/2} \end{aligned} \tag{5.2.5}$$

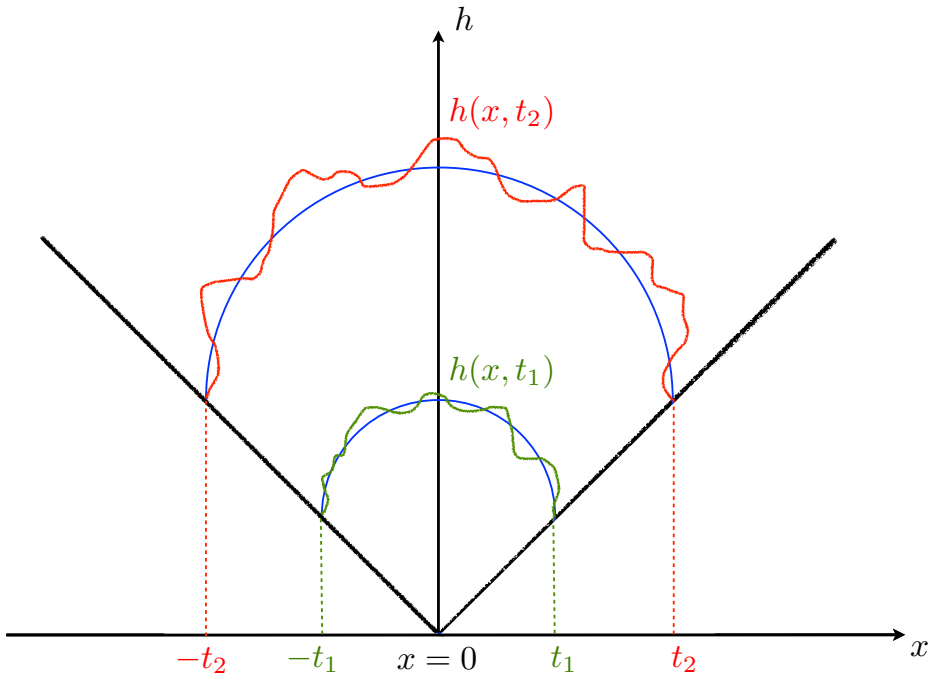

Figure 5.2: The height $h(x,t)$ evolving on a substrate $-t \leqslant x \leqslant t$. The light cone (black lines) describes the growth of the interface. The solid line (in blue) represents the average height at two different times. Figure courtesy of P. Le Doussal, S. N. Majumdar and G. Schehr [187].

One remarkable property of the prediction of the rate of the large deviations is that the PDF $P(H,t)$ is expected to encounter a third-order phase transition, i.e.

$$\lim_{t\to+\infty} -\frac{1}{t^2}\log P(H=zt,t) = \begin{cases} \Phi_-(z) & z \leqslant 0 \\ 0 & z \geqslant 0 \end{cases} \tag{5.2.6}$$

We recall that Φ_- is expected to have a cubic behavior for small argument and that this cubic behavior is a general property of the Tracy-Widom distributions which are the late-time distributions of the KPZ universality class. This answers positively the question of the existence of the famous third-order phase transition [158]. One of the goal of this Thesis will be the derivation of the exact expression of Φ_- for specific initial conditions of the KPZ equation.

Remark 5.2.2. *One may wonder why we are only interested at the fluctuations of the height at a single point. The KPZ fixed point scaling tells us that the fluctuations are correlated on a longitudinal width of order $x \sim t^{2/3}$. Hence if the growing interface is sufficiently long, disparate regions will see roughly independent growth and therefore by standard extreme-value theory, the maximal and minimal height of the entire interface will be determined by the one-point tail behavior.*

In order to get a flavor of these large deviations at late time, let us briefly analyze a directed polymer model belonging to the KPZ universality class introduced and solved by Johansson [52] and we shall again heavily borrow from the elegant presentation of Ref. [187]. This model is equivalent to a discrete space-time (x,t) growth model which takes place on a substrate $-t \leqslant x \leqslant t$, starting from the seed at the origin $x=0$ at initial time. The interface height $h(x,t)$, represented in Fig. 5.2, evolves in the bulk as

$$h(x,t) = \max\left[h(x-1,t-1), h(x+1,t-1)\right] + \eta(x,t) \tag{5.2.7}$$

where $\eta(x,t) \geqslant 0$ are i.i.d positive random variables with exponential distribution. Johansson showed that at late times, the average height has a semi-circular shape

$$\mathbb{E}[h(x,t)] = t\left(1+\sqrt{1-(\frac{x}{t})^2}\right) \tag{5.2.8}$$

In addition, the height at the origin at lates times behaves as

$$h(0,t) \sim 2t + 2t^{1/3}\chi_2 \tag{5.2.9}$$

where χ_2 is GUE Tracy-Widom distributed. By exploiting an exact mapping of the growing height with the largest eigenvalue of complex Wishart matrices, Le Doussal, Majumdar and Schehr obtained precisely in Ref. [187] the large deviations of the height $H = \frac{h(0,t)}{2} - t$ of the form presented in Eq. (5.2.4). The reasoning behind the rates t and t^2 in the large deviations is the following:

- To obtain a configuration of H much smaller than its typical value, the noise variables $\eta(x,t)$ at all sites should be small. The probability of this event, where all noise variables inside the wedge $|x| < t$ of area $\sim t^2$ are small, is proportional to e^{-t^2} since the noise is composed of i.i.d random variables.

- Configurations where H is much bigger than its typical value are realized by concatenating large positive noise at the origin $x = 0$ at all times between 0 and t. Since the noise is i.i.d, the probability of this event is proportional to e^{-t}. This is not a collective action as it solely involves a column of the lattice.

We assume that this argument for the rate of the large deviations in this discrete model holds in the continuum and this will serve as a cornerstone for the rest of this Thesis.

Part II

Short-time height distributions of the solutions to the KPZ equation

Abstract

The second part of this Thesis is devoted to the investigation of the short-time properties of the solutions to the Kardar-Parisi-Zhang equation. We will introduce two recently developed analytic methods which allow to extract complementary exact information about the solutions at short time: *(i)* the Weak Noise Theory and *(ii)* the cumulant method, based on the Fredholm representation of the KPZ solutions. In addition, we will present some recent remarkable numerical progress which allowed to confront the theoretical predictions at short time with high-precision Monte Carlo simulations. The knowledge of the exact short-time distribution for the KPZ solutions will shed some light on how the solutions flow from the Edwards-Wilkinson fixed point, which is Gaussian by essence, to the Kardar-Parisi-Zhang fixed point, developing asymmetric non-Gaussian fluctuations. In particular, we will see that the short-time expansion of the KPZ equation formally identifies with a perturbation theory in its noise. It predicts a non-trivial large deviation regime where the probability distribution of the KPZ height $H(t)$ takes the form

$$P(H,t) \sim \exp(-\frac{\Phi(H)}{\sqrt{t}}). \tag{5.2.10}$$

The calculation of the function $\Phi(H)$ has required to develop new theoretical methods and their presentation is the goal of this second part.

Chapter 6

Perturbative noise rescaling of the KPZ equation: Weak Noise Theory

This Chapter is dedicated to a method introduced to probe the Gaussian fluctuations of the solution to the Kardar-Parisi-Zhang equation, i.e. of its height, at short time as well as the asymmetric tails of the distribution at one point. It has different names in the literature: Instanton method, Macroscopic fluctuation theory, Weak Noise Theory (WNT) and for the sake of this Chapter we shall use the latter. The range of application of this method is wide, but concerning the Kardar-Parisi-Zhang equation and the directed polymer, it was pioneered by Kolokolov and Korshunov in Refs. [202] and then mostly been developed by Meerson and collaborators [203–212]. Although we have not worked directly with this theory in this Thesis, we present it for completeness as it plays an important role in our story and is quite complementary to our work. The Weak Noise Theory is based on a Principle of Least Action for the path integral representation of the Kardar-Parisi-Zhang equation. It can be seen as a perturbative expansion in the magnitude of the noise itself.

In the Weak Noise Theory, the logarithm of the one-point probability distribution of the KPZ height H at time T, $-\log P(H,T)$, is interpreted as the classical action over an optimal path: this is analogous to a semi-classical expansion in quantum mechanics with the parameter $\hbar$ equal to $\sqrt{T}$. The optimal path is then interpreted as the most probable evolution of the interface $h(x,t)$ conditioned on the specified large deviation at final time.

The Weak Noise Theory has been used to study *(i)* the first few cumulants of the solution to the Kardar-Parisi-Zhang equation at short time, *(ii)* the tails of the short-time one-point distribution and *(iii)* as we shall see below, the effect of the initial and boundary conditions [203–212]. It is important to note that the WNT does not rely on the knowledge of the exact solution of the KPZ equation at all times hence is a versatile method. However, the WNT does not provide the analytic full expression of the large deviation function $\Phi(H)$ (5.2.10) at short time but allows for a numerical evaluation for arbitrary value of H. This function $\Phi(H)$ will be calculated explicitly in the next Chapter using another method which we developed, complementary to the WNT.

Before constructing the Weak Noise Theory, we would like to refer for further details the readers to the extensive list of publications [203–212], related to the use of WNT to study short-time properties of the KPZ solutions. The presentation below follows the arguments of these publications.

6.1 Construction of the Weak Noise Theory

For the sake of the Weak Noise Theory, let us reexpress the Kardar-Parisi-Zhang equation with the original system of units.

$$\partial_t h(x,t) = \nu\,\partial_x^2 h(x,t) + \frac{\lambda_0}{2}\,(\partial_x h(x,t))^2 + \sqrt{D}\,\xi(x,t)\;. \tag{6.1.1}$$

We are interested in the probability density $P(H,L,T)$ of observing the height H at position L at a final time T.

$$H = h(L,T)\;. \tag{6.1.2}$$

For convenience, let us introduce the following rescaling[5] $t = T\tilde{t}$, $x = \sqrt{T\nu}\tilde{x}$, and $h = \frac{\nu}{|\lambda_0|}\tilde{h}$, the final time being T and the rescaled time $\tilde{t}$ spanning the interval $[0,1]$. The variables L and H will be rescaled identically $L = \sqrt{T\nu}\tilde{L}$ and $H = \frac{\nu}{|\lambda_0|}\tilde{H}$.

$$\tilde{H} = \tilde{h}(\tilde{x} = \tilde{L}, \tilde{t} = 1)\;. \tag{6.1.3}$$

By a dimensional analysis, $P(H,L,T)$ depends on three parameters: $|\lambda_0|\,H/\nu$, $L/\sqrt{T\nu}$ and ε. One then rewrites the KPZ equation (6.1.1) in these scaled variables (from now on we drop the tildes on all variables including L and H)

$$\sqrt{\varepsilon}\xi(x,t) = \partial_t h - \partial_{xx}^2 h - \frac{1}{2}(\partial_x h)^2, \tag{6.1.4}$$

where

$$\varepsilon = \frac{D\lambda_0^2\sqrt{T}}{\nu^{5/2}} \tag{6.1.5}$$

is the dimensionless noise magnitude and ξ is a unit Gaussian white noise in the rescaled variables. The probability to encounter a realization of the Gaussian white noise is proportional to $\exp(-\frac{S_{\rm dyn}}{\varepsilon})$, where $S_{\rm dyn}$ is called the dynamical action[6]

$$S_{\rm dyn} = \frac{1}{2}\int_0^1 \mathrm{d}t \int_{\mathbb{R}} \mathrm{d}x\,\left[\partial_t h - \partial_{xx}^2 h - \frac{1}{2}(\partial_x h)^2\right]^2\;. \tag{6.1.6}$$

The Weak Noise Theory assumes that ε is small. Hence, in the limit of $\varepsilon \ll 1$, the stochastic problem for the KPZ equation, formulated as a functional integral, will be solved via a saddle-point evaluation (akin to a semi-classical expansion), leading to a minimization problem for the action functional over all fields $h(x,t)$. In our case of interest, the regime $\varepsilon \ll 1$ corresponds to the short-time regime

$$T \ll \frac{\nu^5}{\lambda_0^4 D^2} \tag{6.1.7}$$

and the semi-classical saddle point will lead to a hydrodynamic problem. In all generality, we can associate to the dynamical action $S_{\rm dyn}$ (6.1.6) a Lagrangian functional $\mathcal{L}$

$$\mathcal{L}\{h\} = \frac{1}{2}\int_{\mathbb{R}} \mathrm{d}x\,\left[\partial_t h - \partial_{xx}^2 h - \frac{1}{2}(\partial_x h)^2\right]^2, \tag{6.1.8}$$

and a momentum field $\rho(x,t)$ associated to the height field $h(x,t)$

$$\rho(x,t) = \frac{\delta\mathcal{L}}{\delta(\partial_t h)} = \partial_t h - \partial_{xx}^2 h - \frac{1}{2}(\partial_x h)^2. \tag{6.1.9}$$

[5] The absolute value comes from the fact that people in the literature alternatively use $\lambda_0 > 0$ or $\lambda_0 < 0$ without a consensus, hence we opt for the neutral choice of the absolute value.

[6] We implicitly assume a full-space problem here by integrating over $\mathbb{R}$. The half-space problem problem would instead be formulated only on the half-line $\mathbb{R}_+$.

The momentum field at the saddle point plays the role of the optimal noise and we can express again the dynamical action only in terms of the momentum as

$$S_{\text{dyn}} = \frac{1}{2}\int_0^1 \mathrm{d}t \int_{\mathbb{R}} \mathrm{d}x\, \rho^2(x,t)\ . \tag{6.1.10}$$

For the action to be bounded, we shall require the momentum ρ to vanish fast enough at infinity. Having defined the Lagrangian $\mathcal{L}$, it is possible to define a Hamiltonian $\mathcal{H}$ such that

$$\begin{aligned}\mathcal{H}\{h\} &= \int_{\mathbb{R}} \mathrm{d}x\, \rho(x,t)\partial_t h(x,t) - \mathcal{L}\{h\} \\ &= \int_{\mathbb{R}} \mathrm{d}x\, \rho(x,t)\left[\partial^2_{xx}h + \frac{1}{2}(\partial_x h)^2 + \frac{1}{2}\rho(x,t)\right]\ .\end{aligned} \tag{6.1.11}$$

The second Euler-Lagrange equation governing the dynamics of the momentum $\rho(x,t)$ is then $\partial_t \rho(x,t) = -\frac{\delta \mathcal{H}}{\delta h}$. Gathering both Euler-Lagrange equations, we summarize the system of equations verified by the two conjugated fields h, ρ.

$$\begin{cases} \partial_t h = \partial^2_{xx}h + \frac{1}{2}(\partial_x h)^2 + \rho \\ \partial_t \rho = -\partial^2_{xx}\rho + \partial_x(\rho \partial_x h) \end{cases} \tag{6.1.12}$$

Remark 6.1.1. *The second equation of* (6.1.12) *leads to a conservation law* $\int_{\mathbb{R}} \mathrm{d}x\, \rho(x,t) = cst.$

The initial and boundary conditions of these equations have yet to be defined. To calculate $P(H,L,T)$, we need to fix the constraint

$$h(x = L, t = 1) = H \tag{6.1.13}$$

since $x = L$ is the point at which we probe the distribution. From the principle of least action, if one perturbs the height field h by δh, the resulting perturbation on the dynamical action is

$$\delta S_{\text{dyn}} = \int_0^1 \mathrm{d}t \int_{\mathbb{R}} \mathrm{d}x\, \rho(x,t)\left[\partial_t \delta h - \partial^2_{xx}\delta h - (\partial_x h)(\partial_x \delta h)\right] \tag{6.1.14}$$

Integrating δS_{dyn} by part leads to the second equation of (6.1.12). Upon this integration by part, there are additional boundary terms in time which must vanish independently at $t = 0$ and $t = 1$. In particular, $h(x, t = 1)$ is arbitrary everywhere except at $x = L$ where it is fixed. The boundary term in time (*b.t.*) reads

$$b.t. = \int_{\mathbb{R}} \mathrm{d}x\ \rho(x, t = 1)\delta h(x)\ |_{t=1} - \int_{\mathbb{R}} \mathrm{d}x\ \rho(x, t = 0)\delta h(x)\ |_{t=0} \tag{6.1.15}$$

As there is a single constraint at $t = 1$, the momentum field ρ should act as a Lagrange multiplier at time $t = 1$, hence

$$\rho(x, t = 1) = \Lambda_1 \delta(x - L) \tag{6.1.16}$$

The unknown constant Λ_1 will ultimately be determined by the condition $h(x = L, t = 1) = H$ together with the conservation law on the momentum $\rho(x,t)$. The fact that the constraint appears at $t = 1$ indicates that the equation verified by ρ will be solved backwards in time.

The other constraints arising at $t = 0$ will highly depend on the initial condition of the KPZ equation. For completeness, we present the example of Brownian initial condition to show how to incorporate initial time considerations in the hydrodynamic problem.

6.1.1 Intermediate example: the Brownian initial condition

Consider now Eq. (6.1.1) with an initial field $h(x, t = 0)$ which is a two-sided unit Brownian interface pinned at the origin $h(x = 0, t, 0) = 0$ (note that in this paragraph we use the physical units associated to Eq. (6.1.1)). We express this initial condition and specify the physical constants (in the original system of units) as

$$\frac{\lambda}{2\nu} h(x, t = 0) = \alpha B(x) \tag{6.1.17}$$

where $B(x)$ is the two-sided unit Brownian motion and $\alpha = (2\nu)^{-3/2}\lambda D^{1/2}$. Here the drift is zero and this corresponds to the so-called stationary KPZ initial condition.

Going now to the rescaled units, for this initial condition, in addition to the dynamical action, there is an initial action corresponding to the cost of the initial height. The probability to encounter a realization of the initial condition is proportional to $\exp\left(-\frac{S_{\text{in}}}{\varepsilon}\right)$, where

$$S_{\text{in}} = \int_{\mathbb{R}} \mathrm{d}x (\partial_x h)^2 \mid_{t=0} \tag{6.1.18}$$

The total action is finally given by the sum of the two contributions

$$S = S_{\text{dyn}} + S_{\text{in}} \tag{6.1.19}$$

There is one remaining constraint for this random initial condition case is at $x = 0$ which is $h(x, = 0, t = 0) = 0$. Hence the boundary term should become a Lagrange multiplier. Considering the total action and perturbing the height h by δh, the perturbation of the total action is given by

$$\delta S = \int_0^1 \mathrm{d}t \int_{\mathbb{R}} \mathrm{d}x\, \rho(x, t) \left[\partial_t \delta h - \partial_{xx}^2 \delta h - (\partial_x h)(\partial_x \delta h)\right] + 2 \int_{\mathbb{R}} \mathrm{d}x \partial_x h \partial_x \delta h \mid_{t=0} \tag{6.1.20}$$

There is an extra term appearing at $t = 0$. Once again, the boundary terms in time must vanish independently at $t = 0$ and $t = 1$. Now $h(x, t = 0)$ is arbitrary everywhere except at $x = 0$ where it is fixed and is equal to zero. The boundary term in time b.t.2 reads

$$b.t.2 = \int_{\mathbb{R}} \mathrm{d}x\, \rho(x, t = 1)\delta h(x) \mid_{t=1} - \int_{\mathbb{R}} \mathrm{d}x \left[\rho(x, t = 0) + 2\partial_{xx}^2 h(x, t = 0)\right] \delta h(x) \mid_{t=0} \tag{6.1.21}$$

To ensure the single point constraint at $x = 0$, we naturally add another Lagrange multplier Λ_2 such that

$$\rho(x, t = 0) + 2\partial_{xx}^2 h(x, t = 0) = \Lambda_2 \delta(x) \tag{6.1.22}$$

Using the conservation law $\int_{\mathbb{R}} \mathrm{d}x\, \rho(x, t) = cst$, we can further conclude that $\Lambda_1 = \Lambda_2$.

Remark 6.1.2. *In several papers about WNT, see e.g. [210], it is stated that there exists a general relation to relate Λ_1 to H at the saddle point*

$$\frac{\mathrm{d}S}{\mathrm{d}\Lambda_1} = \Lambda_1 \frac{\mathrm{d}H}{\mathrm{d}\Lambda_1} \tag{6.1.23}$$

This provides another way to relate Λ_1 to H.

We now summarize all boundary conditions of the WNT equations for the Brownian initial condition:

$$\begin{cases} h(x = 0, t = 0) = 0 \\ h(x = L, t = 1) = H \\ \rho(x, t = 0) + 2\partial_{xx}^2 h(x, t = 0) = \Lambda \delta(x) \\ \rho(x, t = 1) = \Lambda \delta(x - L) \end{cases} \tag{6.1.24}$$

To ensure boundedness of the overall action, we also require ρ and all derivatives of h to vanish fast enough at infinity.

6.2 Large deviation function of the Kardar-Parisi-Zhang equation at short time

Assuming that we can solve the hydrodynamic equations for ρ and h of the Weak Noise Theory (6.1.12), the probability density, $P(H, L, T)$, of the one-point Kardar-Parisi-Zhang height H will be given for small time by

$$-\log P(H, L, T) \simeq \frac{\nu^{5/2}}{D\lambda_0^2\sqrt{T}} S(\frac{|\lambda_0|\, H}{\nu}, \frac{L}{\sqrt{\nu T}}) \tag{6.2.1}$$

where the total action S, evaluated at the saddle point, naturally plays the role of the large deviation function at short time. From this general scaling relation at $L = 0$, we can interpret the relative importance of the different terms in the Kardar-Parisi-Zhang equation. If we want the distribution not to depend on the non-linear coefficient λ_0, then the distribution should be Gaussian in H. If we want the distribution not to depend on the diffusion coefficient ν, then the distribution should be a streched-exponential in H with exponent $5/2$.

The general solutions to the WNT equations (6.1.12) and S in Eq. (6.2.1) can globally be obtained numerically but there are some limits which can be studied analytically. The WNT equations are generally solvable for small H using a perturbation theory in the parameter $\Lambda \sim H$. It is possible to probe the typical Gaussian fluctuations for small H and to calculate the first few cumulants. For very large and positive H, the solutions can (up to exponential small corrections) be found analytically using soliton solutions for ρ and ramps for h. For very large and negative H, the solutions can be found using inviscid hydrodynamics, i.e. neglecting the diffusion terms $\partial^2_{xx} h$ and $\partial^2_{xx}\rho$ in the WNT equations. In all generality the negative H tail (in our conventions) for $L = 0$ was shown to take the following form:

$$-\log P(H, L = 0, T) \underset{H\to-\infty}{\simeq} f(\lambda_0, D)\frac{|H|^{5/2}}{\sqrt{T}}, \tag{6.2.2}$$

where the prefactor $f(\lambda_0, D)$ depends on the initial condition of the KPZ equation. The important feature of this tail is that is does not depend on the diffusion coefficient ν, consistent with the inviscid approximation. This tail has also been argued to remain valid at all times. Indeed since this tail does not depend on ν, one could have chosen instead an arbitrary time T and a coefficient $\nu \gg 1$ in order to remain within the validity of the WNT approximation ($\varepsilon \ll 1$). The reasoning presented above would still be valid and the tail would be determined equivalently. For intermediate regimes in H, the equations require to be solved numerically. Once again, we refer the readers to the extensive list of publications [203–212] related to WNT for further details on the analytic solutions at large positive and negative H.

In the rest of this Chapter, we provide some more details about the symmetries of the WNT equations in full-space, and about the half-space problem. We also present the perturbative solution of the WNT equations at small H, and describe the phenomenon of spontaneous symmetry breaking for the Brownian initial condition. Finally, we will report some recent progress of the WNT.

6.3 Symmetries of the WNT equations in full-space and some considerations in half-space

In addition to the previous considerations on the WNT equations, it is interesting to study their symmetries. Indeed if an initial condition verifies some of them, it then provides an ansatz to

solve the equations. The symmetries in the full-space case have been studied extensively in Ref. [208] and we give them here without any proof. The equations (6.1.12) are invariant under the following transformations

- Translation invariance (taking x_0, t_0, C arbitrary)

$$\begin{cases} h(x - x_0, t - t_0) + C \to h(x, t) \\ \rho(x - x_0, t - t_0) \to \rho(x, t) \end{cases} \tag{6.3.1}$$

- Spatial inversion invariance

$$\begin{cases} h(-x, t) \to h(x, t) \\ \rho(-x, t) \to \rho(x, t) \end{cases} \tag{6.3.2}$$

- Galilean invariance (taking v arbitrary)

$$\begin{cases} xv + h(x - vt, t) \to h(x, t) \\ \rho(x - vt) \to \rho(x, t) \end{cases} \tag{6.3.3}$$

- Generalized time reversal invariance I

$$\begin{cases} -h(x, -t) - 2\log|2\rho(x, -t)| \to h(x, t) \\ \rho(x, -t) \to \rho(x, t) \end{cases} \tag{6.3.4}$$

- Generalized time reversal invariance II

$$\begin{cases} -h(x, -t) \to h(x, t) \\ \rho(x, -t) + 2\partial_{xx}^2 h(x, -t) \to \rho(x, t) \end{cases} \tag{6.3.5}$$

- Generalized time reversal invariance III : For any given profiles $h_0(x)$ and $h_1(x)$ such that $\partial_x h_0(|x| \to +\infty) = \partial_x h_1(|x| \to +\infty) = 0$ and for a trajectory $h(x, t)$ such that $h(x, 0) = h_0(x)$ and $h(x, 1) = h_1(x)$, one has

$$S_{\text{in}}[h_0(x)] + S_{\text{dyn}}[h(x, t)] = S_{\text{in}}[-h_1(x)] + S_{\text{dyn}}[h(x, 1 - t)] \tag{6.3.6}$$

Remark 6.3.1. *Some of these symmetries are in general violated by the boundary and initial conditions of the WNT problem. The Brownian initial condition for instance does not verify the spatial inversion invariance.*

In general, if the equations governing a system possess a discrete symmetry, the solution to these equations need not exhibit that symmetry. For example, the differential equation $\ddot{y}(t) = y(t)$ is symmetric under the discrete time-reversal symmetry $t \to -t$, but the solutions $t \mapsto e^t$ and $t \mapsto e^{-t}$ do not exhibit this symmetry whereas $t \mapsto \cosh(t)$ does. The same is true for the WNT equations: even if the WNT equations are symmetric under space reflection, their solution may not be symmetric under space reflection. When the solution is space-reversal symmetric, we say that the symmetry is unbroken. Conversely, if the solution does not possess a space-reversal symmetry, we say that the symmetry is broken. This argument can be extended to all symmetries mentioned above.

In the following, we shall discuss in some details the half-space problem and then we shall provide an example of symmetry breaking.

6.3.1 Some properties of the WNT in half-space

The half-space problem consists in restricting the range of x to $\mathbb{R}_+$ and adding a boundary condition at $x = 0$, which we impose to be

$$\forall t > 0, \quad \partial_x h(x,t) \mid_{x=0} = A \tag{6.3.7}$$

The scaling of the Kardar-Parisi-Zhang equation remains the same in the half-space as given above. The boundary parameter becomes $A = \sqrt{\frac{\nu}{\lambda_0^2 T}}\tilde{A}$. The general WNT scaling arguments can then be extended [210] to show that the height distribution at $x = 0$ takes the form

$$-\log P(H,A,T) = \frac{\nu^{5/2}}{D\lambda_0^2\sqrt{T}} S\left(\frac{\lambda_0 H}{\nu}, A\sqrt{\frac{\lambda_0^2 T}{\nu}}\right) \tag{6.3.8}$$

This scaling regime has the property to introduce a new time-scale which is

$$T_A = \frac{\nu A^2}{\lambda_0^2}, \tag{6.3.9}$$

it is interpreted as the time T above which the boundary condition start to play a role in the large deviations. Recalling that WNT is valid for $T \ll \frac{\nu^5}{D^2\lambda_0^4}$, if the time T_A is greater than the limiting time at which WNT remains valid, i.e. $T_A \gg \frac{\nu^5}{D^2\lambda_0^4}$ the boundary parameter A will play no role and the problem can be simplified using e.g. a reflective boundary condition $A = 0$. This is the case in the short-time regime when A is fixed and of order 1. If, on the contrary, the time T_A is much smaller than the typical limiting time of WNT $T_A \ll \frac{\nu^5}{D^2\lambda_0^4}$ or equivalently $A \gg \frac{D\lambda_0}{\nu^2}$, then there can exist two regimes [210] for the large deviations:

$$\begin{cases} T \ll T_A \\ T_A \ll T \ll \frac{\nu^5}{D^2\lambda_0^4} \end{cases} \tag{6.3.10}$$

controlled respectively by the reflective wall fixed point ($A = 0$) and the hard wall fixed point ($A = +\infty$). In addition to these new timescale considerations, from the Principle of Least Action, it is possible to see that the boundary condition on h also imposes a boundary condition [209] on ρ as

$$\partial_x \rho(x,t) \mid_{x=0} = \tilde{A}\rho(x=0,t). \tag{6.3.11}$$

Finally, from the symmetries of the full-space problem, Meerson and his collaborators found that for any initial condition that is deterministic and mirror symmetric around 0, there is a relation [209, 210] between the large deviations of the Kardar-Parisi-Zhang height in full-space and the one in half-space for $A = 0$ at $x = 0$:

$$S_{\text{half-space}} = \frac{1}{2} S_{\text{full-space}} \tag{6.3.12}$$

In particular, they concluded that this relation implies that it is more likely to observe unusually large values of H in a half-line system than in the full-line system with the same parameters. The same conclusion (6.3.12) was also obtained by us [6] by different arguments, see below.

6.4 From small H to large H and spontaneous symmetry breaking

We now turn to some specific details of the small H expansion of the WNT equations. In this regime, the WNT problem can be solved via a regular perturbation expansion in the powers of

H or Λ. Writing $h = \Lambda h_1 + \mathcal{O}(\Lambda^2)$ and $\rho = \Lambda\rho_1 + \mathcal{O}(\Lambda^2)$, we expand the WNT equations and the first order leads to the Edwards-Wilkinson equation where the Gaussian white noise is replaced by the optimal noise ρ_1:

$$\begin{cases} \partial_t h_1 = \partial^2_{xx} h_1 + \rho_1 \\ \partial_t \rho_1 = -\partial^2_{xx} \rho_1 \end{cases} \tag{6.4.1}$$

with the aforementioned boundary conditions. For small H and at any order of the perturbation, the solution for h was found to be reflection symmetric $h(x) = h(-x)$.

It turns out that for large positive H, the symmetric solution can lose stability and the solution is such that $h(x) \neq h(-x)$, leading to singular behaviors the total action S. This is interpreted as dynamical phase transitions. In Ref. [205], Janas, Kamenev and Meerson have found that for the Brownian initial condition, the action S exhibits a second order phase transition (or singularity of second order). They defined the following order parameter which, in addition, is a conserved quantity in the WNT dynamics

$$\Delta = h(\infty, t) - h(-\infty, t) = \int_{\mathbb{R}} \mathrm{d}x \partial_x h(x, t) \ . \tag{6.4.2}$$

This order parameter describes the asymmetry of the height field. It is equal to zero when the solution is reflection symmetric. A non zero value of Δ will then be associated to a spontaneous breaking of this symmetry, inducing a phase transition or singularity in the large deviation function S. In Figure 6.1, we report the numerical values of Δ for the Brownian initial condition and increasing values of H found in Ref. [205].

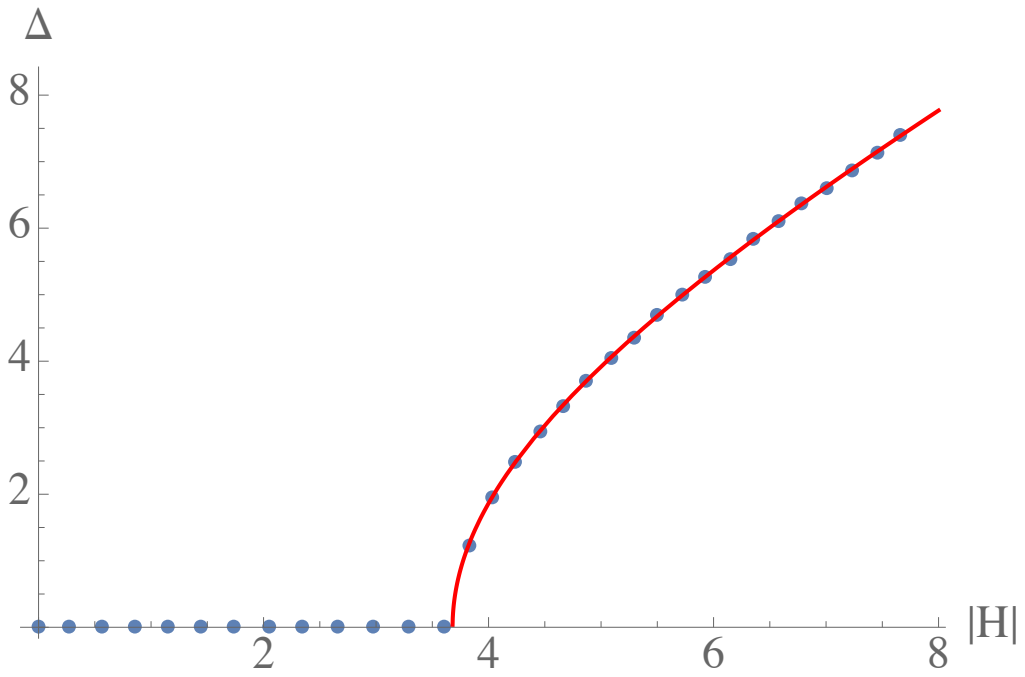

Figure 6.1: Δ vs. $|H|$ at $H < 0$. Symbols: numerical results, solid line: fit of the data for $|H| \geqslant |H_c|$. $|H_c| \simeq 3.7$. These data were originally presented in Ref. [205], courtesy of B. Meerson.

The figure clearly indicates a breaking of the reflection symmetry for some $H = H_c$. Crossing this information with other numerical simulations of Ref. [205] led Janas, Kamenev and Meerson to formulate the following conclusion:

" This suggests a mean-field like second order transition, where the large deviation function S exhibits a discontinuity in its second derivative $\partial^2_{HH} S$ at $H = H_c$. " (Taken from Ref. [205])

This conclusion turned out to be correct as we showed analytically in Ref. [9] by obtaining the analytic value of H_c and $\Phi(H)$ using the exact solution of the Kardar-Parisi-Zhang equation. We will come back to the precise derivation of $\Phi(H)$ for the Brownian initial condition in Section 7.3.2.

6.5 Recent applications of the Weak Noise Theory

Before we end this Chapter on Weak Noise Theory, let us mention a few recent problems related to the KPZ equation at short time to which this theory has been applied.

- The study of the parabolic initial condition $h(x, t = 0) = \frac{x^2}{L}$ in full-space which interpolates between the flat and the droplet initial conditions [204].
- The study of the stationary initial condition, the discovery of the dynamical phase transition due to the symmetry breaking [205, 206] and the development of an effective Landau theory to explain the phenomenon. In particular, the authors of Ref. [207] Smith, Kamenev and Meerson concluded that when studying the one-point height distribution H at position L, $|H|$ plays the role of an inverse temperature and L the role of an external magnetic field in the Landau model.
- The study of finite size effects for the Kardar-Parisi-Zhang height distribution at $x = 0$ on a ring of length $2L$ with flat initial condition [211].
- The study in the half-space of the flat initial condition with different boundary conditions [209, 210].
- The study in the full-space of a relation between the height distribution for stationary and flat initial conditions leading to the exact relation

$$S_{\text{flat}}(H) = \frac{1}{2\sqrt{2}} S_{\text{stat}}(2H) \tag{6.5.1}$$

  for the analytic (or symmetric) branch of $S_{\text{stat}}(2H)$ [208], see below.
- The study of the time-averaged height distribution for flat initial condition in full-space [212]

$$\bar{H}(t) = \frac{1}{t} \int_0^t \mathrm{d}t' \; h(x = 0, t'). \tag{6.5.2}$$

The next Chapter will be dedicated to a method called *the first cumulant approximation* which allows to obtain exactly and entirely the large deviation function S, i.e. not only its tails and the small argument behavior. It would be interesting to see whether the exact solutions we provide in the next Chapter could allow to solve the WNT equations exactly in any regime of H.

Chapter 7

Large deviation solutions at short time: one method to rule them all

In this Chapter, we will present the theoretical framework that we introduced in Refs. [5, 6, 8, 9] building on the pioneering work of Ref. [169] to obtain the exact distribution of the KPZ solutions at short time in a large deviation form. This framework is readily applicable to any initial conditions of the KPZ equation for which the generating function exhibits a Fredholm representation.

7.1 The first cumulant approximation of Fredholm determinants at short time

As presented in the first part of this Thesis, for all known solutions to the KPZ equation there is a duality between the generating function of the exponential of the KPZ height at one point and a linear statistics of a Determinantal or Pfaffian process. Indeed for $z \geqslant 0$, we have the equality

$$\mathbb{E}_{\mathrm{KPZ}}\left[\exp\left(-\frac{z\alpha}{\sqrt{t}}e^{H(t)}\right)\right] = \mathbb{E}_K\left[\prod_{i=1}^{\infty}\frac{1}{[1+ze^{t^{1/3}a_i}]^{\chi}}\right] \tag{7.1.1}$$

where the parameters $\alpha > 0$, $\chi > 0$ depend on the initial condition and where the set of points $\{a_i\}_{i\in\mathbb{N}}$ forms, see Chapter 2,

- either a Determinantal point process with scalar kernel K in which case

$$\mathbb{E}_K\left[\prod_{i=1}^{\infty}\frac{1}{[1+ze^{t^{1/3}a_i}]^{\chi}}\right] = \mathrm{Det}[I-\sigma_{z,t}K]_{\mathbb{L}^2(\mathbb{R})} \tag{7.1.2}$$

- or a Pfaffian point process with 2×2 matrix valued kernel K in which case

$$\mathbb{E}_K\left[\prod_{i=1}^{\infty}\frac{1}{[1+ze^{t^{1/3}a_i}]^{\chi}}\right] = \mathrm{Pf}[J-\sigma_{z,t}K]_{\mathbb{L}^2(\mathbb{R})} \tag{7.1.3}$$

In both cases the "generalized Fermi factor" $\sigma_{z,t}$ is defined as

$$\sigma_{z,t}(a) = 1 - \frac{1}{[1+ze^{t^{1/3}a}]^{\chi}} \tag{7.1.4}$$

Remark 7.1.1. *In practice, the coefficient α will account for an eventual shift in the solution of the KPZ equation to center its distribution around 0. For the solved cases of the KPZ equation, the power in the Fermi factor is either $\chi = 1$ or $\chi = \frac{1}{2}$.*

We recall that the mean density of the associated Determinantal or Pfaffian processes are given by the diagonal elements of the associated kernels, i.e. by $K(v, v)$ for Determinantal processes, see Eq. (2.2.1), and $K_{12}(v, v)$ for Pfaffian processes, see Eqs. (2.2.5) and (2.2.7). It has been observed for all known initial conditions of the KPZ equation that these densities have a similar asymptotic behavior:

Result 7.1.2 (*Density of the point processes related to the KPZ equation I*)

1. *The asymptotic behavior of the densities is given as*

$$\begin{cases} K(at^{-1/3}, at^{-1/3}) & \simeq_{t\ll 1} t^{-1/6}\rho_\infty(a)\Theta(\Xi - a) \\ K_{12}(at^{-1/3}, at^{-1/3}) & \simeq_{t\ll 1} t^{-1/6}\rho_\infty(a)\Theta(\Xi - a) \end{cases}$$

for some finite $\Xi < \infty$ where Θ is the Heaviside function.

This scaling in t is consistent for instance with the behavior of the mean density of the Airy point process which should match the semi-circle for large negative argument. The precise form of ρ_∞ depends on the initial condition.

As the generating function of the exponential of the KPZ height is written as a linear statistics over a Determinantal (or Pfaffian) point process, let us study its first cumulant κ_1. From our introduction of cumulant expansions in the first Part of this Thesis, see Eqs. (2.2.23) and (2.2.28), we know that it reads

$$\kappa_1 = -\chi \int_{\mathbb{R}} \mathrm{d}a \log(1 + ze^{t^{1/3}a}) K(a, a) \tag{7.1.5}$$

and equivalently with $K_{12}(a, a)$. Rescaling the integration variable $a \to t^{-1/3}a$ leads to

$$\kappa_1 = -\chi t^{-1/3} \int_{\mathbb{R}} \mathrm{d}a \log(1 + ze^{a}) K(at^{-1/3}, at^{-1/3}) \tag{7.1.6}$$

Upon the use of the Result 7.1.2, the first cumulant thus admits the following leading order behavior at short time

$$\kappa_1 = -\frac{\Psi(z)}{\sqrt{t}} \tag{7.1.7}$$

where the function $\Psi(z)$ is defined on $z \in \left[-e^{-\Xi}, +\infty\right[$ as

$$\Psi(z) = \chi \int_{-\infty}^{\Xi} \mathrm{d}a \, \log(1 + ze^{a}) \rho_\infty(a) \tag{7.1.8}$$

This first cumulant is a good starting point to investigate the short-time properties. The parameter $1/\sqrt{t}$ being large, it allows to use saddle points or Legendre transforms. This factor matches the same scaling used in Weak Noise Theory. The empirical observation is that higher cumulants are all subdominant and hence one can truncate the cumulant series at the first order at short time. We call this truncation the *first cumulant approximation*, a conjecture which was introduced by us in Ref. [8] and reads:

Result 7.1.3 (*First cumulant approximation for the KPZ solution at short time*)

The first cumulant approximation conjectures that for all solved initial conditions of the Kardar-Parisi-Zhang equation, the following Large Deviation Principle is exact

$$\lim_{t\to 0} -\sqrt{t}\log \mathbb{E}_{\rm KPZ}\left[\exp\left(-\frac{z\alpha}{\sqrt{t}}e^{H(t)}\right)\right] = \Psi(z) \tag{7.1.9}$$

for $\Psi(z)$ given in Eq. (7.1.8). In other words for small time $t \ll 1$,

$$\mathbb{E}_{\rm KPZ}\left[\exp\left(-\frac{z\alpha}{\sqrt{t}}e^{H(t)}\right)\right] \asymp \exp\left(-\frac{\Psi(z)}{\sqrt{t}}\right) \tag{7.1.10}$$

The validity of this conjecture can be understood as follows. As seen from Eq. (2.2.27), the cumulants κ_n are the ones of the random variable $X = \chi\sum_{i=1}^{\infty}\log(1+ze^{t^{1/3}a_i})$ and the set $\{a_i\}$ forms a Determinantal/Pfaffian point process. In the limit $t \ll 1$ many of the a_i's contribute to the sum, and by a law of large number, the fluctuations of X around the mean value are subdominant. This is fully confirmed by us by an explicit calculation of higher order cumulants $n \geqslant 2$ in Ref. [5] where cancellations occur leaving only subdominant powers of t, see Chapter 9.

7.1.1 Towards rigorization: a flavor of the Szegö theorem

Although the first cumulant conjecture is presented non-rigorously within this Thesis, there exists in the case of the droplet initial condition and the Airy $\beta = 2$ point process a rigorous version of it proved by Basor and Widom in Ref. [213].

Theorem 7.1.4 (*Basor & Widom. Theorem 3.8 of Ref. [213]*)

Let $f \in L^\infty(\mathbb{R})$, let $A_t(f)$ an integral operator on $\mathbb{L}^2(\mathbb{R})$ with kernel given by

$$f\left(xt^{1/3}\right)\int_0^\infty {\rm d}z\,{\rm Ai}(x+z){\rm Ai}(z+y) = f\left(xt^{1/3}\right)K_{\rm Ai}(x,y) \tag{7.1.11}$$

Assume that $f(-x^2) \neq -1$ for all x. Then as $t \to 0$, the Fredholm determinant of $A_t(f)$ is given by

$${\rm Det}(I + A_t(f)) = \exp\{\frac{c_1}{\sqrt{t}} + c_2 + o(1)\} \tag{7.1.12}$$

where

$$c_1 = \int_0^{+\infty}{\rm d}x\,\frac{\sqrt{x}}{\pi}\log(1+f(-x)), \quad c_2 = \frac{1}{2}\int_0^\infty {\rm d}x\,xG(x)^2. \tag{7.1.13}$$

with $G(x) = \frac{1}{2\pi}\int_{\mathbb{R}}{\rm d}y\,e^{ixy}\log(1+f(-y^2))$.

From the point of view of the theory of operators, the first cumulant conjecture along with the Theorem of Basor and Widom appear as a continuous version of the Szegö theorem [214] for Toeplitz determinants. The first cumulant provides the weak version of the theorem and we have shown in Ref. [5] that the second cumulant provides the additional term of the strong version of the theorem: the Gaussian free field correction. In the third part of this Thesis, we will extend the Theorem of Basor and Widom up to arbitrary order in the variable t.

7.2 Large deviations for various initial conditions

In the first Part of this Thesis, we recalled various exact solutions to the Kardar-Parisi-Zhang valid at all times. In particular, we provided the asymptotic density ρ_∞ for:

- In full-space: the droplet initial condition and the Brownian initial condition
- In half-space: the droplet initial condition for a wall with parameter $A = -\frac{1}{2}, 0, +\infty$

From the knowledge of the asymptotic density ρ_∞, we have determined the expression of the large deviation function $\Psi(z)$ using Eq. (7.1.8) for various initial conditions and we present our result in the Table 7.1.

$-\Psi(z) \propto$	$\int_{\mathbb{R}} \frac{\mathrm{d}k}{2\pi} \mathrm{Li}_2(-zk^2 e^{-k^2})$	$\int_{\mathbb{R}} \frac{\mathrm{d}k}{2\pi} \mathrm{Li}_2(-ze^{-k^2})$	$\int_{\mathbb{R}} \frac{\mathrm{d}k}{2\pi} \mathrm{Li}_2(-z\frac{e^{-k^2}}{k^2})$
Full space		Droplet	Brownian Flat
Half space	Droplet $(A = \infty)$	Droplet $(A = 0)$ Brownian $(A = \infty)$	Brownian $(A = 0)$ Flat $(A = 0)$

Table 7.1: Large deviation function $\Psi(z)$ resulting from the first cumulant approximation for various initial conditions. The proportionality notation $\propto$ indicates a possible numerical factor such as in the case of the half-space problem, where the function $\Psi(z)$ has a factor $1/2$ compared to the full-space case.

In addition to the four cases for which we performed analytic calculations, the Table 7.1 contains four other cases which we have obtained using the following facts. From a scaling argument at short time given in the Chapter 1 and from the Weak Noise Theory, four rules have been determined to relate the short-time behavior of the KPZ solution in half-space:

1. The solutions to the KPZ equation in half-space for any finite $A < +\infty$ have the same behavior at short time as for $A = 0$;
2. The large deviation function $\Phi(H)$ of the exponential of the KPZ height in half-space for any finite $A < \infty$ is half of the one of the same initial condition in full-space.
3. From the Theorem of Parekh of Ref. [173], the large deviation function for the Brownian initial condition in half-space with a hardwall is the same as for the droplet initial condition with $A = 0$.
4. The short-time distribution of the flat initial condition in full-space is proportional to the analytic branch of the distribution for the Brownian initial condition, see below.

This Table is quite striking to us as it seems to indicate some universality in the short-time behavior of the large deviation function $\Psi(z)$. We have no interpretation at present of why polylogarithm functions appear in the KPZ problem, nor why the different cases involve various quadratic k factors in the polylogarithms.

7.3 Inverting the Legendre transform

From the first cumulant approximation, the next step consists in inverting the generating function to obtain the short-time distribution of the height H of the KPZ equation. As stated before, the short-time scaling in $1/\sqrt{t}$ leads to a natural Large Deviation formulation of the probability distribution of the one-point KPZ height as

$$P(H,t) \asymp \exp\left(-\frac{\Phi(H)}{\sqrt{t}}\right) \tag{7.3.1}$$

where the function Φ is obtained by inverting the following Legendre transform:

$$\min_{H\in\mathbb{R}}\left[\Phi(H) + z\alpha e^{H}\right] = \Psi(z) \tag{7.3.2}$$

The goal of the remainder this Section will be to determine the large deviation function $\Phi(H)$. Before we turn to the inversion of the Legendre transform, we shall need some more properties on the asymptotic densities of the Determinantal (or Pfaffian) processes, since ρ_∞ controls $\Psi(z)$, and hence all the properties of $\Phi(H)$. It has been observed for all known initial conditions of the KPZ equation that these asymptotic densities behave as:

Result 7.3.1 (*Densities of the point processes related to the KPZ equation II*)

2. *The asymptotic density ρ_∞ is positive, real-valued and strictly decreasing on $]-\infty,\Xi]$ and grows towards $-\infty$ as*
$$\rho_\infty(a) \simeq_{-a\gg 1} \beta_1[-a]^{\gamma_1}$$
for some $\beta_1 > 0$ and $\gamma_1 > 0$.

3. *The asymptotic density ρ_∞ vanishes algebraically at the right edge Ξ as*
$$\rho_\infty(a) \simeq_{a\to\Xi} (\Xi - a)^{\nu}$$
for some $0 < \nu \leqslant 1$.

The precise values of all constants β_1, γ_1 and ν will depend on the initial condition. Finally, there exists one last property that is verified by the asymptotic density ρ_∞ of all initial conditions *except* the Brownian initial condition in full-space.

Result 7.3.2 (*Densities of the point processes related to the KPZ equation III*)

4. *The extension of ρ_∞ on the interval $]\Xi,+\infty[$ is purely imaginary-valued and behaves towards $+\infty$ as*
$$\rho_\infty(a) \simeq_{a\gg 1} \beta_2[-a]^{\gamma_2}$$
for some $\beta_2 > 0$ and γ_2 a half-integer.

In the remainder of this Section, we will formulate the result and properties of the function $\Phi(H)$ for all initial conditions *except* the Brownian initial condition in full-space, which we shall treat as a singular case afterwards.

7.3.1 Solution to the general case

Let us first analyze the function $\Psi(z)$ which will be central in the Legendre inversion. To obtain $\Phi(H)$ for all $H \in \mathbb{R}$, it turns out that one needs more information than $\Psi(z)$ for $z \in \left[-e^{-\Xi}, +\infty\right[$:

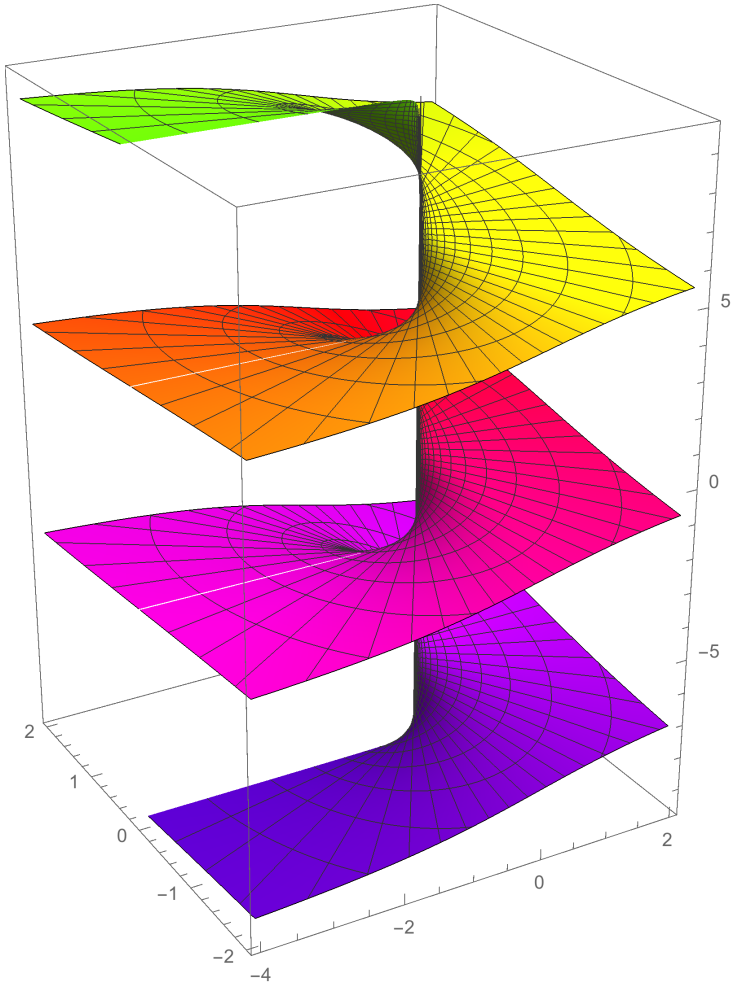

Figure 7.1: Riemann surface of $z \mapsto \Im(\log z)$.

one needs a continuation of $\Psi(z)$. For $z \in \left[-e^{-\Xi}, +\infty\right[$, the expression of $\Psi(z)$ is given by

$$\Psi(z) = \chi \int_{-\infty}^{\Xi} \mathrm{d}a \, \log(1 + ze^{a})\rho_{\infty}(a) \tag{7.3.3}$$

Defining the strictly positive variable $\zeta = e^{-\Xi}$ and the integrated density up to Ξ

$$f(y) = \chi \int_{-\log y}^{\Xi} \mathrm{d}v \, \rho_{\infty}(v), \tag{7.3.4}$$

Ψ also admits the following rewriting $\Psi(z) = \int_{\zeta}^{+\infty} \mathrm{d}y f(y) \frac{z}{y} \frac{1}{y+z}$ by integration by part on Eq. (7.3.3). The pole of the integrand at $y = -z$, coupled to Result 7.3.2 which states that ρ_{∞} rotates to the imaginary axis above Ξ, indicates that $\Psi(z)$ exhibits a branch cut along the interval $z \in]-\infty, -\zeta[$ akin to the one of the usual logarithm along the negative real axis. In Fig. 7.1, we represent some Riemann sheets of the logarithm composing the full associated Riemann surface. Keeping the analogy with the usual logarithm, it is possible to construct $\Psi(z)$ in a Riemann surface. This can be done either by proceeding Riemann sheet by Riemann sheet or by constructing a multi-valued function over the complex plane. Indeed, the jump of Ψ across the branch cut at $]-\infty, -\zeta[$ will be defined as

$$\Delta(z) = \lim_{\epsilon \to 0} \left[\Psi(z + i\epsilon) - \Psi(z - i\epsilon)\right] = 2i\pi f(-z) \tag{7.3.5}$$

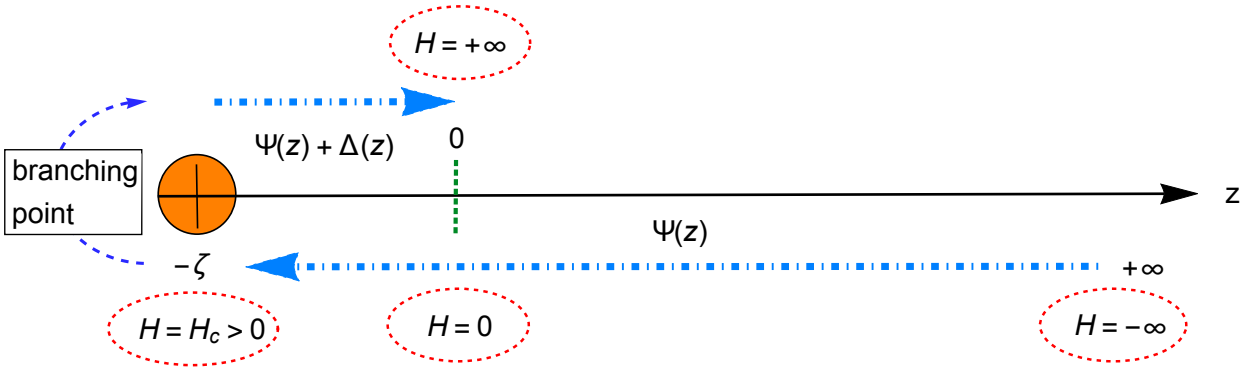

Figure 7.2: Schematic representation of the parametric solution of the optimization problem. For $H \leqslant H_c$ one uses the function Ψ to invert the Legendre transform taking the parameter z to decrease from $+\infty$ to $-\zeta$. At $H = H_c$ or $z = -\zeta$, one needs to turn around the branching point and replace Ψ by its continuation $\Psi + \Delta$ to determine all $H \geqslant H_c$ by increasing the parameter z from $-\zeta$ to 0.

From the result 7.3.2, we know that for $z \in [-\zeta, 0[$, Δ will be real valued and hence we use this interval for the domain of definition of Δ and we subsequently define the continuation of Ψ as a multi-valued function $\Psi_{\text{continued}}$ defined on $[-\zeta, 0[$ as

$$\forall z \in [-\zeta, 0[, \quad \Psi_{\text{continued}}(z) = \Psi(z) + 2i\pi f(-z) \tag{7.3.6}$$

The reason behind this construction of $\Psi_{\text{continued}}$ is that naively, the Legendre transform of the distribution of H gets inverted as

$$\min_{H \in \mathbb{R}} \left[\Phi(H) + z\alpha e^H \right] = \Psi(z) \quad \Rightarrow \quad \Phi(H) = \max_z \left[\Psi(z) - z\alpha e^H \right] \tag{7.3.7}$$

As shown in Ref. [6], this is only partially valid for the solutions of the KPZ equation as this procedure will not provide the full function $\Phi(H)$ on $\mathbb{R}$ but only its expression on some interval $H \in]-\infty, H_c]$ as depicted in Fig. 7.2. We proved in Ref. [6] that continuing Ψ to $\Psi_{\text{continued}}$ allows to obtain the missing part of $\Phi(H)$ on the interval $H \in [H_c, +\infty[$.

In particular, we obtained the complete solution for $\Phi(H)$ in two equivalent forms: one is an implicit equation and the other is a parametric system of equations. The formal statement of our result is the following:

Result 7.3.3 (*Expression of the large deviation function $\Phi(H)$*)

The shifted height defined by $\tilde{H} = H(t) + \log\alpha - \log\Psi'(0)$ is centered, i.e. $\mathbb{E}[\tilde{H}] = 0$. If the parameter α was initially free (due to a shift in the initial condition of H), one could choose at this stage $\alpha = \Psi'(0)$. We further introduce the "branching height" H_c

$$H_c = \log \frac{\Psi'(-e^{-\Xi})}{\Psi'(0)}. \tag{7.3.8}$$

Then, Φ is the solution of the implicit equations

$$\begin{aligned} &\forall H \leqslant H_c,\ \Phi(H) - \Phi'(H) = \Psi(-\frac{e^{-H}\Phi'(H)}{\Psi'(0)}), \\ &\forall H \geqslant H_c,\ \Phi(H) - \Phi'(H) = \Psi(-\frac{e^{-H}\Phi'(H)}{\Psi'(0)}) + 2i\pi f(\frac{e^{-H}\Phi'(H)}{\Psi'(0)}). \end{aligned} \tag{7.3.9}$$

$\Phi(H)$ is also solution to the parametric equations

- *$\forall H \leqslant H_c$, or equivalently, $\forall z \in [-e^{-\Xi}, +\infty[$*

$$\begin{aligned} \Psi'(0)e^H &= \Psi'(z), \\ \Phi(H) &= \Psi(z) - z\Psi'(z). \end{aligned} \tag{7.3.10}$$

- *$\forall H \geqslant H_c$, or equivalently, $\forall z \in [-e^{-\Xi}, 0[$*

$$\begin{aligned} \Psi'(0)e^H &= \Psi'(z) - 2i\pi f'(-z), \\ \Phi(H) &= \Psi(z) - z\Psi'(z) + 2i\pi f(-z) + 2i\pi z f'(-z). \end{aligned} \tag{7.3.11}$$

We recall that $\Psi(z)$ and $f(z)$ are given in (7.3.3) and (7.3.4).

Remark 7.3.4. *The parametric solution is quite useful to plot Φ while the implicit solution is useful to derive the small argument expansion and the large argument asymptotics of Φ.*

In principle, to leading order in the variable t, this result fully solves the problem of determining the short-time one-point height distribution. In addition to the general equations verified by $\Phi(H)$ we have also established some of its properties regarding its regularity and its asymptotic behavior. These results are summarized in the following result.

Result 7.3.5 (*Properties of the large deviation function* $\Phi(H)$)

The properties of Φ *are the following :*

1. Φ *is infinitely differentiable everywhere on the real line, i.e. it has no singularity.*
2. Φ *is quadratic for small argument, i.e.* $\Phi(0) = \Phi'(0) = 0$ *and*

$$\Phi''(0) = -\frac{\Psi'(0)^2}{\Psi''(0)}. \tag{7.3.12}$$

Hence the distribution of H *is Gaussian for small* H *around 0 and its second cumulant reads*

$$\mathbb{E}[H^2] = -\frac{\Psi''(0)}{\Psi'(0)^2}\sqrt{t} \tag{7.3.13}$$

3. *The left tail of* Φ *is given by*

$$\Phi(H) \simeq_{H\to-\infty} \frac{\chi\beta_1}{(\gamma_1+1)(\gamma_1+2)}|H|^{\gamma_1+2}. \tag{7.3.14}$$

4. *The right tail of* Φ *is given by*

$$\Phi(H) \simeq_{H\to+\infty} \frac{2\pi\chi\beta_2}{\gamma_2+1}H^{\gamma_2+1}. \tag{7.3.15}$$

We applied this very general framework to all known solutions to the KPZ equation *except* the Brownian initial condition which violates one of the conditions of application, specifically the Result 7.3.2. The consequence is that the Brownian initial condition has two branching points instead of one and its associated large deviation function $\Phi(H)$ has a singularity, see Section 7.3.2 below. This result additionally allowed us to obtain most of the tails of the distribution of the KPZ height presented in Table 7.2.

Remark 7.3.6. *Although the results are obtained for arbitrary* γ_1 *and* γ_2*, the known solutions to the KPZ equation all exhibit the same exponents*

$$\gamma_1 = \gamma_2 = \frac{1}{2}. \tag{7.3.16}$$

7.3.2 The singular case of the Brownian initial condition

As we announced earlier in this Section and as mentioned in the Section related to Weak Noise Theory, the Brownian initial condition is a singular case where the short-time large deviation function will exhibit a singularity. In the following, we shall present step by step the calculation of large deviation function $\Phi(H)$ and show that our exact results match the numerical simulations obtained through Weak Noise Theory. Our goal here will be to study the short-time behavior of the stationary initial condition, represented by the Brownian initial condition with a drift w equal to 0.

In the case of the Brownian initial condition, the generating function of the exponential of the height comprises an additional term χ, which is a random variable, but nonetheless it is still equal to a Fredholm determinant (see Chapter 3 Eq. (3.2.7)) to which we can apply the first cumulant conjecture. Hence, our starting point is the Large Deviation principle established for Fredholm determinants which reads

$$\mathbb{E}_{\mathrm{KPZ},\chi}\left[\exp(-\frac{z}{t}e^{H(t)+\chi})\right] \asymp e^{-\frac{\Psi(z)}{\sqrt{t}}} \tag{7.3.17}$$

We recall that χ is a real random variable, independent of H with the following distribution $p(\chi)\mathrm{d}\chi = e^{-2w\chi-\exp(-\chi)}\mathrm{d}\chi$ and that starting from a Brownian with drift w, the relevant parameter at short time is $\tilde{w} = wt^{1/2}$ (see Chapter 1 Table 1.1). Proceeding to a saddle point method on the variable χ in the generating function, one shows [9] that the generating function simplifies in the limit $\tilde{w} = 0$ as

$$\mathbb{E}_{\mathrm{KPZ},\chi}\left[\exp(-\frac{z}{t}e^{H(t)+\chi})\right] \asymp \mathbb{E}_{\mathrm{KPZ}}\left[\exp(-\frac{2\sqrt{z}}{\sqrt{t}}e^{\frac{H}{2}})\right] \tag{7.3.18}$$

In addition, in that limit the function $\Psi(z)$ is given by

$$\Psi(z) = \int_{\mathbb{R}} \frac{\mathrm{d}k}{2\pi}\mathrm{Li}_2(-z\frac{e^{-k^2}}{k^2}) = \int_0^{+\infty} \frac{\mathrm{d}y}{\pi}\left[\frac{2}{3}W_0(y)^{3/2} + 2W_0(y)^{1/2}\right]\frac{z}{y}\frac{1}{y+z} \tag{7.3.19}$$

where W_0 is the first real branch of the Lambert function, see Appendix A.1.

Remark 7.3.7. *This function $\Psi(z)$ is not analytic in z at $z = 0$, in fact it admits the following expansion*

$$\forall z \geqslant 0, \qquad \Psi(z) = -\frac{1}{\sqrt{4\pi}}\sum_{n\geqslant 1}(-1)^n\frac{(4z)^{\frac{n}{2}}}{n!}\Gamma\left(\frac{n}{2}\right)\left(\frac{n}{2}\right)^{\frac{n-3}{2}} \tag{7.3.20}$$

The inversion of the Laplace transform of the exponential height requires to perform the following Legendre transform

$$\Phi(H) = \max_{z\geqslant 0}\left[\Psi(z) - 2\sqrt{ze^H}\right] \tag{7.3.21}$$

The inspection of this optimization problem along with the exact expression of Ψ leads to the following observations:

- This optimization problem allows to obtain $\Phi(H)$ for $H \in]-\infty, 0]$;
- The branch cut of $\Psi(z)$ is located along the negative half-line $z \in]-\infty, 0[$.

Similarly as the general case, we may define the continuation of Ψ by adding the corresponding value of the jump towards the upper Riemann sheet. This leads us to define for $z \in \left[0, e^{-1}\right]$ the jump Δ_0 as

$$\Delta_0(z) = \frac{4}{3}\left[-W_0(-z)\right]^{3/2} - 4\left[-W_0(-z)\right]^{1/2}. \tag{7.3.22}$$

In the general case, the jump $\Delta_0(z)$ would diverge along the imaginary axis at the edge of its domain of definition which is $z = e^{-1}$ in the present case. This divergence, mentioned in Result 7.3.2 for all initial conditions except the Brownian one, indicated that it was sufficient to consider $\Psi_{\text{continued}} = \Psi + \Delta_0$ to obtain the rest of the distribution $\Phi(H)$. Since the jump $\Delta_0(z)$ does not diverge at $z = e^{-1}$, this is not true for the Brownian initial condition and this continuation only allows to obtain $\Phi(H)$ for $H \in [0, H_{c_2}]$ where

$$\begin{aligned} H_{c2} &= 2\log[2e - \Psi'(e^{-1})] - 1 \approx 1.85316 \\ \Psi'(e^{-1}) &= \int_0^{+\infty}\frac{\mathrm{d}y}{\pi}\left[1 + \frac{1}{y}\right]\frac{\sqrt{y}}{e^{-1} + ye^y} \end{aligned} \tag{7.3.23}$$

The delicate point here is to define again another continuation of Ψ, yet the continuation has to be taken over Δ_0. In the general case, the Riemann surface associated to Ψ was only a deformation of the one of the logarithm. In the present case, this is modified due to the presence of the Lambert function W: indeed the Lambert function $W(y)$ is multi-valued for $y \in \left[-e^{-1}, 0\right[$ and the two real branches are W_0 and W_{-1}, see Appendix A.1. In Ref. [9], we identified the proper

continuations of the jump Δ_0 allowing to solve the problem. Defining the jump Δ_{-1} where the Lambert function W_0 in Δ_0 is simply substituted by W_{-1}

$$\Delta_{-1}(z) = \frac{4}{3}\left[-W_{-1}(-z)\right]^{3/2} - 4\left[-W_{-1}(-z)\right]^{1/2} \tag{7.3.24}$$

Then the two continuations of $\Psi_{\text{continued}}$ that we have found are defined for $z \in \left]0, e^{-1}\right[$ and are expressed as

$$\begin{aligned} \Psi_{\text{continued},-1}(z) &= \Psi(z) + \Delta_{-1}(z) \\ \Psi_{\text{continued},-1/2}(z) &= \Psi(z) + \frac{\Delta_{-1}(z) + \Delta_0(z)}{2} \end{aligned} \tag{7.3.25}$$

These two continuations allow to find two physical[7] continuations of $\Phi(H)$ in the missing range $[H_{c2}, +\infty[$ which we denote $\Phi_{-1/2}$ and Φ_{-1}. Besides, in Ref. [9] we proved the following properties:

- If we choose to continue $\Phi(H)$ with $\Phi_{-1/2}(H)$, then the second derivative Φ'' has a discontinuity at $H = H_{c2}$.
- If we choose to continue $\Phi(H)$ with $\Phi_{-1}(H)$, then the branching is smooth and all derivatives of any order match between Φ and Φ_{-1}.
- For all $H \geqslant H_{c2}$, these continuations are ordered as $\Phi_{-1}(H) \geqslant \Phi_{-1/2}(H)$. This implies that Φ_{-1} is subdominant in terms of large deviations and hence only $\Phi_{-1/2}$ survives.

These observations lead us to call $\Phi_{-1/2}$ the asymmetric non-analytic continuation and Φ_{-1} the symmetric analytic continuation of Φ. The reason for the names asymmetric and symmetric comes from the fact that these continuations will match the large deviation distributions found in the Weak Noise Theory using asymmetric or symmetric solutions of the hydrodynamic equations. Before comparing our predictions to the estimates obtained in the Weak Noise Theory, we summarize the variational representations of $\Phi(H)$ for the Brownian initial condition for all branches as follows.

[7] As we shall see below, they can be both associated to some initial conditions.

Result 7.3.8 (*Variational solution for the large deviation function $\Phi(H)$*)

The large deviation function $\Phi(H)$ for the Brownian initial condition verifies the following optimization problems.

$$
\begin{aligned}
&\Phi(H) \\
&= \max_{z\in[0,+\infty[} \left[\Psi(z) - 2\sqrt{ze^H}\right], \quad (\textit{for } H \leqslant 0) \\
&= \max_{z\in\left[0,e^{-1}\right]} \left[\Psi(z) + \frac{4}{3}[-W_0(-z)]^{\frac{3}{2}} - 4[-W_0(-z)]^{\frac{1}{2}} + 2\sqrt{ze^H}\right], \quad (\textit{for } 0 \leqslant H \leqslant H_{c2}) \\
&= \min_{z\in\left]0,e^{-1}\right]} \left[\Psi(z) + \frac{4}{3}[-W_{-1}(-z)]^{\frac{3}{2}} - 4[-W_{-1}(-z)]^{\frac{1}{2}} + 2\sqrt{ze^H}\right], \\
&\qquad\qquad (\textit{for } H \geqslant H_{c2}), \quad \textit{analytic branch} \\
&= \min_{z\in\left]0,e^{-1}\right]} \left[\Psi(z) + \frac{2}{3}[-W_0(-z)]^{\frac{3}{2}} + \frac{2}{3}[-W_{-1}(-z)]^{\frac{3}{2}} - 2[-W_0(-z)]^{\frac{1}{2}} - 2[-W_{-1}(-z)]^{\frac{1}{2}} + 2\sqrt{ze^H}\right]. \\
&\qquad\qquad (\textit{for } H \geqslant H_{c2}), \quad \textit{non-analytic branch}
\end{aligned}
\tag{7.3.26}
$$

Although there is coexistence of two branches above H_{c2}, the analytic branch gives a higher contribution in the large deviation function, hence is not optimal and can be neglected compared to the non-analytic one. The function $\Psi(z)$ is given in Eq. (7.3.17), we have inserted the explicit expressions of the different jumps and continuations and we recall that in our system of units $H_{c2} \approx 1.85316$.

Remark 7.3.9. *One can understand the change of sign in front of $2\sqrt{ze^H}$ in the variational problem as follows: we first decrease z from $+\infty$ to 0 and then increase it to e^{-1}. In the complex z-plane, turning around 0 induces a branch change in the square root function $\sqrt{z} \to -\sqrt{z}$. The change from a maximum to a minimum can be seen from a change of convexity in the argument of the variational problem.*

To observe the singularity in the large deviation $\Phi(H)$ we have plotted in Fig. 7.3 the derivative of $\Phi(H)$ for a set of H which allows to observe the different continuations of $\Phi(H)$. It is visible on Fig. 7.3 that the asymmetric non-analytic branch (the dot-dashed brown line) induces a discontinuity in the second derivative of $\Phi(H)$. For completeness, we also plot the whole large deviation function $\Phi(H)$ in Fig. 7.4 displaying both symmetric and asymmetric branches.

We now turn to the comparison of our exact solution for the large deviation function $\Phi(H)$ with the numerical estimates obtained by Janas, Kamenev and Meerson in [205]. In our system of units[8], the comparison is possible for a range $H \in [0, 4]$ which comprises all continuations of $\Phi(H)$. The comparison is made for both symmetric and asymmetric WNT solutions, allowing us to test our hypothesis whether our analytic and non-analytic branches match these two solutions. In our system of units, the critical height at which the phase transition was observed in Ref. [205] is $H_{c2} \approx 1.85$. The exact value that we have found for H_{c2} matches this numerical estimate. That fact already hints that the conclusion of this study will coincide with the one of WNT. We present in Fig. 7.4 our general solution along with the comparison with the results of Janas, Kamenev and Meerson. The interpretation of Fig. 7.4 is that our analytic branch matches point to point the symmetric WNT solution and that our non-analytic branch also matches point to point the asymmetric WNT solution for the interval considered $H \in [0, 4]$. Further numerics would be

[8]Note that Ref. [205] uses a sign of λ_0 opposite to ours. Equivalently, their variable H is opposite to ours, which exchanges right and left tails. More precisely, in our units $\Phi(H) = \frac{1}{8}S(-2H)$ where $S(H)$ is the rescaled total action given in [205].

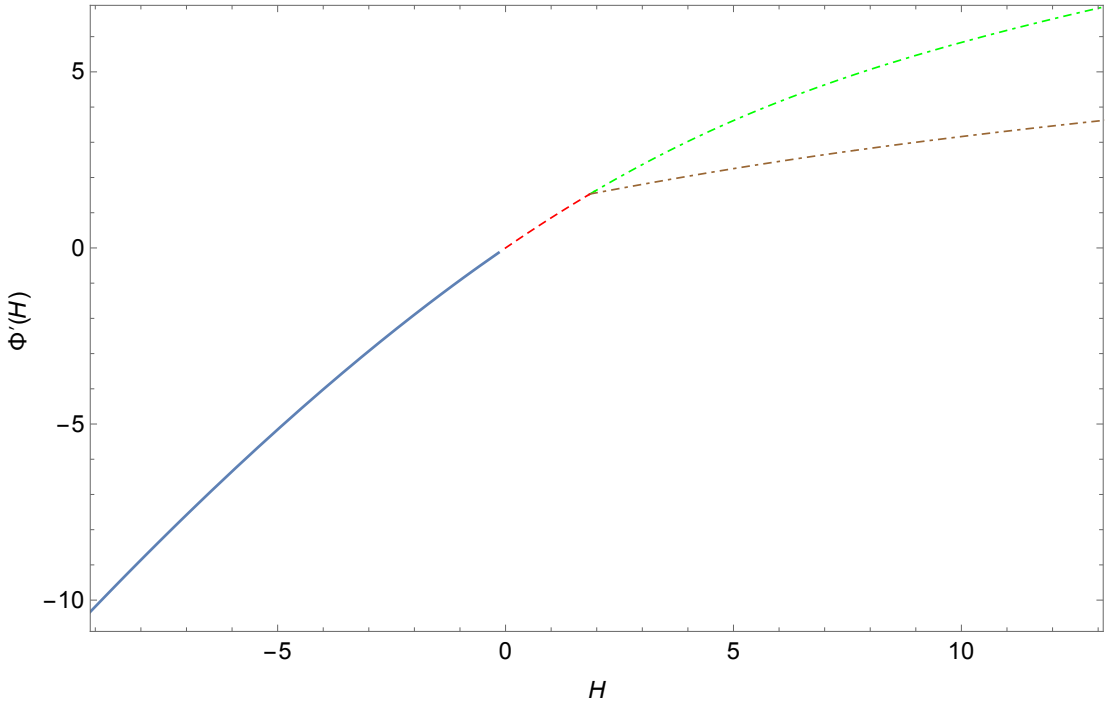

Figure 7.3: The function $\Phi'(H)$ vs H for the Brownian initial condition. The blue line corresponds to the exact solution for $H < 0$, the dashed red line corresponds to a first analytic continuation for $0 < H < H_{c2}$, the dot-dashed green line corresponds to a second symmetric analytic continuation for $H > H_{c2}$ and the dot-dashed brown line corresponds to a second asymmetric non-analytic continuation for $H > H_{c2}$, where $H_{c2} \approx 1.85316$. At the point $H = H_{c2}$ the asymmetric continuation of $\Phi'(H)$ is continuous but not differentiable.

required to allow a comparison outside $H \in [0, 4]$ but according to the overlap of our exact result with numerical estimates, we are confident that our branching point H_{c2} is the critical field where a phase transition was observed in [205].

7.4 A hint of universality for the solutions at short time

Before giving in the next Chapter the explicit formulae for $\Phi(H)$ for all cases mentioned in the Table 7.2, we will discuss the tails properties of the large deviations, i.e. the asymptotics of $\Phi(H)$. We have represented in the Table 7.2 the tails obtained for various initial conditions both in full-space and half-space. These tails are important as they provide the information on how the solutions to the Kardar-Parisi-Zhang equation depart from the Gaussian world. Besides, as we shall discuss in the third Part of this Thesis, these tails seem to be persistent in time hence indicating the presence of conserved quantities or the establishment of some properties of the Kardar-Parisi-Zhang universality class at short time.

We observe that the exponents of the tails are always $5/2$ and $3/2$ and therefore neither side of the distribution is Gaussian and the distribution is highly asymmetric. This asymmetry can be understood from the Kardar-Parisi-Zhang equation where the height field is driven by the square of the gradient of the field which is always positive. Besides, the pre-factors are extremely similar between the different initial conditions, hinting to some form of universality for the large deviations of the solution to the KPZ equation. Finally, aesthetically speaking we observe a difference

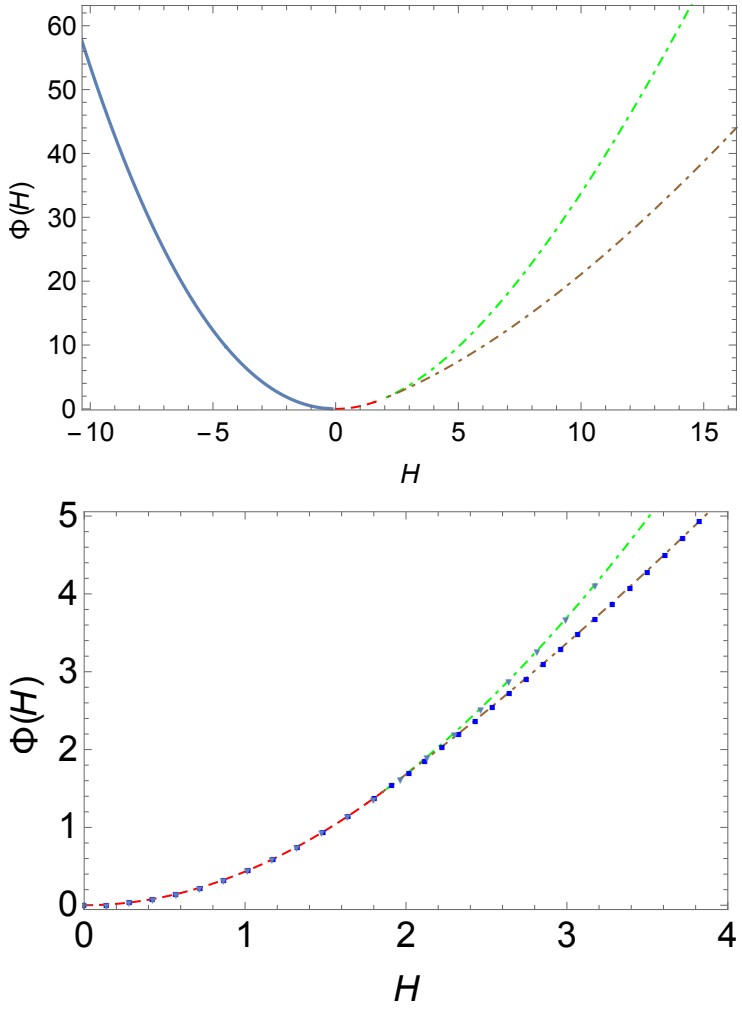

Figure 7.4: Top: The rate function $\Phi(H)$ defined which describes the distribution of the KPZ height $H = H(x = 0, t)$ at small time for the Brownian initial condition with $\Phi(0) = 0$ and $\langle H \rangle = 0$. The blue line corresponds to the exact solution for $H < 0$, the dashed red line corresponds to a first analytic continuation for $0 < H < H_{c2}$, the dot-dashed green line corresponds to a second symmetric analytic continuation for $H > H_{c2}$ and the dot-dashed brown line corresponds to a second asymmetric non-analytic continuation for $H > H_{c2}$, where $H_{c2} \approx 1.85316$. Note the symmetric continuation, is not the optimal one in the sense of WNT and the asymmetric continuation is regarded as the optimal one. **Bottom:** The large deviation function $\Phi(H)$ is compared with the numerical estimates from [205]. The blue squares represent the value of the action obtained from the asymmetric WNT solution and the grey triangles represent the value of the action obtained from the symmetric WNT solution. The numerical estimates of [205] and our exact results match point to point for both branches. Data courtesy of B. Meerson.

in factor of π between the left tail and the right tail. In our construction, a factor π appeared when considering the jump between different Riemann sheets obtained by picking a residue in the integral definition of $\Psi(z)$. It would be interesting to see whether this factor π has a more profound meaning.

The problem of determining the Large Deviation behavior of a random object is in general complicated and in this Chapter we have made a number of predictions in that direction for the short-time KPZ equation. Nonetheless, from the point of view of physics, it would be satisfactory to have some kind of confirmation of these predictions: either experimentally or numerically. Measuring large deviations in experiments is unfortunately a daunting task as the probability of an extreme event to occur is extremely low. Numerically on the contrary, there exist techniques

Initial condition	Left tail	Right tail
Full space		
Droplet	$\frac{4}{15\pi}\lvert H\rvert^{5/2}$	$\frac{4}{3}H^{3/2}$
Brownian	$\frac{4}{15\pi}\lvert H\rvert^{5/2}$	$\frac{2}{3}H^{3/2}$
Flat	$\frac{8}{15\pi}\lvert H\rvert^{5/2}$	$\frac{4}{3}H^{3/2}$
Half space		
Droplet with reflecting wall ($A = 0$)	$\frac{2}{15\pi}\lvert H\rvert^{5/2}$	$\frac{2}{3}H^{3/2}$
Droplet with repulsive hard wall ($A = \infty$)	$\frac{2}{15\pi}\lvert H\rvert^{5/2}$	$\frac{4}{3}H^{3/2}$
Brownian with repulsive hard wall ($A = \infty$)	$\frac{2}{15\pi}\lvert H\rvert^{5/2}$	$\frac{2}{3}H^{3/2}$

Table 7.2: Tails of the large deviation function for various initial conditions.

such as Importance sampling for Monte Carlo algorithms that allow to probe the regions of extreme events. This will constitute the next Chapter of this Thesis.

Chapter 8

High-precision simulations of the short-time large deviations of the KPZ solutions

This Chapter will be devoted to high-precision simulations of Directed Polymers on a square lattice. These numerical estimates will serve as a basis to confirm the theoretical predictions on the short-time distribution of the solutions to the Kardar-Parisi-Zhang equation. We shall first introduce the model of a Directed Polymer on a lattice and explain briefly the idea on how to reach Large Deviation regimes necessary to validate our theoretical predictions. The end of this Chapter will be dedicated to the presentation of these simulations in various geometries, hence probing different initial conditions for the Kardar-Parisi-Zhang equation. We will in addition provide the exact large deviation functions $\Phi(H)$ related to each initial condition presented in the previous Chapter.

The numerical work presented in this Chapter originates from a collaboration with A. Hartmann and we refer the reader to Refs. [1, 215] for further details. As we shall see, the agreement between the theoretical predictions and the simulations is remarkable, even down to probability densities as small as 10^{-1000}.

8.1 Directed polymer on a lattice

Define a polymer on the rotated square lattice (y, τ), see Fig. 8.1, which is allowed to grow according to the following rule

$$(y, \tau) \to (y \pm \frac{1}{2}, \tau + 1) \tag{8.1.1}$$

For each site of the square lattice, define a quenched random variable $V_{y,\tau}$, a temperature T and an associated Boltzmann weight $\exp(-\frac{V_{y,\tau}}{T})$. For a path $\gamma : (0, 0) \to (y_f, L)$, we define its weight by

$$w_\gamma = \prod_{(y,\tau)\in\gamma} e^{-\frac{V_{y,\tau}}{T}}. \tag{8.1.2}$$

For paths of length L with a starting point $(0, 0)$ and an end-point (y_f, L)[9] the partition sum over all possible polymers is given by the sum of the weight of all paths joining these points

$$Z_{y_f,L} = \sum_\gamma w_\gamma. \tag{8.1.3}$$

[9] By construction of the lattice, the final coordinate L means that the polymer will have a length L.

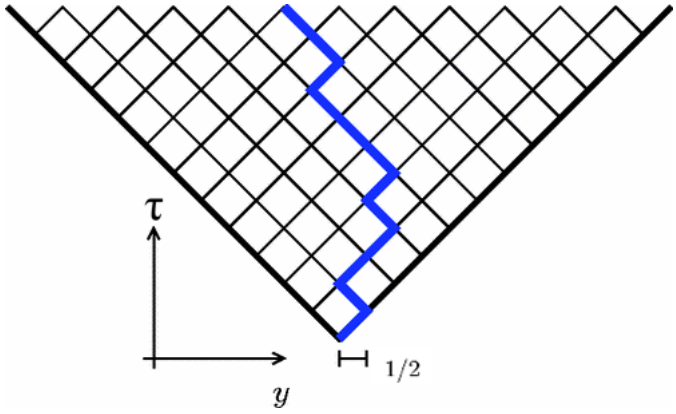

Figure 8.1: Representation of a directed polymer on a square lattice. The square is rotated by 45° and the path of the polymer starts from one of the corner of coordinate $(0, 0)$.

With these definitions, the partition sum verifies a natural recursion formula which constitutes a discretized version of the Stochastic Heat Equation

$$Z_{y,\tau+1} = \left(Z_{y-\frac{1}{2},\tau} + Z_{y+\frac{1}{2},\tau} \right) e^{-\beta V_{y,\tau+1}}. \tag{8.1.4}$$

Numerically, this problem is solved by the transfer matrix method and the complexity to compute the partition sum up to some discrete time τ is of order $\mathcal{O}(\tau^2)$. It is interesting to investigate the extreme regimes of zero temperature and high temperature.

At zero temperature, $T \to 0$, the free energy defines as $F_{y,\tau} = -T \log Z_{y,\tau}$ verifies the optimization/recursion equation

$$F_{y,\tau+1} = \min(F_{y-\frac{1}{2},\tau}, F_{y+\frac{1}{2},\tau}) + V_{y,\tau+1} \tag{8.1.5}$$

which is sometimes referred to as the Bellman equation in the mathematical literature.

In the high temperature regime, $T \to \infty$, the continuum polymer, whose partition function is the solution of the Stochastic Heat Equation, is obtained using the following parametrization [73, 216]

$$x = \frac{4y_f}{T^2}, \qquad t = \frac{2L}{T^4}. \tag{8.1.6}$$

The proper convergence of the partition function is expressed as

$$\lim_{\substack{L\to+\infty \\ T\to+\infty \\ t \text{ fixed}}} 2^{-L} Z_{y_f,L} = Z(x,t) \tag{8.1.7}$$

If the random variables $V_{y,\tau}$ are chosen as independent unit Gaussian (which is the choice made everywhere in this paper) then $Z(x,t)$ is solution of the SHE (1.3.4). We emphasize that for the rest of this Chapter, the coordinates (x,t) will be associated to the continuum limit. From this continuum parametrization, we see that an infinite temperature T and infinite lattice length L limit while keeping the time t small and fixed will be equivalent to a short-time dynamics of the Stochastic Heat Equation or equivalently the Kardar-Parisi-Zhang equation and this is what we should aim for.

Having defined the temperature regime, we now need to choose the geometry of the polymer problem. We consider two type of configurations.

- The point to point polymer whose starting and ending points are fixed.
- The point to line polymer whose starting point is fixed. On the contrary its ending point is arbitrary on some line and, the partition sum will be obtained by summing over all ending points on this line with possibly an additional weight. In the limit of large temperature T and the large lattice size L, this sum will be viewed as a Riemann sum approaching an integral.

For the purpose of comparing our predictions for the solution to the Kardar-Parisi-Zhang and the simulations of a directed polymer, we need to define a height field associated to the partition function of the discrete polymer $\log(Z_{y,\tau})$, which should converge to the KPZ height under the continuum rescaling. In addition, in the following, the discrete partition sum $Z_{y_f,L}$ will be the analog of the propagator for the Stochastic Heat Equation. We recall that if we want to evaluate the final KPZ height at $x = 0$, then its formal expression at time t is given by

$$e^{h(0,t)} = \int_{\mathbb{R}} \mathrm{d}x \, Z(0,t|\, x,0) e^{h(x,t=0)} \tag{8.1.8}$$

where $Z(x,t|\, x',0) = Z(x,t)$ denotes the solution of the SHE with initial condition $Z(x,t = 0|\, x',0) = \delta(x-x')$, and where the initial condition of the KPZ equation in encoded in the weight $e^{h(x,t=0)}$. This tells us that we will need to encode the initial condition of the Kardar-Parisi-Zhang equation in the configuration of the polymer using the correspondence

$$Z(0,t|\, x,0) \longleftrightarrow 2^{-L} Z_{y_f,L} \tag{8.1.9}$$

The usual initial conditions will be encoded as follows:

- The droplet initial condition is $e^{h(x,t=0)} = \delta(x)$ so $e^{h(0,t)} = Z(0,t|0,0)$, this is precisely the point to point polymer;
- The flat initial condition is $e^{h(x,t=0)} = 1$ so $e^{h(0,t)} = \int_{\mathbb{R}} \mathrm{d}x' \, Z(0,t|x',0)$. This integral is obtained on the discrete lattice by summing over all points over the final line: this is precisely the point to line polymer (see Fig 8.1 where the notion of final line is clear);
- The Brownian initial condition is $e^{h(x,t=0)} = e^{B(x)}$ so $e^{h(0,t)} = \int_{\mathbb{R}} \mathrm{d}x' \, Z(0,t|x',0) e^{B(x')}$ where $B(x')$ is the unit two-sided Brownian motion with $B(0) = 0$. This integral will be obtained on the discrete lattice by summing over all point over the final line with an additional weight representing the Brownian contribution, hence this is another type of point to line polymer. The exact method and scaling to introduce the Brownian contribution will be discussed later.

The one-point KPZ height we studied in the short-time case was centered, hence we also require to center the distribution of the height obtained in the simulations. Calling Z_τ the discrete partition function up to time τ (whatever configuration), we will compare our theoretical predictions to the distribution of the quantity $H(t)$ defined by

$$H(t) = \log \frac{Z_L}{\overline{Z_L}} \tag{8.1.10}$$

where $\overline{Z_L}$ is the average value of the partition function over many realizations.

8.2 Introduction to importance sampling

For the purpose of the introduction of the idea of importance sampling, we borrow the very elegant presentation made in Ref. [215].

In principle one could obtain an estimate of the probability distribution $P(H,t)$ numerically from simple sampling. For this, one generates many disorder realisations and calculates the partition function for each. Then $\overline{Z_L}$ is estimated by averaging over all samples, and the distribution is the histogram of the values of H according to Eq. (8.1.10). Nevertheless, this limits the smallest probabilities which can be resolved to the inverse of the number of samples, hence reaching probabilities as small as 10^{-1000} is strictly impossible. Hence, a different approach is required.

To estimate $P(H,t)$ for a much larger range, where probability densities as small as 10^{-1000} may appear, we use a more powerful approach, called importance sampling as discussed in Refs. [217–219]. This approach has been successfully applied in many cases to obtain the tails of distributions arising in equilibrium and non-equilibrium situations, for instance the number of components of Erdős-Rényi (ER) random graphs [220], the distribution of free energies of RNA secondary structures [221], some large-deviation properties of random matrices [222, 223] or the distribution of endpoints of fractional Brownian motion with absorbing boundaries [224].

The idea behind importance sampling is to sample the different disorder realisations with a suitable additional bias [225]. Here we use the bias $\exp(-\theta H(V))$ where θ is an adjustable parameter interpreted as a fictive inverse temperature. If $\theta > 0$ the configurations with a negative H become more likely, conversely if $\theta < 0$ the configurations with a positive H are favored. A standard Markov-chain Monte Carlo simulation is used to sample the biased configurations [226, 227]. At each time step a new disorder realisation V^* is proposed by replacing on the current realisation V a certain fraction r of the random numbers $V_{y,\tau}$ by new random numbers. The new disorder realisation is then accepted with the usual Metropolis-Hastings probability

$$p_{\mathrm{Met}} = \min\left[1, e^{-\theta\left[H(V^*)-H(V)\right]}\right], \tag{8.2.1}$$

otherwise the old configuration is kept [228]. Note that the average partition function $\overline{Z_L}$ appearing in the definition of H (8.1.10) drops out of the Metropolis probability. By construction, the algorithm fulfils detailed balance and is ergodic, since within a sufficient number of steps, each possible realisation may be constructed. Thus, in the limit of infinitely long Markov chains, the distribution of biased disorder realisations will follow the probability

$$q_\theta(V) = \frac{1}{Q(\theta)} P_{\mathrm{dis}}(V) e^{-\theta H(V)}, \tag{8.2.2}$$

where $P_{\mathrm{dis}}(V)$ is the original disorder distribution and $Q(\theta) = \sum_V P_{\mathrm{dis}}(V) e^{-\theta H(V)}$ is the normalization factor. Note that $Q(\theta)$ also depends on L and T because of finite size and temperature effects. $Q(\theta)$ is generally unknown but can be determined. The output of this Markov chain allows to construct a biased histogram $P_\theta(H,t)$. In order to get the correct empirical probability density $P(H,t)$ one should debias the result so that

$$P(H,t) = e^{\theta H} Q(\theta) P_\theta(H,t). \tag{8.2.3}$$

Hence, the target distribution $P(H,t)$ can be estimated, up to a normalisation constant $Q(\theta)$. The method used to determine $Q(\theta)$ is described in Ref. [215]. For each value of the parameter θ, a specific range of the distribution $P(H,t)$ will be sampled and using a positive (respectively, negative) parameter allows to sample the region of a distribution at the left (respectively, at the right) of its center.

8.3 Comparison of the theoretical predictions with the simulations

In this Section, we will compare the theoretical predictions of the probability distribution of the solutions to the Kardar-Parisi-Zhang equation with the numerical simulations of the directed polymer on a lattice for each initial condition. The purpose of this Section is three-fold (i) to give explicitly the large deviation solutions for every initial condition, (ii) to proceed to the comparison of both the center of the distribution and its tails and finally (iii) to provide details on how to encode the random weights on the lattice to account for particular initial conditions. We will address here both full-space and half-space initial conditions and hence the construction of the lattice for the directed polymer will be introduced carefully when required.

We recall that the large deviation function $\Phi(H)$ has been constructed so that it is centered around 0 and hence for a fair comparison, the probability densities obtained in the simulations will be shifted so that their maximum is also reached at 0. Finally, we insist on the fact that the comparison will be done without any fitting parameter.

8.3.1 The droplet initial condition in full-space

To provide the short-time probability distribution for the droplet initial condition in full-space, let us first define the branching field $H_c = \log \zeta(\frac{3}{2})$, where ζ is the Riemann zeta function and denote the intervals:

$$\begin{aligned} I_1 &= [-1, +\infty[\,, \quad & I_2 &= [-1, 0[\,, \\ J_1 &=]-\infty, H_c]\,, \quad & J_2 &= [H_c, +\infty[\,. \end{aligned} \tag{8.3.1}$$

The associated large deviation function $\Phi(H)$ is expressed by the parametric system

$$e^H = \begin{cases} -z^{-1}\mathrm{Li}_{\frac{3}{2}}(-z), & z \in I_1, H \in J_1 \\ -z^{-1}\Big[\mathrm{Li}_{\frac{3}{2}}(-z) + 4\sqrt{\pi}\,\Big[\log(-\frac{1}{z})\Big]^{\frac{1}{2}}\Big], & z \in I_2, H \in J_2 \end{cases} \tag{8.3.2}$$

$$\Phi(H) = \begin{cases} \frac{1}{\sqrt{4\pi}}\Big[\mathrm{Li}_{\frac{3}{2}}(-z) - \mathrm{Li}_{\frac{5}{2}}(-z)\Big], & z \in I_1 \\ \frac{1}{\sqrt{4\pi}}\Big[\mathrm{Li}_{\frac{3}{2}}(-z) - \mathrm{Li}_{\frac{5}{2}}(-z)\Big] + \frac{2}{3}[\log(-\frac{1}{z})]^{\frac{3}{2}} + [\log(-\frac{1}{z})]^{\frac{1}{2}}, & z \in I_2 \end{cases}$$

The numerical simulations for the droplet initial condition were originally presented in Ref. [215]. There were run for polymers of length $L = \{64, 128, 256\}$ and temperature T chosen so that the corresponding time for the Kardar-Parisi-Zhang equation is fixed at $t = 1/16$. Convergence to the analytic predictions is expected for $L \to +\infty$. We now display the simulations in Figs. 8.2 and 8.3 and we observe that the agreement between numerical and analytical results is spectacular (on the left tail, down to values of the order 10^{-800}).

8.3.2 The flat and stationary initial conditions in full-space

To provide the short-time probability distribution for the flat and the stationary initial condition in full-space, let us first define the critical height $H_{c2} = 2\log(2e - \mathcal{I}) - 1 \simeq 1.85316$ with

$$\mathcal{I} = \int_0^{+\infty} \frac{\mathrm{d}y}{\pi}\left[1 + \frac{1}{y}\right]\frac{\sqrt{y}}{e^{-1} + ye^y}. \tag{8.3.3}$$

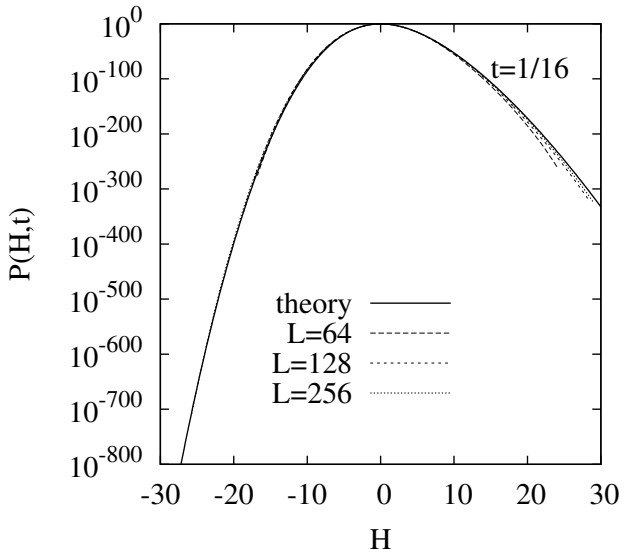

Figure 8.2: Distribution of $P(H,t)$ for a short time $t = 1/16$ for three different polymer lengths $L = \{64, 128, 256\}$ for the droplet initial condition in full-space. The solid line indicates the analytical result in Eq. (8.3.2) obtained in Ref. [169]. Plot taken from Ref. [215]

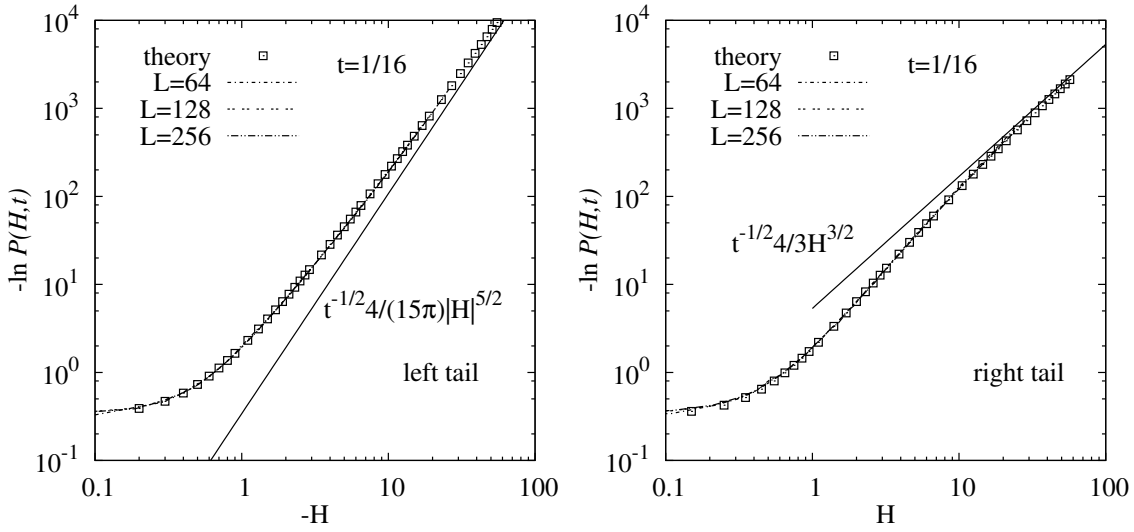

Figure 8.3: Blow up of the left and right tails of the data shown of Fig. 8.2 compared to the prediction given in the Table 7.2. Plots taken from Ref. [215].

together with the function $\Psi(z)$ expressed as

$$\Psi(z) = -\int_{\mathbb{R}} \frac{\mathrm{d}k}{2\pi} \mathrm{Li}_2(-\frac{ze^{-k^2}}{k^2}), \tag{8.3.4}$$

and its reduced version $\psi(z) = \Psi(z) - 2z\Psi'(z)$. We further denote the intervals:

$$\begin{aligned} I_1 &= [0, +\infty[\,,\ I_2 = \left[0, e^{-1}\right],\ I_3 = \left]0, e^{-1}\right], \\ J_1 &=]-\infty, 0]\,,\ J_2 = [0, H_{c2}]\,,\ J_3 = [H_{c2}, +\infty[\,. \end{aligned} \tag{8.3.5}$$

We define a large deviation function $\Phi(H)$ given in a parametric form by

$$\begin{aligned} e^H &= \begin{cases} z\Psi'(z)^2, & z \in I_1, H \in J_1 \\ z\left[\Psi'(z) - 2z^{-1}[-W_0(-z)]^{\frac{1}{2}}\right]^2, & z \in I_2, H \in J_2 \end{cases} \\ \Phi(H) &= \begin{cases} \psi(z), & z \in I_1 \\ \psi(z) + \frac{4}{3}[-W_0(-z)]^{\frac{3}{2}}, & z \in I_2 \end{cases} \end{aligned} \tag{8.3.6}$$

For $z \in I_3, H \in J_3$, we define two continuations of $\Phi(H)$: a symmetric analytic one (resp. asymmetric non-analytic) denoted $\Phi_{\mathbf{A}}$ (resp. $\Phi_{\mathbf{NA}}$) such that their parametric representations read

$$\begin{cases} e^H = z\left[\Psi'(z) - 2z^{-1}[-W_{-1}(-z)]^{\frac{1}{2}}\right]^2 \\ \Phi_{\mathbf{A}}(H) = \psi(z) + \frac{4}{3}[-W_{-1}(-z)]^{\frac{3}{2}} \end{cases}$$

and

$$\begin{cases} e^H = z\left[\Psi'(z) - z^{-1}\Big([-W_{-1}(-z)]^{\frac{1}{2}} + [-W_0(-z)]^{\frac{1}{2}}\Big)\right]^2 \\ \Phi_{\mathbf{NA}}(H) = \psi(z) + \frac{2}{3}[-W_{-1}(-z)]^{\frac{3}{2}} + \frac{2}{3}[-W_0(-z)]^{\frac{3}{2}} \end{cases} \tag{8.3.7}$$

The large deviation solutions for the flat and the Brownian initial conditions are by far the most difficult to study as a two successive continuations are required. Indeed, the large deviation functions for the stationary and flat initial conditions in full-space are given by

$$\forall H \in \mathbb{R}, \qquad \Phi_{\text{Brownian}}(H) = \Phi_{\mathbf{NA}}(H), \quad \Phi_{\text{flat}}(H) = 2^{-\frac{3}{2}}\Phi_{\mathbf{A}}(2H). \tag{8.3.8}$$

The indices **A** and **NA** are explicitly indicated for the region $H \in [H_{c2}, +\infty[$ where the two continuations are distinct and can be omitted for the region where $H \in]-\infty, H_{c2}]$ where the two functions are the same. We further recall that W_0 and W_{-1} are the two real branches of the Lambert function, see Appendix A.1.

The result for the Brownian which follows the **NA** branch was already obtained in Section 7.3.2. The result for the flat initial condition arises from (i) the identification made in the context of the WNT in Ref. [208] (mentioned in Eq. (6.5.1)) of the analytic branch and the large deviation function of the flat initial condition (the rationale being that no phase transition is expected for the flat initial initial condition) and (ii) the analytic result for the **A** branch in Eq. (8.3.7) obtained in Ref. [9].

The verification of (8.3.8) will be an important point to seek in numerical simulations. Before we introduce the results of the simulations obtained through the importance sampling method, we will explain in some details the lattice construction of these initial conditions.

Point to line directed polymer mapping

We first introduce the reader to the mapping of the flat initial condition of the KPZ equation to the directed polymer model on the lattice and then extend the discussion to the Brownian initial condition. As mentioned earlier, contrary to the droplet initial condition, the flat initial condition requires to perform a summation of the partition sum over the final line of the lattice, *i.e.*

$$Z_L = \sum_{k=-L}^{L} Z_{y_k,L}. \tag{8.3.9}$$

where the points $\{y_k\}$ are all the points over the final line of the lattice.

Remark 8.3.1. *Note that this amounts to set a uniform weight over the final line. Comparatively, for the droplet initial condition, all the weight was concentrated at $k = 0$ (the above sum with a Kronecker delta at $k = 0$ yields the droplet).*

Recalling the continuum parametrization of Eq. (8.1.6), the infinite temperature limit (up to a proportionality constant)

$$Z_{y_k,L} \longleftrightarrow Z(x = \frac{4y_k}{T^2}, t = \frac{2L}{T^4}), \tag{8.3.10}$$

by a Riemann summation using a step of size $\Delta x = \frac{4}{T^2} \ll 1$ we obtain the partition function of the flat condition (up to a proportionality constant)

$$\frac{4}{T^2} \sum_{k=-L}^{L} Z_{y_k,L} \underset{T\gg 1}{\longrightarrow} \int_{-4L/T^2}^{4L/T^2} \mathrm{d}x\, Z(x,t) \tag{8.3.11}$$

Remark 8.3.2. *We emphasize that because of our construction of the height (8.1.10), the proportionality constants are irrelevant.*

As we renormalize the partition sum by its average according to Eq. (8.1.10), the prefactor $4/T^2$ can be discarded and will play strictly no role in the numerics. To approximate the integral as being over the real line, the factor $4L/T^2$ should be taken as large as possible: its finiteness might induce additional finite size and discretization effects as compared to the point to point continuum polymer. To provide orders of magnitude, the simulations that we will present will have a time $t = 1/16$ and the factor $4L/T^2$ is then in the range $[4, 8]$ for the different lattice sizes used.

The extension of this mapping to the stationary initial condition is obtained by adding Brownian weights $e^{B(x)}$ on the final line on the lattice.

$$Z_{y_k,L} e^{B(\frac{4y_k}{T^2})} \to Z(x = \frac{4y_k}{T^2}, t) e^{B(x)} \tag{8.3.12}$$

By self-similarity, we have $B(\frac{4y_k}{T^2}) \equiv \frac{2}{T} B(y_k)$ and hence $B(y_k)$ can be easily sampled by a random walk with Gaussian increments with unit variance. Note that the final partition function assumes an additional average over the Brownian motion compared to a deterministic initial condition, hence this provides an extra challenge on the numerical side.

Presentation of the simulations

The numerical simulations for the flat and Brownian initial conditions in full-space are displayed in Ref. [1]. They were run for polymers of length $L = \{32, 64, 128\}$ and temperature T chosen so that the corresponding time for the Kardar-Parisi-Zhang equation is fixed at $t = 1/16$. Convergence to the analytic predictions is expected for $L \to +\infty$. We present the simulations in Figs. 8.4 and 8.5. We observe for the flat and Brownian initial conditions that the agreement between the numerics and the theory is fairly good and improves as L increases. We should note that there are additional sources of finite size effects and statistical errors since for the flat and the Brownian initial conditions we need to perform a summation of the partition function over the final line in both cases and an additional average over the Brownian weights in the second case. Nonetheless, the simulations are able to probe both tails of the distribution of $P(H, t)$ for quite a range of values for both initial conditions as can be seen in Fig. 8.5.

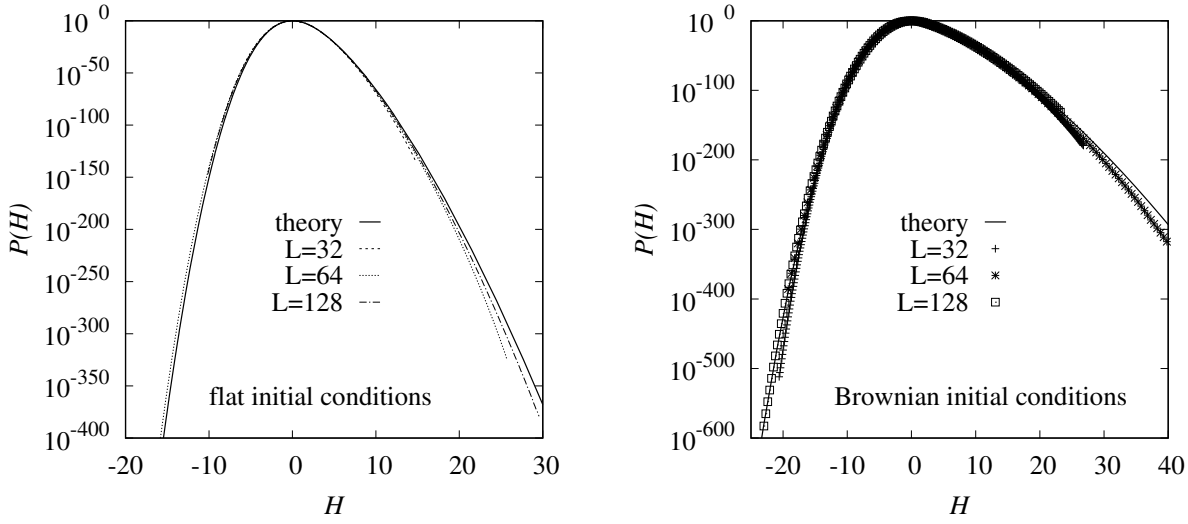

Figure 8.4: Distribution of $P(H,t)$ for a short time $t = 1/16$ for three different polymer lengths $L = \{32, 64, 128\}$. The solid lines indicates on the **left** plot the analytical result in Eq. (8.3.8) obtained in Ref. [208] for the flat initial condition and on the **right** plot the analytical result in Eq. (8.3.8) obtained in Ref. [9] for the Brownian (stationary) initial condition. Plots taken from Ref. [1].

Discussion around the choice of branch $\Phi_{\mathbf{A}}/\Phi_{\mathbf{AN}}$ for flat and Brownian initial conditions

We now turn to the crucial discussion of the choice of branch $\Phi_{\mathbf{A}}/\Phi_{\mathbf{AN}}$ for both flat and Brownian initial conditions. We recall that considerations coming from Weak Noise Theory [208] together with the precise study of the Fredholm determinant associated to the solution for the Brownian initial condition [9] concluded that

$$\forall H \in \mathbb{R}, \qquad \Phi_{\text{Brownian}}(H) = \Phi_{\mathbf{NA}}(H), \quad \Phi_{\text{flat}}(H) = 2^{-\frac{3}{2}}\Phi_{\mathbf{A}}(2H). \tag{8.3.13}$$

This implies that if we rescale the simulation data for the flat initial condition, they should coincide pointwise up to the critical height H_{c2} and then separate to the symmetric and asymmetric branches. We emphasize that the choice of branch is critical as it determines the tails of the distribution and the existence of a singularity in the large deviation function.

We present in Fig. 8.6 the comparison in a region around H_{c2} between the exact expression of the different branches of $\Phi(H)$ written in Eqs. (8.3.6) and (8.3.7) and the directed polymer simulations of length $L = 128$ at a time $t = 1/16$ for the Brownian and the flat initial conditions. Note that we rescaled the distribution for the flat initial condition according to the scaling proposed in Eq. (8.3.8) for a fair comparison. Figure 8.6 confirms in a remarkable way that each condition corresponds to the one of the two branches we have obtained analytically. The coincidence of the two distributions before the point $H = H_{c2}$ is also quite spectacular.

8.3.3 The droplet initial condition in half-space with a hard-wall $A = +\infty$

To provide the short-time probability distribution for the droplet initial condition in a half-space in presence of a hard wall, let us first define the branching height $H_c = \log(8\sqrt{\pi}\,\mathcal{I}) \simeq 0.9795$ with

$$\mathcal{I} = \int_0^{+\infty} \frac{\mathrm{d}y}{\pi}\left[1 - \frac{1}{y}\right]\frac{\sqrt{y}}{e^y/y - e}. \tag{8.3.14}$$

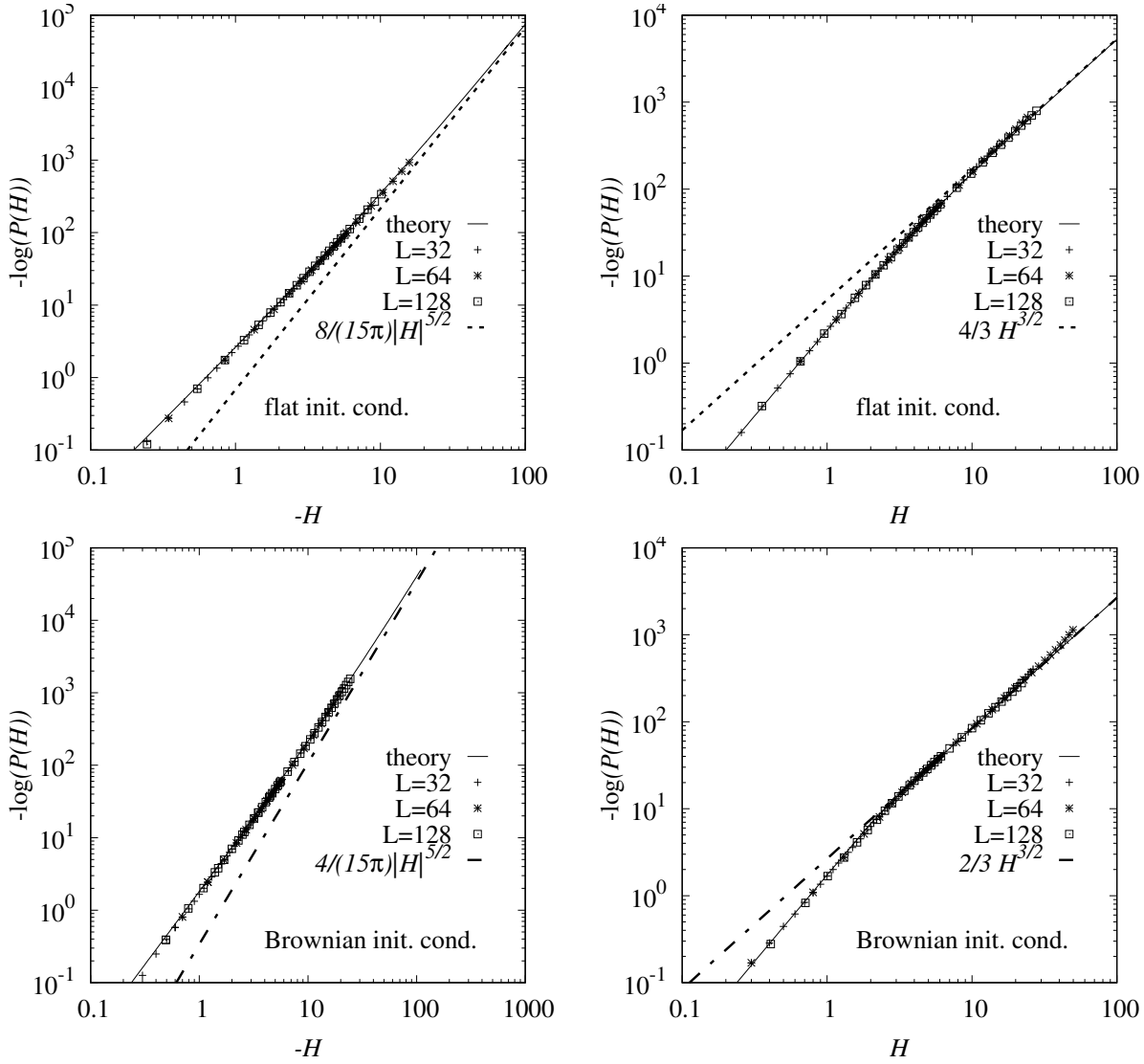

Figure 8.5: Top: blow up of the left and right tails of the data shown in the left plot of Fig. 8.4 for the flat initial condition. **Bottom**: blow up of the left and right tails of the data shown in the right plot of Fig. 8.4 for the Brownian initial condition. In all four plots the solid line is the analytical prediction given in Eq. (8.3.8), together with Eqs. (8.3.6) and (8.3.7). The leading tails at large $|H|$ given in the Table 7.2 are also plotted in each case. Plots taken from Ref. [1].

The functions $\Psi(z)$, $\Delta(z)$ and its derivative $\Delta'(z)$ are expressed as

$$\begin{aligned}
\Psi(z) &= -\int_{\mathbb{R}} \frac{\mathrm{d}k}{4\pi} \mathrm{Li}_2(-zk^2 e^{-k^2}) \\
\Delta(z) &= \frac{2}{3}\left[W_0(\frac{1}{z})\right]^{\frac{3}{2}} + \frac{2}{3}\left[W_{-1}(\frac{1}{z})\right]^{\frac{3}{2}} + 2\left[W_0(\frac{1}{z})\right]^{\frac{1}{2}} + 2\left[W_{-1}(\frac{1}{z})\right]^{\frac{1}{2}} \\
\Delta'(z) &= -\frac{1}{z}\left[W_0(\frac{1}{z})\right]^{\frac{1}{2}} - \frac{1}{z}\left[W_{-1}(\frac{1}{z})\right]^{\frac{1}{2}}
\end{aligned} \tag{8.3.15}$$

and we define their reduced versions ψ and δ

$$\psi(z) = \Psi(z) - z\Psi'(z), \quad \delta(z) = \Delta(z) - z\Delta'(z). \tag{8.3.16}$$

We further denote the intervals:

$$\begin{aligned}
I_1 &= [-e, +\infty[\,, \quad I_2 = [-e, 0[\,, \\
J_1 &=]-\infty, H_c]\,, \quad J_2 = [H_c, +\infty[\,.
\end{aligned} \tag{8.3.17}$$

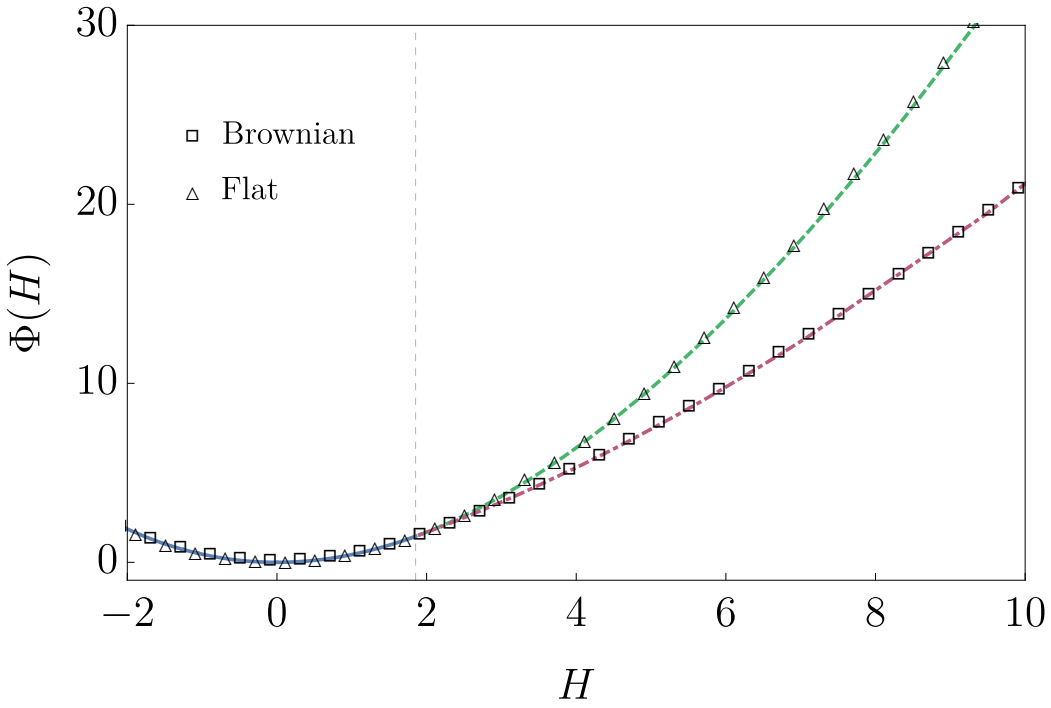

Figure 8.6: The analytic expression of $\Phi(H)$ obtained in Eqs. (8.3.6) and (8.3.7) is compared with the simulation data obtained for the flat and for Brownian initial conditions. In the case of the flat initial condition, the data are rescaled according to Eq. (8.3.8) for a fair comparison. The blue line corresponds to the function $\Phi(H)$ before the critical point $H_{c2} \simeq 1.85316$ which position is indicated by a vertical grey dotted line. The green dashed line corresponds to the symmetric analytic branch $\Phi_{\mathbf{A}}$ and the red dot-dashed line corresponds to the asymmetric non-analytic branch $\Phi_{\mathbf{NA}}$. The square markers represent the Brownian initial condition simulation data and the triangle markers represent the rescaled flat initial condition data.

The associated large deviation function $\Phi(H)$ is expressed by the parametric system

$$\begin{aligned} e^H &= \begin{cases} 8\sqrt{\pi}\Psi'(z), & z \in I_1, H \in J_1 \\ 8\sqrt{\pi}[\Psi'(z) + \Delta'(z)], & z \in I_2, H \in J_2 \end{cases} \\ \Phi(H) &= \begin{cases} \psi(z), & z \in I_1 \\ \psi(z) + \delta(z), & z \in I_2 \end{cases} \end{aligned} \tag{8.3.18}$$

Before we introduce the results of the simulations obtained through the importance sampling method, we will explain in some details the lattice construction of the half-space problem in the presence of a wall.

Point to point directed polymer mapping in a half-space with a hard-wall $A = +\infty$

To mimic a hard-wall type problem, one can forbid the polymer to visit some edges and introduce a tabu list for edges bringing the polymer towards the diagonal of the lattice. Indeed, the partition function should be strictly zero on the diagonal so that the probability of crossing the diagonal is strictly zero. We introduce this idea of forbidden edges in Fig. 8.7. Finally, extension of this construction to a generic value of A would be interesting.

Presentation of the simulations

The numerical simulations for the droplet initial condition in half-space in the presence of a hardwall are displayed in Ref. [1]. They were run for polymers of length $L = \{64, 128, 256\}$ and

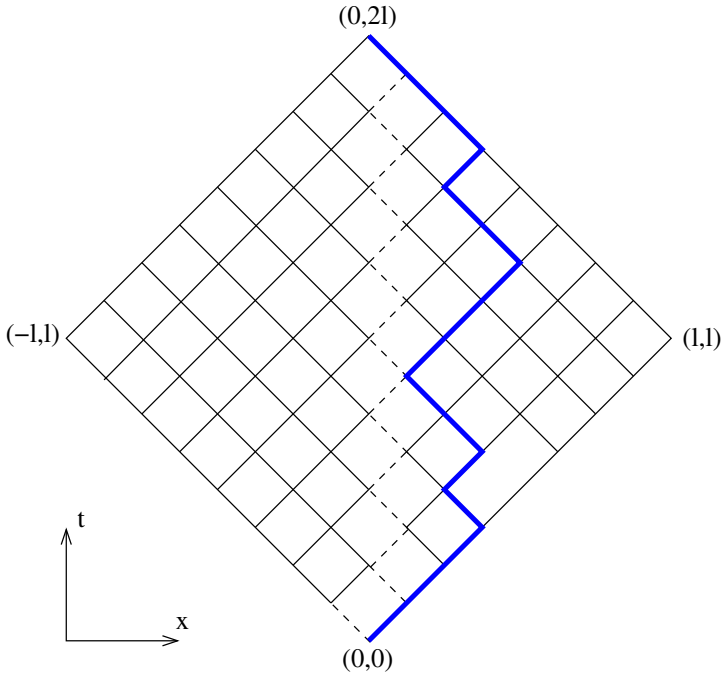

Figure 8.7: Square lattice designed for the half-space problem with a hard-wall. The dashed lines are forbidden edges for the polymer constraining it to stay on the right of the lattice. An example of a polymer realization is drawn on the blue line.

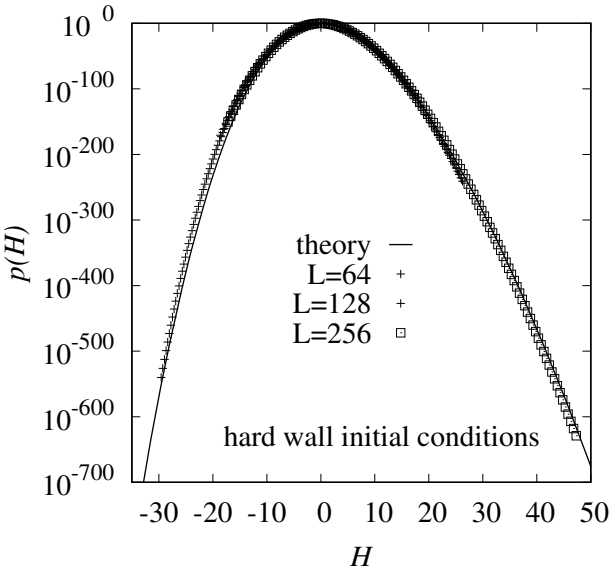

Figure 8.8: Probability distribution $P(H,t)$ for a short time $t = 1/16$ for three different polymer lengths $L = \{64, 128, 256\}$ for the droplet initial condition in a half-space with an infinite hard-wall at the origin. The solid line indicates the analytical result displayed in Eq. (8.3.18) obtained in [6]. Plots taken from Ref. [1]

temperature T chosen so that the corresponding time for the Kardar-Parisi-Zhang equation is fixed at $t = 1/16$. Convergence to the analytic predictions is expected for $L \to +\infty$. We present the simulations in Figs. 8.8 and 8.9 and we observe that the agreement between numerical and analytic results is remarkable in the tails (for $H \leqslant -25$ and all $H \geqslant 0$), but nonetheless there is an intermediate region for negative H ($-20 \leqslant H \leqslant -10$) where the matching is not entirely perfect: this could possibly come from finite size effects but it still need to be further investigated.

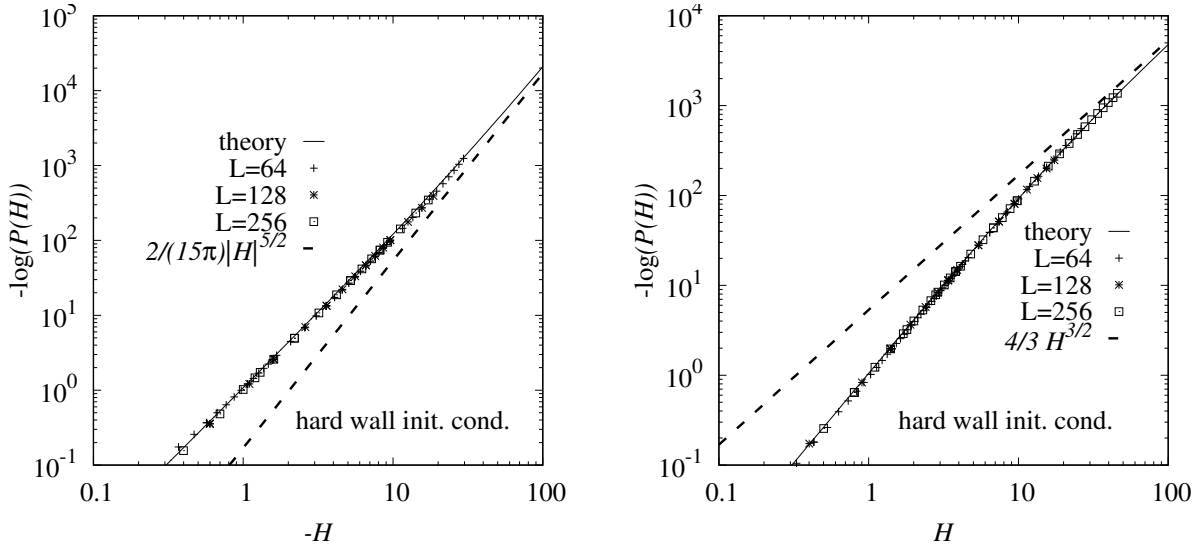

Figure 8.9: Blow up of the left and right tails of the data shown of Fig. 8.8. The solid lines indicate the analytical prediction displayed in Eq. (8.3.18) obtained in [6]. The data is also compared with the leading behavior of each tail as displayed in the Table 7.2. Plots taken from Ref. [1].

8.4 What do the large deviation polymers look like ?

Before we conclude this Chapter on the numerical simulations of the short-time distributions of the solutions to the Kardar-Parisi-Zhang equation, let us now change the point of view and briefly discuss the physics of directed polymers and the implications of our large deviation studies. This Section will act as an outlook on the subject.

It is quite intuitive that the polymers which will contribute to the large deviations of the Kardar-Parisi-Zhang height are atypical and will have a special shape and a special roughness. Additionally, we expect that the configurations of the polymer which contribute to the left tail of the distribution of H will be quite different from the ones which contribute to the right tail. It would be extremely interesting to determine the roughness exponent of these atypical polymers. The knowledge of the shape of such polymers could be of great benefits as we could hope to learn or at least get some insight on how to sample from atypical polymer distributions.

Finally, to summarize this Chapter, we introduced a large-deviation sampling approach to measure the distribution $P(H,t)$ of heights for the KPZ for various initial conditions. This was achieved using a directed polymer on a lattice, whose partition function converges, in the high temperature limit, to the solution of the SHE where the boundary condition of the polymer maps to the initial condition of the SHE. This allowed us to determine numerically the probability distribution of the height over a large range of values, allowing for a precise comparison with the theoretical predictions. We find that the agreement with the short-time large-deviation function $\Phi(H)$ predicted by the theory, which differs according to the geometry and the initial condition, is very good over hundreds of decades in probability, even very far in the tails. The existence and location of a phase transition for the stationary initial condition are fully confirmed, as well as the close connection of the rate function for the flat and stationary initial conditions.

Part III

From the large deviations of KPZ at late time to linear statistics at the edge of Gaussian β random matrices.

Abstract

The third and final part of this Thesis will focus on the late-time properties of the solutions to the Kardar-Parisi-Zhang equation. We will smoothly shift from short time to late time by showing that the left tail of the short-time distribution is conserved during the dynamics and by extending our cumulant expansion of the Fredholm representation of the KPZ solutions from short time to large time. Quite surprisingly, we will show that the late-time KPZ problem lies within a more general framework which is the linear statistics at the edge of Gaussian random matrices. The capstone of the end of this Thesis will be the unification of four a priori unrelated methods to solve this microscopic linear statistics problem.

Chapter 9

From small times to large times

In this Chapter, we will be interested in developing a systematic approach to study the late-time behavior of the Kardar-Parisi-Zhang solutions. Here and below, we will focus on the solution to the droplet initial in full-space which is related at all times to a Fredholm determinant involving the Airy kernel. Most of this Chapter will based on our publications [5, 8].

Our first focal point will be dedicated to the left tail of the distribution of the KPZ height and particularly to the recent developments showing that the left tail is a conserved quantity in the KPZ dynamics. The second spotlight of this Chapter will be the presentation of a time expansion of a Fredholm determinant involving the Airy kernel, allowing us to confirm the first cumulant conjecture by calculating corrections to a high order. Quite surprisingly, there will be several other outcomes of our study, some unexpected. Firstly, a careful examination of the structure of the short-time expansion allows to obtain some results at long time which apply to the solution to the KPZ equation. The second outcome relates to random matrix theory. There has been a lot of interest recently in linear statistics and central limit theorems for eigenvalues of large random matrices in the Gaussian Unitary Ensemble (GUE) [104], see e.g. [166, 229, 230] but there are not so many results concerning the linear statistics near the edge of the GUE. Our systematic expansion will shed some new light on this edge.

The inspiration for this work comes from the connection between the KPZ equation with droplet initial condition and the Airy point process, which describes the (scaled) eigenvalues of the GUE at the edge [43, 72–75, 106, 231]. Here and in the following Chapters, we will be able to use that connection to make several detailed predictions for (i) the higher cumulants of the linear statistics of the Airy point process (ii) the large deviations of the linear statistics.

9.1 How negative can the solution of KPZ be ?

As any calculation on the solution to the Kardar-Parisi-Zhang equation is obtained by the Cole-Hopf mapping $Z = e^h$, it is paramount to guarantee that the solution to the Stochastic Heat Equation remains positive at all time. More than the positivity of the solution to the SHE, we might want to control how small it can become, or equivalently, how negative can the solution of the KPZ equation be. At short time, we have determined that the left tail of the distribution of the KPZ height is a stretched exponential with exponent $5/2$ as stated in Table 7.2 in the second part of this Thesis.

At short time, this negative tail for the distribution of the KPZ height can be obtained either from the Weak Noise Theory or the cumulant method on the Fredholm representation of the solutions. In Refs. [6, 8], we showed that the first cumulant approximation remains valid at all

times for the far negative tail

$$-\log \mathbb{P}(h(0,t)+\frac{t}{12}\leqslant -st^{1/3}) \simeq_{s\gg 1} \frac{4}{15\pi}t^{1/3}s^{5/2} \tag{9.1.1}$$

which thus remains a stretched exponential with exponent $5/2$ and the indicated prefactor for all time t. This is quite an important statement as the left tail of the distribution of the KPZ height is therefore a conserved quantity in the dynamics. In addition, this provides a direct way to control how small the solution to the Stochastic Heat Equation is. This statement about the left tail was proved rigorously by Corwin and Ghosal in Ref. [232] where they provided the following theorem for the solution to the KPZ equation in full-space with droplet initial condition.

Theorem 9.1.1 (*Corwin & Ghosal, Theorem 1.1 of Ref. [232]*)

Fix $\epsilon,\delta\in]0,\frac{1}{3}[$ and $t_0>0$. Then, there exist $S=S(\epsilon,\delta,t_0)$, $C=C(t_0)>0$, $K_1=K_1(\epsilon,\delta,t_0)>0$ and $K_2=K_2(t_0)>0$ such that for all $s\geqslant S$ and $t\geqslant t_0$,

$$\mathbb{P}\Big(h(0,t)+\frac{t}{12}\leqslant -st^{1/3}\Big)\leqslant e^{-\frac{4(1-C\epsilon)}{15\pi}t^{\frac{1}{3}}s^{5/2}}+e^{-K_1s^{3-\delta}-\epsilon t^{1/3}s}+e^{-\frac{(1-C\epsilon)}{12}s^3}, \tag{9.1.2}$$

and

$$\mathbb{P}\Big(h(0,t)+\frac{t}{12}\leqslant -st^{1/3}\Big)\geqslant e^{-\frac{4(1+C\epsilon)}{15\pi}t^{\frac{1}{3}}s^{5/2}}+e^{-K_2s^3}. \tag{9.1.3}$$

Let us briefly comment on this result. For $t^{2/3}\gg s\gg 1$, the second and third terms of the upper bound (9.1.2) dwarf the first term and represent a cubic decay (in the exponential) in s. In particular, as t gets large, only the third term survives and provides the predicted Tracy-Widom tail $\frac{1}{12}s^3$. On the other hand, for $s\gg t^{2/3}$ the first term of the lower bound dwarfs the others and one recovers the $\frac{4}{15\pi}s^{5/2}$ decay for all t. Prior to the Theorem 9.1.1 of Corwin and Ghosal, the only finite time bounds were in [67] which provided a Gaussian upper-bound on the decay, hence a weaker result than the stretched exponentials with exponent $5/2$ and 3. Theorem 9.1.1 was also recently extended in two cases: (i) for the half-space droplet initial condition with Robin boundary coefficient $A=-1/2$ by Kim in Ref. [233] and (ii) for larger class of initial conditions by Corwin and Ghosal in Ref. [234].

At infinite time, we have seen in the first part of this Thesis that the cumulative distribution of the KPZ height is a Tracy-Widom distribution with a stretched exponential left tail with exponent 3. At all times, we have also seen that the left tail of the distribution of the KPZ height is a stretched exponential with exponent $5/2$. To fully understand how this is consistent, we have to reconcile both tails. The upper bound (9.1.2) provides a visual way to compare both tails which seem in competition at large time. We have to balance the following terms

$$s^3\sim t^{1/3}s^{5/2}\,. \tag{9.1.4}$$

This implies that there is an intermediate region with $s\sim t^{2/3}$ where the tail of the KPZ height interpolates between the extreme 3 and $5/2$ exponents. In this regime, denoting $s=t^{2/3}u$, the cumulative probability that we study is thus $\mathbb{P}(h(0,t)+\frac{t}{12}\leqslant -ut)$. It probes fluctuations of the KPZ height of order $h\sim t$ rather than $t^{1/3}$. This scaling in t indicates a large deviation regime whereas the scaling $t^{1/3}$ is affiliated to typical fluctuations. In that regime, the KPZ interface has an average velocity different than $-1/12$ at large time.

The rest of the third part of this Thesis will be devoted to understand this large deviation regime. This will be achieved by studying the right hand side of Eq. (3.2.1), i.e. the Fredholm

determinant associated to the KPZ solution with droplet initial condition in full-space. As a first step, we will introduce a systematic time expansion of this Fredholm determinant which we call the edge GUE Fredholm determinant. This will validate the first cumulant approximation that we used at short times and will lead the path towards describing the late-time properties of the solutions to the KPZ equation.

9.2 Systematic time expansion of the edge GUE Fredholm determinant

In this Section, we will present a systematic time expansion of the edge GUE Fredholm determinant developed in Ref. [5] in collaboration with S. Prolhac, which goes much beyond previous studies. We will see that, although initially devised for short time, a resummation of the series expansion allows to obtain also a *long-time large deviation function*. This also extends a result of Basor and Widom [213] to a much higher order. The main motivation for this systematic expansion in Ref. [5] was to investigate corrections to the first cumulant approximation for the KPZ problem at short time. In addition, it also allowed us to study the late-time behavior of the KPZ solution for droplet initial condition.

We study the linear statistics for the Airy $\beta = 2$ point process, namely averages over the Airy point process $\{a_i\}$ of the type $\mathbb{E}_{\mathrm{Ai}}[\exp(\sum_{i=1}^{+\infty} f(a_i))]$. Since explicit expressions are difficult to obtain for arbitrary function $f(x)$, we focus on two problems which will include a parameter $t > 0$ denoting the time since it will exactly identify with the time of the KPZ equation in the applications.

- We calculate the following average in an expansion *for short time* t

$$\mathbb{E}_{\mathrm{Ai}}\left[\exp\left(\sum_{i=1}^{+\infty} f(t^{1/3}a_i)\right)\right] \tag{9.2.1}$$

  for a large class of functions f. It allows us to obtain the cumulants of the scaled empirical measure $\mu(at^{-1/3}) = \sum_{i=1}^{+\infty} \delta(at^{-1/3} - a_i)$ of the Airy point process, in an expansion in small t, i.e. for value $a_i \sim t^{-1/3}$ which correspond to a region close to the bulk of the GUE spectrum. We are thus studying the matching region with the bulk going towards the edge. In the bulk of the GUE, it was shown by Borodin and Ferrari [235, 236] that the second cumulant of linear statistics can be obtained equivalently using the Gaussian free field. We will show that our result for the second cumulant for small t matches theirs. In addition, we will obtain systematic corrections to the Gaussian free field (higher cumulants, expansion towards the edge) and we will additionally extend a classical result of Basor and Widom to a much higher order [213].

- We calculate the following average in an expansion *for large time* t

$$\mathbb{E}_{\mathrm{Ai}}\left[\exp\left(-t\sum_{i=1}^{+\infty} \phi(t^{-2/3}a_i)\right)\right] \sim \exp\left(-t^2\Sigma_\phi\right) . \tag{9.2.2}$$

  This is a large deviation result, with a rate function Σ_ϕ which we obtain explicitly for a class of functions ϕ.

Both results are obtained in a single framework by studying the following generating function

$$Q_{t,\alpha}(\sigma) = \mathbb{E}_{\mathrm{Ai}}\left[\exp\left(\sum_{i=1}^{\infty} \alpha g(\sigma e^{t^{1/3}a_i})\right)\right] = \mathrm{Det}\left[1-(1-e^{\alpha \hat{g}_{t,\sigma}})K_{\mathrm{Ai}}\right] \tag{9.2.3}$$

where α is a book-keeping parameter which we will set to 1 at the very end of the calculation, where we used the shorthand notation $\hat{g}_{t,\sigma}(a) = g(\sigma e^{t^{1/3}a})$. For the purpose of this Chapter, we consider general functions g with $g(0) = 0$ which is mandatory for convergence, and $g(-\infty) < 0$.

After some manipulations on the Fredholm determinant (9.2.3), we will obtain the alternative series expression (9.2.12), from which the short and large-times expansions (9.2.1) and (9.2.2) of $\log Q_{t,\alpha}(\sigma)$ will be obtained in a systematic way. We will present below some crucial steps of the derivation of the expansion and we refer the readers to Ref. [5] for the complete presentation of the calculation.

9.2.1 Manipulations on the Fredholm determinant

The overall goal on the systematic expansion of the edge GUE Fredholm determinant is to derive Large Deviation principles for small and large t. To this aim, it is advantageous to consider the logarithm of our generating function (9.2.3), i.e. $\log Q_{t,\alpha}(\sigma) = q_{t,\alpha}(\sigma)$ defined as

$$q_{t,\alpha}(\sigma) = \log \mathbb{E}_{\mathrm{Ai}}\left[\exp\left(\alpha \sum_{j=1}^{\infty} g(\sigma e^{t^{1/3}a_j})\right)\right]. \tag{9.2.4}$$

We recall that $\{a_j\}$ forms the Airy point process. The expectation value over the Airy point process has the Fredholm determinant expression to which we apply the identity $\log \mathrm{Det} = \mathrm{Tr} \log$.

$$\begin{aligned} q_{t,\alpha}(\sigma) &= \log \mathrm{Det}\left[I-(1-e^{\alpha \hat{g}_{t,\sigma}})K_{\mathrm{Ai}}\right] \\ &= -\sum_{m=1}^{\infty} \frac{1}{m} \int_{\mathbb{R}^m} \mathrm{d}u_1 \dots \mathrm{d}u_m \left(\prod_{j=1}^{m}\left[1-\exp\left(\alpha g(\sigma e^{t^{1/3}u_j})\right)\right] K_{\mathrm{Ai}}(u_j,u_{j+1})\right). \end{aligned} \tag{9.2.5}$$

Here and below cyclicity on the variables u_j is assumed, $u_{j+m} \equiv u_j$. It turns out that it is more convenient for the following to consider the derivative $q'_{t,\alpha}(\sigma)$. This leads to a sum over $k \in [1,m]$ of terms where the factor $\exp\left(\alpha g(\sigma e^{t^{1/3}u_j})\right)$ is replaced by $\partial_\sigma \exp\left(\alpha g(\sigma e^{t^{1/3}u_j})\right)$. By cyclicity of the product over j, one can make the derivative act only on the factor with $k=1$ after renaming the variables u_j cancelling the factor $1/m$ of the Fredholm expansion. The crucial identities allowing to pursue the calculation are the following

$$\partial_\sigma \exp\left(\alpha g(\sigma e^{t^{1/3}u_1})\right) = \frac{t^{-1/3}}{\sigma}\partial_{u_1} \exp\left(\alpha g(\sigma e^{t^{1/3}u_1})\right), \quad (\partial_u+\partial_v)\,K_{\mathrm{Ai}}(u,v) = -\mathrm{Ai}(u)\mathrm{Ai}(v) \tag{9.2.6}$$

After one partial integration on u_1, $q'_{t,\alpha}(\sigma)$ reads

$$q'_{t,\alpha}(\sigma) = -\frac{t^{-1/3}}{\sigma}\sum_{m=1}^{\infty}\int_{\mathbb{R}^m}\prod_{j=1}^{m}\left[\mathrm{d}u_j\left(1-\exp\left(\alpha g(\sigma e^{t^{1/3}u_j})\right)\right)\right]\mathrm{Ai}(u_1)\left(\prod_{j=1}^{m-1}K_{\mathrm{Ai}}(u_j,u_{j+1})\right)\mathrm{Ai}(u_m) \tag{9.2.7}$$

Writing the Airy kernels explicitly in terms of Airy functions, expanding the prefactors as

$$K_{\mathrm{Ai}}(x,y) = \int_0^{+\infty}\mathrm{d}z\,\mathrm{Ai}(x+z)\mathrm{Ai}(y+z), \qquad 1-\exp\left(\alpha g(\sigma e^{t^{1/3}u})\right) = -\sum_{n=1}^{\infty} a_{n,\alpha}\,\sigma^n e^{t^{1/3}nu}, \tag{9.2.8}$$

and introducing the Airy propagator

$$\int_{\mathbb{R}} \mathrm{d}u\, e^{nu} \mathrm{Ai}(u+a)\mathrm{Ai}(u+b) = \frac{e^{\frac{n^3}{12} - \frac{(a+b)n}{2} - \frac{(a-b)^2}{4n}}}{\sqrt{4\pi n}}, \tag{9.2.9}$$

the integration over the variables $\{u_j\}$ can be performed upon the introduction of $m-1$ variables $\{z_j\}$ arising from the integral representation of the Airy kernel. At this stage, we obtain a first intermediate representation for $q'_{t,\alpha}(\sigma)$ as

$$\begin{aligned} q'_{t,\alpha}(\sigma) = -\frac{1}{\sigma\sqrt{t}} \sum_{m=1}^{\infty} (-1)^m \sum_{n_1,\dots,n_m=1}^{\infty} \left(\prod_{j=1}^{m} \frac{a_{n_j,\alpha}\, \sigma^{n_j}\, e^{\frac{t}{12} n_j^3}}{\sqrt{4\pi n_j}} \right) \\ \int_{\mathbb{R}_+^{m-1}} \mathrm{d}z_1 \dots \mathrm{d}z_{m-1} \left(\prod_{j=1}^{m} e^{-\frac{(z_{j-1}+z_j)n_j\sqrt{t}}{2} - \frac{(z_j - z_{j-1})^2}{4n_j}} \right)_{z_0 = z_m = 0}. \end{aligned} \tag{9.2.10}$$

After a consequent amount of combinatorial manipulations on Eq. (9.2.10), we have obtained in Ref. [5] a second representation of $q'_{t,\alpha}(\sigma)$ presented in Eq. (9.2.12). This other expression depends on a quantity $L_\alpha(\sigma, a, b)$ defined as

$$L_\alpha(\sigma, a, b) = -\sum_{m=1}^{\infty} (-1)^m \int_{\mathbb{R}_+^{m-1}} \mathrm{d}z_1 \dots \mathrm{d}z_{m-1} \prod_{\ell=1}^{m} \left(\sum_{n=1}^{\infty} \frac{a_{n,\alpha}\, \sigma^n}{\sqrt{4\pi n}}\, e^{-\frac{(z_\ell - z_{\ell-1})^2}{4n}} \right)_{\substack{z_0 = a \\ z_m = b}}. \tag{9.2.11}$$

As we will see in the rest of this Chapter, this second representation is much more suited to the systematic expansion we wish to obtain. It reads

$$\begin{aligned} q'_{t,\alpha}(\sigma) = \frac{1}{\sigma\sqrt{t}}\, e^{\frac{t}{12}(\sigma\partial_\sigma)^3} \left(\sum_{p=0}^{\infty} \left[\prod_{j=1}^{p} \frac{e^{\sqrt{t}\,(\sum_{i=0}^{j-1} \sigma_i \partial_{\sigma_i})(\sum_{i=j}^{p} \sigma_i \partial_{\sigma_i})\partial_{z_j}} - 1}{\partial_{z_j}} \right] \right. \\ \left. \times \prod_{j=0}^{p} L_\alpha(\sigma_j, z_j, z_{j+1}) \right)_{\substack{z_0 = \dots = z_{p+1} = 0 \\ \sigma_0 = \dots = \sigma_p = \sigma}}. \end{aligned} \tag{9.2.12}$$

At this stage, it is hard to see why the expansion (9.2.12) is a formidable interpretation of the initial Fredholm determinant as it depends on the quantity L_α which itself depends on a certain Taylor expansion of g. We will now present a systematic procedure or algorithm to obtain the successive time contributions of the Fredholm determinant, this algorithm will highly depend on four remarkable recursion properties of L_α.

9.2.2 Algorithm for the short-time expansion of $q_{t,\alpha}(\sigma)$

In this Section, we explain how the short-time expansion of (9.2.12) can be performed systematically to arbitrary order in t. This leads to the short-time expansion (9.2.22) for $\log Q_t(\sigma)$. The algorithm giving the expansion is based on the following identities verified by the functions $L_\alpha(\sigma, a, b)$ defined in (9.2.11):

$$\begin{aligned} &L_\alpha(\sigma, 0, 0) = \frac{\alpha}{\pi} \sigma\partial_\sigma \int_0^\infty \mathrm{d}x\, \sqrt{x}\, g(\sigma e^{-x}) \\ &L_\alpha(\sigma, a, b) = L_\alpha(\sigma, b, a) \\ &(\partial_a + \partial_b) L_\alpha(\sigma, a, b) = -L_\alpha(\sigma, a, 0) L_\alpha(\sigma, 0, b) \\ &\sigma\partial_\sigma \partial_a L_\alpha(\sigma, a, b) = \frac{b-a}{2} L_\alpha(\sigma, a, b) - L_\alpha(\sigma, a, 0)\, \sigma\partial_\sigma L_\alpha(\sigma, 0, b)\,. \end{aligned} \tag{9.2.13}$$

Remark 9.2.1. *These identities are proved in Ref. [5] and we recall the proof of Eq. (9.2.13) in Appendix B.3 as it is highly non-trivial and quite elegant.*

From (9.2.12), each term in the short-time expansion of $\sigma g'_{t,\alpha}(\sigma)$ is a polynomial in the variables $\mathfrak{L}_{i,j,k} = (\sigma\partial_\sigma)^i L_\alpha^{(0,j,k)}(\sigma,0,0)$, where $(i,j,k) \geqslant 0$ indicates the order of partial derivatives with respect to each variable of L_α. In terms of the $\mathfrak{L}_{i,j,k}$, the identities (9.2.13) imply

$$\mathfrak{L}_{i,0,0} = \frac{\alpha}{\pi}(\sigma\partial_\sigma)^{i+1}\int_0^\infty \mathrm{d}x\,\sqrt{x}\,g(\sigma e^{-x}) = \frac{\alpha}{2\pi}(\sigma\partial_\sigma)^i\int_{\mathbb{R}}\mathrm{d}p\,g(\sigma e^{-p^2}) \tag{9.2.14}$$

$$\mathfrak{L}_{i,j,k} = \mathfrak{L}_{i,k,j} \tag{9.2.15}$$

$$\mathfrak{L}_{i,j+1,k} + \mathfrak{L}_{i,j,k+1} = -\sum_{\ell=0}^{i}\binom{i}{\ell}\mathfrak{L}_{\ell,j,0}\mathfrak{L}_{i-\ell,0,k} \tag{9.2.16}$$

$$\mathfrak{L}_{i+1,j+1,0} = -\frac{j}{2}\,\mathfrak{L}_{i,j-1,0} - \sum_{\ell=0}^{i}\binom{i}{\ell}\mathfrak{L}_{\ell,j,0}\mathfrak{L}_{i+1-\ell,0,0}\,. \tag{9.2.17}$$

At each order in t in (9.2.12), the index k of the variables $\mathfrak{L}_{i,j,k}$ can be set to zero everywhere after applying recursively (9.2.16). Then, using (9.2.17), the index j can be reduced as well, as long as $i \geqslant 1$. Because of this constraint on i, it is not guaranteed that (9.2.17) will be sufficient in order to make $j = 0$ everywhere. In practice, we observed that using repeatedly (9.2.17) does eliminate all variables $\mathfrak{L}_{i,j,k}$ with either $j > 0$ or $k > 0$: only variables of the form $\mathfrak{L}_{i,0,0}$ remain. Hence, we define the notation

$$\mathfrak{L}_i(\sigma) := \mathfrak{L}_i = \mathfrak{L}_{i,0,0} = \frac{\alpha}{\pi}(\sigma\partial_\sigma)^{i+1}\int_0^\infty \mathrm{d}x\,\sqrt{x}\,g(\sigma e^{-x}). \tag{9.2.18}$$

Applying our algorithm recursively, we find the first orders in t as

$$q'_{t,\alpha}(\sigma) = \frac{1}{\sigma\sqrt{t}}\,e^{\frac{t}{12}(\sigma\partial_\sigma)^3}\left(\mathfrak{L}_0 + \mathfrak{L}_1^2\sqrt{t} + 2\,\mathfrak{L}_1^2\mathfrak{L}_2\,t + \left(\frac{4}{3}\,\mathfrak{L}_1^3\mathfrak{L}_3 + 4\,\mathfrak{L}_2^2\mathfrak{L}_1^2 - \frac{1}{6}\,\mathfrak{L}_2\mathfrak{L}_3\right)t^{3/2} + \mathcal{O}(t^2)\right) \tag{9.2.19}$$

Computing explicitly the action of the operator $e^{\frac{t}{12}(\sigma\partial_\sigma)^3}$ and integrating with respect to σ, we observe empirically that the integral at each order can be performed explicitly, except the one at order t^0. The term at order t^0 is given by

$$\int_0^\sigma \frac{\mathrm{d}u}{u}\,\mathfrak{L}_1(u)^2 = \frac{\alpha^2}{4\pi^2}\int_0^\sigma \mathrm{d}u\,u\left[\partial_u\int_{\mathbb{R}}\mathrm{d}p\,g(ue^{-p^2})\right]^2 \tag{9.2.20}$$

Remark 9.2.2. *This second term can also be written equivalently in the form*

$$\int_0^\sigma \frac{\mathrm{d}u}{u}\,\mathfrak{L}_1(u)^2 = \frac{\alpha^2}{8\pi^2}\int_0^\infty \mathrm{d}u\,u\left|\int_{\mathbb{R}}\mathrm{d}p\,e^{iup}g(\sigma e^{-p^2})\right|^2 \tag{9.2.21}$$

The equality is checked by Taylor expanding the function g in both r.h.s of (9.2.20) and (9.2.21) and checking that the series match. This representation of the t^0 contribution will be used later on to comment on the emergence of a Gaussian free field for the edge GUE Fredholm determinant.

We finally obtain our main result for the expansion of $q_{t,\alpha}(\sigma)$ defined in (9.2.5) for an arbitrary function g as shown in Ref. [5]. We present in the following result the first orders of this expansion.

Result 9.2.3 (*Systematic time expansion of the edge GUE Fredholm determinant*)

The first five orders of the systematic expansion of the edge GUE Fredholm determinant read

$$\begin{aligned} q_{t,\alpha}(\sigma) &= \frac{\alpha}{\pi\sqrt{t}} \int_0^\infty \mathrm{d}x\, \sqrt{x}\, g(\sigma e^{-x}) + \frac{\alpha^2}{4\pi^2} \int_0^\sigma \mathrm{d}u\, u \left[\partial_u \int_{\mathbb{R}} \mathrm{d}p\, g(u e^{-p^2})\right]^2 \\ &+ \left(\frac{2\mathfrak{L}_1^3}{3} + \frac{\mathfrak{L}_2}{12}\right)\sqrt{t} + \left(\frac{4}{3}\,\mathfrak{L}_1^3\mathfrak{L}_2 + \frac{\mathfrak{L}_2^2}{12} + \frac{\mathfrak{L}_1\mathfrak{L}_3}{6}\right) t \\ &+ \left(\frac{8}{3}\,\mathfrak{L}_1^3\mathfrak{L}_2^2 + \frac{\mathfrak{L}_2^3}{9} + \frac{2}{3}\,\mathfrak{L}_1^4\mathfrak{L}_3 + \frac{2}{3}\,\mathfrak{L}_1\mathfrak{L}_2\mathfrak{L}_3 + \frac{\mathfrak{L}_1^2\mathfrak{L}_4}{6} + \frac{\mathfrak{L}_5}{288}\right) t^{3/2} + \mathcal{O}(t^2)\,, \end{aligned} \tag{9.2.22}$$

where the $\mathfrak{L}_i$ are defined in (9.2.18).

The first two terms can also be rewritten as

$$\begin{aligned} \frac{\alpha}{\pi} \int_0^\infty \mathrm{d}x\, \sqrt{x}\, g(\sigma e^{-x}) &= \mathfrak{L}_{-1} \\ \frac{\alpha^2}{4\pi^2} \int_0^\sigma \mathrm{d}u\, u \left[\partial_u \int_{\mathbb{R}} \mathrm{d}p\, g(u e^{-p^2})\right]^2 &= \int_0^\sigma \frac{\mathrm{d}u}{u} \mathfrak{L}_1(u)^2 \end{aligned} \tag{9.2.23}$$

Now that we obtained a procedure to expand the edge GUE Fredholm determinant in successive orders in time, our goal is to relate it to the cumulant expansion that we have previously introduced in Eq. (2.2.19). This allows to justify the first cumulant approximation at short time and control the behavior of the higher order cumulants, both at short and large times. We recall that all terms proportional to α^n in the expansion of $q_{t,\alpha}(\sigma)$ belong to the n-th cumulant: each term $\mathfrak{L}$ includes a factor α and hence the combinatorics is easy.

9.3 Cumulants of the Airy point process: from small times to large times

It is interesting to note that the degree in terms of $\mathfrak{L}$ indicates from which cumulant each term originates (i.e. a product of n factors $\mathfrak{L}$ comes from the n-th cumulant). We compared in Ref. [5] the expansion in Eq. (9.2.22) and the explicit calculation of the first three cumulants which coincide term by term. We shall present in this Section the time properties of the different cumulants and explain how their large-time behavior can be extrapolated from their short-time behavior.

9.3.1 Linear statistics at the edge of the GUE at short time: Gaussian free field and beyond

By inspection on the series (9.2.22), we have determined in Ref. [5] a few orders in time of the first five cumulants, which we present in Eqs. (9.3.1).

Cumulant	First order	Second order	Third order
κ_1	$t^{-1/2}$	$t^{1/2}$	$t^{3/2}$
κ_2	1	t	t^2
κ_3	$t^{1/2}$	$t^{3/2}$	$t^{5/2}$
κ_4	t	t^2	t^3
κ_5	$t^{3/2}$	$t^{5/2}$	$t^{7/2}$

Table 9.1: Leading orders in times for the contributions to a given order of each cumulant of the Airy point process κ_n, up to $n = 5$.

$$
\begin{aligned}
\kappa_1 &= \frac{1}{\pi\sqrt{t}} \int_0^{+\infty} \mathrm{d}x \sqrt{x} g(\sigma e^{-x}) + \frac{\mathfrak{L}_2}{12}\sqrt{t} + \frac{\mathfrak{L}_5}{288} t^{3/2} + \mathcal{O}(t^{5/2}) \\
\kappa_2 &= \frac{1}{2\pi^2} \int_0^{\sigma} \mathrm{d}u\, u \left[\partial_u \int_{\mathbb{R}} \mathrm{d}p\, g(u e^{-p^2})\right]^2 + \left(\frac{\mathfrak{L}_2^2}{6} + \frac{\mathfrak{L}_1\mathfrak{L}_3}{3}\right) t + \left(\frac{29}{360}\mathfrak{L}_3\mathfrak{L}_4 + \frac{\mathfrak{L}_2\mathfrak{L}_5}{24} + \frac{\mathfrak{L}_1\mathfrak{L}_6}{72}\right) t^2 + \mathcal{O}(t^3) \\
\kappa_3 &= 4\mathfrak{L}_1^3\sqrt{t} + \left(\frac{2\mathfrak{L}_2^3}{3} + 4\mathfrak{L}_1\mathfrak{L}_3\mathfrak{L}_2 + \mathfrak{L}_1^2\mathfrak{L}_4\right) t^{3/2} + \mathcal{O}(t^{5/2}) \\
\kappa_4 &= 32\mathfrak{L}_1^3\mathfrak{L}_2 t + \left(4\mathfrak{L}_2^4 + 48\mathfrak{L}_1\mathfrak{L}_3\mathfrak{L}_2^2 + 24\mathfrak{L}_1^2\mathfrak{L}_4\mathfrak{L}_2 + 16\mathfrak{L}_1^2\mathfrak{L}_3^2 + \frac{8}{3}\mathfrak{L}_1^3\mathfrak{L}_5\right) t^2 + \mathcal{O}(t^3) \\
\kappa_5 &= (80\mathfrak{L}_3\mathfrak{L}_1^4 + 320\mathfrak{L}_2^2\mathfrak{L}_1^3) t^{3/2} + \mathcal{O}(t^{5/2})
\end{aligned}
\tag{9.3.1}
$$

where the $\mathfrak{L}_j$ are defined in (9.2.14) and where we did set α to 1. We presented in the second Part of the Thesis the first cumulant conjecture, i.e. that the first cumulant $\kappa_1 = \kappa_1(g)$ gives the leading order in the short-time expansion. The expansion presented in Eq. (9.3.1), summarized in Table 9.1 validates our conjecture, higher cumulants being indeed subdominant at small t. The systematic expansion in time Eq. (9.3.1) additionally extends considerably the theorem of Basor and Widom presented in Theorem 7.1.4 (see also Ref. [213]).

At short time, we see that only the first two cumulants are relevant: κ_1 provides the $1/\sqrt{t}$ necessary to study the large deviations of the linear statistics over the Airy point process and κ_2 provides a correction of order $\mathcal{O}(1)$ which was already present in the result of Basor and Widom. We shall now interpret these two contributions in terms of the first two cumulants of the empirical measure of the Airy point process. Indeed, let us recall the expression of the empirical measure μ, and define the height field H of the Airy point process as

$$
\mu(a) = \sum_{i=1}^{+\infty} \delta(a - a_i), \qquad \mathsf{H}(a) = -\int_a^{+\infty} \mu(a')\mathrm{d}a'. \tag{9.3.2}
$$

The height field counts the number of points above a certain level with $\mathsf{H}'(a) = \mu(a)$. The linear statistics problem has a natural rewriting in terms of the empirical measure μ

$$
\mathbb{E}_{\mathrm{Ai}}\left[\exp\left(\sum_{i=1}^{\infty} g(\sigma e^{t^{1/3}a_i})\right)\right] = \mathbb{E}_{\mathrm{Ai}}\left[\exp\left(\int_{\mathbb{R}} \mathrm{d}a\, g(\sigma e^{t^{1/3}a})\mu(a)\right)\right] \tag{9.3.3}
$$

By definition, the cumulants of the empirical measure are determined from κ_g as

$$
\int_{\mathbb{R}^n} \mathrm{d}a_1 \dots \mathrm{d}a_n \prod_{j=1}^{n} g(\sigma e^{a_j}) t^{-n/3} \overline{\mu(t^{-1/3}a_1)\dots\mu(t^{-1/3}a_n)}^{c} = \kappa_n(g) \tag{9.3.4}
$$

In Ref. [5], we were able to determine the first cumulant κ_1 at any order in t as

$$\kappa_1(g) = \frac{e^{\frac{t}{12}(\sigma\partial_\sigma)^3}}{\pi\sqrt{t}} \int_0^{+\infty} \mathrm{d}x \sqrt{x} g(\sigma e^{-x}) \tag{9.3.5}$$

which allowed us to obtain the expected value of the empirical measure to any order in t.

Result 9.3.1 (*Mean density of the Airy point process*)

The expected value of the empirical measure of the Airy point process has the following expansion to all orders in t from the bulk towards the edge

$$t^{-1/6}\overline{\mu(at^{-1/3})} = \frac{\Theta(-a)}{\pi} e^{-\frac{t}{12}(\partial_a)^3}\sqrt{-a} \tag{9.3.6}$$

We can compare this result to the known exact result for the mean density of the Airy point process $\overline{\mu(a)} = K_{\mathrm{Ai}}(a,a) = \mathrm{Ai}'(a)^2 - a\mathrm{Ai}(a)^2$. Asymptotics of the Airy functions allow indeed to recover (9.3.6), but only upon discarding terms which are fast oscillating for large negative a. Hence Eq. (9.3.6) is valid in the weak sense. Additionally, by identification, we obtained in Ref. [5] the second cumulant of the height field at short time.

Result 9.3.2 (*Two-point correlator of the height field of the Airy point process*)

The two-point correlation function of the Airy point process integrated density reads at leading order

$$\overline{\mathsf{H}(a_1 t^{-1/3})\mathsf{H}(a_2 t^{-1/3})}^c \underset{t\ll 1}{=} -\frac{1}{2\pi^2}\log\left|\frac{\sqrt{-a_1}-\sqrt{-a_2}}{\sqrt{-a_1}+\sqrt{-a_2}}\right| \Theta(-a_1)\Theta(-a_2) + \mathcal{O}(t) \tag{9.3.7}$$

This logarithmic correlator is a particular case of the correlator of the Gaussian free field. In [235, 236] it is shown that the height field associated to the GUE in the bulk, H_{GUE} defined likewise by counting the number of eigenvalues above a certain level, is described upon rescaling by a Gaussian free field with a specific correlator (see also [237]). We have shown that it matches precisely Eq. (9.3.7) when taking the limit to the edge.

To summarize, we have been able to validate the first cumulant conjecture at short time for the linear statistics $\mathbb{E}_{\mathrm{Ai}}\left[\exp\left(\sum_{i=1}^{\infty} g(\sigma e^{t^{1/3}a_i})\right)\right]$ and we have obtained its corrections to any order in t, deep in intermediate time regime. Our main result is that the fluctuations around the first cumulant are to leading order at small t the one of the Gaussian free field: this echoes a continuous version of the strong Szegö theorem as we already mentioned in the second Part of this Thesis. However, the higher orders in our expansion thus allow to calculate the deviations from the Gaussian free field in the edge region. In the rest of this Section, we shall see that quite remarkably, the short-time structure of the cumulants can be used to infer their late-time behavior.

9.3.2 Linear statistics at the edge of the GUE at late time

Since we are studying formally an expansion in t, but for arbitrary fixed σ, it turns out that one can in fact obtain some results for arbitrary t and even for large t. Obtaining such results assumes that the observed structure of the series in t when $\sigma \to -\infty$ holds to arbitrary order (and in a non perturbative sense). The examination of our results (9.3.1) for the cumulants led us to formulate in Ref. [5] the following conjecture for the structure of the cumulant expansion.

Conjecture 9.3.3 (*Behavior of various contributions in the cumulant expansion*)

The contribution in time of each cumulant within the expansion $q_t(\sigma)$ at fixed σ in power of t can be expressed as

$$q_t(\sigma) = \sum_{n\geqslant 1} \frac{\kappa_n(g)}{n!} \tag{9.3.8}$$

$$\kappa_n(g) = t^{\frac{n}{2}-1}\kappa_n^0(\sigma) + \sum_{p\geqslant 1} t^{\frac{n}{2}-1+p}\,\kappa_n^p(\sigma) \tag{9.3.9}$$

The leading order for $n \geqslant 1$ is conjectured to be equal to

$$\kappa_n^0(\sigma) = 2^{n-1}(\sigma\partial_\sigma)^{n-3}\mathfrak{L}_1(\sigma)^n. \tag{9.3.10}$$

The general terms $\kappa_n^p(\sigma)$ was conjectured to have the following homogeneity

$$\kappa_n^p(\sigma) \equiv [(\sigma\partial_\sigma)^{n-3+3p}][\mathfrak{L}_1(\sigma)^n]. \tag{9.3.11}$$

Remark 9.3.4. *A direct consequence of this decomposition is that each cumulant at short time is dominated by the leading order $\kappa_n^0(\sigma)$.*

The result for the dominant term $\kappa_n^0(g)$ holds for $n = 1$ since $\mathfrak{L}_1 = (\sigma\partial_\sigma)^2\mathfrak{L}_{-1}$ and $\kappa_1 = t^{-1/2}\mathfrak{L}_{-1}$ and for $n = 2$, from (9.2.20) interpreting $(\sigma\partial_\sigma)^{-1} = \int_0^\sigma \frac{du}{u}$. Let us understand the homogeneity relation by recalling the relation from Eq. (9.2.18)

$$\mathfrak{L}_i = (\sigma\partial_\sigma)^{i-1}\mathfrak{L}_1 = \frac{1}{\pi}(\sigma\partial_\sigma)^{i+1}\int_0^\infty \mathrm{d}x\,\sqrt{x}\,g(\sigma e^{-x}). \tag{9.3.12}$$

and by examining the expression of the second cumulant

$$\kappa_2 = \frac{1}{2}\int_0^\sigma \frac{\mathrm{d}u}{u}\mathfrak{L}_1(u)^2 + \left(\frac{\mathfrak{L}_2^2}{6} + \frac{\mathfrak{L}_1\mathfrak{L}_3}{3}\right)t + \left(\frac{29}{360}\,\mathfrak{L}_3\mathfrak{L}_4 + \frac{\mathfrak{L}_2\mathfrak{L}_5}{24} + \frac{\mathfrak{L}_1\mathfrak{L}_6}{72}\right)t^2 + \mathcal{O}(t^3) \tag{9.3.13}$$

The homogeneity of the first order in t has been checked above. For the second order in t:

- Each factor $\mathfrak{L}_2$ provides one factor $(\sigma\partial_\sigma)$ and one factor $\mathfrak{L}_1$;
- The factor $\mathfrak{L}_3$ provides two factors $(\sigma\partial_\sigma)$ and one factor $\mathfrak{L}_1$.

Hence the combinatorics agree with (9.3.11) and similarly for the third term. More generally, the number of factors $\mathfrak{L}_1$ is fixed by the index of the cumulant (as each $\mathfrak{L}_1$ was carrying one α) and the power of $(\sigma\partial_\sigma)$ is given by the multiplication of the power of each factor $\mathfrak{L}$ by its index minus one.

Equation (9.3.9) can now be studied at fixed t but in the limit $\sigma \to -\infty$. In that limit the first term in (9.3.9), $t^{\frac{n}{2}-1}\kappa_n^0(\sigma)$, is the dominant one, which gives the leading asymptotics of $q_t(\sigma)$ for $\sigma \to -\infty$ for any t. Indeed we see from (9.3.1) and the above conjecture that the term $t^{\frac{n}{2}-1+p}\,\kappa_n^p(\sigma)$ contains $n-3+3p$ derivatives $\sigma\partial_\sigma$. Each derivative makes the term more subdominant: more precisely, setting $\sigma = -e^v$, the condition on $g(x)$ for this to hold is that

$$g(-e^v) \underset{v\to+\infty}{=} o(e^v) \tag{9.3.14}$$

i.e. $g(-e^v)$ is a sub-exponential function of v. A remarkable consequence of the $\sigma \to -\infty$ limit for structure of the series (9.3.9) is that its *large-time limit* is also controlled by the term $t^{\frac{n}{2}-1}\kappa_n^0(\sigma)$.

This can be seen as follows. Let us choose $\sigma = -e^{ut}$, with fixed $u > 0$. From the conjecture above we can write in a symbolic form the general term of (9.3.9) as

$$\begin{aligned} t^{\frac{n}{2}-1+p}\,\kappa_n^p(\sigma = -e^{ut}) &\sim t^{\frac{n}{2}-1+p}[(\sigma\partial_\sigma)^{n-3+3p}][\mathfrak{L}_1(\sigma)^n] \\ &\sim t^{\frac{n}{2}-1+p}[(\frac{1}{t}\partial_u)^{n-3+3p}][\mathfrak{L}_1(-e^{ut})^n] \end{aligned} \tag{9.3.15}$$

where here we just count the degree of homogeneity in derivatives and function $\mathfrak{L}_1$. Since the p dependence in the power of t now behaves t^{-2p} we see that $p = 0$ is the leading term for each fixed n in the large t limit.

Until now our considerations where valid for general function g. Inspired by a family of functions appearing in the Kardar-Parisi-Zhang problem, we shall consider functions g_t which exhibit the following asymptotics

$$\lim_{t\to+\infty} -\frac{g_t(-e^{tu})}{t} = \phi(u) \tag{9.3.16}$$

and $g_t(0) = 0$ which implies that $\phi(x) = 0$ for $x \leqslant 0$.

Example 9.3.5. *The family of polylogarithms verifies this property, i.e.*

$$g_t(x) = t^{1-\gamma}\Gamma(\gamma+1)\mathrm{Li}_\gamma(x). \tag{9.3.17}$$

With this asymptotic expression of g_t, as announced in Eq. (9.2.2), our original linear statistics problem reads

$$\mathbb{E}_{\mathrm{Ai}}\left[\exp\left(\sum_{j=1}^{\infty} g_t(\sigma e^{t^{1/3}a_j})\right)\right] \underset{t\gg1}{=} \mathbb{E}_{\mathrm{Ai}}\left[\exp\left(-t\sum_{j=1}^{\infty}\phi(u+t^{-2/3}a_j)\right)\right]. \tag{9.3.18}$$

Inserting $\sigma = -e^{ut}$ into the expression of the leading term of each cumulant $\kappa_n^0(\sigma)$ in Eq. (9.3.10), recalling the expression of $\mathfrak{L}_1$ in (9.3.12) and taking the large-time limit of the function g_t, Eq. (9.3.16), the n-th cumulant reads

$$\kappa_n^0(\sigma = -e^{ut}) \underset{t\gg1}{=} t^{\frac{n}{2}-1}\frac{2^{n-1}}{\pi^n}(\frac{1}{t}\partial_u)^{n-3}\left(-\frac{1}{t}(\partial_u)^2\int_0^{+\infty}\mathrm{d}x\sqrt{x}\phi(u-\frac{x}{t})\right)^n \tag{9.3.19}$$

Regrouping the different time factors, one observes that all leading terms of κ_n are proportional to t^2 and we can then write the summation over the cumulant index n.

Result 9.3.6 (*Large-time resummation of the cumulant series*)

At large time, the dominant contribution of the cumulant expansion is of magnitude t^2 and enjoys the following expression

$$q_t(\sigma = -e^{ut}) \underset{t\gg1}{=} \sum_{n\geqslant1}\frac{\kappa_n}{n!} = -t^2\Sigma_\phi(u), \quad \Sigma_\phi(u) = -\frac{1}{2}\sum_{n\geqslant1}\frac{1}{n!}(-\frac{2}{\pi})^n\partial_u^{n-3}f(u)^n. \tag{9.3.20}$$

where

$$f(u) = \int_{\mathbb{R}_+}\mathrm{d}b\,\sqrt{b}\,\phi''(u-b) \tag{9.3.21}$$

From the subleading contributions of the different cumulants (see Eq. (9.3.15)) we also know that the next contribution in time for $q_t(u)$ will be of order $\mathcal{O}(t^0)$.

To conclude, we have been able to obtain some information at late time about our linear statistics starting from the short-time expansion. This allowed us in Ref. [5] to derive a large deviation principle for the solution to the KPZ equation with droplet initial condition. As we shall see in the next Chapter, this also allowed us to investigate more general linear statistics at the edge of Gaussian matrices. We refer the reader to Refs. [4, 5] for the complete picture of this work.

9.3.3 Open questions related to a systematic expansion at hard edges or in the bulk

The problem of linear statistics we have investigated in this Chapter concerned the edge of Hermitian Gaussian random matrices and we based the whole calculation on the representation of our linear statistics in terms of a Fredholm determinant involving the Airy kernel. It would be interesting as well to study the same linear statistics at the hard edge of the spectrum of Laguerre random matrices using the Bessel kernel or in the bulk of generic random matrices using the Sine kernel.

In the next Chapter, we shall pursue the investigation of the linear statistics at large time, and we shall unveil some surprising connections between our systematic expansion of the edge GUE Fredholm determinant, the Stochastic Airy Operator and a Coulomb gas at the edge of Gaussian matrices. We will start from recalling the original motivation of the problem: the study of the late-time behavior of the solution to the Kardar-Parisi-Zhang equation for droplet initial condition. Then we will generalize our results to consider perturbations localized at the edge of Gaussian matrices, represented as a certain linear statistics.

Chapter 10

Introduction to the linear statistics at the edge of Gaussian matrices

10.1 The late-time large deviations of KPZ as a microscopic linear statistics

In this Section, we will describe the problem of the late-time behavior of the solution to the Kardar-Parisi-Zhang equation in full-space for the droplet initial condition. This will motivate the introduction to the problem of linear statistics at the edge of random matrices. We recall the duality relation between the KPZ solution and the Airy point process, see Eqs. (3.2.1) and (2.2.3).

$$\mathbb{E}_{\rm KPZ}\left[\exp\left(-e^{h(0,t)+\frac{t}{12}+ut}\right)\right]=\mathbb{E}_{{\rm Ai},\beta=2}\left[\prod_{i=1}^{\infty}\frac{1}{1+e^{t^{1/3}a_i+ut}}\right] \tag{10.1.1}$$

We investigate the convergence of both sides of Eq. (10.1.1), in the late-time regime, $t\to\infty$

- The left hand side of Eq. (10.1.1) approaches the cumulative distribution of the one-point KPZ height at large time:

$$\mathbb{E}_{\rm KPZ}\left[\exp\left(-e^{h(0,t)+\frac{t}{12}+ut}\right)\right]\underset{t\gg 1}{\longrightarrow}\mathbb{P}(h(0,t)+\frac{t}{12}\leqslant -ut) \tag{10.1.2}$$

- The right hand side of Eq. (10.1.1) can also be manipulated in the following fashion:

$$\frac{1}{1+e^{t^{1/3}a_i+ut}}=\exp\left(-\log(1+e^{t^{1/3}a_i+ut})\right)\underset{t\gg 1}{\longrightarrow}\exp\left(-t(t^{-2/3}a_i+u)_+\right) \tag{10.1.3}$$

where $(x)_+=\max(0,x)$.

This allows us to rewrite the duality between the solution to the Kardar-Parisi-Zhang equation and the Airy point process at large time as

$$\mathbb{P}(h(0,t)+\frac{t}{12}\leqslant -ut)\underset{t\gg 1}{=}\mathbb{E}_{{\rm Ai},\beta=2}\left[\exp\left(-t\sum_{i=1}^{\infty}(t^{-2/3}a_i+u)_+\right)\right]. \tag{10.1.4}$$

The right hand side of Eq. (10.1.4) has a very particular structure and is reminiscent of the type of expressions studied in the systematic time expansion of the edge GUE Fredholm determinant, see Eq. (9.2.2) with $\phi(z)=(z+u)_+$. It takes the form of a linear statistics problem

(which we precisely define in the next Section) over the Airy point process. As the Airy point process arises at the edge of the spectrum of random matrices, this linear statistics problem can also be viewed as a microscopic linear statistics for a large random matrix. To our knowledge, the late-time KPZ problem was the first in the literature to motivate an actual study of microscopic linear statistics at the edge of Gaussian random matrices, i.e. on the scale of the first few points of the Airy process.

Very recently, no less than *four methods* were devised to evaluate the right hand side of Eq. (10.1.4): *(i)* the electrostatics of a Coulomb gas [7] *(ii)* a random Schrödinger problem known as the stochastic Airy operator [238] *(iii)* a cumulant expansion explained in the previous Chapter [5] *(iv)* a non-local non-linear differential Painlevé type equation [239]. Although apparently unrelated, they lead to the same large deviation principle expressed in the Result 10.1.1 for the late-time KPZ problem with droplet initial condition. The aim of this Chapter and the following Chapters is to unveil the connections between these methods, make explicit the underlying structure and apply them to more general microscopic linear statistics.

Result 10.1.1 (*Large deviation principle for KPZ at large time: first part*)

For all $u \geqslant 0$, the probability that the KPZ interface, starting from a droplet initial condition, has a velocity smaller than $-1/12$ at large time is given by the following large deviation principle of rate t^2

$$\lim_{t\to+\infty} -\frac{1}{t^2}\log \mathbb{P}(h(0,t)+\frac{t}{12}\leqslant -ut) = \frac{4}{15\pi^6}(1+\pi^2 u)^{5/2} - \frac{4}{15\pi^6} - \frac{2}{3\pi^4}u - \frac{1}{2\pi^2}u^2 \quad (10.1.5)$$

This result was first obtained in Ref. [239].

As expected from the beginning of Section 9.1, the right hand side of (10.1.5) interpolates between a u^3 behavior for small u and a $u^{5/2}$ behavior for large u.

Remark 10.1.2. *From an experimental point of view, these large deviations correspond to an interface with an excess growth.*

The other side of the large deviations has also been obtained in Ref. [187] (see also [234]). We provide here the result for completeness but we will not discuss it in this Thesis.

Result 10.1.3 (*Large deviation principle for KPZ at large time: second part*)

For all $u \leqslant 0$, the probability that the KPZ interface, starting from a droplet initial condition, has a velocity larger than $-1/12$ at large time is given by the following large deviation principle of rate t

$$\lim_{t\to+\infty} -\frac{1}{t}\log \mathbb{P}(h(0,t)+\frac{t}{12}\geqslant -ut) = \frac{4}{3}|u|^{3/2} \quad (10.1.6)$$

In the next Section, we will recall the definition of a linear statistics problem in Random Matrix Theory, review some cases where it has been investigated and show how to change scale to turn from a macroscopic problem into a microscopic one.

10.2 From macroscopic to microscopic linear statistics

10.2.1 Introduction to macroscopic linear statistics

A classical problem, called linear statistics, amounts to study the probability distribution function (PDF) of sums $\mathcal{L} = \sum_{i=1}^{N} f(\lambda_i)$ over eigenvalues λ_i of a size N random matrix. Varying

the function f and the ensemble, it describes e.g. conductance and shot noise [240, 241], Renyi entropies [242], interfaces center of mass [123] and more, see below.

Definition 10.2.1 (*Linear statistics in Random Matrix Theory*)

The linear statistics problem amounts to determine the probability distribution of the following quantity

$$\mathcal{L} = \sum_{i=1}^{N} f(\lambda_i) \tag{10.2.1}$$

where the λ_i are the eigenvalues of an $N \times N$ random matrix. In practice, we will evaluate the generating function of $\mathcal{L}$, i.e. $\mathbb{E}[e^{-\mathcal{L}}]$ and invert the Laplace transform to obtain the distribution.

We call this problem macroscopic linear statistics which natural extension is the truncated linear statistics.

Definition 10.2.2 (*Truncated linear statistics in Random Matrix Theory*)

The truncated linear statistics is a refinement of the macroscopic linear statistics where we consider solely the N_1 largest eigenvalues of the consider random matrix.

$$\mathcal{L} = \sum_{i=1}^{N_1} f(\lambda_i) \tag{10.2.2}$$

Truncated linear statistics were first considered in Ref. [229].

In the Table 10.1 which data are extracted from Ref. [229], we summarize a few cases where linear statistics have been investigated in the physics community. At large N, central limit theorems, universality, and connections to the Gaussian free field were shown [5, 166, 235–237, 243–247] for typical fluctuations of $\mathcal{L}$ in the bulk of the spectrum.

Large deviations of the linear statistics have also been studied in the bulk [164, 192, 248–250], from the Coulomb gas representation or from special Selberg integrals, and these studies have been recently extended to truncated linear statistics [229, 230], showing numerous phase transitions. These phase transitions share remarkable properties with ones observed in several other physics models related to random matrices [158, 251], including large-N gauge theories [252–255], longest increasing subsequences of random permutations [256], random tilings [257, 258].

Recalling the Coulomb gas picture of the eigenvalues of Gaussian β random matrices, the linear statistics problem amounts to study this Coulomb gas with an external potential $f(\lambda)$. Hence, we shall call it a perturbed gas. In this context, two observables of the linear statistics have a particularly simple interpretation:

- The quantity $\mathbb{E}[e^{-\mathcal{L}}]$ is the ratio of the partition functions of the perturbed gas and the unperturbed one ;
- The quantity $\log \mathbb{E}[e^{-\mathcal{L}}]$ is the free energy difference between perturbed and unperturbed gas. We shall also refer to this quantity as the excess energy.

10.2.2 From the bulk towards the edge

From now on, we shall only consider Gaussian random matrices with general β and in particular, we will be interested at linear statistics near their right edge $\lambda_i = 2 + \frac{a_i}{N^{2/3}}$ where the set $\{a_i\}$

Physical observable	Matrix ensemble	Ref.
Linear statistics		
Wigner time delay $\sum_n \lambda_n^{-1}$	Laguerre	[135]
Renyi entropy $\sum_n \lambda_n^q$	Laguerre	[259]
Conductance $\sum_n \lambda_n$	Jacobi	[241, 260]
Shot noise $\sum_n \lambda_n(1-\lambda_n)$	Jacobi	[260]
Moments $\sum_n \lambda_n^k$	Jacobi	[260]
Normal metal - superconductor conductance $\sum_n \lambda_n^2(2-\lambda_n)^{-2}$	Jacobi	[261]
Largest eigenvalue λ_1	Gaussian, Laguerre	[192] [158, 262]
Index $\sum_n \Theta(\lambda_n)$	Gaussian, Laguerre, Cauchy, ...	[249, 250] [125, 263]
Index (2D) $\sum_n \Theta(\|\lambda_n\| - r)$	Complex Ginibre	[264]
Mean radius (2D) $\sum_n \|\lambda_n\|$	Complex Ginibre	[265]
Center of mass of interface $\sum_n \sqrt{\lambda_n}$	Laguerre	[123]
Truncated linear statistics		
$\sum_{i=1}^{N_1} \sqrt{\lambda_i}$	Laguerre	[229, 230]
$\sum_{i=1}^{N_1} \lambda_i$	Jacobi	

Table 10.1: *List of different linear statistics problem studied in the physics literature. The information of this Table is extracted from Ref. [229].*

form the Airy β point process. In this case, for large N, the truncated linear statistics $\mathcal{L}$ reads

$$\mathcal{L} = N_1 f(2) + \sum_{i=1}^{N_1} f'(2) \frac{a_i}{N^{2/3}} + \mathcal{O}(N^{-4/3}) \tag{10.2.3}$$

If the linear statistics function f is smooth at the edge, we observe that the observable which determines the fluctuations of $\mathcal{L}$ is $\sum_{i=1}^{N_1} a_i$. Hence the following natural question arises:

How to study truncated linear statistics at the edge, such as $\mathsf{L} = \sum_{i=1}^{N_1} g(a_i)$ *?*

The answer to this question requires new mathematical tools dedicated to the edge of random matrices: the linear statistics at the edge are not a simple extension of macroscopic linear statistics. The purpose of the rest of this Thesis will be devoted to answering this question and to providing applications of such linear statistics at the edge.

Studying the Airy$_\beta$ point process by itself is complicated, even at the simplest level of the mean, variance, skewness of the Tracy-Widom distributions, there do not exist closed expressions in the literature. Hence, keeping in mind our main goal which is to describe the late-time behavior of the Kardar-Parisi-Zhang equation, we want to study the following linear statistics at the edge:

$$\mathsf{L} = t \sum_{i=1}^{\infty} \phi(t^{-2/3} a_i + u) \tag{10.2.4}$$

where u is a positive parameter and t is taken to be positive and large: $t \gg 1$ (this is exactly the time of the KPZ dynamics). In the following and for rest of the third Part of this Chapter, we will be interested in a class of functions ϕ that we call *monomial soft walls*.

Definition 10.2.3 (*Monomial soft walls*)

Let $\gamma > 1/2$, the monomial soft wall potential is defined by the function

$$\phi(x) = (x)_+^\gamma = \max(0, x^\gamma) \tag{10.2.5}$$

Remark 10.2.4. *The late-time behavior of the KPZ equation is considered by taking $\gamma = 1$.*

Remark 10.2.5. *From our estimates in Eq. (10.2.3), we have seen that any truncated macroscopic linear statistics over a sufficiently smooth function at the edge converges to the linear statistics (10.2.4), (10.2.5) for $\gamma = 1$ which is precisely the case associated to the KPZ equation. Hence, we may wonder whether there exist a deeper connection between the edge limit of macroscopic linear statistics and the Kardar-Parisi-Zhang problem at late time which belongs to the KPZ universality class.*

Although we restrict here to the monomial walls, a wider class of walls and functions ϕ have been studied in Ref. [4].

The truncated linear statistics were originally introduced by truncating the sum of the linear statistics at a certain index. Here we reformulate the truncation by the use of the positive parameters t and u and we will study the limit of fixed u and $t \to +\infty$. Indeed, due to our choice of function ϕ, there is only a finite number of a_i's that contribute to the linear statistics. For a point a_i to contribute, we have the following constraint

$$a_i \geqslant -ut^{2/3} \tag{10.2.6}$$

Heuristically, for large negative a, the density of the Airy point process grows proportionally to $\sqrt{-a}$, hence the number of particles perturbed by this potential is

$$N_1 \propto \int_{-ut^{2/3}}^{0} \mathrm{d}a \, \sqrt{-a} \propto u^{3/2} t \tag{10.2.7}$$

The interpretation of this dependence of N_1 with t is that in our problem, we shall perturb an effective gas containing $\mathcal{O}(t)$ particles. Because we have roughly t non zero terms in the linear statistics and we added an extra t factor in front of the sum, the overall (truncated) linear statistics will be of magnitude $\mathcal{O}(t^2)$. As we shall see in the next Section, this magnitude for the microscopic linear statistics matches the magnitude of macroscopic linear statistics which is N^2 for a matrix that has N eigenvalues (or equivalently a Coulomb gas that has N particles).

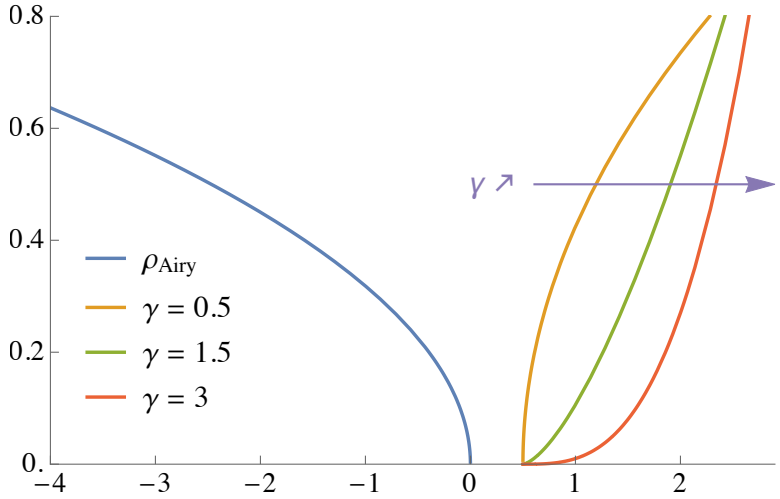

Figure 10.1: Plot of the density of the semi-circle at the right edge (blue line) and of the monomial soft wall function ϕ for three values of γ: 1/2 (orange), 3/2 (green) and 3 (red).

For the following of this Chapter, we will define an empirical density (depending on a parameter t) for the rescaled points $b = -t^{-2/3}a$ as [10]

$$\rho(b) = \frac{1}{t}\sum_{i=1}^{+\infty} \delta(b + t^{-2/3}a_i) \tag{10.2.8}$$

With this definition, the linear statistics reads

$$\mathsf{L} = t^2 \int_{\mathbb{R}} \mathrm{d}b\, \rho(b)\phi(u-b), \tag{10.2.9}$$

and we can calculate the average of L to leading order at large t using the asymptotics of the density of the Airy point process

$$\mathbb{E}[\mathsf{L}] = t^2 \int_0^{+\infty} \mathrm{d}b\, \frac{\sqrt{b}}{\pi}\phi(u-b) + o(t^2). \tag{10.2.10}$$

Remark 10.2.6. *The expected value of* L *(which we also refer to as the first cumulant) can be interpreted as an overlap between the potential* ϕ *and the edge of the semi-circle which has density* $\rho_{\text{Ai}}(b) = \sqrt{(b)_+}/\pi$.

We represent in Fig. 10.1 the density of the semi-circle at the right edge on a scale $t^{-2/3}$ together with the monomial soft walls ϕ. We see from Fig. 10.1 that as γ increases, the potential ϕ becomes less and less sharp at its point of application. Besides, since the potentials that we consider are positive they will compress or push the edge of the Coulomb gas. Since ϕ is not infinite, the potential ϕ acts as soft or permeable wall.

Our goal for the rest of this Thesis will be to derive the following result through four apparently unrelated methods:

[10] As it will be made clear in the next Section, we reverse the points $a \to -a$ since either the left or the right edge of the semi-circle are considered in the literature.

Result 10.2.7 (*Large deviation principle for the linear statistics at the GβE edge*)

The linear statistics L *in Eq.* (10.2.4) *at the edge of Gaussian* β *random matrices, with the scaling previously introduced, and for the monomial soft walls* (10.2.5)*, admits the large deviation principle*

$$\lim_{t\to\infty} -\frac{1}{t^2}\log \mathbb{E}[e^{-\mathsf{L}}] = \Sigma_\phi(u) \tag{10.2.11}$$

where $\mathbb{E}[e^{-\mathsf{L}}]$ *is the ratio of partitions function of the perturbed Coulomb gas at the edge and the unperturbed one and* $\Sigma_\phi(u)$ *is the excess energy resulting from the reorganization of the gas.*

In addition to deriving the large deviation principle, we will be interested in four subsequent questions.

1. How does the Coulomb gas look like after its reorganization ? Or, what is the density of the gas after the rearrangement ?

2. What is the expression of the excess free energy Σ_ϕ of the gas after its reorganization ?

3. How rigid is the soft edge of a random matrix ? In other words, what is the nature of the transition between the perturbed (pushed, $u \geqslant 0$) gas and the unperturbed (free, $u \leqslant 0$) one ?

4. What are the physical applications of the linear statistics at the soft edge of random matrices ?

We will discover in the rest of this Chapter that the problem of linear statistics at the edge is much richer than in the bulk. Indeed, four independent methods have been used to solve the problem and we refer to them as the four paths to the large deviations. This problem is also richer as new physical phenomena are found to exist at the edge which are absent in the bulk. This will be related to the physics of phase transitions: while they are usually of third-order in the bulk, they can exhibit continuously varying exponent larger than three at the edge.

Before we introduce the four methods to solve the linear statistics problem at the edge, we require one last tool: the Coulomb gas at the edge of Gaussian β random matrices which we define now. As linear statistics in the bulk are generally solved by the means of Coulomb gas methods, we first construct properly the gas at the edge by following the approach undertaken in our work in Ref. [7].

10.3 From the bulk of the Coulomb gas to its edge

We choose to focus from now on to the edge of the spectrum of Gaussian β random matrices of size $N \times N$ and recall that the joint probability distribution function (JPDF) of the eigenvalues λ_i reads

$$P[\lambda] \sim \exp\left(\beta \sum_{1\leqslant i<j\leqslant N} \log|\lambda_i - \lambda_j| - \frac{\beta N}{4}\sum_{i=1}^{N}\lambda_i^2\right). \tag{10.3.1}$$

so that the eigenvalue density has support $[-2, 2]$. We also recall that this JPDF (10.3.1) can be seen as the Gibbs measure of a Coulomb gas with logarithmic repulsion between the eigenvalues, which, at large N, can be described by a continuous density. Indeed, the empirical measure $\Lambda_N(\lambda) := N^{-1}\sum_{i=1}^{N}\delta_{\boldsymbol{\lambda}_i}(\lambda)$ converges as $N \to \infty$ to the Wigner semi-circle distribution with density $\Lambda_{\rm sc}(\lambda) = \frac{1}{2\pi}\sqrt{4-\lambda^2}\mathbb{1}_{\{|\lambda|<2\}}$.

In the following, our aim will be to study here the eigenvalues located near the *left* edge of this Coulomb gas, in a window of width $\sim N^{-2/3}$. In that window for $N \to \infty$, we finally recall that the scaled eigenvalues $b_i \equiv N^{2/3}(\lambda_i + 2)$ define the space-reversed Airy$_\beta$ point process (APP)[11]. Our aim will be to provide a large deviation principle for the empirical measure rescaled near the edge.

It was proved in the work of Ben Arous and Guionnet, see Ref. [266], that the macroscopic empirical measure $\Lambda_N(\lambda)$ enjoys an large deviation principle, so that for a given density function Λ, in the large N limit, $\mathbb{P}(\Lambda_N \approx \Lambda) \approx \exp(-N^2 I_\beta(\Lambda))$, where $I_\beta(\Lambda) = \beta(\mathcal{E}(\Lambda) - \mathcal{E}(\Lambda_{\rm sc}))$, and

$$\mathcal{E}(\Lambda) = \frac{1}{4}\int_{\mathbb{R}} \mathrm{d}\lambda\, \lambda^2 \Lambda(\lambda) - \frac{1}{2}\iint_{\mathbb{R}^2} \log|\lambda_1 - \lambda_2| \prod_{i=1}^{2} \mathrm{d}\lambda_i \Lambda(\lambda_i). \tag{10.3.2}$$

We now manipulate this formula to a form that will be amenable to the rescaling to the Airy$_\beta$ point process. Since the semicircle law $\Lambda_{\rm sc}$ is the minimizer of $\mathcal{E}$ among the set of densities $\Lambda(\lambda)$ with unit normalization $\int_{\mathbb{R}} \mathrm{d}\lambda \Lambda(\lambda) = 1$, it satisfies

$$\frac{\lambda^2}{4} - \int_{\mathbb{R}} \mathrm{d}\lambda' \log|\lambda - \lambda'| \Lambda_{\rm sc}(\lambda') = \frac{1}{2} V(\lambda) + \text{const.} \tag{10.3.3}$$

for some potential V that vanishes $V|_{\{\lambda \in [-2,2]\}} = 0$ within the support $[-2,2]$ of the semi-circle density $\Lambda_{\rm sc}$, and is nonnegative $V|_{\{|\lambda|>2\}} \geqslant 0$ off the support. More explicitly, by calculating the Hilbert transform of the semi-circle density $\int_{-2}^{2} \frac{\mathrm{d}\lambda' \Lambda_{\rm sc}(\lambda')}{\lambda - \lambda'}$, and then integrating the result with respect to λ, we find

$$V(\lambda) = \int_0^{|\lambda|} \mathrm{d}\lambda' \sqrt{(\lambda'^2 - 4)_+} = \left(\frac{|\lambda|}{2}\sqrt{\lambda^2 - 4} - 2\log\left(\frac{\sqrt{\lambda^2 - 4} + |\lambda|}{2} \right) \right) \mathbb{1}_{\{|\lambda|>2\}} \tag{10.3.4}$$

Remark 10.3.1. *Near the edge $|\lambda| \approx 2$, the potential V behaves as $V(\lambda) \simeq \frac{4}{3}\Big(|\lambda| - 2\Big)^{3/2} \mathbb{1}_{\{|\lambda|>2\}}$. The exponent and pre-factors are reminiscent of the one of the right large deviations of the largest eigenvalue of a Gaussian β random matrix.*

Now, given a generic density Λ with unit mass, we write $\Lambda = (\Lambda - \Lambda_{\rm sc}) + \Lambda_{\rm sc}$, and insert this into the electrostatic energy function $\mathcal{E}(\Lambda)$ to get

$$\mathcal{E}(\Lambda) - \mathcal{E}(\Lambda_{\rm sc}) = \frac{1}{2} J(\Lambda) + \int_{\mathbb{R}} \mathrm{d}\lambda \Big(\Lambda(\lambda) - \Lambda_{\rm sc}(\lambda) \Big) \left(\frac{\lambda^2}{4} - \int_{\mathbb{R}} \mathrm{d}\lambda' \log|\lambda - \lambda'| \Lambda_{\rm sc}(\lambda') \right), \tag{10.3.5}$$

where $J(\Lambda) = -\iint_{\mathbb{R}^2} \log|\lambda_1 - \lambda_2| \prod_{i=1}^{2} \mathrm{d}\lambda_i (\Lambda(\lambda_i) - \Lambda_{\rm sc}(\lambda_i))$. We may substitute (10.3.3) into the last term above. Recall that we normalized the empirical measure Λ_N so as to have total mass 1, which implies $\int_{\mathbb{R}} \mathrm{d}\lambda (\Lambda(\lambda) - \Lambda_{\rm sc}(\lambda)) = 0$. Thus, the constant in (10.3.3) does not contribute after integrating over λ. From these considerations we obtain

$$I_\beta(\Lambda) = \beta(\mathcal{E}(\Lambda) - \mathcal{E}(\Lambda_{\rm sc})) = \frac{\beta}{2} J(\Lambda) + \frac{\beta}{2} \int_{\mathbb{R}} \mathrm{d}\lambda\, V(\lambda) \Lambda(\lambda). \tag{10.3.6}$$

Note that in deriving this, we have also used the fact that Eq. (10.3.6) indeed vanishes for $\Lambda = \Lambda_{\rm sc}$ (since the potential $V(\lambda) = 0$ on the support $[-2,2]$ of $\Lambda_{\rm sc}$). We now may consider the edge limit of the spectrum.

[11] For consistency and to avoid further headaches, we shall keep the letter a for the Airy point process (i.e. the right edge of the semi-circle) and the letter b for the space-reversed process (i.e. the left edge of the semi-circle).

In accordance with earlier work of Dean and Majumdar in Refs. [192,248], it is more convenient to work with the space-reversed Airy point process which arises as a scaling limit of the Gaussian β random matrices spectrum near its lower edge $\lambda = -2$. To relate the GβE large deviation principle to the Airy$_\beta$ point process large deviation principle, we introduce the scaling $\lambda = -2+t^{2/3}N^{-2/3}b$ with an extra parameter $t > 0$. In the $N \to \infty$ limit, the change of measure should read (recalling the definition of ρ in Eq. (10.2.8))

$$N \mathrm{d}\lambda \, \Lambda_N(\lambda) \simeq t \mathrm{d}b \, \rho(b) \tag{10.3.7}$$

Inserting this ansatz in large deviation function of Eq. (10.3.6), we find

$$\begin{aligned} \frac{2}{\beta} N^2 I_\beta(\Lambda) \simeq & - t^2 \iint_{\mathbb{R}^2} \log|b_1 - b_2| \prod_{i=1}^{2} \mathrm{d}b_i \left(\rho(b_i) - t^{-1/3} N^{1/3} \Lambda_{\mathrm{sc}}(-2 + t^{2/3} N^{-2/3} b_i) \right) \\ & - t^2 \int_{\mathbb{R}} \mathrm{d}b \, \rho(b) t^{-1} N V(-2 + t^{2/3} N^{-2/3} b_i). \end{aligned} \tag{10.3.8}$$

Taking $N \to \infty$ on the r.h.s., with t fixed, we obtain the Airy$_\beta$ point process large deviation rate function $I_{\mathrm{Ai}}(\rho) = J_{\mathrm{Ai}}(\rho) + U(\rho)$, where the two contributions are given by

$$\begin{aligned} J_{\mathrm{Ai}}(\rho) &= - \iint_{\mathbb{R}^2} \log|b_1 - b_2| \prod_{i=1}^{2} \mathrm{d}b_i \Big[\rho(b_i) - \rho_{\mathrm{Ai}}(b_i) \Big], \\ U(\rho) &= \frac{4}{3} \int_{-\infty}^{0} \mathrm{d}b \, |b|^{\frac{3}{2}} \rho(b), \\ \rho_{\mathrm{Ai}}(b) &= \frac{\sqrt{b}}{\pi} \mathbb{1}_{\{b>0\}}. \end{aligned} \tag{10.3.9}$$

Remark 10.3.2. *A crucial assumption is that the mass-conservation* $\int_{\mathbb{R}} \mathrm{d}b \, (\rho(b) - \rho_{\mathrm{Ai}}(b)) = 0$ *is still verified after having taken the large* N *limit for any candidate* ρ*.*

We therefore conclude that the empirical density ρ enjoys a large deviation principle, so that for a given density function μ, in the large t limit, $\mathbb{P}(\rho \approx \mu) \approx \exp(-t^2 \frac{\beta}{2} I_{\mathrm{Ai}}(\mu))$. We observe that the rate of the large deviations is now t^2 rather N^2 which has the following interpretation: the magnitude of macroscopic large deviations is of order N^2 because they involve the interactions between $\sim N^2$ pairs of particles (hence roughly N particles are involved in the fluctuations). The rate t^2 hence means that the number of points in the Airy$_\beta$ process involved in the microscopic large deviations is of order t.

The Airy density ρ_{Ai} is the equilibrium density at the *left* edge of the semi-circle. Let us take a moment to interpret the functional $U(\rho)$ in Eq. (10.3.9). At equilibrium, the density has support on $\mathbb{R}_+$ and hence, $U(\rho_{\mathrm{Ai}}) = 0$. If we perturb the edge of the Coulomb gas out of equilibrium, then two different situations arise. If we decide to compress the gas so that the support ρ is strictly included in $\mathbb{R}_+$, then $U(\rho)$ will still have a zero contribution. On the contrary, if we decide to expand the gas so that ρ has a support with a non-zero intersection with $\mathbb{R}_-$, then the functional $U(\rho)$ will play a role. In the rest of this Thesis, we will be interested in the former situation to which we now refer to as the *pushed* Coulomb gas.

Chapter 11

The four tales of the one tail: solving the linear statistics at the edge

In this Chapter, we will solve the linear statistics problem at the edge of Gaussian β random matrices by the means of four methods and we will closely follow our work from Ref. [4]. The problem is non-trivial since at the edge of the spectrum of a random matrix, fluctuations are stronger and much fewer results exist [213]. For the classical random matrix ensembles, an array of methods exists to study spectral correlations [104, 105, 120, 121], such as the Coulomb gas, resolvant, orthogonal polynomials, Selberg integrals, determinantal processes, Painlevé equations, the Dimitriu-Edelman tridiagonal representation [153] and the stochastic operators [155,267,268]. These methods however often appear disconnected but in this Chapter we unveil relations between some of them, valid at the edge. The quantity of interest for the linear statistics at the edge is $Q_t(u)$ expressed as follows

$$Q_t(u) = \mathbb{E}\left[\exp\left(-t\sum_{i=1}^{\infty}\phi(t^{-2/3}a_i + u)\right)\right] \tag{11.0.1}$$

where the set $\{a_i\}$ forms the Airy β point process. The linear statistics considered are for positive and increasing functions ϕ which vanish for negative argument. This amounts to study a Coulomb gas *delicately* pushed at its edge. For further purpose, we shall also recall the shorthand notation

$$\mathsf{L} = t\sum_{i=1}^{\infty}\phi(t^{-2/3}a_i + u)\ . \tag{11.0.2}$$

11.1 From the cumulants of the linear statistics to the free energy

In this Section, we study the linear statistics from the point of view of a cumulant expansion following Refs. [4, 5]. Although initially introduced for the GUE ($\beta = 2$), we have been able to extrapolate the large-time cumulants for any β ensemble. From our work on the cumulants of the Airy point process for $\beta = 2$ [4, 5], we have determined that at large t all cumulants have a dominant term of order t^2

$$\log \mathbb{E}_\beta[e^{-\mathsf{L}}] = \sum_{n\geqslant 1}\frac{(-1)^n}{n!}\mathbb{E}_\beta[\mathsf{L}^n]^c \simeq -t^2\Sigma_\phi(u) \tag{11.1.1}$$

From Eq. (9.3.20) for $\beta = 2$ and from the extension to any β found in [4], identifying order by order we obtain

$$\mathbb{E}_\beta[\mathsf{L}^n]^c = (-1)^n\kappa_n \simeq \frac{\beta}{4}t^2\left(\frac{4}{\beta\pi}\right)^n\partial_u^{n-3}f(u)^n \tag{11.1.2}$$

The function f relates to the potential ϕ as follows

$$f(u) = \frac{1}{2}\int_0^{+\infty} \frac{\mathrm{d}b}{\sqrt{b}}\phi'(u-b). \tag{11.1.3}$$

Note that for soft monomial walls the function f is positive and vanishes for negative arguments $f(u \leqslant 0) = 0$. It is possible and convenient to perform the summation of the series representation of Σ_ϕ by writing its third derivative as

$$\Sigma_\phi'''(u) = -\frac{\beta}{4}\sum_{n\geqslant 1}\frac{1}{n!}(-\frac{4}{\beta\pi})^n(\partial_u)^n f(u)^n \tag{11.1.4}$$

To proceed to the summation, we use a Mellin-Barnes summation method presented in the Appendix B.1, and displayed in Eq. (B.1) with $a = -\frac{4}{\beta\pi}$ and $\Sigma_\phi'''(u) = -\frac{\beta}{4}\mathcal{S}(u)$. The summation requires solving the following equation for $w = w(u)$

$$f(u - \frac{4}{\beta\pi}w) = w \tag{11.1.5}$$

In the context of monomial soft walls, the function f is positive, increasing and vanishes for negative argument hence w is also positive. This ensures that there is a unique solution of Eq. (11.1.5) which can be written

$$u := u(w) = f^{-1}(w) + \frac{4}{\beta\pi}w, \quad \forall w > 0, \quad \text{and } u(0) = 0 \tag{11.1.6}$$

It is convenient to extend w and u to negative values setting $u(w \leqslant 0) = 0$ and $w(u \leqslant 0) = 0$. Given the uniqueness, from Eq. (B.1) and (B.9) in the Appendix, Σ_ϕ''' is given by

$$\Sigma_\phi'''(u) = \frac{1}{\pi}w'(u) \tag{11.1.7}$$

To obtain back Σ_ϕ, we perform successive integrations, using that for $u \to -\infty$ the Coulomb gas is not affected by the wall and hence $\Sigma_\phi(u)$ and its derivatives should vanish. For monomial soft walls, both f and w vanish for $u \leqslant 0$, so we can even use that $\Sigma(0) = \Sigma'(0) = \Sigma''(0) = 0$. The successive integrations of Σ_ϕ''' give the following result.

Result 11.1.1 (*Free energy from the cumulant method*)

The large deviation function Σ_ϕ obtained by the cumulant method reads

$$\Sigma_\phi(u) = \frac{1}{2\pi}\int_0^{w(u)} \mathrm{d}w' \left[u - u(w')\right]^2 = \frac{1}{\pi}\int_0^u \mathrm{d}u'\, w(u')\left[u - u'\right] \tag{11.1.8}$$

where $u(w)$ is given in Eq. (11.1.6).

The forms as integrals in w' are quite useful in practice when $f^{-1}(w)$ has a simple form, since $u(w)$ is then explicit using (11.1.6) and the integral can often be calculated. The second form allows easy comparison with the other methods we will subsequently present in this Chapter. Having understood how to obtain the large deviation function through the cumulant expansion, we now turn to the second method which deals with a semi-classical WKB treatment of the Stochastic Airy Operator.

11.2 A WKB semi-classical density of states for the Stochastic Airy Operator

The second tale of the linear statistics relies on the Stochastic Airy Operator (SAO) [267] and is an extension of the method introduced by Tsai for the late-time Kardar-Parisi-Zhang problem in

Ref. [238]. It is known [155] that the Airy point process $\{a_i\}$ can be generated as $-a_i = \varepsilon_i$ where ε_i are the eigenvalues of the following Schrödinger problem on the half-line $y > 0$, defined by the Hamiltonian

$$\mathcal{H}_{\rm SAO} = -\partial_y^2 + y + \frac{2}{\sqrt{\beta}} V(y) \tag{11.2.1}$$

where $V(y)$ is a unit white noise and the wave functions vanish at $y = 0$. Since we are interested in energy levels of order $t^{2/3}$ we can rescale $y = t^{2/3}x$, $V(y) = t^{2/3}\frac{\sqrt{\beta}}{2}v(x)$, $\mathcal{H}'_{\rm SAO} = t^{-2/3}\mathcal{H}_{\rm SAO}$ with energy levels $b_i = t^{-2/3}\varepsilon_i = -t^{-2/3}a_i$ and obtain

$$\mathcal{H}'_{\rm SAO} = -t^{-2}\partial_x^2 + x + v(x) \tag{11.2.2}$$

This corresponds to a Schrödinger problem on the half-line $x > 0$ for a particle of mass $m = 1/2$ with $\hbar = 1/t$. At $\hbar \to 0$ in the large-time limit, we can treat the Hamiltonian $\mathcal{H}'_{\rm SAO}$ using a semi-classical Wentzel-Kramer-Brilloin (WKB) approach.

In particular, we use the standard WKB argument [269, 270] which we state in its generality to obtain the semi-classical density of states associated to a Schrödinger Hamiltonian describing a quantum particle of mass m in a potential $W(x)$ in one dimension

$$\mathcal{H}(p,x) = \frac{p^2}{2m} + W(x) \quad , \quad p = \frac{\hbar}{i}\partial_x \tag{11.2.3}$$

One considers classical periodic trajectories between two consecutive turning points $x_\pm$ where the classical momentum $p(x) = \sqrt{2m(E - W(x))}$ vanishes. In the limit of small $\hbar$, or for high energy levels, the quantification condition for the n-th level becomes well approximated by $\int_{x_-}^{x_+} \mathrm{d}x\, p(x) = \pi n\hbar$. Hence the integrated density of states, i.e. the number of levels below the energy E reads

$$N(E) = \frac{1}{\hbar\pi}\int \mathrm{d}x \sqrt{2m(E - W(x))} \tag{11.2.4}$$

Taking $\mathcal{H} = \mathcal{H}'_{SAO}$, which corresponds to $W(x) = x + v(x)$, $m = 1/2$, $E = b$ and $\hbar = 1/t$, we can apply for large t this WKB estimate for the density of energy levels of (11.2.2), $\hat\rho(b) = \sum_i \delta(b - b_i)$ as $\hat\rho(b) \simeq t\rho(b)$ with

$$\rho(b) = \frac{1}{\pi}\frac{\mathrm{d}}{\mathrm{d}b}\int_0^{+\infty} \mathrm{d}x \sqrt{(b - x - v(x))_+}. \tag{11.2.5}$$

In the present case there is an infinite barrier at $x = 0$, hence $x_- = 0$ and x_+ denotes the first turning point.

The linear statistics is an average over the Airy Point Process and can also be interpreted as an average over the white noise of the SAO $V(y)$

$$Q_t(u) = \int \mathcal{D}V\, e^{-t\sum_{i=1}^{+\infty}\phi(-t^{-2/3}a_i(V)+u) - \frac{1}{2}\int \mathrm{d}y\, V(y)^2} \tag{11.2.6}$$

where $a_i(V) = -\varepsilon_i(V)$ and $\varepsilon_i(V)$ denote the eigen-energies in the potential V. Under the proposed rescaling adapted to the WKB method, the measure of the white noise rescales to

$$e^{-\frac{1}{2}\int \mathrm{d}y\, V(y)^2} = e^{-\frac{\beta}{8}t^2\int \mathrm{d}x v(x)^2}. \tag{11.2.7}$$

Since the linear statistics is itself proportional to t^2 and the measure of the rescaled white noise is also proportional to t^2, the large t limit allows to obtain $\Sigma_\phi(u)$ as the solution of the following variational problem for $x > 0$

$$\Sigma_\phi(u) = \min_{v(x)}\Big[\int_{\mathbb{R}} \mathrm{d}b\, \rho(b)\phi(u - b) + \frac{\beta}{8}\int_0^{+\infty} \mathrm{d}x\, v(x)^2\Big] \tag{11.2.8}$$

where $\rho(b)$ is defined in Eq. (11.2.5). This approach was made rigorous in the case $\phi_{\rm KPZ} = (x)_+$ in Ref. [238] using explosions in the Riccati formulation of the SAO.

Remark 11.2.1. *The highly surprising, and quite non-trivial point is that the WKB method can be a useful approximation despite the fact that the typical $v(x)$ is a white noise hence not at all smooth. One way to understand it is to remember that the approximation is used for describing the optimal $v(x)$ (or near optimal one) which by contrast is smooth.*

The expression of $\Sigma_\phi(u)$ taken at the saddle point expression is now

$$\Sigma_\phi(u) = \int_{\mathbb{R}} \mathrm{d}b\, \rho_*(b)\phi(u-b) + \frac{\beta}{8}\int_0^{+\infty} \mathrm{d}x\, v_*(x)^2 \tag{11.2.9}$$

where $v_*(x)$ is the solution of the saddle point SP1 and $\rho_*(b)$ is the optimal density

$$\frac{\beta}{4}v_*(x) = \frac{1}{2\pi}\int_0^{+\infty} \frac{\mathrm{d}b}{\sqrt{b}}\phi'(u-b-x-v_*(x)) \quad , \quad \rho_*(b) = \frac{1}{2\pi}\int_0^{+\infty} \mathrm{d}x\, \frac{1}{\sqrt{(b-x-v_*(x))_+}} \tag{11.2.10}$$

By simple manipulations, one can find a virial identity at the saddle point of the SAO method which reads

$$\int_{\mathbb{R}} \mathrm{d}b\, \rho_*(b)\phi(u-b) = \frac{\beta}{4}\int_0^{+\infty} \mathrm{d}x \left(x v_*(x) - \frac{v_*(x)^2}{2}\right) \tag{11.2.11}$$

Combining the virial identity with the expression of the free energy at the optimum (11.2.8) provides a simple expression for Σ_ϕ presented in the following result.

Result 11.2.2 (*Free energy simplified at the saddle point of the SAO*)

The large deviation function Σ_ϕ obtained by the Stochastic Airy Operator method reads

$$\Sigma_\phi(u) = \frac{\beta}{4}\int_0^{+\infty} \mathrm{d}x\, x v_*(x) \tag{11.2.12}$$

11.2.1 From the Stochastic Airy Operator back to the cumulant expansion

As an intermediate step of our presentation, we now relate the two first tales, i.e. the cumulant expansion and the Stochastic Airy Operator method. The saddle point of the SAO (11.2.10) can be expressed in terms of the function f (11.1.3) as

$$\frac{\beta}{4}v_*(x) = \frac{1}{2\pi}\int_{\mathbb{R}} \frac{\mathrm{d}b}{\sqrt{(b)_+}}\phi'(u-b-x-v_*(x)) = \frac{1}{\pi}f(u-x-v_*(x)) \tag{11.2.13}$$

To make contact with the method of cumulants, we study a solution $v_*(x)$ which has the form

$$v_*(x) = \frac{4}{\beta\pi}w(u-x), \qquad 0 \leqslant x \leqslant u \tag{11.2.14}$$

with $v_*(x) = 0$ for $x \geqslant u$. With this parametrization, the saddle point equation becomes

$$f(u - \frac{4}{\beta\pi}w(u)) = w(u) \tag{11.2.15}$$

This is precisely the equation (11.1.5) encountered in the resummation of the series in the cumulant method. In addition, using this parametrization, the resulting equation for $\Sigma_\phi(u)$ within the SAO method Eq. (11.2.12) reads

$$\Sigma_\phi(u) = \frac{\beta}{4}\int_0^{+\infty} \mathrm{d}x\, x\, v_*(x) = \frac{1}{\pi}\int_0^u \mathrm{d}u' w(u')[u-u'] \tag{11.2.16}$$

This identifies with the Result 11.1.1 from the cumulant method. We now derive through the SAO method the series expansion previously obtained from the cumulant method: this is realized by the means of the Lagrange inversion formula which we recall.

Lemma 11.2.3 (*Lagrange inversion formula*)

The Lagrange inversion formula states that for a sufficiently nice function f, the equation $z = x + yf(z)$ can be inverted as

$$z = x + \sum_{n\geqslant 1} \frac{y^n}{n!} (\partial_x)^{n-1} f(x)^n \tag{11.2.17}$$

The identification

$$x = u, \quad z = u - \frac{4}{\beta\pi} w, \quad y = -\frac{4}{\beta\pi} \tag{11.2.18}$$

leads to a series representation for the solution $w(u)$ of Eq. (11.2.15)

$$-\frac{4}{\beta\pi} w(u) = \sum_{n\geqslant 1} \frac{1}{n!} (-\frac{4}{\beta\pi})^n \partial_u^{n-1} f(u)^n \tag{11.2.19}$$

From Eq. (11.2.16), we also have $\Sigma''_\phi(u) = \frac{1}{\pi} w(u)$ and hence we obtain

$$\Sigma''_\phi(u) = -\frac{\beta}{4} \sum_{n\geqslant 1} \frac{1}{n!} (-\frac{4}{\beta\pi})^n \partial_u^{n-1} f(u)^n \tag{11.2.20}$$

which coincides precisely with the second derivative of the series expansion obtained for the cumulant method.

11.2.2 Optimal density from the semi-classical Stochastic Airy Operator point of view

We now derive an explicit formula for the optimal density obtained by the SAO method. Let us start from the correspondence between the saddle points of the SAO and the cumulant methods: $v_*(x) = \frac{4}{\beta\pi} w(u-x)$ for $0 \leqslant x \leqslant u$ and $v_*(x) = 0$ for $x \geqslant u$. Then the WKB semi-classical density of states at the optimal v_* reads

$$\rho_*(b) = \frac{1}{2\pi} \int_0^{+\infty} \frac{\mathrm{d}x}{\sqrt{(b - x - v_*(x))_+}} = \frac{1}{2\pi} \int_0^u \frac{\mathrm{d}u'}{\sqrt{(b - u + u' - \frac{4}{\beta\pi} w(u'))_+}} + \frac{\sqrt{(b-u)_+}}{\pi} \tag{11.2.21}$$

Using the saddle point SP1 or equivalently the functional relation verified by w: $f(u' - \frac{4}{\beta\pi} w(u')) = w(u')$, we have found in Ref. [4] that the optimal density can be factorized in a simple and compact form.

Result 11.2.4 (*Optimal density of state for the linear statistics problem at the edge*)

The optimal density obtained through the WKB approximation on the Stochastic Airy Operator for the linear statistics problem reads

$$\rho_*(b) = \frac{\sqrt{(b - \frac{4}{\beta\pi} w(u))_+}}{\pi} \left[1 + \frac{1}{\beta\pi} \fint_{\mathbb{R}} \frac{\mathrm{d}b'}{b + b' - u} \frac{\phi'(b')}{\sqrt{(u - \frac{4}{\beta\pi} w(u) - b')_+}} \right] \tag{11.2.22}$$

In particular, the edge of the support can be identified easily as

$$u_0 = \frac{4}{\beta\pi} w(u) \tag{11.2.23}$$

Remark 11.2.5. *Using this result, we have shown in Ref. [4] that for fixed u, in the large b limit, one recovers the density of the Airy process, i.e. the edge limit of the semi-circle density. More precisely, we have controlled the difference between the optimal density ρ_* and the Airy density $\rho_{\rm Ai}$, i.e.*

$$\rho_*(b) - \rho_{\rm Ai}(b) \underset{b\gg 1}{=} \mathcal{O}(\frac{1}{b^{3/2}}) \tag{11.2.24}$$

As both densities behave asymptotically as the semi-circle, i.e. $\rho(b) = \mathcal{O}(\sqrt{b})$, it is not trivial to see that the difference between the optimal density and the Airy one is of order $1/b^{3/2}$ and not $1/b^{1/2}$.

We now turn to the third tale of the linear statistics which is the story of the Electrostatic Coulomb gas, originally introduced in the context of the late-time KPZ dynamics in Ref. [7] and extended to linear statistics at the edge in Ref. [4].

11.3 Electrostatic Coulomb gas approach to the linear statistics

In Section 10.3, we have determined the measure of the Coulomb gas at the edge which we shall use to express our linear statistics: this constitutes the third tale. Indeed from Eqs. (10.3.8) and (10.3.9), the linear statistics is written as

$$\mathbb{E}\left[\exp\left(-t\sum_{i=1}^{\infty}\phi(t^{-2/3}a_i+u)\right)\right] \asymp \int \mathcal{D}\rho\ \exp\Big(-t^2[\int_{\mathbb{R}} \mathrm{d}b\,\rho(b)\phi(u-b) + \mathcal{J}(\rho) + U(\rho)]\Big) \tag{11.3.1}$$

where $\mathcal{J}(\rho) = -\frac{\beta}{2}\iint_{\mathbb{R}^2}\log|b_1-b_2|\prod_{i=1}^2 \mathrm{d}b_i(\rho(b_i)-\rho_{\rm Ai}(b_i))$ and $U(\rho)$ is irrelevant for our linear statistics problem as we study a pushed phase ($U(\rho)$ is relevant solely for a pulled gas). The free energy is then obtained readily as

$$\Sigma_\phi(u) = \min_\rho\Big[\int_{\mathbb{R}}\mathrm{d}b\,\rho(b)\phi(u-b) + \mathcal{J}(\rho)\Big] \tag{11.3.2}$$

The optimal density $\rho^*(b)$ is then the unique solution[12] of the variational equation

$$\phi(u-b) - \beta\int_{\mathbb{R}}\mathrm{d}b'\log|b-b'|(\rho_*(b')-\rho_{\rm Ai}(b')) \geqslant c \tag{11.3.3}$$

for some real c, with equality on the support of ρ^*. The derivative of Eq. (11.3.3) on the support of the density provides a saddle point SP2. The Coulomb gas problem is usually solved through the use of the Tricomi theorem but here we shall completely bypass this approach by unveiling a connection between the Coulomb gas and the Stochastic Airy Operator method. Indeed, comparing the variational formulation of the free energy Σ_ϕ for the SAO (Eq. (11.2.8)) and the Coulomb gas (Eq. (11.3.2)) methods, there should exist a mapping to relate the following objects

$$-\frac{\beta}{2}\iint_{\mathbb{R}^2}\log|b_1-b_2|\prod_{i=1}^2\mathrm{d}b_i(\rho(b_i)-\rho_{\rm Ai}(b_i)) \quad\longleftrightarrow\quad \frac{\beta}{8}\int_0^{+\infty}\mathrm{d}x\,v(x)^2 \tag{11.3.4}$$

We have found in Ref. [4] a general parametrization of the density ρ which relates the two objects and we now present it.

[12] See Theorem 2.6.1, Lemma 2.6. from Ref. [164].

11.3.1 Reparametrization of the Coulomb gas

The Stochastic Airy Operator method suggests to study a parametrization of the density $\rho(b)$ of a Coulomb gas in terms of a function $v(x)$ for $x > 0$ as

$$\rho(b) = \frac{1}{2\pi} \int_0^{+\infty} \mathrm{d}x \, \frac{1}{\sqrt{(b - x - v(x))_+}} \tag{11.3.5}$$

where $v(x)$ encodes the deviation from the Airy density which is recovered for $v(x) = 0$.

$$\rho_{\mathrm{Ai}}(b) = \frac{\sqrt{(b)_+}}{\pi} = \frac{1}{2\pi} \int_0^{+\infty} \mathrm{d}x \, \frac{1}{\sqrt{(b - x)_+}} \tag{11.3.6}$$

Remark 11.3.1. *At this stage, nothing is assumed on the function v, in particular, we do not assume that it is a saddle point: it is completely arbitrary!*

Remark 11.3.2. *This parametrization of the density verifies the bare condition of mass conservation* $\int_{\mathbb{R}} \mathrm{d}b(\rho(b) - \rho_{\mathrm{Ai}}(b)) = 0$

The extraordinary property of this change of variable is that the electrostatic energy of the Coulomb gas adopts the remarkably simple representation in terms of the above function v.

Result 11.3.3 (*Parametrization of the logarithmic energy of the Coulomb gas*)

Under the parametrization of Eq. (11.3.5), the logarithmic energy of the Coulomb gas is equal to the quadratic energy of a white noise.

$$\mathcal{J}(\rho) = -\frac{\beta}{2} \iint_{\mathbb{R}^2} \log|b_1 - b_2| \prod_{i=1}^{2} \mathrm{d}b_i(\rho(b_i) - \rho_{Ai}(b_i)) = \frac{\beta}{8} \int_0^{+\infty} \mathrm{d}x \, v(x)^2 \tag{11.3.7}$$

This equality precisely identifies the Brownian weight in the SAO method. It is valid under some mild assumptions on v (see Ref. [4]). In particular it does not assume any saddle point property of v, hence the scope of this mapping is much more general than what we use it for.

We proved in Ref. [4] that if one chooses the optimal v_* in the reparametrization of the Coulomb gas density, then for all b in $\mathbb{R}$, the following inequality holds

$$\phi(u - b) - \beta \int_{\mathbb{R}} \mathrm{d}b' \, \log\left|b - b'\right| (\rho_*(b') - \rho_{\mathrm{Ai}}(b')) \geqslant 0 \tag{11.3.8}$$

which turns to be an equality in the support of the optimal density ρ_*, i.e. $b \in [u_0, +\infty[$. As we have mapped the Coulomb gas problem to the Stochastic Airy Operator method, we fully rely on the results obtained through the latter which concludes this Section on the electrostatic approach. It would be of utter importance to have a more in-depth understanding of this mapping and to determine whether it holds in the bulk of the spectrum as well and whether it holds for tridiagonal random matrices of finite size. We now turn to the fourth and final method able to investigate the linear statistics at the edge of GUE matrices: the semi-classical treatment of the non-local Painlevé II equation.

11.4 A WKB approximation for the Painlevé II representation of the linear statistics

The fourth and last method we present in this Section was first introduced in the context of the large deviations in [187], (based on [75]) and later pushed much further in [239] to study the

late-time behavior of the solution to the KPZ equation for droplet initial condition. It was then extended in Ref. [4] for the purpose of linear statistics at the edge of GUE random matrices (this method applies solely for $\beta = 2$). For $\beta = 2$ the set $\{a_i\}$ forms the usual Airy point process and one rewrites the linear statistics

$$Q_t(u) = \mathbb{E}\left[\exp\left(-t\sum_{i=1}^{\infty}\phi(t^{-2/3}a_i + u)\right)\right] \tag{11.4.1}$$

for all t as a Fredholm determinant $Q_t(u) = \mathrm{Det}[I - \sigma_t K_{\mathrm{Ai}}]$ where $\sigma_t(a) = 1 - e^{-t\phi(u+t^{-2/3}a)}$ and K_{Ai} is the standard Airy kernel. This Fredholm determinant was shown in Ref. [75] to obey the following equation, with $s = -ut^{2/3}$

$$\log Q_t(u) = \int_s^{+\infty} \mathrm{d}r(s-r)\Psi_t(r) \tag{11.4.2}$$

$$\Psi_t(r) = -\int_{\mathbb{R}} \mathrm{d}v(q_t(r,v))^2 \frac{\mathrm{d}}{\mathrm{d}v} e^{-t\phi(vt^{-2/3})} \tag{11.4.3}$$

$$\partial_r^2 q_t(r,v) = [v + r + 2\Psi_t(r)]q_t(r,v) \tag{11.4.4}$$

with $q_t(r,v) \simeq_{r\to+\infty} \mathrm{Ai}(r+v)$. Let us recall here the analysis of Ref. [239] to treat the problem and present its generalization. To make it easier we stick to the notations of Ref. [239]. Starting from Eqs. (11.4.2) we introduce as in Ref. [239] the scaled variables $r = t^{2/3}X$, $v = t^{2/3}V$ and make the ansatz

$$q_t(r,v) = t^{-1/6}\tilde{q}_t(X,V), \qquad \Psi_t(r) = t^{2/3}g_t(X), \tag{11.4.5}$$

with $g_t(X) > 0$. The remarkable fact is that the function $g_t(X)$ becomes independent of t at large t, and one denotes $g(X) = \lim_{t\to+\infty} g_t(X)$. Performing the large-time rescaling, the second equation in (11.4.2) becomes

$$g(X) = \int_{\mathbb{R}} \mathrm{d}V[\tilde{q}_t(X,V)]^2\phi'(V)e^{-t\phi(V)}. \tag{11.4.6}$$

The condition that the r.h.s. of Eq. (11.4.6) does not eventually depend on t at large t will lead to two stationary equations SP1 and SP2 which we will obtain in Eq. (11.4.12). To obtain these equations, let us first perform the large-time rescaling, under which the third equation of (11.4.2) becomes

$$-t^{-2}\partial_X^2\tilde{q}_t(X,V) + (V + X + 2g(X))\tilde{q}_t(X,V) = 0 \tag{11.4.7}$$

with the boundary condition $\tilde{q}_t(X,V) \to_{X\to+\infty} t^{1/6}\mathrm{Ai}(t(X+V)) \simeq \frac{\exp(-\frac{2}{3}t(X+V)^{3/2})}{2\sqrt{\pi}(X+V)^{1/4}}$.

Remark 11.4.1. *This boundary condition implies the condition $\phi(+\infty) = +\infty$. If this is not the case, e.g. $\phi(+\infty) = \phi_\infty < \infty$ then the boundary condition becomes $\tilde{q}_t(X,V) \to_{X\to+\infty} t^{1/6}\sqrt{1-e^{-t\phi_\infty}}\mathrm{Ai}(t(X+V))$, see Ref. [60], hence generalizing Proposition 5.2 of Ref. [75].*

Equation (11.4.7) can be interpreted as the Schrödinger equation of a quantum particle of mass $m = 1/2$ at energy $-V$ in the potential $X + 2g(X)$, in the semi-classical limit since $\hbar = 1/t$ is small. As in Ref [239] we consider cases such that $g(X)$ is a positive and monotonic decreasing function, and, as seen below, $g(X)$ vanishes for $X > 0$. The potential $X + 2g(X)$ is however an increasing function of X. Hence there is a unique classical turning point at $X = a$ with $V + a + 2g(a) = 0$. The classical momentum of the particle is $p(X,V) = \sqrt{-V - X - 2g(X)}$, which is positive in the the classically allowed region $X < a$, and imaginary for $X > a$, the forbidden region. The standard WKB method then gives the following approximation of the

wave function for large t

$$\tilde{q}_t(X,V) \simeq \frac{C_t(V)}{|V+X+2g(X)|^{1/4}}\Bigg(\cos\left[t\int_{-\infty}^{X}\mathrm{d}X'\sqrt{(-V-X'-2g(X'))_+}-\frac{\pi}{4}\right]\Theta(-V-X-2g(X)) \\ +\frac{1}{2}\exp\Big[-t\int_{-\infty}^{X}\mathrm{d}X'\sqrt{(V+X'+2g(X'))_+}\Big]\,\Theta(V+X+2g(X))\Bigg) \tag{11.4.8}$$

The boundary condition determines the amplitude $C_t(V)$ as

$$C_t(V)=\frac{1}{\sqrt{\pi}}\exp\left(t\int_{\mathbb{R}}\mathrm{d}X'\Big[\sqrt{(V+X'+2g(X'))_+}-\sqrt{(V+X')_+}\Big]\right) \tag{11.4.9}$$

Inserting $\tilde{q}_t(X,V)$ into Eq. (11.4.6) we obtain a sum of two contributions

$$g(X)=\int_{\mathbb{R}}\mathrm{d}V\frac{C_t(V)^2\phi'(V)e^{-t\phi(V)}}{|V+X+2g(X)|^{1/2}} \\ \left(\frac{\Theta(-V-X-2g(X))}{2}+\frac{\Theta(V+X+2g(X))}{4}e^{-2t\int_{-\infty}^{X}\mathrm{d}X'\sqrt{(V+X'+2g(X'))_+}}\right) \tag{11.4.10}$$

The second term can be neglected at large t compared to the first (see Ref. [239] for more discussion of the validity of the WKB approximations) leading to

$$g(X)=\frac{1}{2\pi}\int_{-\infty}^{-X-2g(X)}\frac{\mathrm{d}V\phi'(V)}{\sqrt{-V-X-2g(X)}} \\ \exp\left(t\Big(2\int_{\mathbb{R}}\mathrm{d}X'[\sqrt{(V+X'+2g(X'))_+}-\sqrt{(V+X')_+}]-\phi(V)\Big)\right) \tag{11.4.11}$$

The condition of t independence gives two equations SP1 and SP2 that have to be solved simultaneously

$$g(X)=\frac{1}{2\pi}\int_{-\infty}^{-X-2g(X)}\frac{\mathrm{d}V\phi'(V)}{\sqrt{-V-X-2g(X)}} \tag{11.4.12}$$

$$\phi(V)=2\int_{\mathbb{R}}\mathrm{d}X'\left[\sqrt{(V+X'+2g(X'))_+}-\sqrt{(V+X')_+}\right] \tag{11.4.13}$$

Remark 11.4.2. *The authors of Ref. [239] qualified the compatibility of these two equations for the late-time KPZ problem as a "miracle". In Ref. [4], we explained and proved this compatibility and showed that the two equations were in fact the saddle points of the SAO and the Coulomb gas methods upon the identification* $w(X)=\frac{\beta\pi}{2}g(-X)$.

We shall suppose that ϕ is increasing $\phi'(V)\geqslant 0$ and strictly vanishes for all $V<0$, hence one finds that $g(X)\geqslant 0$ with $g(X)=0$ for $X>0$. Hence the upper bound of the integral in the second equation of (11.4.12) can be chosen to be $X'=0$. Finally, performing the large-time rescaling in the first equation of (11.4.2) and introducing the excess energy Σ_ϕ leads to the following result.

Result 11.4.3 (*Free energy from the analysis of the Painlevé equation*)

The large deviation function Σ_ϕ *obtained by the WKB analysis of the Painlevé equation reads*

$$\Sigma_\phi(u)=\int_{-u}^{0}\mathrm{d}X(u+X)g(X). \tag{11.4.14}$$

By consistency with the other methods, see Ref. [4], the formula for general β is obtained by multiplying the r.h.s of (11.4.14) by $\beta/2$ and by replacing the potential ϕ in Eqs. (11.4.12) by $2\phi/\beta$.

The stationary equations being identified to the saddle point equations of the SAO and Coulomb gas methods, we finally rely on the solutions obtained through the first three methods to conclude. This method based on the Painlevé representation of the linear statistics for $\beta = 2$ was proved to be extremely useful for the developments of this Thesis. Indeed, as the saddle points of all methods appeared simultaneously this provided the first hints of their equivalence.

Brief summary of the results

So far we have introduced four methods to solve the linear statistics problem at the edge: each method has its own saddle points. For clarity we briefly provide a dictionary between the different variables introduced. The saddle points of the different methods are related as

$$\forall x \geqslant 0, \quad v_*(x) = \frac{4}{\beta\pi} w(u-x) = 2g(x-u). \tag{11.4.15}$$

The different variables vanish for

$$v_*(x \leqslant u) = 0, \qquad w(u \leqslant 0) = 0, \qquad g(X \geqslant 0) = 0. \tag{11.4.16}$$

The lower edge of the support of the perturbed Airy gas is

$$u_0 = \frac{4}{\beta\pi} w(u) = v_*(0). \tag{11.4.17}$$

Finally, let us emphasize that quite remarkably, the sole knowledge of the edge u_0 as a function of u determines completely the energy $\Sigma_\phi(u)$ since $\Sigma''_\phi(u) = \frac{\beta}{4} u_0$. By construction for positive and increasing potentials ϕ, the position of the edge is positive $u_0 \geqslant 0$, ensuring the convexity of the excess energy.

11.5 Solution for monomial walls with parameter γ

Our considerations on the four methods have been quite general in the choice of the potential ϕ, the only requirements being that ϕ is positive, increasing and vanishes for negative arguments. We now specify the problem to the monomial soft walls $\phi(x) = (x)_+^\gamma$ for which the function f introduced in Eq. (11.1.3) is

$$f(u) = \frac{\gamma}{2} \int_0^{+\infty} \frac{\mathrm{d}b}{\sqrt{b}} (u-b)_+^{\gamma-1} = C_\gamma (u)_+^{\gamma-\frac{1}{2}} \quad , \quad C_\gamma = \frac{\sqrt{\pi}}{2} \frac{\Gamma(\gamma+1)}{\Gamma(\gamma+\frac{1}{2})}. \tag{11.5.1}$$

The rest of this Section will be dedicated to obtaining the exact expression of the excess energy of the Coulomb gas subject to the monomial soft wall and the related optimal density. For completeness and clarity we shall also provide a couple of examples for some values of γ and some figures to represent the optimal density at different values of γ and the parameter u.

11.5.1 Expression of the excess energy

We present the excess energy for general γ in terms of two representations: firstly as a series in u and secondly as a solution to a parametric system involving a trinomial equation. We start by

recalling the series expansion of $\Sigma_\phi(u)$ obtained from the cumulant method, as given in Result 11.1.1. Inserting the expression (11.5.1) of $f(u)$ for monomial soft walls, the excess energy reads

$$\Sigma_\phi(u) = -\frac{\beta}{4}\sum_{n\geqslant 1}\frac{(-1)^n}{n!}\left(\frac{2}{\beta\sqrt{\pi}}\frac{\Gamma(\gamma+1)}{\Gamma(\frac{1}{2}+\gamma)}\right)^n \partial_u^{n-3}u^{n(\gamma-\frac{1}{2})} \tag{11.5.2}$$

The derivative can be taken explicitly and we finally obtain the following result.

Result 11.5.1 (*Free energy expressed as a series*)

The series expansion of the free energy of a Coulomb gas pushed by a soft monomial wall of parameter γ is given by

$$\Sigma_\phi(u) = -\frac{\beta}{4}\sum_{n\geqslant 1}\frac{(-1)^n}{n!}\left(\frac{2}{\beta\sqrt{\pi}}\frac{\Gamma(\gamma+1)}{\Gamma(\frac{1}{2}+\gamma)}\right)^n \frac{\Gamma(n(\gamma-\frac{1}{2})+1)}{\Gamma(4-n(\frac{3}{2}-\gamma))}u^{3-n(\frac{3}{2}-\gamma)} \tag{11.5.3}$$

Following the cumulant method, we have to solve the following equation for $w = w(u)$, $f(u-\frac{4}{\beta\pi}w(u)) = w(u)$ where $f(u)$ is given in (11.5.1). This leads to a trinomial algebraic equation for w from which we retain only the positive root (with the additional constraint that this root should vanish for $u = 0$)

$$u = \frac{4}{\beta\pi}w + (\frac{w}{C_\gamma})^{\frac{1}{\gamma-1/2}}. \tag{11.5.4}$$

Result 11.1.1 on the expression of the excess energy from the SAO method provides another representation for Σ_ϕ as

$$\Sigma_\phi(u) = \frac{1}{2\pi}\int_0^{w(u)} \mathrm{d}w'(u(w')-u)^2 = \frac{1}{2\pi}\int_0^{w(u)} \mathrm{d}w'(\frac{4}{\beta\pi}w' + (\frac{w'}{C_\gamma})^{\frac{1}{\gamma-1/2}} - u)^2 \tag{11.5.5}$$

The integrals over w can be taken explicitly, yielding a parametric representation for Σ_ϕ.

Result 11.5.2 (*Free energy expressed as a parametric system*)

The parametric representation of the free energy of a Coulomb gas pushed by a soft monomial wall of parameter γ is given by

$$\Sigma_\phi(u) = \frac{4u^2w(u)}{\pi(2\gamma+1)(2\gamma+3)} + \frac{(2\gamma-3)(6\gamma+1)uw(u)^2}{\pi^2\beta\gamma(2\gamma+1)(2\gamma+3)} + \frac{4(2\gamma-3)^2w(u)^3}{3\pi^3\beta^2\gamma(2\gamma+3)} \tag{11.5.6}$$

where C_γ was given in Eq. (11.5.1) and $w(u)$ is the unique positive root of Eq. (11.5.4) which vanishes for $u = 0$.

In Table 11.1 we give a few examples of closed analytic forms which can be obtained for some values of γ. These have been obtained by summing the cumulant series using Mathematica. The same result (in a different, though equivalent form) can be obtained by solving the trinomial equation, generally by the means of hypergeometric functions.

Now that we have a complete picture for the excess energy of a Coulomb gas perturbed at its edge by a soft monomial wall, we shall continue our story by answering to the question of the nature of the rearrangement of the gas after its perturbation: we now provide an exact expression for the optimal density of the perturbed gas.

γ	$\Sigma_\phi(u)$	Around $u=0^+$	Around $u=+\infty$
1	$\frac{4}{15\pi^6}(1+\pi^2u)^{5/2}-\frac{4}{15\pi^6}-\frac{2}{3\pi^4}u-\frac{1}{2\pi^2}u^2$	$\frac{u^3}{12}-\frac{\pi^2u^4}{96}+\mathcal{O}(u^5)$	$\frac{4u^{5/2}}{15\pi}-\frac{u^2}{2\pi^2}+\mathcal{O}(u^{3/2})$
$\frac{3}{2}$	$\frac{u^3}{28}$	$\frac{u^3}{28}$	$\frac{u^3}{28}$
2	$\frac{16u^{7/2}}{105\pi}\,{}_2F_1\left(\frac{5}{6},\frac{7}{6};\frac{9}{2};\frac{48u}{\pi^2}\right)$ $+\frac{81\pi^6}{29360128}\,{}_2F_1\left(-\frac{8}{3},-\frac{7}{3};-\frac{5}{2};\frac{48u}{\pi^2}\right)$ $\frac{u^3}{12}-\frac{3\pi^2u^2}{256}+\frac{27\pi^4u}{81920}-\frac{81\pi^6}{29360128}$	$\frac{16u^{7/2}}{105\pi}-\frac{4u^4}{9\pi^2}+\mathcal{O}(u^{9/2})$	$\frac{u^3}{12}-\frac{9(3\pi)^{2/3}u^{8/3}}{320}+\mathcal{O}(u^{7/3})$
$\frac{5}{2}$	$\frac{u^3}{12}+\frac{2u^2}{15}+\frac{32u}{675}-\frac{8(4+15u)^{5/2}}{50625}+\frac{256}{50625}$	$\frac{5u^4}{128}-\frac{45u^5}{1024}+\mathcal{O}(u^6)$	$\frac{u^3}{12}-\frac{8u^{5/2}}{15\sqrt{15}}+\mathcal{O}(u^2)$
$\frac{7}{2}$	$\frac{8u}{105}\,{}_2F_1\left(-\frac{2}{3},-\frac{1}{3};\frac{3}{2};-\frac{945u^2}{128}\right)+\frac{u^3}{12}-\frac{8u}{105}$	$\frac{7u^5}{256}-\frac{175u^7}{4096}+\mathcal{O}(u^9)$	$\frac{u^3}{12}-\frac{9u^{7/3}}{14\times 70^{1/3}}+\mathcal{O}(u^{5/3})$

Table 11.1: Excess energies $\Sigma_\phi(u)$ for $\beta=2$ for different values of γ for $u>0$ with the two first orders of their expansion around $u=0^+$ and $u=+\infty$.

11.5.2 Expression of the optimal density

Before providing the exact expression of the optimal density of the gas, let us discuss briefly the properties of its support. In the case of soft monomial walls, the optimal density has a single support of the form $[u_0,+\infty[$ where u_0 is the unique positive solution of the following trinomial equation:

$$(u-u_0)^{\gamma-\frac{1}{2}}=\frac{\beta\pi}{4C_\gamma}u_0 \quad , \quad C_\gamma=\frac{\sqrt{\pi}}{2}\frac{\Gamma(\gamma+1)}{\Gamma(\gamma+\frac{1}{2})} \tag{11.5.7}$$

The edge of the support enjoys some elementary properties:

1. u_0 should be chosen positive (because we are in a pushed phase);
2. u_0 is smaller than u (because the monomial walls are soft, the position of the new edge should be smaller than the point of application of the wall)
3. u_0 should vanish for $u=0$ (because the gas is unperturbed for $u=0$).

The asymptotic behaviors of u_0 as a function of u exhibit a change at $\gamma=3/2$, indeed

- for $\gamma<3/2$, for $u\gg 1$, $u_0\simeq\frac{4C_\gamma}{\beta\pi}u^{\gamma-1/2}$ and for $u\ll 1$, $u_0\simeq u$.
- for $\gamma\geqslant 3/2$, for $u\gg 1$, $u_0\simeq u$ and for $u\ll 1$, $u_0\simeq\frac{4C_\gamma}{\beta\pi}u^{\gamma-1/2}$.

Remark 11.5.3. *The regime $u_0\simeq u$ should be interpreted as a hard-wall type situation as the point of application of the wall provides the new edge of the gas.*

We consider soft monomial walls which can possibly have an extra positive amplitude B (amounting to replace ϕ by $B\phi$) and we additionally consider general β ensembles. It is interesting in the first place to understand how the density behaves with respect to these parameters.

We have determined in Ref. [4] the scaling property of the optimal density for the soft-monomial walls $\phi(z) = (z)_+^\gamma$, with $\gamma > 1/2$ and $\gamma \neq 3/2$.

Result 11.5.4 (*Scaling properties of the optimal density*)

Let $\gamma > 1/2$ and $\gamma \neq 3/2$, the optimal density scales in B and β as

$$\begin{aligned} \rho_{B,u}(b) &= B^{\frac{1}{3-2\gamma}} \rho_{1, uB^{\frac{2}{2\gamma-3}}}(bB^{\frac{2}{2\gamma-3}}) \\ \rho_u^{(\beta)}(b) &= (\frac{2}{\beta})^{\frac{1}{3-2\gamma}} \rho^{(2)}_{u(\frac{2}{\beta})^{\frac{2}{2\gamma-3}}}(b(\frac{2}{\beta})^{\frac{2}{2\gamma-3}}) \end{aligned} \tag{11.5.8}$$

where $\rho_{B,u}(b)$ (resp. $\rho_u^{(\beta)}(b)$) denotes here the optimal density associated to the monomial wall $\phi(z) = B(z)_+^\gamma$ (resp. to β) for a parameter u. In particular, we may from now on consider only $\beta = 2$ and $B = 1$, all other regimes will be obtained simply by a scaling transformation.

Having the scaling laws in mind, we now present the expression of the optimal density ρ_* derived from Eq. (11.2.22) upon the insertion of the expression of the potential ϕ.

Result 11.5.5 (*Expression of the optimal density with a hypergeometric function*)

Defining the positive parameter $\tau = \frac{u-u_0}{b-u_0}$, where u_0 is the lower edge of the support of the optimal density, we have

$$\begin{aligned} \forall b \geqslant u, \quad \rho_*(b) &= \frac{\sqrt{(b-u_0)_+}}{\pi}\left[1 + \frac{u_0}{2(b-u_0)}\ {}_2F_1(1, \frac{1}{2}, \gamma+\frac{1}{2}, \tau)\right] \\ \forall b \leqslant u, \quad \rho_*(b) &= \frac{\sqrt{(b-u_0)_+}}{\pi}\left[1 + \frac{(\gamma-\frac{1}{2})u_0}{u-u_0}\ {}_2F_1(1, \frac{3}{2}-\gamma, \frac{3}{2}, \frac{1}{\tau})\right] \end{aligned} \tag{11.5.9}$$

A remarkable property is that the monomial soft walls keep the semi-circle property at the new edge of the gas $b = u_0$. Indeed the expansion of the optimal density around this point reads

$$\rho_*(b) = \frac{\sqrt{(b-u_0)_+}}{\pi} + \frac{u_0\,(2\gamma-1)\,\sqrt{(b-u_0)_+}}{2\pi(u-u_0)} + \frac{(4(2-\gamma)\gamma-3)u_0\,(b-u_0)_+^{3/2}}{6\pi\,(u-u_0)^2} + \mathcal{O}\left(b-u_0\right)^{\frac{5}{2}} \tag{11.5.10}$$

Hence it is not possible to create a different order of cancellation at the edge with such kind of potentials. From the scaling law of the optimal density, we also recover the result for a hard-wall by taking $B \to +\infty$. For any γ, we have

$$\rho_{B=+\infty,u}(b) = \rho_{HW}(b) = \frac{2b-u}{2\pi\sqrt{(b-u)_+}} \tag{11.5.11}$$

We now provide a few examples of these optimal densities for $\gamma = 1, 2$ at $\beta = 2$ and $B = 1$.

- For $\gamma = 1$, using $C_\gamma = 1$, $u_0 = \frac{4}{\beta\pi}\sqrt{u-u_0}$ we find for all b the optimal density

$$\rho_*(b) = \left[\frac{\sqrt{b-u_0}}{\pi} + \frac{2}{\beta\pi^2}\log\left(\frac{\sqrt{b-u_0}+\sqrt{u-u_0}}{\sqrt{|b-u|}}\right)\right]\Theta(b-u_0) \tag{11.5.12}$$

  We represent in Fig. 11.1 this optimal density (seen from the right edge of the spectrum) for $\gamma = 1$ and for two values $u = \{0.05, 25\}$. For $u = 25$ the deformation of the semi-circle is small and the logarithmic divergence due to the accumulation of particles at the application

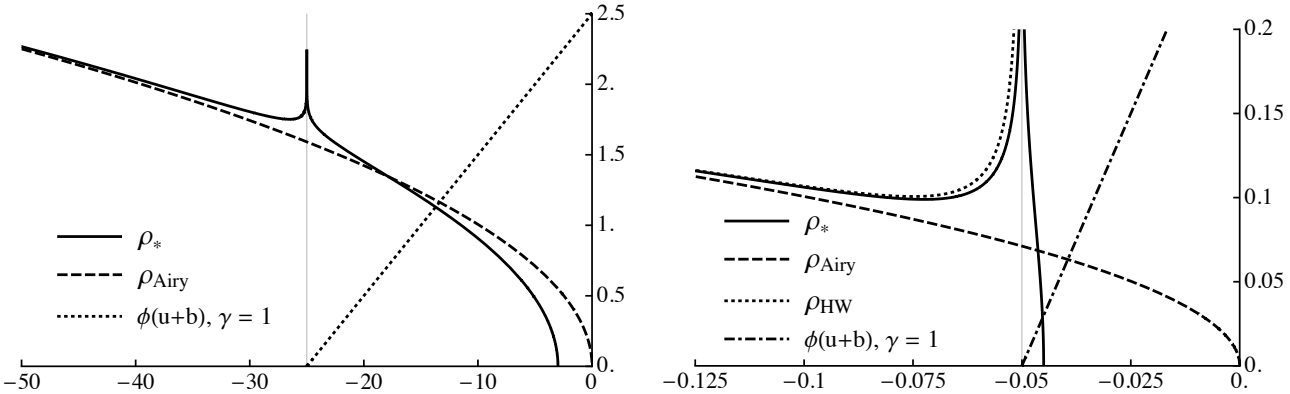

(a) $u = 25$ **(b)** $u = 0.05$

Figure 11.1: Optimal density $\rho_*(-b)$ for $\beta = 2$ and the linear wall $\gamma = 1$ (solid line) with $u = 25$ and $u = 0.05$, compared to the semi-circle density $\rho_{\rm Ai}(-b)$ (dashed line), to the potential $\phi(u + b)$, and to the infinite hard-wall density $\rho_{HW}(-b)$. The optimal density for $u = 0.05$ shows a good agreement with the hard-wall density.

point of the wall is seen easily. For $u = 0.05$, the deformation of the semi-circle is much more important, and the optimal density strongly resembles the hard-wall density.

- For $\gamma = 2$, we find for all b the optimal density

$$\rho_*(b) = \left[\frac{\sqrt{b-u_0}}{\pi} + \frac{2}{\pi^2 \beta} \left(2\sqrt{b-u_0}\sqrt{u-u_0} + (b-u) \log \left| \frac{\sqrt{b-u_0} - \sqrt{u-u_0}}{\sqrt{b-u_0} + \sqrt{u-u_0}} \right| \right) \right] \Theta(b-u_0) \tag{11.5.13}$$

We represent in Fig. 11.2 this optimal density (seen from the right edge of the spectrum) for $\gamma = 2$ and for two values $u = \{1, 100\}$. For $u = 1$ the deformation of the semi-circle is small and there is no divergence at the application point of the wall as the potential is not sharp enough[13]. For $u = 100$, the deformation of the semi-circle is much more important, and the optimal density strongly starts to resemble the hard-wall density.

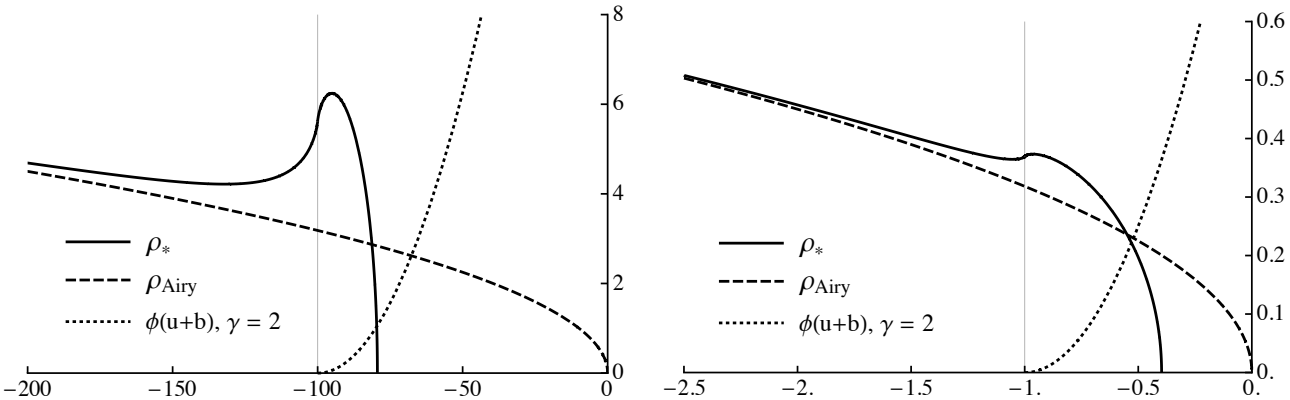

(a) $u = 100$ **(b)** $u = 1$

Figure 11.2: Same as Fig. 11.1 for the quadratic wall $\gamma = 2$ with $u = 100$ and $u = 1$.

[13] We have proved in Ref. [4] that a divergence occurs only for $\gamma \leqslant 1$.

11.5.3 Relation to truncated linear statistics: matching bulk and edge

To conclude this Chapter on the soft monomial walls, we would like to mention a final result about the matching of the truncated linear statistics in the bulk and at the edge of the spectrum. Indeed, we have shown in Ref. [4] that there is a smooth matching between the results of Ref. [229] for truncated linear statistics in the bulk and the results presented in this Thesis at the edge for the linear wall $\gamma = 1$. The details of the matching are non-trivial and instructive and furthermore it can be shown a form of universality, i.e. that any macroscopic linear statistics problem which is smooth around the edge of a Gaussian β random matrix yields the same results as for $\gamma = 1$.

11.6 Where all the physics hides: upper bounds of the excess energy

The presentation of the linear statistics at the edge of Gaussian β random matrices has been so far quite mathematical. In this Section, we will trade technicality with simple arguments to discuss the physics of phase transitions in the perturbation of a Coulomb gas at its edge. In particular, we will show the existence of a general free-to-pushed transition of order larger than or equal to three and we will show that this transition can be of two types depending on the value of the parameter γ: *(i)* a perturbative rearrangement of the edge ($\gamma > 3/2$) and *(ii)* a non-perturbative hard-wall-like breaking of the edge of the Coulomb gas ($\gamma < 3/2$). The critical value $\gamma = 3/2$ will be called the critical rigidity of the edge.

The two simple ingredients we shall require for our discussion are two upper bounds for the free energy Σ_ϕ: a convexity bound and a linear statistics comparison bound. The key ingredient is that these bounds are shown to be saturated in some regime.

Lemma 11.6.1 (*Jensen's bound*)

Jensen's convexity inequality states that $\mathbb{E}_\beta[e^{-\mathsf{L}}] \geqslant e^{-\mathbb{E}_\beta[\mathsf{L}]}$. *Specifying to the linear statistics*

$$\mathsf{L} = t^2 \int_{\mathbb{R}} \mathrm{d}b\, \rho(b)\phi(u-b), \tag{11.6.1}$$

and recalling the expected value of L *in Eq.* (10.2.10)*, this inequality provides an upper bound for* $\Sigma_\phi(u)$ *valid for any potential* ϕ

$$\Sigma_\phi(u) \leqslant \int_0^{+\infty} \mathrm{d}b \frac{\sqrt{b}}{\pi} \phi(u-b). \tag{11.6.2}$$

The interpretation of this bound is that the free energy is not larger than the first cumulant, *i.e.* the energy provided by the additional potential on the unperturbed gas. This is intuitive as the gas will tend to reorganize itself to lower its energy when the new potential is applied.

The second upper bound will relate two different linear statistics with two different potentials that are ordered.

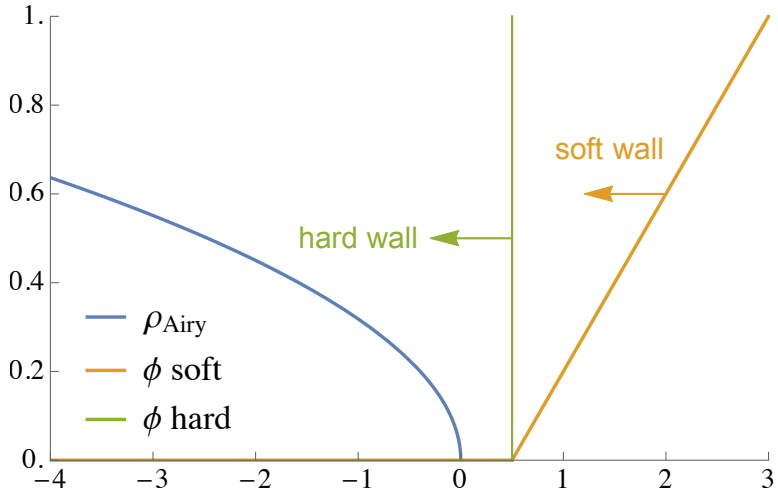

Figure 11.3: Right edge of the semi-circle (blue line) and two wall potentials: a hard-wall (green line) and a soft wall with coefficient $\gamma = 1$ (orange line).

Lemma 11.6.2 (*Comparison bound*)

Let two linear statistics with potentials ϕ_1 and ϕ_2 ordered such that $\phi_1 \leqslant \phi_2$. Then for all $u \geqslant 0$,

$$\mathbb{E}_\beta\left[\prod_{i=1}^{+\infty} e^{-t\phi_2(u+t^{-2/3}a_i)}\right] \leqslant \mathbb{E}_\beta\left[\prod_{i=1}^{+\infty} e^{-t\phi_1(u+t^{-2/3}a_i)}\right] \tag{11.6.3}$$

In particular, this allows to compare the excess energies of both problems as

$$\forall u \geqslant 0, \quad \Sigma_{\phi_1}(u) \leqslant \Sigma_{\phi_2}(u) \tag{11.6.4}$$

The interpretation of this bound is that the larger the additional potential is, the more free energy the system gains. Hence, if one increases the amplitude of the perturbing potential, there cannot exist a rearrangement of the particles that decreases the free energy.

The second upper bound is potential specific in the sense that to be able to have an upper bound, we require the exact knowledge of another linear statistics problem. Since the beginning of this Chapter, we have considered soft permeable walls ϕ and we shall compare them to a hard impermeable wall potential which is defined by the function ϕ_{HW} defined by part as

$$\begin{cases} \phi_{\mathrm{HW}}(z \leqslant 0) = 0 \\ \phi_{\mathrm{HW}}(z \geqslant 0) = +\infty \end{cases} \tag{11.6.5}$$

We represent in Fig. 11.3 the edge of the semi-circle along with two potentials used for the linear statistics: a permeable wall with coefficient $\gamma = 1$ and a hard wall.

By construction all monomial soft walls verify the inequality $\phi \leqslant \phi_{\mathrm{HW}}$, which leads to, using the comparison bound of Lemma 11.6.2,

$$\mathbb{E}_\beta\left[\prod_{i=1}^{+\infty} e^{-t\phi_{\mathrm{HW}}(u+t^{-2/3}a_i)}\right] \leqslant \mathbb{E}_\beta\left[\prod_{i=1}^{+\infty} e^{-t\phi(u+t^{-2/3}a_i)}\right] \tag{11.6.6}$$

Denoting the largest point $a_{\max} = \max_i\{a_i\}$, the left hand side of Eq. (11.6.6) is equal to the cumulative distribution of the largest Airy point, i.e. $\mathbb{E}_\beta\left[\prod_{i=1}^{+\infty} e^{-t\phi_{\mathrm{HW}}(u+t^{-2/3}a_i)}\right] = \mathbb{P}\left(a_{\max} < -ut^{2/3}\right)$

which leads to the following inequality

$$\mathbb{P}\left(a_{\max} < -ut^{2/3}\right) \leqslant \mathbb{E}_\beta \left[\prod_{i=1}^{+\infty} e^{-t\phi(u+t^{-2/3}a_i)}\right]. \tag{11.6.7}$$

Using the standard result for the large deviations of the largest eigenvalue of β-ensembles (*i.e.* from Tracy Widom for $\beta = 1, 2, 4$ [158]) leads to an upper bound of the excess energy of the Coulomb gas subject to a soft wall potential.

$$\Sigma_\phi(u) \leqslant \frac{\beta}{24}u^3 \tag{11.6.8}$$

Remark 11.6.3. *By construction, this upper bound is saturated by the hard wall, hence if one multiplies ϕ by an amplitude B, then for any positive potential ϕ, $\lim_{B\to+\infty} \Sigma_{B\phi}(u) = \frac{\beta}{24}u^3$.*

Gathering the two upper bounds of Eqs. (11.6.2) and (11.6.8) brings a strong constraint on the free energy $\Sigma_{B\phi}(u)$, indeed we find after the precise calculation of the first cumulant the following result.

Result 11.6.4 (*Saturation of the bounds*)

$$\Sigma_{B\phi}(u) \leqslant \min_{u\geqslant 0}\left(\frac{\beta}{24}u^3, \frac{\Gamma(\gamma+1)B}{\sqrt{4\pi}\Gamma(\frac{5}{2}+\gamma)}u^{\gamma+\frac{3}{2}}\right) \tag{11.6.9}$$

From the precise mathematical treatment of the previous Section, it is easy to show that this upper bound is tight for small and large u.

Let us take a moment to comment on this upper bound.

- The u^3 bound describes a non-perturbative response of the gas to the external potential. It is equivalent to the application of a hardwall which inevitably breaks the edge of the gas.
- The $u^{\gamma+\frac{3}{2}}$ bound described a perturbative response of the gas to the external potential. Indeed, coming from the first cumulant, it is seen as an elastic or linear deformation of the edge of the gas.

In particular, we deduce the small $u > 0$ behavior of the free energy $\Sigma_\phi(u)$

$$\Sigma_\phi(u) \propto \begin{cases} u^3, & \gamma < \frac{3}{2} \\ u^{\gamma+\frac{3}{2}}, & \gamma > \frac{3}{2} \end{cases} \tag{11.6.10}$$

As the potentials ϕ are positive, one should also have $\Sigma_\phi(u < 0) = 0$. This is easily seen as the free energy is positive as the potential is positive, and for negative u the first cumulant is equal to zero, hence by Jensen's inequality the free energy should be zero for negative u.

Result 11.6.5 (*Critical rigidity of the edge*)

The consequence of this study is the appearance of a singularity in the free energy of order ν at $u = 0$, where

$$\nu = \max(3, \gamma + \frac{3}{2}) \tag{11.6.11}$$

The soft wall parameter γ has a critical value at $\gamma = \frac{3}{2}$ which we call the critical rigidity of the edge of the semi-circle. The reason for this name is quite transparent as this critical value is the frontier between the elastic and inelastic regimes.

In the previous Chapter, we introduced the soft monomial walls with their coefficient γ and interpreted γ as a measure of the sharpness of the potential at the point of application. This interpretation is now even more transparent as we unveiled the existence of a critical rigidity for the edge of Gaussian β random matrices for a critical value of γ.

There are many applications of the study of linear statistics at the edge, the late KPZ equation being one of them. We refer the reader to Ref. [4] for a broader discussion on this matter. In the next Section, we will introduce one of these applications, the non-intersecting Brownian interfaces, and we will propose a possible experimental realization of our predictions.

11.7 Application to non-intersecting Brownian interfaces subject to a needle potential

The results presented in this Thesis additionally apply to non-intersecting Brownian interfaces representing elastic domain walls between different surface phases adsorbed on a crystalline substrate and perturbed by a soft, needle like potential. Here we heavily borrow from the very elegant presentation given in Refs. [123, 229]. There is a related extensive work on the fluctuations of vicinal surfaces: a vicinal surface of a crystal can be obtained by cutting a crystal at a small angle from a high-symmetry direction, as represented in Fig. 11.4. Because of the discrete periodicity of the crystal, the cut gives a sequence of terraces separated by irregular steps. Seen from above, the steps are described by one-dimensional non intersecting random walks. We refer to [271] for further details on vicinal surfaces.

Consider N non-intersecting ordered interfaces at heights $h_1(x) < \cdots < h_N(x)$ that live around a cylinder of radius $L/(2\pi)$, they can be thought as random walkers with periodic boundary condition. Add a hard wall at $h = 0$ (so that $h_i(x) > 0$ for all i) induces some effective potential for each interface and consider the large system limit, i.e. $L \to \infty$, where the interfaces reach equilibrium. We now introduce four contributions to the energy of the interfaces:

1. An elastic energy $E_{\text{elastic}}(h) = \frac{1}{2}(\frac{\mathrm{d}h}{\mathrm{d}x})^2$,
2. A confining energy $V(h) = \frac{b^2h^2}{2} + \frac{\alpha(\alpha-1)}{2h^2}$ with $b > 0$ and $\alpha > 1$,
3. A pairwise interaction between interfaces $V_{\text{pair}}(h_i, h_j) = \frac{\beta}{2}(\frac{\beta}{2} - 1)\left[\frac{1}{(h_i+h_j)^2} + \frac{1}{(h_i-h_j)^2}\right]$ with $\beta > 0$,
4. An external *needle* soft potential probing the interfaces at the position $x = 0$ on the cylinder, $V_{\text{needle}}(h, x, U) = \delta(x)W(h(x)-U)$ (see Fig. 11.5). The parameter $U > 0$ controls the depth of the probe and the exact form of W controls the type of measurement on the interfaces. The δ function indicates that the probe is sufficiently local in space. It could be realized in practice as an Scanning Tunneling Microscope tip.

The choice of the confining energy comes from the fact that confinement is necessary not to have a zero mode, so for simplicity we consider a quadratic one, plus a repulsive inverse square potential natural from entropic considerations as shown by Fisher in Ref. [272]. By a path integral calculation, it was proved in Ref. [123] that the equilibrium joint distribution of heights at a fixed space point can be obtained from the spectral properties of the quantum Calogero-Moser Hamiltonian. However, concerning the edge properties that we are probing here, these are not important details. From the universality of the soft edge, a purely quadratic confining potential with no hard wall at $h = 0$, as considered in [271], would do as well.

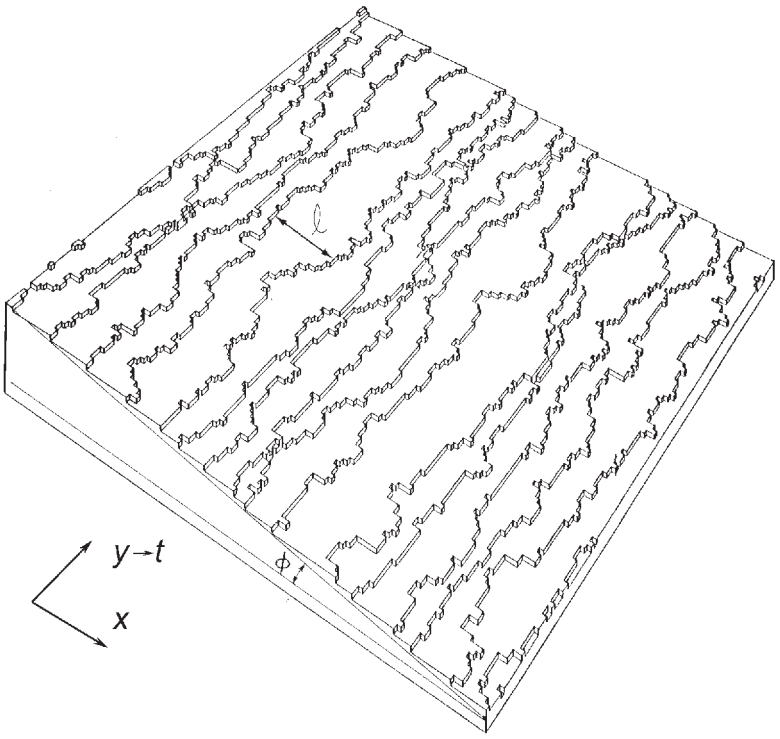

Figure 11.4: Vicinal surface of a crystal: the terrace-step-kink picture is obtained by cutting a crystal at a small angle from a high-symmetry direction. The figure is a Monte Carlo simulation of Einstein [271].

Indeed, at equilibrium, the probability to observe a particular realization of N lines is given by the Boltzmann weight (in units where temperature is unity)

$$P\left[\{h_i(x)\}_{i\in[1,N]}\right] \propto \exp\left(-\sum_{i=1}^{N} E\left[h_i(x)\right] - \sum_{1\leqslant i<j\leqslant N} V_{\text{pair}}(h_i,h_j)\right) \mathbb{1}_{h_i(x)>0} \tag{11.7.1}$$

where the total energy reads $E[h] = E_{\text{elastic}}(h) + V(h) + V_{\text{needle}}(h,x,u)$. The joint probability to see interfaces at positions $\{h_1,\ldots,h_N\}$ at $x=0$ and $x=L$ (because of the periodic boundary condition) is given by the path integral

$$P(h) \propto \prod_{i=1}^{N} \int_{h_i(0)=h_i}^{h_i(L)=h_i} \mathcal{D}h_i(x) \mathbb{1}_{h_i(x)>0}\, e^{-E\left[h_i(x)\right]} \prod_{1\leqslant i<j\leqslant N} e^{-V_{\text{pair}}(h_i,h_j)} \tag{11.7.2}$$

which in turn can be seen as a propagator of N quantum particles

$$P(h_1,\ldots,h_N) \propto e^{-\sum_{i=1}^{N} W(h_i-U)} \left\langle h_1,\ldots,h_N\right| e^{-L\mathcal{H}_{\text{interface}}} \left|h_1,\ldots,h_N\right\rangle \tag{11.7.3}$$

subject to the many-body Hamiltonian

$$\mathcal{H}_{\text{interface}} = \sum_{i=1}^{N}\left[-\frac{1}{2}\frac{\mathrm{d}^2}{\mathrm{d}h_i^2} + V(h_i)\right] + \sum_{1\leqslant i<j\leqslant N} V_{\text{pair}}(h_i,h_j) \tag{11.7.4}$$

In the large L limit, the marginal PDF is given by the N-body ground state of $\mathcal{H}_{\text{interface}}$ which is exactly the Calogero-Moser model [273]. As the brownian interfaces are non-intersecting, the corresponding quantum particles are fermionic and the ground state is formed by filing the first N

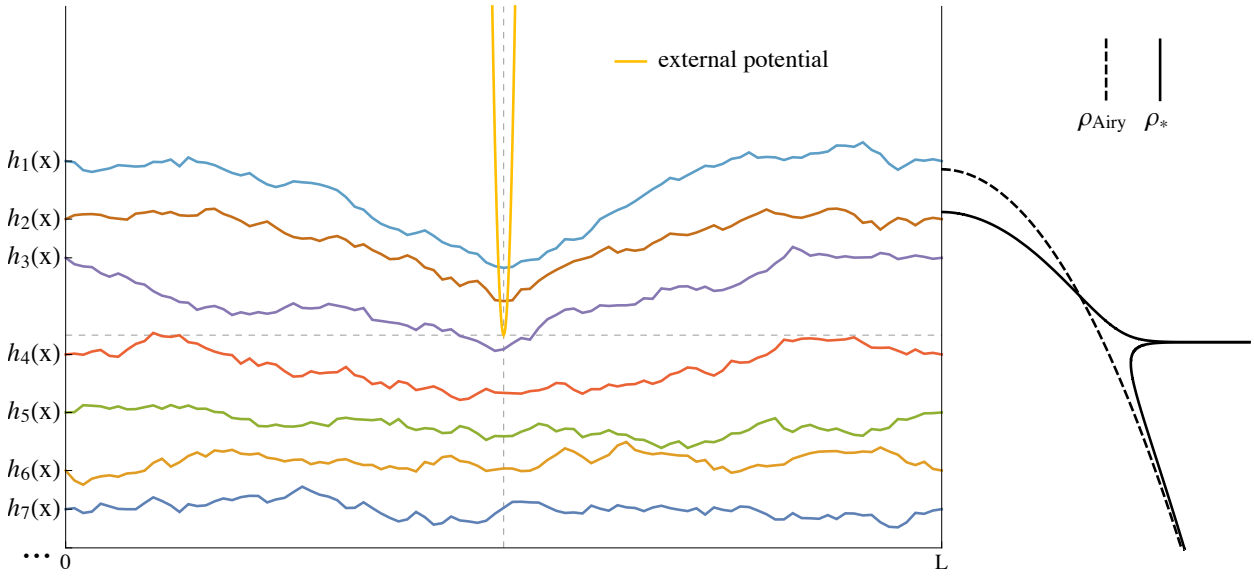

Figure 11.5: Representation of the seven top Brownian lines subject to the needle external potential. In absence of the potential, the density of the top lines as a function of the depth is described by the edge of the semi-circle $\rho_{\rm Ai}$ (dashed lined on the right) and in presence of a smooth potential, the reorganization of the interfaces imposes a new optimal density ρ_* (black line on the right).

eigenstates of the Hamiltonian and given by the Slater determinant of the first N eigenfunctions $\{\psi_i\}_{i\in\mathbb{N}}$. This determinant was computed in Ref. [123] using exacts results on the Calogero-Moser Hamiltonian eigenstates.

$$\begin{aligned} P(h_1,\dots,h_N) &\propto \prod_{i=1}^{N} e^{-W(h_i-U)} \left|\det[\psi_i(h_j)]_{i,j\in[1,N]}\right|^2 \\ &\propto \prod_{i=1}^{N} h_i^{2\alpha} e^{-W(h_i-U)-bh_i^2} \prod_{1\leqslant i<j\leqslant N} (h_i^2-h_j^2)^\beta \end{aligned} \tag{11.7.5}$$

After the change of variable $bh_i^2=\lambda_i$, this PDF corresponds to the general Wishart ensemble with arbitrary $\beta\geqslant 0$ and an external potential W. In the large N limit and in the absence of the potential W, the arrangement of the top brownian lines is described by the soft edge of the Marcenko-Pastur distribution around $\lambda\sim 4N$ or equivalently $h\sim 2\sqrt{N}$.

The results of this Thesis readily apply to describe the linear statistics of the top non-intersecting Brownian interfaces in the ground state in a region of width $N^{-1/6}$ around the top line located at a height $\sim 2\sqrt{N}$. Indeed, if one considers the rescaled heights $\tilde{h}_i=(\sqrt{b}h_i-2\sqrt{N})4^{1/3}N^{1/6}$, then these behave for large N jointly as the Airy$_\beta$ process $\tilde{h}_i:=a_i$. One observable studied in [229] in the bulk is the center of mass position of the N_1 top interfaces $H(N_1)=\frac{1}{N_1}\sum_{i=1}^{N_1}h_i$. In presence of the needle potential W, parameters can be adjusted so that the soft potential W translate into the soft potential ϕ in our units, using the correspondence $W(h_i-U)\equiv t\phi(u+t^{-2/3}a_i)$ with $\sqrt{b}h_i\equiv 2\sqrt{N}+4^{-1/3}N^{-1/6}a_i$. A practical way to measure the value of u is to measure the position of the center of mass $H(N_1)$, from which we can determine the optimal density of the first N_1 brownian lines. Finally, we represent in Fig. 11.5 the top interfaces (at a distance of order $N^{-1/6}$ to the first line) subject to an external potential and the optimal density for the first top lines.

Note that other applications of our work have been studied in Ref. [4], in particular to fermions.

11.8 Open questions regarding linear statistics at the edge of random matrix spectra

The work we have presented on the linear statistics at the edge of Gaussian random matrices was, to the best of our knowledge, the first to provide a precise picture of phenomena such as free-to-pushed phase transitions at the edge or to propose a definition of the rigidity of the soft edge, describing its stability against small perturbation localized around the edge.

Let us mention that our work in Ref. [4] does not restrict to soft monomial walls, indeed we have analytically solved the problem (i.e. determined the exact expression of the excess energy and the optimal density) for other potentials which contrary to the monomial walls can penetrate the entire spectrum:

- The exponential wall $\phi(z) = e^z$;
- The inverse monomial wall $\phi(z) = (-z)^{-\delta}$ with $\delta > 3/2$ for $z < 0$ and $\phi(z) = +\infty$ else. The inverse monomial wall can be viewed as a wall which penetrates the semi-circle as a power law for $u \leqslant 0$ and as a hardwall for $u > 0$.

There are still many open directions which we would like to briefly discuss before closing this Chapter.

11.8.1 Pulling the edge rather than pushing it

The original motivation for the linear statistics problem at the edge arose from the determination of the left tail of the solution to the Kardar-Parisi-Zhang for droplet initial condition at late time. In this setting, the problem amounted to study a Coulomb gas in its pushed phase, i.e. by adding an additional confining potential localized at the edge: these were the soft monomial walls we have extensively discussed.

It would be extremely interesting to extend this research program to pulled Coulomb gases by applying a potential which decreases the confinement of the gas in order to expand it. From the knowledge of macroscopic linear statistics, this problem will turn out to be much more complicated due to the fact that the density of the gas can have multiple supports. It will be extremely interesting to see how the support splitting occurs in the Stochastic Airy Operator method. We believe that in this case the WKB method will be more involved due to the presence of multiple classical turning points and the saddle points or stationary equations will have non-unique solutions: there will be one solution for each interval of support of the optimal density of the Coulomb gas. We also believe that at the moment, the most natural way to initiate this research direction would be by the cumulant method, where our Mellin-Barnes summation trick provides a way of summing over all solutions of the saddle point equation, see Appendix B.1.

11.8.2 Linear statistics at hard edges

The linear statistics problem we have treated so far concerns the soft edge of random matrices where the Airy β point process arises. Another interesting direction would be to extend our research to the hard edge of random matrices in the Laguerre β ensemble for instance. We believe that the problem is well posed and that all tools necessary to solve it exist: indeed there is an analog of the Stochastic Airy Operator at the hard edge which is the Stochastic Bessel Operator. Additionally, a Coulomb gas formulation near the hard edge could easily be obtained from the joint probability distribution of the eigenvalues in the Laguerre β ensemble.

11.8.3 Universality of the linear statistics at soft edges of generic random matrices

In this Thesis, we have presented our results on the linear statistics problem at the soft edge of Gaussian random matrices. For the sake of universality, it would be interesting to prove that our results hold for a larger class of random matrices exhibiting a soft edge. A possible direction would come from the Stochastic Airy Operator whose universality has been investigated by Krishnapur, Rider and Virág [274] by an operator approach, by Bekerman, Figalli and Guionnet [275] by the means of measure transportation and by Bourgade, Erdös and Yau [276] by their relaxation of Dyson Brownian motion approach. In particular, it would be interesting to know whether the order of the free-to-pushed phase transition is always larger than three for all soft edges and if the critical rigidity is always 3/2.

Conclusion

In conclusion to this Chapter on linear statistics at the edge of Gaussian random matrices, we presented and unified *four* apparently distinct methods to study the large deviations for linear statistics at the edge of the β ensemble of random matrices. It equivalently describes the response of a logarithmic Coulomb gas pushed *delicately* at its edge. The results of this Thesis raise multiple questions such as the extensions to more general soft potentials leading to possibly non-unique solutions of the saddle points or multiple supports for the optimal density.

Conclusion and perspectives

> "*One never notices what has been done; one can only see what remains to be done.*"
>
> — Marie Curie

In this Thesis, we have made meaningful progress in the understanding of the properties of the solutions to the Kardar-Parisi-Zhang equation. We have revisited the KPZ equation in a half-space, extending previous exact solutions obtained in the literature. In addition we have introduced in a self-contained way a general framework to understand the large deviations of the solutions to the KPZ equation at short time. This framework allowed us to discover analytically the singularity of the large deviation function of the KPZ height at short time for the Brownian initial condition. At large time, we have unveiled and unified different perspectives to obtain the large deviations of the solutions to the KPZ equation. This was intimately connected to the understanding of linear statistics at the edge of Gaussian random matrices at the microscopic level for which we have obtained new results.

We have tried to highlight in this Thesis that the physics surrounding the Kardar-Parisi-Zhang equation is extremely rich, ranging from its origin in out-of-equilibrium physics to its remarkable mathematical ties. In particular, we have presented some intriguing connections between the solutions to the KPZ equation, Random Matrix Theory, Brownian functionals and the theory of Coulomb gases. Nonetheless, we think that these connections are just the tip of an iceberg and that further developments will shed some light on a more general physics, especially regarding the various cross-overs appearing in the KPZ universality class. This is the reason why we stated a large number of open questions all along this Thesis.

There is an extensive number of research directions to undertake regarding the Kardar-Parisi-Zhang equation. The first and maybe most difficult one is the question of solving the equation for any initial condition. Even without going to that level of ambition, the existing solutions raise already a number of questions. Can one construct an appropriate generating function of the KPZ solution which could always be expressed by a Fredholm determinant or Pfaffian ? Can we relate other initial conditions to random matrix ensembles at all times ? Can we establish general properties of the large deviations of the KPZ solution at short time for a general initial condition ? Could we use the integrability of the KPZ equation to discover new integrability features in the WNT ? Could we use the exact short-time solutions obtained with the cumulant method to solve the hydrodynamic equations of the Weak Noise Theory ? At the moment, the large-time behavior of the solution to the KPZ equation is well understood in two restricted cases: the droplet in full-space and in half-space in the critical case. Can we extend our study and obtain the large-time behavior of the solutions for other initial conditions such as the flat initial condition ? We have made a conjecture in this direction for the stationary initial condition in Ref. [6].

To finally conclude, let us say that we hope to have raised enough interesting questions in this Thesis to stimulate the interest of the ever-growing Kardar-Parisi-Zhang community.

Appendix

A Properties of some functions (Airy, Lambert)

A.1 The Lambert W function

We introduce the Lambert W function [171] which we use extensively throughout this thesis. Consider the function defined on $\mathbb{C}$ by $f(z) = ze^z$, the W function is composed of all inverse branches of f so that $W(ze^z) = z$. It does have two real branches, W_0 and W_{-1} defined respectively on $[-e^{-1}, +\infty[$ and $[-e^{-1}, 0[$. On their respective domains, W_0 is strictly increasing and W_{-1} is strictly decreasing. By differentiation of $W(z)e^{W(z)} = z$, one obtains a differential equation valid for all branches of $W(z)$

$$\frac{\mathrm{d}W}{\mathrm{d}z}(z) = \frac{W(z)}{z(1+W(z))} \tag{A.1}$$

Concerning their asymptotics, W_0 behaves logarithmically for large argument $W_0(z) \simeq_{z\to+\infty} \log(z) - \log\log(z)$ and is linear for small argument $W_0(z) =_{z\to 0} z - z^2 + \mathcal{O}(z^3)$. W_{-1} behaves logarithmically for small argument $W_{-1}(z) \simeq_{z\to 0^-} \log(-z) - \log(-\log(-z))$. Both branches join smoothly at the point $z = -e^{-1}$ and have the value $W(-e^{-1}) = -1$. These remarks are summarized on Fig. 6. More details on the other branches, W_k for integer k, can be found in [171].

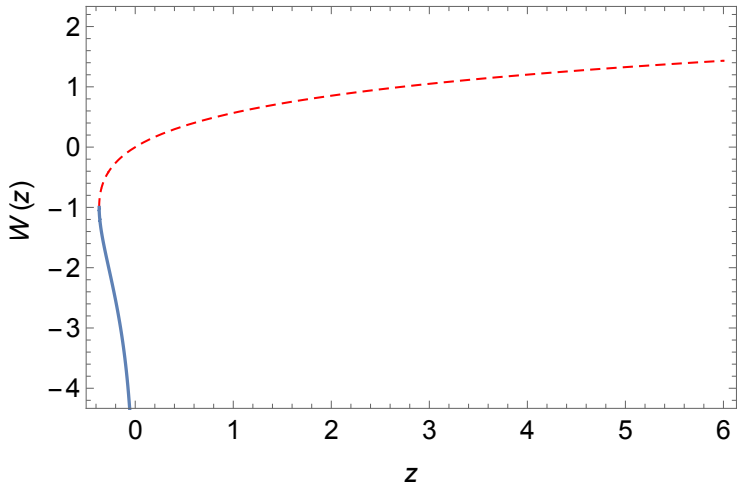

Figure 6: The Lambert function W. The dashed red line corresponds to the branch W_0 whereas the blue line corresponds to the branch W_{-1}.

A.2 Airy function

The Airy function is defined for $v \in \mathbb{R}$ as

$$\mathrm{Ai}(v) = \int_{\mathbb{R}+i\varepsilon} \frac{\mathrm{d}\eta}{2\pi} \exp\left(i\frac{\eta^3}{3} + iv\eta\right) \tag{A.2}$$

where $\varepsilon = 0^+$. The Airy function verifies the second order differential equation

$$\mathrm{Ai}''(v) = v\mathrm{Ai}(v), \tag{A.3}$$

It is normalized $\int_{\mathbb{R}} \mathrm{d}v\, \mathrm{Ai}(v) = 1$ and we recall the following asymptotics of the Airy function

- As $v \to +\infty$, $\mathrm{Ai}(v) \sim \dfrac{e^{-\frac{2}{3}v^{3/2}}}{\sqrt{4\pi}v^{1/4}}$

- As $v \to -\infty$, $\mathrm{Ai}(v) \sim \dfrac{\sin(\frac{2}{3}(-v)^{3/2} + \frac{\pi}{4})}{\sqrt{\pi} v^{1/4}}$

A.3 Airy kernel

The Airy kernel is defined either by its integral representation for $u, v \in \mathbb{R}$ as

$$K_{\mathrm{Ai}}(u,v) = \int_0^{+\infty} \mathrm{d}r\, \mathrm{Ai}(u+r)\mathrm{Ai}(r+v), \tag{A.4}$$

or by its Christoffel-Darboux representation

$$K_{\mathrm{Ai}}(u,v) = \frac{\mathrm{Ai}(u)\mathrm{Ai}'(v) - \mathrm{Ai}'(u)\mathrm{Ai}(v)}{u-v}. \tag{A.5}$$

The Airy kernel also verifies the separation relation

$$(\partial_u + \partial_v) K_{\mathrm{Ai}}(u,v) = -\mathrm{Ai}(u)\mathrm{Ai}(v). \tag{A.6}$$

B Some technical theorems and lemmas

B.1 Mellin-Barnes derivation of the Lagrange inversion formula

Here we perform the summation of the series which appears in (11.1.4). We use a Mellin-Barnes summation method inspired from Lemma 6 of Ref. [170] which was introduced to calculate the sum over replicas in the context of the KPZ equation. For benign real test functions f, assumed to be positive, the following series admits a closed algebraic form

$$\mathcal{S}(u) = \sum_{n \geqslant 1} \frac{a^n}{n!} (\partial_u)^n f(u)^n = \sum_i \frac{1}{|a f'(u + a w_i) - 1|} - 1 \tag{B.1}$$

where the $\{w_i\}$'s are the positive solutions of the equation $f(u + aw) = w$. We use this formula in this Thesis only in the case of a unique solution. The present Mellin-Barnes method proposes a formula in the case of multiple solutions.

Physicist's heuristics. Let us start by manipulating the summand

$$\frac{a^n}{n!} (\partial_u)^n f(u)^n = \int_{\mathbb{R}} \mathrm{d}y\, \delta(y) \frac{a^n}{n!} (\partial_u)^n f(u)^{n+iy} \tag{B.2}$$

Let us express the delta in Fourier space and proceed to the change of variable $z = n + iy$,

$$\frac{a^n}{n!} (\partial_u)^n f(u)^n = \int_{n+i\mathbb{R}} \mathrm{d}z \int_{\mathbb{R}} \frac{\mathrm{d}r}{2i\pi}\, e^{-r(z-n)} \frac{a^n}{n!} (\partial_u)^n f(u)^z \tag{B.3}$$

Let us suppose that we can shift the contour of integration of z such that there is no n dependency anymore. Let us call Γ the new shifted contour.

$$\frac{a^n}{n!} (\partial_u)^n f(u)^n = \int_{\Gamma} \frac{\mathrm{d}z}{2i\pi} \int_{\mathbb{R}} \mathrm{d}r\, e^{-r(z-n)} \frac{a^n}{n!} (\partial_u)^n f(u)^z \tag{B.4}$$

Let us choose the contour $\Gamma = a + i\mathbb{R}$ for some $a \in]0,1[$ so that Γ is parallel to the imaginary axis and let us proceed to the summation over n.

$$\sum_{n \geqslant 1} \frac{a^n}{n!} (\partial_u)^n f(u)^n = \int_{\Gamma} \frac{\mathrm{d}z}{2i\pi} \int_{\mathbb{R}} \mathrm{d}r\, e^{-rz} \left(\sum_{n \geqslant 1} \frac{e^{rn} a^n}{n!} (\partial_u)^n \right) f(u)^z \tag{B.5}$$

One recognizes an exponential series, and more particularly, the series of a translation operator.

$$\begin{aligned}\sum_{n\geqslant 1}\frac{a^n}{n!}(\partial_u)^n f(u)^n &= \int_\Gamma \frac{\mathrm{d}z}{2i\pi}\int_{\mathbb{R}}\mathrm{d}r\, e^{-rz}\left[e^{ae^r\partial_u}-1\right]f(u)^z \\ &= \int_\Gamma \frac{\mathrm{d}z}{2i\pi}\int_{\mathbb{R}}\mathrm{d}r\, e^{-rz}\left[f(u+ae^r)^z - f(u)^z\right]\end{aligned} \tag{B.6}$$

As Γ is parallel to the imaginary axis and as both r and f are real valued, one recognizes the integral over z as Fourier transform and we therefore have

$$\begin{aligned}\sum_{n\geqslant 1}\frac{a^n}{n!}(\partial_u)^n f(u)^n &= \int_{\mathbb{R}}\mathrm{d}r\,\left[\delta(\log f(u+ae^r)-r)-\delta(r)\right] \\ &= \sum_i \frac{1}{\left|af'(u+ae^{r_i})-1\right|}-1\end{aligned} \tag{B.7}$$

where r_i are the real solutions of the equation $f(u+ae^r)=e^r$. As r is real, we define $w=e^r>0$ which concludes the derivation. □

Furthermore suppose now, as in this Thesis, that there exists a unique real solution $w=w(u)$ to the equation $f(u+aw)=w$ and that $1-af'(u+aw)>0$ for this solution. It is possible to further simplify the series. Indeed, differentiating the equation $f(u+aw)=w$ leads to

$$\left[1-af'(u+aw)\right]\mathrm{d}w = f'(u+aw)\mathrm{d}u \tag{B.8}$$

Inserting this differential relation into Eq. (B.1) yields

$$\mathcal{S}(u)=\sum_{n\geqslant 1}\frac{a^n}{n!}(\partial_u)^n f(u)^n = \frac{af'(u+aw)}{1-af'(u+aw)} = a\frac{\mathrm{d}w}{\mathrm{d}u}. \tag{B.9}$$

B.2 Sparre Andersen theorem

The Sparre-Andersen theorem lies in the framework of random partial sums $S_i = X_1+\cdots+X_i$ of a sequence of random variables $\{X_i\}$. Here we make the hypothesis that our process forms a bridge, i.e. $S_0 = S_{n+1} = 0$ and we are interested in N_n^* be the number of points (j, S_j), $j=1,\ldots,n$ which lie above the straight line from $(0,0)$ to $(n+1, S_{n+1}=0)$.

Theorem B.1 (*Sparre Andersen Corollary 1, Ref. [277]*)

If the random variables $X_1,\ldots,X_{n+1}$ are independent and each has a continuous distribution, or if the random variables are symmetrically dependent and the joint distribution function is absolutely continuous, then for any C which is symmetric with respect to $X_1,\ldots,X_{n+1}$ and has $\mathbb{P}(C)>0$, we have

$$\forall m\in[0,n],\ \mathbb{P}(N_n^*=m\mid C)=\frac{1}{n+1} \tag{B.10}$$

For our case of interest, the event C will be our hypothesis that the process is a bridge.

$$C=\{S_0=0\}\cap\{S_{n+1}=0\} \tag{B.11}$$

B.3 Proof of the identity (9.2.13) for the systematic expansion of the Fredholm terminant of the Airy kernel

In this Appendix, we prove the identity (9.2.13) for the function $L_\alpha(\sigma, a, b)$. Starting from the definition in Eq. (9.2.11), one has

$$L_\alpha(\sigma,0,0) = \sum_{k=1}^{\infty}(-1)^{k-1} \sum_{n_1,\dots,n_k=1}^{\infty} \left(\prod_{\ell=1}^{k} a_{n_l,\alpha}\,\sigma^{n_\ell}\right) \int_0^\infty \mathrm{d}z_1 \dots \mathrm{d}z_{k-1} \left(\prod_{\ell=1}^{k} K_{n_j}(z_\ell - z_{\ell-1})\right)_{\substack{z_0=0\\ z_k=0}} \tag{B.12}$$

where $K_n(z) = \frac{e^{-\frac{z^2}{4n}}}{\sqrt{4\pi n}}$ is the Gaussian kernel. The integral in the expression above can be interpreted as the probability that a random walker, starting initially at position 0, ends at position 0 after $k-1$ steps after staying only on positive positions for all intermediate steps. The transition probabilities depend on the variables n_j, but in a symmetric way since each n_j has the same weight. Thus, it is possible to use the Sparre Andersen theorem (see Appendix B.2) to replace the integral by $\frac{1}{k}\,K_{n_1+\dots+n_k}(0)$. This leads to

$$\begin{aligned}
L_\alpha(\sigma,0,0) &= \frac{1}{\sqrt{4\pi}} \sum_{k=1}^{\infty} \frac{(-1)^{k-1}}{k} \sum_{n_1,\dots,n_k=1}^{\infty} \frac{\prod_{\ell=1}^{k} a_{n_l,\alpha}\,\sigma^{n_\ell}}{\sqrt{n_1+\dots+n_k}} \\
&= \frac{1}{2\pi} \int_0^{+\infty} \frac{\mathrm{d}x}{\sqrt{x}} \sum_{k=1}^{\infty} \frac{(-1)^{k-1}}{k} \sum_{n_1,\dots,n_k=1}^{\infty} \prod_{\ell=1}^{k} a_{n_\ell,\alpha}\,(\sigma e^{-x})^{n_\ell} \\
&= \frac{1}{2\pi} \int_0^{+\infty} \frac{\mathrm{d}x}{\sqrt{x}} \sum_{k=1}^{\infty} \frac{(-1)^{k-1}}{k} (\exp(\alpha g(\sigma e^{-x})) - 1)^k \\
&= \frac{\alpha}{2\pi} \int_0^{+\infty} \frac{\mathrm{d}x}{\sqrt{x}} g(\sigma e^{-x}) \\
&= \frac{\alpha}{\pi} (\sigma\partial_\sigma) \int_0^{+\infty} \mathrm{d}x \sqrt{x}\, g(\sigma e^{-x})
\end{aligned} \tag{B.13}$$

With no boundary term using that $g(0) = 0$ as long as $\sqrt{x}g(\sigma e^{-x}) \to 0$ for $x \to +\infty$. We precisely obtain (9.2.13).

Publications related to this Thesis

[10] L. D. Landau and E. M. Lifshitz. Course of theoretical physics, Statistical Physics, Volume 5. Elsevier.

[11] L. Onsager. *Crystal statistics. I. a two-dimensional model with an order-disorder transition.* Physical Review, 65(3-4):117–149, (1944).

[12] K. G. Wilson. *The renormalization group: Critical phenomena and the kondo problem.* Reviews of Modern Physics, 47(4):773–840, (1975).

[13] W. Bialek, A. Cavagna, I. Giardina, T. Mora, E. Silvestri, M. Viale, and A. Walczak. *Statistical mechanics for natural flocks of birds.* *PNAS; Proceedings of the National Academy of Sciences*, 109(13):4786–4791, (2012).

[14] M. Kardar, G. Parisi and Y-C. Zhang, *Dynamic Scaling of Growing Interfaces*, Physical Review Letters **56**, 889, (1986).

[15] T. Halpin-Healy, Y-C. Zhang, *Kinetic roughening phenomena, stochastic growth, directed polymers and all that.* Phys. Rep. **254**, 215, (1995).

[16] J. Krug, *Origins of scale invariance in growth processes.* Adv. Phys. **46**, 139 (1997).

[17] M. Hairer, *Solving the KPZ equation*, Ann. Math. **178**, 559, (2013).

[18] I. Corwin, *The Kardar-Parisi-Zhang equation and universality class*, Random Matrices: Theory Appl. **01** 1130001, (2012).

[19] T. Halpin-Healy, K. A. Takeuchi, *A KPZ cocktail-shaken, not stirred: Toasting 30 years of kinetically roughened surfaces* J. Stat. Phys. **160**, 794 , (2015).

[20] K. A. Takeuchi. *An appetizer to modern developments on the Kardar–Parisi–Zhang universality class.* Physica A: Statistical Mechanics and its Applications, 504:77– 105, (2018).

[21] I. Gupta and B. C. Mohanty *Dynamics of surface evolution in semiconductor thin films grown from a chemical bath* *Sci. Rep.* **6** 33136 (2016). P. A. Orrillo, S. N. Santalla, R. Cuerno, L. Vazquez, S. B. Ribotta, L. M. Gassa, F. J. Mompean, R. C. Salvarezza and M. E. Vela *Morphological stabilization and KPZ scaling by electrochemically induced co-deposition of nanostructured NiW alloy films* Sci. Rep. **7** 17997, (2017).

[22] J. Maunuksela, M. Myllys, O.-P. Kähkönen, J. Timonen, N. Provatas, M. J. Alava, and T. Ala-Nissila *Kinetic roughening in slow combustion of paper.* Physical Review Letters, 79(8):1515–1518, (1997).

[23] M. A. C. Huergo, M. A. Pasquale, P. H. González, A. E. Bolzán, A. J. Arvia, *Growth dynamics of cancer cell colonies and their comparison with noncancerous cells*, Phys. Rev. E 85 011918, (2012).

[24] O. Hallatschek, P. Hersen, S. Ramanathan, and D. Nelson. *Genetic drift at expanding frontiers promotes gene segregation.* PNAS; Proceedings of the National Academy of Sciences, 104(50):19926–19930, (2007).

[25] K. A. Takeuchi, M. Sano, *Universal fluctuations of growing interfaces: Evidence in turbulent liquid crystals*, Physical Review Letters **104** 230601, (2010).

[26] K. A. Takeuchi, M. Sano, T. Sasamoto, H. Spohn, *Growing interfaces uncover universal fluctuations behind scale invariance*, Scientific Reports 1 34, (2011).

[27] K. A. Takeuchi, M. Sano, *Evidence for geometry-dependent universal fluctuations of the Kardar-Parisi-Zhang interfaces in liquid-crystal turbulence*, J. Stat. Phys. 147 853–890, (2012).

[28] K. A. Takeuchi, *Experimental approaches to universal out-of-equilibrium scaling laws: turbulent liquid crystal and other developments*, J. Stat. Mech. P01006, (2014).

[29] Y. T. Fukai, K. A. Takeuchi, *Kardar-Parisi-Zhang interfaces with inward Growth*, Physical Review Letters **119** 030602, (2017).

[30] K. A. Takeuchi, *Crossover from growing to stationary interfaces in the Kardar-Parisi-Zhang class*, Physical Review Letters **110** 210604, (2013).

[31] I. Ito, K. A. Takeuchi, *When fast and slow interfaces grow together: connection to the half-space problem of the Kardar-Parisi-Zhang class*, arXiv:1802.10284, Phys. Rev. E 97, 040103 (2018).

[32] S. F. Edwards and D. R. Wilkinson, *The surface statistics of a granular aggregate.* Proc. R. Soc. London Ser. **A 381**, 17, (1982).

[33] D. A. Huse, C. L. Henley, D. S. Fisher, Physical Review Letters **55**, 2924, (1985);

[34] D. Forster, D. R. Nelson, and M. J. Stephen *Large-distance and long-time properties of a randomly stirred fluid.* Physical Review A, 16(2):732–749, (1977).

[35] I. Corwin, J. Quastel, et D. Remenik, *Renormalization fixed point of the KPZ universality class*, J Stat Phys 160: 815, (2015).

[36] M. Hairer et J. Quastel, *A class of growth models rescaling to KPZ*, arXiv:1512.07845, (2015).

[37] M. Henkel and X. Durang. *Spherical model of growing interfaces.* Journal of Statistical Mechanics: Theory and Experiment, 2015(5):P05022, (2015).

[38] M. Prähofer and H. Spohn. *Universal distributions for growth processes in 1+ 1 dimensions and random matrices.* Physical Review Letters, 84(21):4882, (2000).

[39] J. Baik, E. M. Rains, *Limiting distributions for a polynuclear growth model with external sources*, J. Stat. Phys. 100 523–541, (2000).

[40] M. Prähofer, H. Spohn, *Scale invariance of the PNG droplet and the Airy process*, J. Stat. Phys. 108 1071–1106, (2002).

[41] J. Ortmann, J. Quastel, D. Remenik, *A Pfaffian representation for flat ASEP*, Comm. Pure Appl. Math. **70** 1, 3, (2015).

[42] A. Borodin and I. Corwin, *Macdonald processes*, Prob. Theor. Rel. Fields 158 (2014), no. 1-2, 225–400, arXiv:1111.4408.

[43] A. Borodin, *Stochastic higher spin six vertex model and Macdonald measures*, J. Math. Phys. 59, 023301, (2018); A. Borodin and G. Olshanski, *The ASEP and determinantal point processes*, Commun. Math. Phys. 353: 853 (2017).

[44] C. A. Tracy, H. Widom, *Asymptotics in ASEP with step initial condition,* Commun. Math. Phys. 290 129–154, (2009).

[45] M. Prahofer and H. Spohn *Current fluctuations for the totally asymmetric simple exclusion process*, Progress in Probability, Vol. 51, edited by V. Sidoravicius (Birkhauser,Boston, 2002) 185, arXiv:cond-mat/0101200.

[46] T. Thiery et P. Le Doussal, *Log-gamma directed polymer with fixed endpoints via the replica Bethe Ansatz,* Journal of Statistical Mechanics: Theory and Experiment **10**, 10018, (2014).

[47] T. Thiery et P. Le Doussal, *On integrable directed polymer models on the square lattice,* Journal of Physics A Mathematical General **48**, 465001 (2015).

[48] N. O'Connell. *Directed polymers and the quantum toda lattice.* The Annals of Probability, 40(2):437–458, (2012).

[49] Auffinger, A., Baik, J., Corwin, I. *Universality for directed polymers in thin rectangles.* arXiv:1204.4445, (2012)

[50] N. O'Connell and M. Yor. *Brownian analogues of Burke's theorem.* Stochastic Processes and their Applications, 96(2):285 – 304, (2001).

[51] T. Thiery. *Stationary measures for two dual families of finite and zero temperature models of directed polymers on the square lattice.* Journal of Statistical Physics, 165(1):44–85, (2016).

[52] K. Johansson, *Shape fluctuations and random matrices.* Commun. Math. Phys. **209**, 437 (2000).

[53] A. Borodin, I. Corwin, et D. Remenik, *Log-gamma polymer free energy fluctuations via a fredholm determinant identity.* Communications in Mathematical Physics **324**, 215–232 , (2013).

[54] I. Corwin, T. Seppäläinen, et H. Shen, *The strict-weak lattice polymer,* Journal of Statistical Physics **160**, 1027–1053,, (2015).

[55] G. Barraquand and I. Corwin. *Random-walk in beta-distributed random environment.* Probab. Theo. Rel. Fields **167**, 1057 (2017).

[56] P. Le Doussal and T. Thiery. *Diffusion in time-dependent random media and the Kardar-Parisi-Zhang equation.* Phys. Rev. E **96**, 010102 (2017).

[57] J. Baik, P. Deift, K. Johansson, *On the distribution of the length of the longest increasing subsequence of random permutations*, J. Am. Math. Soc. 12 1119–1178, (1999).

[58] L. M. Sieberer, G. Wachtel, E. Altman and S. Diehl, *Lattice duality for the compact Kardar-Parisi-Zhang equation*, arXiv:1604.01043, Phys. Rev. B **94**, 104521 (2016).

[59] L . He, L. M. Sieberer, E. Altman and S. Diehl, *Scaling properties of one-dimensional driven-dissipative condensates* Phys. Rev. B **92,** 155307 (2015).

[60] C. A. Tracy, H. Widom, *Level-spacing distributions and the Airy kernel*, Commun. Math. Phys. **159**, 151, (1994).

[61] C. A. Tracy and H. Widom, *On orthogonal and symplectic matrix ensembles* Commun. Math. Phys. **177**, 727, (1996).

[62] K. Matetski, J. Quastel, and D. Remenik. *The KPZ fixed point.* arXiv:1701.00018, (2016).

[63] H. Spohn *Stochastic integrability and the KPZ equation* arXiv:1204.2657, (2012).

[64] T. Thiery, *Analytical methods and field theory for disordered systems.* PhD thesis available online at https://tel.archives-ouvertes.fr/tel-01361896/document.

[65] L. Bertini, G. Giacomin, *Stochastic Burgers and KPZ equations from particle systems*, Commun. Math. Phys. 183 571–607, (1997).

[66] J. Bec et K. Khanin, *Burgers turbulence,* Phys. Rep. **447**, 1–66, (2007).

[67] C. Mueller, *On the support of solutions to the heat equation with noise*, Stochastics, **37**, 225 (1991).

[68] C. Mueller and D. Nualart, *Regularity of the density for the stochastic heat equation*, Elect. J. Prob. **13**, 2248 (2008).

[69] G. Moreno Flores, *On the (strict) positivity of solutions of the stochastic heat equation.* Ann. Probab. **42**, 1635 (2014).

[70] A.-L. Barabási, H. E. Stanley, *Fractal Concepts in Surface Growth*, Cambridge Univ. Press, Cambridge, (1995).

[71] T. Gueudré, P. Le Doussal, *Directed polymer near a hard wall and KPZ equation in the half-space*, Europhys. Lett. **100**, 26006, (2012).

[72] T. Sasamoto, H. Spohn, *One-dimensional Kardar-Parisi-Zhang equation: an exact solution and its universality*, Physical Review Letters **104**, 230602, (2010).

[73] P. Calabrese, P. Le Doussal, A. Rosso, *Free-energy distribution of the directed polymer at high temperature*, Europhys. Lett. **90**, 20002, (2010).

[74] V. Dotsenko, *Bethe ansatz derivation of the Tracy-Widom distribution for one-dimensional directed polymers* EPL **90**, 20003 (2010); *Replica Bethe ansatz derivation of the Tracy–Widom distribution of the free energy fluctuations in one-dimensional directed polymers*, J. Stat. Mech. P07010, (2010); V. Dotsenko and B. Klumov, *Bethe ansatz solution for one-dimensional directed polymers in random media* J. Stat. Mech. P03022, (2010).

[75] G. Amir, I. Corwin, J. Quastel, *Probability distribution of the free energy of the continuum directed random polymer in 1 + 1 dimensions*, Comm. Pure and Appl. Math. **64**, 466, (2011).

[76] P. Calabrese, P. Le Doussal, *Exact solution for the Kardar-Parisi-Zhang equation with flat initial conditions*, Physical Review Letters **106**, 250603, (2011); *The KPZ equation with flat initial condition and the directed polymer with one free end*, J. Stat. Mech. P06001, (2012).

[77] T. Imamura, T. Sasamoto, *Exact solution for the stationary Kardar-Parisi-Zhang equation*, Physical Review Letters **108**, 190603, (2012).

[78] A. Borodin, I. Corwin, P. L. Ferrari. B. Veto, *Height fluctuations for the stationary KPZ equation*, Math. Phys. Anal. Geom. **18**, 20, (2015).

[79] A. Borodin, A. Bufetov, I. Corwin, *Directed random polymers via nested contour integrals.* Annals of Physics, **368** 191–247, (2016).

[80] G. Barraquand, A. Borodin, I. Corwin, M. Wheeler, *Stochastic six-vertex model in a half-quadrant and half-line open ASEP*, arXiv:1704.04309, (2017).

[81] M. Kardar, *Replica Bethe ansatz studies of two-dimensional interfaces with quenched random impurities*. Nucl. Phys. B **290**, 582, (1987).

[82] I. Corwin, *Macdonald processes, quantum integrable systems and the Kardar-Parisi-Zhang universality class*, Proceedings of the ICM, arXiv:1403.6877.

[83] E. H. Lieb and W. Liniger, *Exact Analysis of an Interacting Bose Gas. I. The General Solution and the Ground State*, Phys. Rev. **130**, 1605, (1963).

[84] B. Paredes, A. Widera, V. Murg, O. Mandel, S. Fölling, I. Cirac, G. V. Shlyapnikov, T. W. Hänsch, and I. Bloch. *Tonks–Girardeau gas of ultracold atoms in an optical lattice*. Nature, 429(6989):277, (2004).

[85] M. Cazalilla. *Bosonizing one-dimensional cold atomic gases*. Journal of Physics B: Atomic, Molecular and Optical Physics, 37(7):S1, (2004).

[86] J. B. McGuire, *Study of Exactly Soluble One-Dimensional N-Body Problems*. J. Math. Phys. **5**, 622, (1964).

[87] P. Calabrese and J.-S. Caux. *Correlation functions of the one-dimensional attractive bose gas*. Physical Review letters, 98(15):150403, (2007).

[88] D. Muth and M. Fleischhauer. *Dynamics of pair correlations in the attractive lieb-liniger gas*. Physical Review letters, 105(15):150403, (2010).

[89] P. Bienias, K. Pawlowski, M. Gajda, and K. Rzazewski. *Statistical properties of one-dimensional attractive bose gas*. EPL (Europhysics Letters), 96(1):10011, (2011).

[90] P. J. Everitt, M. A. Sooriyabandara, G. D. McDonald, K. S. Hardman, C. Quinlivan, M. Perumbil, P. Wigley, J. E. Debs, J. D. Close, C. C. Kuhn, N. Robins *Observation of breathers in an attractive bose gas*. arXiv:1509.06844, (2015).

[91] S. Lepoutre, L. Fouché, A. Boissé, G. Berthet, G. Salomon, A. Aspect and T. Bourdel. *Production of strongly bound* $39K$ *bright solitons*. Physical Review A, 94(5):053626, (2016).

[92] L. Piroli, P. Calabrese, and F. Essler. *Quantum quenches to the attractive one-dimensional Bose gas: exact results*. SciPost Phys. 1, 001 , (2016).

[93] Tschischik, W., Haque, M. (2015). *Repulsive-to-attractive interaction quenches of a one-dimensional Bose gas in a harmonic trap*. Physical Review A, 91(5), 053607.

[94] Zill, J., Wright, T., Kheruntsyan, K., Gasenzer, T., Davis, M. . *Quantum quench dynamics of the attractive one-dimensional Bose gas via the coordinate Bethe ansatz*. SciPost Physics, 4(2), 011, (2018).

[95] M. Gaudin, *Boundary Energy of a Bose Gas in One Dimension* , Phys. Rev. A 4 386, (1971).

[96] C. Tracy, H. Widom, *The Bose Gas and Asymmetric Simple Exclusion Process on the Half-Line* J. Stat. Phys., 150:1, (2013).

[97] N. Oelkers, M.T. Batchelor, M. Bortz, X.W. Guan, *Bethe Ansatz study of one-dimensional Bose and Fermi gases with periodic and hard wall boundary conditions*, arXiv:cond-mat/0511694, J. Phys. A **39** 1073 (2006).

[98] M. Gaudin and J-S Caux. *The Bethe Wavefunction*. Cambridge University Press, (2014).

[99] I. P. Castillo, T. Dupic, *Reunion Probabilities of N One-Dimensional Random Walkers with Mixed Boundary Conditions*, J. Stat Phys **3** 156:606–616, arXiv:1311.0654 (2014).

[100] J.F. van Diejen, E. Emsiz, *Orthogonality of Bethe Ansatz eigenfunctions for the Laplacian on a hyperoctahedral Weyl alcove* Commun. Math. Phys. 350, no. 3, 1017, (2017), J.F. van Diejen, E. Emsiz, I.N. Zurrian, *Completeness of the Bethe Ansatz for an open q-boson system with integrable boundary interactions*, arXiv:1611.05922, Ann. Henri Poincaré 19: 1349, (2018).

[101] E. Emsiz, *Completeness of the Bethe ansatz on Weyl alcoves*, Lett. Math. Phys. 91, 61–70 (2010)

[102] E. Gutkin, B. Sutherland, *Completely integrable systems and groups generated by reflections*, PNAS, 76:6057, (1979).

[103] G. J. Heckman, E. M. Opdam, *Yang's System of Particles and Hecke Algebras* Ann. Math., 145:139–173, (1997).

[104] M. L. Mehta, *Random Matrices*, 2nd ed. (New York: Academic), (1991).

[105] P. J. Forrester, *Log-gases and random matrices (LMS-34)*. London Mathematical Society Monographs Series, 34. Princeton University Press, (2010).

[106] D. S. Dean, P. Le Doussal, S. N. Majumdar, and G. Schehr. *Finite-temperature free fermions and the Kardar-Parisi-Zhang equation at finite time*. Physical Review Letters **114** (11):110402, (2015).

[107] J. Baik, E. M. Rains, *Symmetrized random permutations* , arXiv:math/9910019, (1999).

[108] T. Sasamoto, T. Imamura, *Fluctuations of a one-dimensional polynuclear growth model in a half space* J. Stat. Phys. **115** 749, arXiv:cond-mat/0307011, (2004) ; T. Sasamoto, *Fluctuations of the one-dimensional asymmetric exclusion process using random matrix techniques* J. Stat. Mech. 2007, P07007 (2007).

[109] N. O'Connell, T. Seppäläinen, N. Zygouras, *Geometric RSK correspondence, Whittaker functions and symmetrized random polymers*, arXiv:1210.5126, (2012).

[110] G. Barraquand, A. Borodin, and I. Corwin. *Half-space Macdonald processes*. arXiv:1802.08210, (2018).

[111] E. Bisi, N. Zygouras, *Point-to-line polymers and orthogonal Whittaker functions*, arXiv:1703.07337, (2017).

[112] J. de Nardis, A. Krajenbrink, P. Le Doussal, T. Thiery, *Delta Bose gas on a half-line and the KPZ equation: boundary bound states and unbinding transitions*, In preparation, (2019).

[113] M. Kardar, *Depinning by quenched randomness*. Physical Review Letters **55**, 2235, (1985).

[114] A. Somoza, P. Le Doussal, M. Ortuno, *Unbinding transition in semi-infinite two-dimensional localized systems*. Phys. Rev. B, **91** (15):155413, (2015).

[115] S. Parekh. *The KPZ limit of ASEP with boundary*. Communications in Mathematical Physics, 365(2):569–649, (2019).

[116] J. Baik, G. Barraquand, I. Corwin, T. Suidan, *Pfaffian Schur processes and last passage percolation in a half-quadrant*, arXiv:1606.00525, (2016).

[117] J. Baik, G. Barraquand, I. Corwin, and T. Suidan, *Facilitated exclusion process*, arXiv:1707.01923 (2017).

[118] P. Le Doussal, *Crossover between various initial conditions in KPZ growth: flat to stationary*, J. Stat. Mech. 2017 053210, (2017).

[119] P. Le Doussal, *Crossover from droplet to flat initial conditions in the KPZ equation from the replica Bethe ansatz* arXiv:1401.1081, J. Stat. Mech. P04018, (2014).

[120] B. Eynard, T. Kimura, and S. Ribault. *Random matrices*. arXiv:1510.04430.

[121] K. Johansson, *Random matrices and determinantal processes*, arXiv:math-ph/0510038, (2005).

[122] J. Bun, J.-P. Bouchaud, and M. Potters. *Cleaning large correlation matrices: tools from random matrix theory*. Physics Reports, 666:1–109.

[123] C. Nadal and S. N. Majumdar. *Nonintersecting Brownian interfaces and Wishart random matrices*. Phys. Rev. E, **79**,061117, (2009).

[124] V. Eisler, *Universality in the Full Counting Statistics of Trapped Fermions*. Physical Review Letters **111**, 080402, (2013).

[125] R. Marino, S. N. Majumdar, G. Schehr, P. Vivo, *Phase Transitions and Edge Scaling of Number Variance in Gaussian Random Matrices* Physical Review Letters **112**, 254101 (2014).

[126] R. Marino, S. N. Majumdar, G. Schehr, P. Vivo. *Number statistics for β-ensembles of random matrices: Applications to trapped fermions at zero temperature* Phys. Rev. E **94**, 032115, (2016).

[127] I. Pérez-Castillo, *Spectral order statistics of Gaussian random matrices: Large deviations for trapped fermions and associated phase transitions* Phys. Rev. E **90**, 040102(R), (2014).

[128] P. Calabrese, P. Le Doussal, S. N. Majumdar. *Random matrices and entanglement entropy of trapped Fermi gases* Phys. Rev. A **91**, 012303, (2015).

[129] D. S. Dean, P. Le Doussal, S. N. Majumdar, and G. Schehr. *Noninteracting fermions at finite temperature in a d-dimensional trap: Universal correlations*. Phys. Rev. A, **94** (6):063622, (2016).

[130] P. Le Doussal, S. N. Majumdar, G. Schehr, *Multicritical edge statistics for the momenta of fermions in non-harmonic traps* arXiv:1802.06436, Physical Review Letters **121**, 030603.

[131] É. Brézin *Matrix models of two dimensional quantum gravity*, in les Houches lectures notes, Ed. B. Julia, J. Zinn Justin, North Holland.

[132] J. S. Cotler, G. Gur-Ari, M. Hanada, J. Polchinski, P. Saad, S. H. Shenker, D. Stanford, A. Streicher, M. Tezuka, *Black Holes and Random Matrices*, arXiv:1611.04650, JHEP 1705:118.

[133] A. D. Mirlin, Y. V. Fyodorov, F.-M. Dittes, J. Quezada, and T. H. Seligman. *Transition from localized to extended eigenstates in the ensemble of power-law random banded matrices*. Phys. Rev. E, **54**(4):3221.

[134] C. W. Beenaker. *Random-matrix theory of quantum transport*. Reviews of modern physics, **69**(3):731.

[135] C. Texier and S. N. Majumdar. *Wigner time-delay distribution in chaotic cavities and freezing transition.* Physical Review Letters **110 250602**, (2013).

[136] A. Altland, D. Bagrets, *Quantum ergodicity in the SYK model* arXiv:1712.05073, Nucl. Phys. B 930, 45-68.

[137] A. Chan, A. De Luca and J.T. Chalker, *Spectral statistics in spatially extended chaotic quantum many-body systems*, arXiv:1803.03841, Physical Review Letters 121, 060601.

[138] B. Bertini, P. Kos, T. Prosen, *Exact Spectral Form Factor in a Minimal Model of Many-Body Quantum Chaos* arXiv:1805.00931.

[139] J. Keating and B. Odgers. *Symmetry transitions in random matrix theory & L-functions*, Communications in Mathematical Physics, 281(2):499–528, (2008).

[140] E. B. Bogomolny and J. P. Keating. *Random matrix theory and the riemann zeros. i. three- and four-point correlations*, Nonlinearity, 8(6):1115, (1995).

[141] E. B. Bogomolny and J. P. Keating. *Random matrix theory and the riemann zeros ii: n-point correlations*, Nonlinearity, 9(4):911, (1996).

[142] J. P. Keating and N. C. Snaith. *Random matrix theory and* $\zeta(1/2+it)$; Communications in Mathematical Physics, 214(1):57–89, (2000).

[143] H. L. Montgomery. *The pair correlation of zeros of the zeta function.* In Proc. Symp. Pure Math, volume 24, pages 181–193, (1973).

[144] Y.V. Fyodorov, P. Le Doussal, A. Rosso, and C. Texier. *Exponential number of equilibria and depinning threshold for a directed polymer in a random potential* Annals of Physics **397**, 1–64, (2018).

[145] Y. V Fyodorov and P. Le Doussal. *Hessian spectrum at the global minimum of high-dimensional random landscapes*, J.Phys. A: Math. Theor, **51**, 474002, (2018)

[146] Y. V. Fyodorov and C. Nadal, *Critical Behavior of the Number of Minima of a Random Landscape at the Glass Transition Point and the Tracy-Widom Distribution*, Physical Review Letters **109**, 167203, (2012).

[147] V. Ros, G. Ben Arous, G. Biroli, C. Cammarota. *Complex energy landscapes in spiked-tensor and simple glassy models: ruggedness, arrangements of local minima and phase transitions.* Phys. Rev. X **9**, 011003 (2019)

[148] A. Auffinger, G. Ben Arous, and J. Cerny. *Random matrices and complexity of spin glasses.* Commun. Pure. Appl. Math. **66** no.2, 165–201 (2013).

[149] Y. V Fyodorov and P. Le Doussal, *Manifolds pinned by a high-dimensional random landscape: Hessian at the global energy minimum*, arXiv:1903.07159, (2019)

[150] C. Nadal, *Matrices aléatoires et leurs applications à la physique statistique et physique quantique.* PhD thesis, Université Paris-Sud, (2011).

[151] S. Karlin, J. McGregor, *Coincidence probabilities*, Pacific J. Math. **9**, 4, 1141-1164, (1959).

[152] G. Schehr, S. N. Majumdar, A. Comtet, and J. Randon-Furling. *Exact distribution of the maximal height of p vicious walkers*, Physical Review Letters 101(15):150601, (2008).

[153] I. Dumitriu, A. Edelman, *Matrix models for beta ensembles*, J. Math. Phys. **43** 5830-5847.

[154] Dyson, F. J. *A Brownian-motion model for the eigenvalues of a random matrix.* Journal of Mathematical Physics, 3(6), 1191-1198, (1962).

[155] J. Ramirez, B. Rider and B. Virag, *Beta ensembles, stochastic Airy spectrum and a diffusion*, J. Amer. Math. Soc. **24** 919-944.

[156] C. A. Tracy and H. Widom, *Correlation functions, cluster functions, and spacing distributions for random matrices.* J. Stat. Phys. **92** (5-6):809–835, (1998).

[157] C. A. Tracy, H. Widom, *Distribution functions for largest eigenvalues and their applications*, Proceedings of the ICM Beijing, **1**, 587, (2002).

[158] S. N. Majumdar and G. Schehr. *Top eigenvalue of a random matrix: large deviations and third order phase transition.* J. Stat. Mech. P01012, (2014).

[159] P.J. Forrester, *Painleve transcendent evaluation of the scaled distribution of the smallest eigenvalue in the Laguerre orthogonal and symplectic ensemble*, arXiv:nlin/0005064, (2000).

[160] P. L. Ferrari and H. Spohn, *A determinantal formula for the GOE Tracy-Widom distribution*, Journal of Physics A: Mathematical and General, **38** (33):L557, (2005).

[161] J. Baik, R. Buckingham, and J. DiFranco, *Asymptotics of Tracy-Widom distributions and the total integral of a Painlevé II function*, Communications in Mathematical Physics, **280** (2):463–497, (2008).

[162] S. P. Hastings and J. B. Mcleod, *A boundary value problem associated with the second Painlevé transcendent and the Korteweg-de Vries equation.* Archive for Rational Mechanics and Analysis, 73(1):31–51, (1980).

[163] A. Soshnikov, *Determinantal random point fields.* Russian Mathematical Surveys, 55(5):923, (2000).

[164] G. W. Anderson, A. Guionnet and O. Zeitouni, *An Introduction to Random Matrices*, volume 118 of Cambridge Studies in Advanced Mathematics **118**.

[165] E. M. Rains, *Correlation functions for symmetrized increasing subsequences* , arXiv:math/0006097, (2000).

[166] K. Johansson and G. Lambert, *Gaussian and non-Gaussian fluctuations for mesoscopic linear statistics in determinantal processes.* arXiv:1504.06455, (2015).

[167] N. De Bruijn, *On some multiple integrals involving determinants.* J. Indian Math. Soc, **19** 133–151, (1955).

[168] A. Borodin and E. Kanzieper, *A note on the Pfaffian Integration Theorem.* Journal of Physics A: Mathematical and Theoretical, **40** (36):F849, (2007).

[169] P. Le Doussal, S. N. Majumdar, A. Rosso, G. Schehr, *Exact short-time height distribution in 1D KPZ equation and edge fermions at high temperature*, Physical Review Letters **117**, 070403, (2016).

[170] T. Imamura, T. Sasamoto, *Stationary correlations for the 1D KPZ equation*, J. Stat. Phys. **150**, 908-939 , (2013).

[171] R. M. Corless, G. H. Gonnet, D. E. Hare, D. J. Jeffrey, D. E. Knuth *On the Lambert W function*, Advances in Computational Mathematics, **5** 329–359, (1996).

[172] P. Le Doussal, *Unpublished notes.* (2016)

[173] S. Parekh. *Positive random walks and an identity for half-space SPDEs*. arXiv:1901.09449, (2019).

[174] Y. Hao, Y. Zhang, J. Q. Liang and S. Chen, *Ground-state properties of one-dimensional ultracold Bose gases in a hard-wall trap*, Phys. Rev. A **73**,063617 (2006).

[175] P. J. Forrester, T. Nagao, E. M. Rains, *Correlation functions for random involutions*, arXiv:math/0503074

[176] P. J. Forrester, E. M. Rains, *Correlations for superpositions and decimations of Laguerre and Jacobi orthogonal matrix ensembles with a parameter*. E. Probab. Theory Relat. Fields 130: 518, (2004).

[177] V. Gorin and S. Sodin. *The KPZ equation and moments of random matrices*. arXiv:1801.02574, (2018).

[178] T. Tao and V. Vu. *Random matrices: Universal properties of eigenvectors*. Random Matrices: Theory and Applications, 1(01):1150001, (2012).

[179] Diaconis, P. W., Eaton, M. L., Lauritzen, S. L. *Finite de Finetti theorems in linear models and multivariate analysis*. Scandinavian Journal of Statistics, 289-315. (1992).

[180] Diaconis, P., Freedman, D. *A dozen de Finetti-style results in search of a theory*. In Annales de l'IHP Probabilités et statistiques (Vol. 23, No. S2, pp. 397-423), (1987).

[181] D. Revuz and M. Yor. *Continuous martingales and Brownian motion*, volume 293. Springer Science & Business Media, (2013).

[182] A. N. Borodin, *Brownian local time*, Russian Math. Surveys, **44:2:1-51**, (1989).

[183] J. Pitman, *The distribution of local times of a Brownian bridge*, Séminaire de probabilités de Strasbourg **33**, 388-394 (1999).

[184] P. Ghosal, *Moments of the SHE under delta initial measure*, arXiv:1808.04353, (2018).

[185] P. Forrester, S. V. E. N. Warnaar, *The importance of the Selberg integral*, B. Am. Math. Soc. **45**(4), 489-534, (2008).

[186] P. Calabrese, M. Kormos and P. Le Doussal, *From the sine-Gordon field theory to the Kardar-Parisi-Zhang growth equation*, arXiv:1405.2582, EPL 107 10011, (2014).

[187] P. Le Doussal, S. N. Majumdar, G. Schehr, *Large deviations for the height in 1D Kardar-Parisi-Zhang growth at late times*, Europhys. Lett. **113**, 60004, (2016).

[188] Dembo, Amir, and Ofer Zeitouni. *Large deviations techniques and applications*. Applications of Mathematics 38, (1998).

[189] H. Touchette. *The large deviation approach to statistical mechanics*. Physics Reports, 478(1-3):1–69, (2009).

[190] E. J. Gumbel. *Statistics of extremes*. Columbia University Press, New York, 1958.

[191] J.-P. Bouchaud and M. Mézard. *Universality classes for extreme-value statistics*. Journal of Physics A: Mathematical and General, 30(23):7997–8015, (1997).

[192] D. S. Dean and S. N. Majumdar. *Extreme value statistics of eigenvalues of Gaussian random matrices*. Phys. Rev. E **77**, 041108.

[193] B. Derrida and J.L. Lebowitz, *Exact Large Deviation Function in the Asymmetric Exclusion Process* Physical Review Letters **80**:209-213, (1998)

[194] S. Prolhac *Finite-time fluctuations for the totally asymmetric exclusion process*, Physical Review Letters **116**:090601, (2016).

[195] A. Lazarescu and K. Mallick *An exact formula for the statistics of the current in the TASEP with open boundaries.* J. Phys. A: Math. Theor. **44**:315001, (2011)

[196] M. Gorissen, A. Lazarescu, K. Mallick and C. Vanderzande *Exact Current Statistics of the Asymmetric Simple Exclusion Process with Open Boundaries.* Physical Review Letters **109**:170601, (2012)

[197] H. Moriya, R. Nagao, and T. Sasamoto. *Exact large deviation function of spin current for the one dimensional XX spin chain with domain wall initial condition.* arXiv:1901.07228, (2019).

[198] A. Lazarescu *The physicist's companion to current fluctuations: one-dimensional bulk-driven lattice gases* J. Phys. A: Math. Theor. **48**:503001, (2015)

[199] B. Derrida, *Non-equilibrium steady states: fluctuations and large deviations of the density and of the current.* J. Stat. Mech. P07023, (2007).

[200] B. Derrida and A. Gerschenfeld, *Current fluctuations of the one dimensional symmetric simple exclusion process with step initial condition*, J. Stat. Phys. **136**, pp 1-15, (2009).

[201] L. Bertini, A. De Sole, D. Gabrielli, G. Jona-Lasinio, C. Landim, *Macroscopic fluctuation theory for stationary nonequilibrium states.* J. Stat. Phys. **107**, 635-675, (2002) .

[202] I. V. Kolokolov, S. E. Korshunov, *Explicit solution of the optimal fluctuation problem for an elastic string in random potential.* Phys. Rev. E **80**, 031107, (2009); *Universal and non-universal tails of distribution functions in the directed polymer and KPZ problems.* Phys. Rev. B **78**, 024206, (2008); *Optimal fluctuation approach to a directed polymer in a random medium.* Phys. Rev. B **75**, 140201, (2007).

[203] B. Meerson, E. Katzav, A. Vilenkin, *Large Deviations of Surface Height in the Kardar-Parisi-Zhang Equation*, Physical Review Letters **116**, 070601, (2016).

[204] A. Kamenev, B. Meerson, P. V. Sasorov, *Short-time height distribution in 1D KPZ equation: starting from a parabola*, Phys. Rev. E **94**, 032108, (2016).

[205] M. Janas, A. Kamenev, B. Meerson. *Dynamical phase transition in large-deviation statistics of the Kardar-Parisi-Zhang equation*, Phys. Rev. E **94**, 032133, (2016).

[206] B. Meerson, J. Schmidt, *Height distribution tails in the Kardar-Parisi-Zhang equation with Brownian initial conditions*, J. Stat. Mech. 103207, (2017).

[207] N. R. Smith, A. Kamenev, B. Meerson, *Landau theory of the short-time dynamical phase transition of the Kardar-Parisi-Zhang interface* , arXiv:1802.07497, (2018).

[208] N. R. Smith and B. Meerson, *Exact short-time height distribution for the flat Kardar-Parisi-Zhang interface* , arXiv:1803.04863, (2018).

[209] T. Asida, E. Livne, and B. Meerson. *Large fluctuations of a Kardar-Parisi-Zhang interface on a half-line: the height statistics at a shifted point.* Phys. Rev. E 99, 042132, arXiv:1901.07608, (2019).

[210] B. Meerson and A. Vilenkin. *Large fluctuations of a Kardar-Parisi-Zhang interface on a half line*. Physical Review E, 98(3):032145, (2018).

[211] N. R. Smith, B. Meerson, and P. Sasorov. *Finite-size effects in the short-time height distribution of the Kardar–Parisi–Zhang equation*. Journal of Statistical Mechanics: Theory and Experiment,2018(2):023202, (2018).

[212] N. R. Smith, B. Meerson, and A. Vilenkin. *Time-averaged height distribution of the Kardar-Parisi-Zhang interface*. arXiv:1902.08110, (2019).

[213] E. Basor and H. Widom. *Determinants of Airy Operators and Applications to Random Matrices*. J. Stat. Phys. **96** (1-2):1–20, (1999).

[214] E. Basor. *A brief history of the strong Szegö limit theorem*. In *Mathematical methods in systems, optimization, and control, pages 73–83. Springer*, (2012).

[215] A. K. Hartmann, P. Le Doussal, S. N. Majumdar, A. Rosso, G. Schehr, *High-precision simulation of the height distribution for the KPZ equation*, Europhys. Lett. 121, 67004 (2018)

[216] E. Brunet *Influence des effets de taille finie sur la propagation d'un front — Distribution de l'énergie libre d'un polymère dirigé en milieu aléatoire*, Available on E. Brunet's webpage, (2000).

[217] A. K. Hartmann *Sampling rare events: Statistics of local sequence alignments* Phys. Rev. E 65 2002 056102, (2001).

[218] A. K. Hartmann *Large-deviation properties of largest component for random graphs* Eur. Phys. J. B 84 2011 627, (2011).

[219] A. K. Hartmann, *Big Practical Guide to Computer Simulations*, World Scientific, Singapore, (2015)

[220] A. Engel A., R. Monasson, A. K. Hartmann *On Large Deviation Properties of Erdös–Rényi Random Graphs* J. Stat. Phys. 117 2004 387,(2004).

[221] S. Wolfsheimer, A. K. Hartmann, *Minimum-free-energy distribution of RNA secondary structures: Entropic and thermodynamic properties of rare events* Phys. Rev. E 82 2010 021902, (2010).

[222] T. A. Driscoll, K. L. Maki *Searching for Rare Growth Factors Using Multicanonical Monte Carlo Methods* SIAM Review 49 2007 673, (2007).

[223] N. Saito, Y. Iba, K. Hukushima *Multicanonical sampling of rare events in random matrices* Phys. Rev. E 82 2010 031142, (2010).

[224] A. K Hartmann, S. N. Majumdar, A. Rosso *Sampling fractional Brownian motion in presence of absorption: A Markov chain method* Phys. Rev. E 88 2013 022119, (2013).

[225] J, M. Hammersley, K. W. Morton, *A new Monte Carlo technique: antithetic variates*, Math. Proc. Cambr. Phil. Soc. **52**, 449–475, (1956).

[226] M. E. J. Newman , G. T. Barkema *Monte Carlo Methods in Statistical Physics*, (Clarendon Press, Oxford) (1999).

[227] D. P. Landau, K. Binder *A Guide to Monte Carlo Simulations in Statistical Physics* Cambridge University Press, Cambridge, (2000).

[228] N. Metropolis, A. W. Rosenbluth , M. N. Rosenbluth , A. Teller, E. Teller *Equation of State Calculations by Fast Computing Machines* J. Chem. Phys. 21 1953 1087, (1953).

[229] A. Grabsch, S. N. Majumdar, and C. Texier. *Truncated linear statistics associated with the top eigenvalues of random matrices.* J. Stat. Phys. **167** (2):234–259, (2017).

[230] A. Grabsch, S. N. Majumdar, and C. Texier. *Truncated linear statistics associated with the eigenvalues of random matrices II. Partial sums over proper time delays for chaotic quantum dots.* J. Stat. Phys. 167(6):1452–1488, (2017).

[231] A. Borodin and V. Gorin. *Moments match between the KPZ equation and the Airy point process*, Symmetry, Integrability and Geometry. Methods and Applications, 12, (2016).

[232] I. Corwin, P. Ghosal, *Lower tail of the KPZ equation.* arXiv:1802.03273, (2018).

[233] Y. H. Kim, *The lower tail of half-space KPZ equation*, arXiv:1905.07703, (2019).

[234] I. Corwin and P. Ghosal. *KPZ equation tails for general initial data.* arXiv:1810.07129, (2018).

[235] A. Borodin, P. Ferrari, *Anisotropic growth of random surfaces in 2+1 dimensions* arXiv:0804.3035v2, Comm. Math. Phys. **325**, 603-684.

[236] A. Borodin. *CLT for spectra of submatrices of Wigner random matrices*, arXiv:1010.0898, (2010).

[237] Z. Bai, X. Wang, and W. Zhou. *CLT for linear spectral statistics of Wigner matrices.* Electron. J. Probab. 14:no. 83, 2391, (2009).

[238] L.-C. Tsai. *Exact lower tail large deviations of the KPZ equation.* arXiv:1809.03410, (2018).

[239] P. Sasorov, B. Meerson, S. Prolhac, *Large deviations of surface height in the 1+1 dimensional Kardar-Parisi-Zhang equation: exact long-time results for* $\lambda H < 0$, J. Stat. Mech. 063203, (2017).

[240] H.-J. Sommers, W. Wieczorek, and D. Savin. *Statistics of conductance and shot-noise power for chaotic cavities.* arXiv:0710.5370.

[241] P. Vivo, S. N. Majumdar, and O. Bohigas. *Distributions of conductance and shot noise and associated phase transitions.* Physical Review Letters **101** (21):216809, (2008).

[242] C. Nadal, S. N. Majumdar, and M. Vergassola. *Phase transitions in the distribution of bipartite entanglement of a random pure state.* Physical Review Letters **104**, 110501.

[243] M. Duits, K. Johansson *On mesoscopic equilibrium for linear statistics in Dyson's Brownian Motion*, arXiv:1312.4295.

[244] I. Dumitriu, E. Paquette. *Spectra of Overlapping Wishart Matrices and the Gaussian Free Field* arXiv:1410.7268, Random Matrices: Theory and Applications 7(02): 1850003.

[245] I. Dumitriu, E. Paquette. *Global fluctuations for linear statistics of* β*-Jacobi ensembles.* Random Matrices Theory Appl. 1(4), 1250,013, 60.

[246] F. D. Cunden and P. Vivo. *Universal covariance formula for linear statistics on random matrices.* Physical Review Letters **113** 070202.

[247] T. Maciazek*et al.*, *The probability distribution of spectral moments for the Gaussian beta-ensembles*, arXiv:1510.03898, Acta Physica Polonica A, vol. 128, no.6, pp 983.

[248] D. S. Dean and S. N. Majumdar. *Large deviations of extreme eigenvalues of random matrices.* Physical Review Letters **97** (16):160201.

[249] S. N. Majumdar, C. Nadal, A. Scardicchio, and P. Vivo. *Index Distribution of Gaussian Random Matrices.* Physical Review Letters **103** 220603.

[250] S. N. Majumdar, C. Nadal, A. Scardicchio, and P. Vivo. *How many eigenvalues of a Gaussian random matrix are positive?* Phys. Rev. E, **83** 041105.

[251] F. D. Cunden, P. Facchi, and P. Vivo. *A shortcut through the Coulomb gas method for spectral linear statistics on random matrices.* Journal of Physics A: Mathematical and Theoretical, 49(13):135202, (2016).

[252] A. Barranco and J. G. Russo. *Large N phase transitions in supersymmetric Chern-Simons theory with massive matter.* Journal of High Energy Physics, 2014(3):12, (2014).

[253] D. J. Gross and E. Witten. *Possible third-order phase transition in the large N lattice gauge theory.* In The Large N Expansion In Quantum Field Theory And Statistical Physics: From Spin Systems to 2-Dimensional Gravity, pages 584–591. World Scientific, (1993).

[254] L. Santilli and M. Tierz. *Phase transitions and Wilson loops in antisymmetric representations in Chern-Simons-matter theory.* arXiv:1808.02855, (2018).

[255] S. R. Wadia. *$N = \infty$ phase transition in a class of exactly soluble model lattice gauge theories.* Physics Letters B, 93(4):403–410, (1980).

[256] K. Johansson. *The longest increasing subsequence in a random permutation and a unitary random matrix model.* Mathematical Research Letters, 5(1):68–82, (1998).

[257] F. Colomo and A. Pronko. *Third-order phase transition in random tilings.* Physical Review E, 88(4):042125, (2013).

[258] F. Colomo and A. G. Pronko. *Thermodynamics of the six-vertex model in an L-shaped domain.* Communications in Mathematical Physics, 339(2):699–728, (2015).

[259] C. Nadal, S. N. Majumdar, and M. Vergassola, *Statistical Distribution of Quantum Entanglement for a Random Bipartite State*, J. Stat. Phys. **142**(2), 403–438, (2011).

[260] P. Vivo, S. N. Majumdar, and O. Bohigas, *Probability distributions of Linear Statistics in Chaotic Cavities and associated phase transitions*, Phys. Rev. B **81**, 104202, (2010).

[261] K. Damle, S. N. Majumdar, V. Tripathi, and P. Vivo, *Phase transitions in the distribution of the Andreev conductance of superconductor-metal junctions with multiple transverse modes*, Physical Review Letters **107**, 177206, (2011).

[262] S. N. Majumdar and M. Vergassola, *Large deviations of the maximum eigenvalue for Wishart and Gaussian random matrices.* Physical Review Letters **102**, 060601, (2009).

[263] R. Marino, S. N. Majumdar, G. Schehr, and P. Vivo, *Index distribution of Cauchy random matrices.* J. Phys. A: Math. Theor. **47**, 055001, (2014).

[264] R. Allez, J. Touboul, and G. Wainrib, *Index distribution of the Ginibre ensemble.* J. Phys. A: Math. Theor. **47**, 042001, (2014).

[265] F. D. Cunden, A. Maltsev, and F. Mezzadri, *Fluctuations in the two-dimensional one-component plasma and associated fourth-order phase transition*, Phys. Rev. E **91**, 060105 (2015).

[266] G. Ben Arous and A. Guionnet, *Large deviations for Wigner's law and Voiculescu's non-commutative entropy*. Probab. Theo. Rel. Fields **108**, 517 (1997).

[267] A. Edelman, B. Sutton, *From random matrices to stochastic operators*. J. Stat. Phys. **127**, no. 6, 1121-1165.

[268] B. Virag, *Operator limits of random matrices*, arXiv:1804.06953.

[269] C. Cohen-Tannoudji, B. Diu, F. Laloe, *Quantum mechanics* Wiley, New York, (1977).

[270] L. D. Landau, E. M. Lifshitz, *Quantum mechanics*, Pergamon, (1977).

[271] T. L. Einstein, *Applications of Ideas from Random Matrix Theory to Step Distributions on Misoriented Surfaces* arXiv:cond-mat/0306347, Ann. Henri Poincaré 4, Suppl. 2, S811-S824 (2003).

[272] M. E. Fisher, *Walks, walls, wetting, and melting.* Journal of Statistical Physics, **34** (5-6):667–729, (1984).

[273] J. Moser, *Three integrable hamiltonian systems connected with isospectral deformations.* Surveys in Applied Mathematics, pages 235–258. Elsevier, (1976).

[274] M. Krishnapur, B. Rider, and B. Virág, *Universality of the stochastic airy operator*. Communications on Pure and Applied Mathematics, 69(1):145–199, (2016).

[275] F. Bekerman, A. Figalli, and A. Guionnet, *Transport maps for β -matrix models and universality*. Communications in Mathematical Physics, 338(2):589–619, (2015).

[276] P. Bourgade, L. Erdös, and H.-T. Yau, *Edge universality of beta ensembles*. Communications in Mathematical Physics, 332(1):261–353, (2014).

[277] E. S. Andersen, *On the fluctuations of sums of random variables*, Mathematica Scandinavica, pp 263-285, (1954).

RÉSUMÉ

Cette thèse de doctorat porte sur l'étude du modèle de croissance stochastique Kardar-Parisi-Zhang (KPZ) en 1+1 dimensions et en particulier de l'équation qui le régit. Cette thèse est d'une part destinée à effectuer un état de l'art et dresser un portrait moderne de la recherche des solutions exactes de l'équation KPZ, de leurs propriétés en terme de théorie des grandes déviations et également de leurs applications (en théorie des matrices aléatoires ou en calcul stochastique notamment). D'autre part cette thèse a pour but de formuler un certain nombre de questions ouvertes à l'interface avec la théorie de l'intégrabilité, la théorie des matrices aléatoires et la théorie des gaz de Coulomb.

Cette thèse est divisée en trois parties distinctes portant (i) sur les solutions exactes de l'équation KPZ, (ii) sur les solutions à temps court sous la forme d'un principe grandes déviations et (iii) sur les solutions à temps long et leurs extensions aux statistiques linéaires au bord de spectre de matrice aléatoire.

Nous présenterons les résultats de cette thèse comprenant notamment (a) une nouvelle solution de l'équation KPZ à tout temps dans un demi-espace, (b) une méthodologie générale pour établir à temps court un principe de grandes déviations pour les solutions de KPZ à partir de leur représentation sous forme de déterminant de Fredholm et (c) une unification de quatre méthodes permettant d'obtenir à temps long un principe de grandes déviations pour les solutions de l'équation KPZ et de manière plus générale d'étudier des statistiques linéaires au bord du spectre de matrices aléatoires.

MOTS CLÉS

Systèmes désordonnés et hors équilibre, polymère dirigé, Kardar-Parisi-Zhang, modèles exactement solubles, large déviations, théorie des matrices aléatoires, statistique linéaire, processus ponctuel d'Airy, fermions froids.

ABSTRACT

Throughout this Ph.D thesis, we will study the Kardar-Parisi-Zhang (KPZ) stochastic growth model in 1+1 dimensions and more particularly the equation which governs it. The goal of this thesis is two-fold. Firstly, it aims to review the state of the art and to provide a detailed picture of the search of exact solutions to the KPZ equation, of their properties in terms of large deviations and also of their applications to random matrix theory or stochastic calculus. Secondly, is it intended to express a certain number of open questions at the interface with integrability theory, random matrix theory and Coulomb gas theory.

This thesis is divided in three distinct parts related to (i) the exact solutions to the KPZ equation, (ii) the short-time solutions expressed by a Large Deviation Principle and the associated rate functions and (iii) the solutions at large time and their extensions to linear statistics at the edge of random matrices.

We will present the new results of this thesis including (a) a new solution to the KPZ equation at all times in a half-space, (b) a general methodology to establish at short time a Large Deviation Principle for the solutions to the KPZ equation from their representation in terms of Fredholm determinant and (c) the unification of four methods allowing to obtain at large time a Large Deviation Principle for the solution to the KPZ equation and more generally to investigate linear statistics at the soft edge of random matrices.

KEYWORDS

Disordered and out-of-equilibrium systems, directed polymer, Kardar-Parisi-Zhang, exactly solvable models, large deviations, random matrix theory, linear statistics, Airy point process, cold fermions.